



HAL
open science

Etude géomorphologique de la dynamique sédimentaire de torrents à lave (Alpes Françaises)

Joshua Theule

► **To cite this version:**

Joshua Theule. Etude géomorphologique de la dynamique sédimentaire de torrents à lave (Alpes Françaises). Sciences de la Terre. Université de Grenoble, 2012. Français. NNT : 2012GRENU021 . tel-00864986

HAL Id: tel-00864986

<https://theses.hal.science/tel-00864986>

Submitted on 23 Sep 2013

HAL is a multi-disciplinary open access archive for the deposit and dissemination of scientific research documents, whether they are published or not. The documents may come from teaching and research institutions in France or abroad, or from public or private research centers.

L'archive ouverte pluridisciplinaire **HAL**, est destinée au dépôt et à la diffusion de documents scientifiques de niveau recherche, publiés ou non, émanant des établissements d'enseignement et de recherche français ou étrangers, des laboratoires publics ou privés.

THÈSE

Pour obtenir le grade de

DOCTEUR DE L'UNIVERSITÉ DE GRENOBLE

Spécialité : **Science de la Terre, de l'Univers et de l'Environnement**

Arrêté ministériel : 7 août 2006

Présentée par

Joshua I. Theule

Thèse dirigée par **Frédéric Liébault** et
Dominique Laigle

préparée au sein de l'**IRSTEA, Unité de Recherche ETNA
(Erosion Torrentielle, Neige et Avalanches)**
dans l'**École Doctorale Terre, Univers et Environnement**

Geomorphic study of sediment dynamics in active debris-flow catchments (French Alps)

Thèse soutenue publiquement le **29 novembre 2012**,
devant le jury composé de :

Prof. Oldrich Hungr

University of British Columbia, Rapporteur

Prof. John Pitlick

University of Colorado, Rapporteur

Prof. Michel Jaboyedoff

Université de Lausanne, Examineur

Dr. Alexandre Remaître

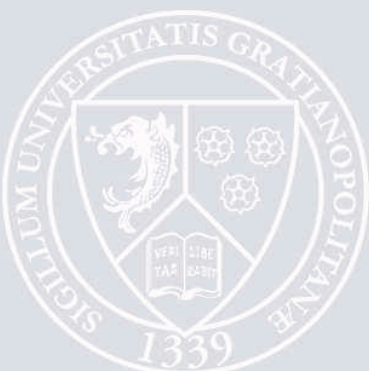
Université de Strasbourg, Examineur

Dr. Dominique Laigle

IRSTEA ETNA, Directeur

Dr. Frédéric Liébault

IRSTEA ETNA, Encadrant



ACKNOWLEDGEMENTS

This research was supported by the European Interreg-Alpine Space-PARAMount project, the Interreg-Alcotra-Risknat project and the PGRN (*Pôle Grenoblois d'étude et de recherche pour la prévention des Risques Naturels, Conseil Général de l'Isère*). The ONF-RTM 38 is acknowledged for facilitating field access to the Manival Torrent and the ONF-RTM 06 for the Réal Torrent.

I am very grateful for my reviewers, Oldrich Hungr (University of British Columbia) and John Pitlick (University of Colorado), who have decided to spend their time and energy for examining my thesis.

A special thank you goes to my advisor Frédéric Liébault who decided to put me through this endeavor. I have learned a great deal from him to become a tedious and honest researcher who can contribute effectively to the scientific community. He has also given me the independence and trust for taking my own strides.

My thesis has also been guided by a committee with great input and direction. Thanks go to my HDR advisor, Dominique Laigle, and to Christophe Peteuil, Nicolle Mathys, and Alexandre Remaître. I must give further gratitude to Michel Jaboyedoff who has collaborated with my project and allowed me to use the terrestrial laser scanner from the IGAR institute.

Other thanks must be given to my close colleagues and friends Oldrich Navratil and Alexandre Loye who have had parallel studies with me in the Manival and Réal. We have spent many days in the field, have had many discussions, and collaborated with each others research.

I have spent over one hundred days in the field during my study and was hardly ever alone. Thank you everybody for bearing the cold, heat, snow, rain, and falling rocks: Bruno Bacq (you were a great sla... uhh master student), Christophe Bigot (and his tick-proof suit), Adeline Heymann (vin chaud in Manival was awesome), Sandrine Tacon (don't worry, Fred barks more than he bites), Mathieu Cassel, Michael Deschatres, Hugo Jantzi, Mathieu Labbé, Emilien Parisot, Nicolas Talaska, Greg Tucker, Philippe Chavignon, Luc Demirdjian, Eric Travaglini and Nathalie Andreis.

For my friends who lacked the opportunity (or courage) to help me in the field, I still appreciated the many discussions, encouragements and high spirits during and after work: grandpa Paolo Caccamo (our Alicia coffee maker barely survived our entire PhD program), Vito Bacchi, Philomène Favier, Pauline Leduc, Nicolas Lafarge, Nejib Hadda, Benoit Chanut, Caroline Le Bouteiller and the list can go on...

During my program in France I have spent very little time with my family in the United States and China. Despite the long distances, I could still count on their encouragement, support and love.

Finally, I must thank my dear Steph, who has been by my side during the hardest times. Rather than me analyzing my work in circles, she helped me to breathe and to be part of the world. Je te remercie de me faire aimer, vivre et sourire.

TABLE OF CONTENTS

ACKNOWLEDGEMENTS	I
TABLE OF CONTENTS	II
ABSTRACT	V
RESUME	VI
CHAPTER 1: INTRODUCTION	1
1 GENERAL UNDERSTANDING OF DEBRIS-FLOWS	2
1.1 DEBRIS-FLOW FEATURES.....	2
1.1.1 Classification of debris-flows.....	4
1.1.2 Conditions for occurrence.....	6
1.2 SCIENTIFIC STUDY OF DEBRIS-FLOWS.....	7
1.2.1 Field Observations.....	7
1.2.2 Experimental laboratory studies.....	9
1.2.3 Debris-flow modeling.....	10
2 SEDIMENT TRANSFER BY DEBRIS-FLOWS	11
2.1 CATCHMENT-SCALE SEDIMENT CASCADE.....	11
2.1.1 Sediment supply from hillslopes.....	11
2.1.2 Sediment yields.....	12
2.2 INTERACTIONS WITH THE CHANNEL.....	14
2.2.1 Channel scouring.....	14
2.2.2 Controlling factors.....	16
2.3 CHANNEL STORAGE CHANGES OVER TIME.....	17
3 THESIS OBJECTIVES	19
CHAPTER 2: STUDY SITES	21
1 STUDY SITES OVERVIEW	22
2 THE MANIVAL TORRENT CATCHMENT	22
3 THE REAL TORRENT CATCHMENT	27
CHAPTER 3: SEDIMENT BUDGET MONITORING OF DEBRIS-FLOW AND BEDLOAD TRANSPORT IN THE MANIVAL TORRENT	33
1 INTRODUCTION	34
2 MATERIAL AND METHODS	35
2.1 SEDIMENT BUDGET.....	35
2.1.1 Channel storage changes.....	35
2.1.2 Sediment output.....	39
2.2 SEDIMENT SUPPLY FROM LOW-ORDER HEADWATERS.....	42
2.3 INITIAL CHANNEL STORAGE QUANTIFICATION.....	43
2.4 RAINFALL MONITORING.....	45
3 RESULTS	46
3.1 RAINFALL AND CHANNEL RESPONSES.....	46
3.2 TORRENT SEDIMENT BUDGETS.....	48
3.3 SEDIMENT SUPPLY FROM FIRST-ORDER HEADWATERS.....	51
3.4 FLUCTUATING CHANNEL STORAGE OVER TIME.....	55
4 DISCUSSION	56

5	CONCLUSIONS	64
CHAPTER 4: DEBRIS-FLOW PROPAGATION AND CHANNEL INTERACTIONS: THE CASE OF THE REAL TORRENT		
1	INTRODUCTION	66
2	MATERIAL AND METHODS.....	67
2.1	POST-EVENT FIELD SURVEYS.....	67
2.1.1	Cross-section surveying.....	67
2.1.2	Backcalculating debris-flow velocity	70
2.2	HIGH-FREQUENCY DEBRIS-FLOW MONITORING STATIONS	70
3	RESULTS	72
3.1	FLOW RECORDS.....	72
3.1.1	Rainfall conditions and flow occurrence	72
3.1.2	Event descriptions and results (P1-P6)	74
3.1.3	Debris-flow volume measurement comparisons.....	81
3.1.4	Surge dynamics for June 29, 2011 debris-flow	81
3.2	JUNE 29, 2011 DEBRIS-FLOW VELOCITY AND DISCHARGE	83
3.2.1	Reach-scale comparison (Station 3)	83
3.2.2	Full channel comparison.....	86
4	DISCUSSION	90
4.1	RELIABILITY OF POST-EVENT SURVEYS	90
4.1.1	Sediment transport volumes	90
4.1.2	Backcalculation of velocities	90
4.2	INFLUENCE OF CHANNEL INTERACTION AND SURGE COALESCENCE	91
4.3	FLOW RESISTANCE CHARACTERIZATION	93
4.4	SEDIMENT TRANSPORT TRENDS BY PROCESS TYPE	97
5	CONCLUSIONS	100
CHAPTER 5: SPATIAL VARIABILITY OF CHANNEL EROSION BY DEBRIS-FLOWS		
1	INTRODUCTION	104
2	METHODS.....	105
2.1	CHANNEL OBSERVATIONS FROM CROSS-SECTION SURVEYING.....	105
2.2	DATA COMPILATION FROM LITERATURE.....	107
2.3	LASER SCANNING FOR THE CHARACTERIZATION OF ERODIBLE MATERIAL.....	109
3	RESULTS	112
3.1	SPATIAL VARIABILITY OF SCOUR AND FILL.....	112
3.1.1	Scour and fill for the Manival.....	112
3.1.2	Scour and fill for the Réal.....	114
3.1.3	Comparison between debris-flow and bedload transport.....	116
3.2	GLOBAL RELATION OF DEBRIS-FLOW SCOUR AND CHANNEL SLOPE.....	120
3.3	CHARACTERIZING ERODIBLE MATERIAL WITH TLS.....	122
3.3.1	Sequence of events and topographic descriptions	122
3.3.2	Classifying erodible material with roughness.....	126
3.4	REACH-SCALE ROUGHNESS	128
4	DISCUSSION	130
4.1	COMPARING DEBRIS-FLOW AND BEDLOAD SCOURING	130
4.2	INFLUENCE OF SLOPE AND STORAGE ON DEBRIS-FLOW SCOURING.....	130
4.3	MAPPING POTENTIAL DEBRIS-FLOW SCOUR AND VOLUME.....	133
5	CONCLUSIONS	135

CHAPTER 6: GENERAL CONCLUSIONS	137
1 SUMMARY OF CONCLUSIONS	138
2 OUTCOMES AND PERSPECTIVES.....	140
REFERENCES.....	143
APPENDIX: LIST OF PUBLICATIONS.....	151

ABSTRACT

Steep mountain catchments typically experience large sediment pulses from hillslopes which are stored in headwater channels and remobilized by debris-flows or bedload transport. The purpose of this research was to investigate the coarse sediment transport through steep catchments and how channel storage can influence debris-flows. This required intensive field-based geomorphic monitoring of flow events in the Manival and Réal torrent catchments which can experience debris-flows and bedload transport every year.

In the Manival Torrent, the sediment transfers were characterized at a seasonal time scale by a complete sediment budget of the catchment derived from multi-date topographic measurements between important flow events (cross-section surveying and terrestrial laser scanning). Two debris-flows were observed, as well as several bedload transport flow events. Sediment budget reconstitution of the two debris-flows revealed that most of their volumes were supplied by channel scouring (more than 92%). Bedload transport during autumn contributed to the sediment recharge of high-order channels by the deposition of large gravel wedges. This process is recognized as being fundamental for debris-flow occurrence during the subsequent spring and summer. A time shift of scour-and-fill sequences was observed between low- and high-order channels, revealing the discontinuous sediment transfer in the catchment during common flow events. A conceptual model of sediment routing for different event magnitudes is proposed.

In the Réal Torrent, post-event surveying and high-frequency monitoring stations were used to compare and compile measurements of flow events. Three debris-flow events and three periods of bedload transport with small headwater debris-flows were observed. Sediment transport volumes for debris-flows were very similar to the Manival with important volume growth in the channel. The largest observed debris-flow was examined in detail revealing a downstream decrease of maximum flow heights, shear stress, velocity, and flow resistance. We hypothesize with supporting evidence that the debris-flow front scours and destabilizes the channel, but it cannot transport the material because of its high sediment concentration. Therefore, the trailing hyperconcentrated surge picks up the remaining material, grows in volume, and coalesces with the decelerating debris-flow. Both the front and following surges play an integral role for net erosion during a debris-flow event.

Multi-date cross-sections in both the Manival and Réal have clearly shown that debris-flows have significant scouring with large spatial variability. Bedload transport was observed to be at equilibrium with little variability. Field observations of channel deformations show that debris-flow scouring is strongly controlled by upstream slope and storage conditions. A logarithmic relationship is proposed as an empirical fit for the prediction of channel erosion. The most susceptible materials for erosion in the Manival are the unconsolidated gravel wedges developed from bedload transport. This material has a smooth surface within the rugged channel which can be automatically mapped with a 20 cm digital elevation model from either terrestrial or airborne laser scans by calculating roughness with a one meter window. This provides an automatic assessment of erodible areas in a channel at the time of the laser scan survey.

This study has contributed to the need of quantitative field observations in the realm of debris-flow research. Complete and thorough databases were obtained by integrating multi-date cross-section surveys, multi-date laser scans, and high-frequency monitoring stations. Quantified evidence revealing sediment transfers, channel interactions/controls, debris-flow dynamics, and storage characterizations in two different catchments provides a strong basis in the development of conceptual and statistical models. These observations also highlighted the significant field parameters that have an influence on debris-flows and steep catchment systems.

RESUME

Dans les bassins versants abrupts de montagne, de larges quantités de sédiments provenant des pentes escarpées viennent se déposer dans la partie supérieure des torrents et sont remobilisées par les laves torrentielles ou par charriage. Le but de ces travaux était d'étudier le transport des sédiments grossiers dans les petits bassins versants torrentiels et d'analyser l'influence du stockage de ces sédiments dans le chenal sur les laves torrentielles. Cela a requis sur le terrain une intense surveillance géomorphologique des événements d'écoulement dans les bassins versants des torrents du Manival et du Réal, susceptibles de produire des laves torrentielles et du transport solide par charriage chaque année.

Dans le torrent du Manival, le transport de sédiment a été caractérisé par un suivi saisonnier du bilan sédimentaire du bassin versant, réalisé grâce à des mesures topographiques répétées entre les événements importants d'écoulements (sections transversales et relevés au scan laser terrestre). Deux événements de laves torrentielles ont pu être observés, ainsi que plusieurs événements de charriage. La reconstitution du budget sédimentaire de ces deux laves torrentielles a révélé que la majeure partie de leurs volumes a été apportée par l'érosion du chenal (à plus de 92%). Les événements de charriage qui ont eu lieu au cours de l'automne ont contribué à la recharge sédimentaire du chenal principal par le dépôt de grands bancs de gravier. Ce processus est fondamental au déclenchement de laves torrentielles lors des printemps et été suivants. Un décalage dans le temps des séquences érosion /dépôt a été observé entre les parties supérieure et inférieure du chenal, révélant un transfert discontinu de sédiments dans le bassin versant pendant les événements d'écoulement communs. Un modèle conceptuel de transfert des sédiments est proposé pour les différentes magnitudes d'écoulement.

Dans le torrent du Réal, les inspections après événement et les stations de mesure à haute fréquence ont permis de comparer et de compiler les mesures des écoulements. Trois laves torrentielles et trois périodes de charriage avec de petites laves torrentielles en amont ont été observées. Le volume de sédiment transporté lors des laves torrentielles du Réal est similaire à celui du Manival avec une augmentation importante du volume dans le chenal. La plus importante lave torrentielle observée a été examinée en détail et a révélé une diminution en aval des hauteurs d'écoulement maximales, des contraintes de cisaillement, de la vitesse et de la résistance à l'écoulement. Nos résultats suggèrent que le front de la lave torrentielle érode et déstabilise le chenal, mais qu'il ne peut pas transporter les matériaux en raison de sa concentration élevée en sédiments. Par conséquent, la vague hyperconcentrée qui suit se charge des matériaux restants, croît en volume, et fusionne avec la lave torrentielle en décélération. A la fois le front et les vagues suivantes jouent un rôle essentiel pour l'érosion lors d'un événement de lave torrentielle.

Les multiples relevés dans les sections transversales du Manival et du Réal ont clairement montré que les laves torrentielles ont créé une érosion significative à la variabilité spatiale importante. En revanche, les déformations du lit induites par le charriage sont en équilibre. Les observations sur le terrain de la déformation du chenal montrent que l'érosion par les laves torrentielles est contrôlée étroitement par la pente en amont et les conditions de stockage des sédiments. Cette érosion du chenal peut être prédite par une relation logarithmique. Les matériaux les plus sensibles à l'érosion dans le Manival sont les bancs de gravier non consolidés formés par le charriage. Ce matériau constitue une surface lisse au sein du chenal rugueux et peut être automatiquement cartographié avec 20 cm de précision à partir de données de laser scan terrestre ou aérien. La rugosité peut être calculée avec une fenêtre d'un mètre. Ceci fournit une évaluation automatique des zones sensibles à l'érosion dans un chenal au moment du relevé au scan laser.

Cette étude a permis d'alimenter le domaine des laves torrentielles en observations quantitatives sur le terrain. Des bases de données complètes et détaillées ont été obtenues par l'intégration de multiples relevés des différentes sections transversales, des nombreux balayages laser, et des données des stations de mesure à haute fréquence. Les mesures de transfert de sédiments, des interactions/contrôles dans le chenal, de la dynamique des laves torrentielles, et la caractérisation des stockages dans deux bassins différents fournissent une base solide pour le développement de modèles conceptuels et statistiques. Ces observations ont également mis en évidence les paramètres importants à mesurer sur le terrain qui ont une influence sur les laves torrentielles.

Chapter 1: INTRODUCTION

1 GENERAL UNDERSTANDING OF DEBRIS-FLOWS

1.1 Debris-flow features

A debris-flow is generally defined as “*a very rapid to extremely rapid flow of saturated non-plastic debris in a steep channel*” (Hungri et al., 2001). Poorly sorted sediments mixed with water and organic debris typically form destructive surges with sediment concentrations higher than 50% by volume or 70% by mass (Costa, 1984; Phillips and Davies, 1991). The flow undergoes longitudinal grain size sorting which develops a steep bouldery front (or head) and is followed by a slurry in the tail (Pierson, 1986; Iverson, 1997) (Figure 1). Multiple pulses can occur with the first pulse typically consisting of boulders as a large isolated surge and the secondary pulses are often characterized as muddy waves (Zanuttigh and Lamberti, 2007). The most striking feature of debris-flows is their ability to transport a considerable volume of sediment (10^3 and 10^5 m³ in alpine environments) over long distances (several km) and at relatively high velocities (generally between 2 to 20 m s⁻¹) (Iverson, 1997; Rickenmann, 1999). The volume of a debris-flow is known to dramatically grow during propagation by entrainment of in-channel sediment (Iverson, 1997; Hungri et al., 2005). This process is referred as bulking.

Debris-flows typically occur in steep, small to average size mountain streams (referred as torrents in Latin Europe) and induce each year disturbances and/or damages to infrastructures. These steep channel processes are one of the most common and widespread hazards in many mountain environments worldwide (Jakob et al., 2005; Shroder et al., 2012). Landslides and debris-flows cause 25-50 deaths and a two billion dollar loss each year in the United States (National Research Council, 2004). They occur in 950 cities in China with an annual economic loss of 228-304 million dollars (Ding et al., 2012). In the Himalayas, 350 lives are lost each year (Dahal and Hasegawa, 2008). In the European Alps, channelized debris-flows and floods cause 5-10 deaths each year (Arnaud-Fassetta et al., 2009). Many debris-flows are not reported because they occur in remote and unoccupied areas. The growth of urbanization and the increasing frequency of extreme climatic events in mountainous regions make the impact of debris-flow hazards increase (Pierce et al., 2004; Stoffel and Beniston, 2006; Bollschweiler and Stoffel, 2010).

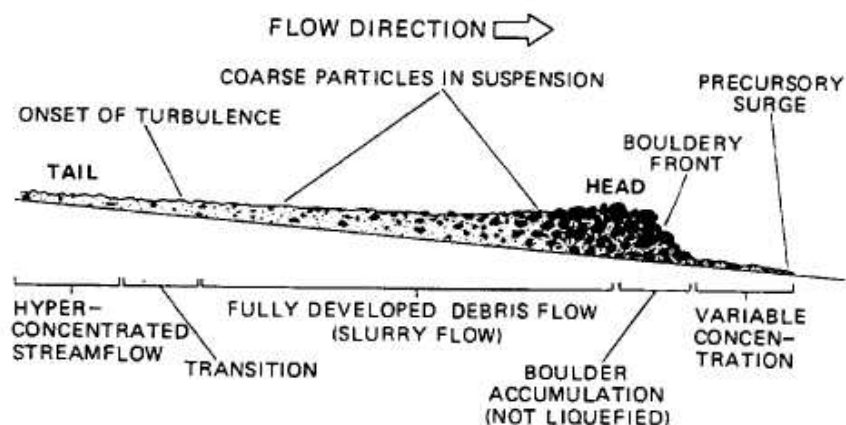


Figure 1 Schematic representation of a debris-flow surge with a bouldery front (from Pierson, 1986)

Debris-flows are important geomorphic agents in upland environments (Dietrich and Dunne, 1978; Swanson et al., 1988; Stock and Dietrich, 2006). Bedrock incision by debris-flows in steep valleys was recently recognized as a key process for the understanding of landscape evolution models in unglaciated mountains (Stock and Dietrich, 2003). Debris-flows are also known to produce extremely high punctuated sediment supply to river networks with considerable effects on low-order channel morphology and texture (Miller and Benda, 2000). Although their occurrence is relatively rare, their legacy on upland valley floor landscape is long lasting (Benda, 1990). Alluvial terraces formed by the propagation of sediment waves coming from debris-flows are common landforms in upland environments. It is also recognized that sediment and woody debris supplied to larger channels by debris-flows play an important role for the diversity of mountain streams aquatic habitats (Benda et al., 2005). Large woody debris and boulders provide essential structural elements for habitats in fish-bearing streams (Bigelow et al., 2007). Debris-flows can be destructive in the short-term, burying habitat and biota, destroying spawning beds and filling pools (Everest et al., 1987; Nawa and Frissell, 1993); however the long-term effect is positive for habitat heterogeneity (Benda et al., 2003).

Debris-flow magnitude and frequency are strongly controlled by climate changes. Local dendrogeomorphological reconstitutions in the Swiss Alps clearly showed an increasing frequency of debris-flow events during wet periods of the Little Ice Age (Stoffel and Beniston, 2006). Contrasting expectations have been made concerning the effect of global warming on debris-flow activity. The expected shifting of rainfall events from summer to spring and autumn may decrease the occurrence of debris-flow events (Stoffel and Beniston, 2006). Projected climate changes may also modify the frequency of extreme debris-flows under the effect of storm intensity increase and permafrost degradation (Stoffel, 2010). Nevertheless, recent investigations of debris-flow activity in the French Alps since the 1980s (Dévoluy and Massif des Ecrins) revealed a decreasing frequency at low-elevations (< 2200 m) (Jomelli et al., 2004; Jomelli et al., 2007). This trend is related to the recorded increase of temperature and decrease of the number of freezing days, which can explain a decrease of

the sediment recharge rate between debris-flow events (Jomelli et al., 2004). In the Massif des Ecrins, it was also demonstrated that the response of hillslope debris-flows to the increase of extreme summer rainfall events is characterized by an important variability conditioned by the lithology and nature of the sediment storage in the triggering slopes (Jomelli et al., 2007).

1.1.1 Classification of debris-flows

Successive landslide classifications from Hutchinson (1968), Johnson (1970), and Varnes (1978) have proposed a variety of terms for debris-flows and other mass movements used in practice. In general, they describe a debris-flow as an intermediate process between landslides and water runoff. For this study, we refer to a simple classification of flow types and landslide processes according to sediment concentration and typical velocity ranges (Jakob and Jordan, 2001) (Figure 2). Bedload transport occurs during flow events (eg. Figure 3A) with low sediment concentrations (<20% by volume). A debris flood is defined as “*a very rapid, surging flow of water, heavily charged with debris, in a steep channel*” (Hungri et al., 2001). Sediment concentrations range from 20 to 50% and they have similar peak discharges to water runoff (Wilford et al., 2004; Hungri, 2005). However, debris flood is not a well accepted term and it is difficult to distinguish debris flood from small debris-flow with low peak discharges. Therefore, we do not make use of the term in this report. Hyperconcentrated flow is generally similar to a debris-flow but with a lower sediment concentration of 20-60% (Lavigne and Suwa, 2004). Both hyperconcentrated flows and debris-flows can occur during a same event according to changes of water content or sediment concentration during propagation (explained later in this chapter).

Debris-flows (eg. Figure 3B) can be classified according to the triggering mechanisms. Most frequently, debris-flows are initiated from landslides or runoff (Blijenberg, 2007).

1) Landslide initiated debris-flows: long duration rainfall saturates hillslopes which typically trigger shallow landslides, and with enough water content, the landslide can transform into a debris-flow by dilatancy or liquefaction during movement (Johnson and Rahn, 1970; Fleming et al., 1989; Iverson et al., 1997). The landslides can also be triggered by seismic activity, and with saturated slopes, the vibrations can liquefy large slopes which transforms into catastrophic debris-flow events (Ni et al., 2012).

2) Runoff initiated debris-flows: high intensity rainfall forms water surges that scour channel beds and gradually become a mature (well-developed) debris-flow (Takahashi, 1981). This situation is common in many parts of the world including Japan (Imaizumi et al., 2005), European Alps (Gregoretto and Fontana, 2008), United States (Coe et al., 2008) and more. In the Front Range of Colorado during a monsoon,

runoff initiated debris-flows have been found to be more common and hazardous than landslide initiated debris-flows (Godt and Coe, 2007). Other triggers that form water surges include dam bursts and glacial lake outburst floods which are less frequent but more catastrophic (Caine, 1980; O'Connor and Costa, 1993; Rickenmann et al., 2003; Coe et al., 2008; Guzzetti et al., 2008).

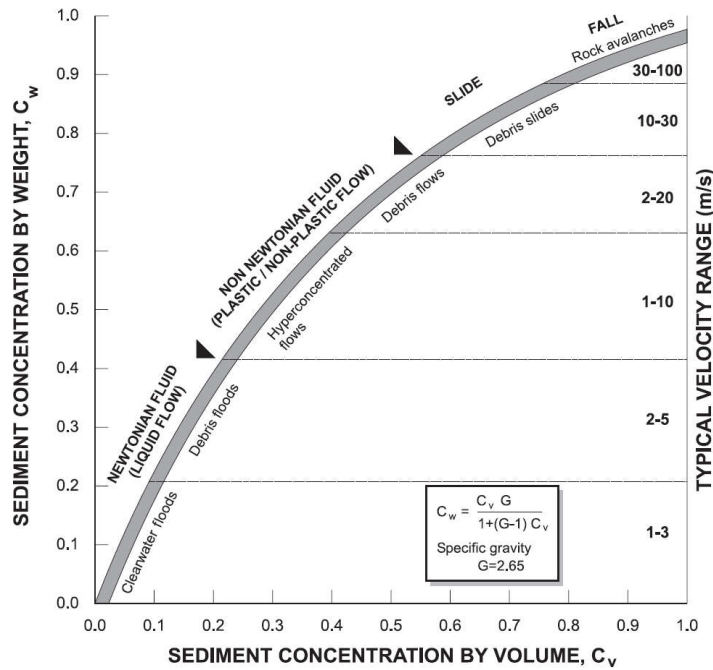


Figure 2 Classification of flow and landslide processes by sediment concentration (volume and weight), velocity, and behavior. Figure from Jakob and Jordan (2001), modified with compiled data from Hungr (2000) and Pierson and Costa (1987).



Figure 3 Example of (A) a flood in the Manival torrent (photo by Joshua Theule) and (B) a debris-flow in the Illgraben torrent, Switzerland (photo from Hürlimann et al., 2003)

Debris-flows can also be classified according to the runout environment. Confined- (or channelized-) debris-flows travel along pre-existing channels. Unconfined- (or hillslope-) debris-flows are not restricted by pre-existing channels over the majority of their length (Conway et al., 2010). In a rheological point of view, debris-flows can generally be classified as either (1) granular (non-cohesive) at which the fine particle fraction is low enough for direct grain contact which influences the mass behavior or (2) cohesive (muddy) at which the fine fraction (containing clay) is large enough for a fine particle-water mixture to form an interstitial fluid which lubricates grain motion and imposes its behavior type on the whole material (Coussot and Meunier, 1996).

1.1.2 Conditions for occurrence

Debris-flows occur with the critical combination of sediment supply, water input and gravitational energy (Takahashi, 1981). Typically the water input is the trigger induced by rainfall and sometimes enhanced by snowmelt (Rickenmann and Zimmermann, 1993). Rainfall intensity-duration relationships are often proposed for determining triggering thresholds (Caine, 1980; Badoux et al., 2008; Coe et al., 2008; Gregoretti and Fontana, 2008; Guzzetti et al., 2008).

Even with a critical water supply, debris-flows will not occur unless sediment is available (eg. Coe et al., 2008). Storage that typically supplies sediment to debris-flows in the Alps includes colluvial deposits (e.g. talus slopes, tills, landslide deposits) and alluvial fills (Theler et al., 2010). The frequency of debris-flows therefore strongly depends on the geomorphic activity of hillslopes (Jakob et al., 2005). Bovis and Jakob (1999) proposed to distinguish transport- and supply-limited debris-flow catchments according to the conditions of sediment recharge (Figure 4). In transport-limited catchments, there is always enough sediment available for a debris-flow to occur and the limiting factor for debris-flow occurrence is the rainfall. In supply-limited catchments, a lower sediment recharge rate prevails and it takes a long time for the channel to replenish after a debris-flow event. In this situation, the limiting factor for debris-flow occurrence is the sediment availability.

Critical slopes for debris-flow initiation and deposition have been characterized in different environmental settings. The analysis of summer 1987 debris-flow events in Switzerland provided ranges of triggering slopes for different geomorphological contexts: 51-78% for talus slopes, 45-70% for rock gullies, and 23-65% for channels (Rickenmann and Zimmermann, 1993). The lower slope threshold in channels is explained by the higher water discharge supplied by higher drainage areas. Inverse power laws of channel slope vs. drainage areas rarely extend to slopes greater than 0.03 to 0.1, which is interpreted as the morphological signature of debris-flows (Stock and Dietrich, 2003), and gives an indication of the critical slope for debris-flow deposition. It is also recognized that the deposition slope depends on the debris-flow volume and rheology (Rickenmann, 1995).

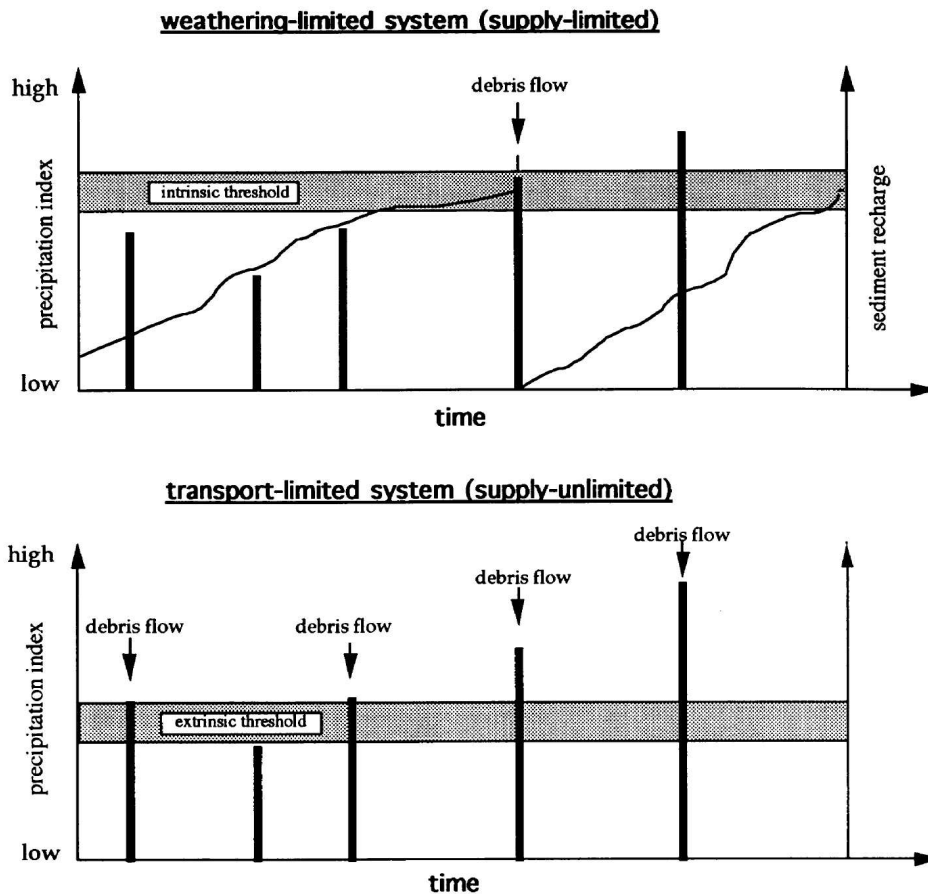


Figure 4 Conceptual model from Bovis and Jakob (1999) showing the debris-flow occurrence for supply-limited and transport-limited systems which highlights the importance of sediment recharge.

1.2 Scientific study of debris-flows

1.2.1 Field Observations

Field studies contributed to important advances in the understanding of debris-flow dynamics. Different types of observations can be made in the field to obtain information about debris-flow geomorphology, sedimentology, flow properties, and past activity.

At the reach scale, post-event topographic surveying can be used to obtain debris-flow heights, widths, and superelevations in bends. These data are used to back-calculate velocity and discharge (eg. Johnson and Rodine, 1984; Berti et al., 1999; Hürlimann et al., 2003). Multi-date surveying within a reach is commonly used to capture erosion and deposition and to determine yield rates and sediment budgets. These measurements are usually made with levels, range finders, total stations, and most recently differential GPS (dGPS) and terrestrial laser scanning (TLS). The advantage for using TLS is that it provides a fast way to obtain very accurate (± 2 to 4 mm) and high resolution (0.4 to 20 cm) digital elevation models (DEM) for a large spatial coverage (Schürch et al., 2011a; Staley et al., 2011)

(Table 1). TLS-derived DEMs can also be used to characterize channel roughness and surface grain-size. This was already tested with success in gravel-bed rivers (Heritage and Milan, 2009), but not for debris-flow channels (to the best of our knowledge). For long channel reaches, TLS surveying becomes more difficult because of the time requirement for scanning at many positions and data processing. In this case, cross-section surveys with total station and dGPS provide a practical way to detect channel changes along several kilometers (eg. Fannin and Wise, 2001; Nyman et al., 2011).

Catchment-scale erosion and deposition can be obtained from photogrammetry and airborne laser scans (ALS). High resolution airphotos are more readily available, however the steep topography and vegetation cover makes morphologic monitoring very difficult (Veyrat-Charvillon and Memier, 2006; Breien et al., 2008; Berger et al., 2011b). ALS data is becoming more common in terrain analysis with its capability of measuring high resolution DEMs by filtering ground point echos. Multi-date ALS scans are expensive however it is the most complete and efficient method for capturing surface deformations of a debris-flow affected area and for quantifying accurate volume changes (Bull et al., 2010). Resolution and accuracy can vary for both photogrammetry and ALS depending on flight elevation and speed. Their volumetric errors will therefore vary from 8 to 14% (Table 1). Since debris-flows are unpredictable, ALS or photogrammetric derived DEMs can be used as preliminary surfaces and fast post-event surveys can be made with dGPS (eg. Conway et al., 2010) or TLS (eg. Bremer and Sass, 2012).

Table 1 Examples of DTM accuracies and resolutions derived from ALS, TLS, photogrammetry (Photo.) and GPS in debris-flow catchments. Measured volume changes, errors and level of detection (LoD) are shown for debris-flow events in the catchments.

Source of study	Method		Height Accuracy (cm)	DTM Resolution (m)	Net Volume Changes (m ³)	Volumetric Error (%)	LoD (cm)
	t ₀	t+1					
Berger et al., 2011b	Photo.	Photo.	28	2	1 000 - 14 000	--	40
Breien et al., 2008	Photo.	Photo.	28	3.33	240 000	10	--
Veyrat-Charvillon and Memier, 2006	Photo.	Photo.	116	--	5 000 - 23 000	12	--
Bremer and Sass, 2012	ALS	ALS	15 - 35	1	6 000 - 12 000	8.2	--
Bull et al., 2010	ALS	ALS	40	4	350 000	14	--
Schürch et al., 2011a	TLS	TLS	--	0.2	90 - 2000	0.2 - 7	10
Staley et al., 2011	TLS	TLS	0.2 - 0.4	0.004	50 - 250	1 - 4	0.4 - 0.5
Scheidl et al., 2008	ALS	ALS	30 - 144	1	30 000 - 90 000	28 - 50	--
Conway et al., 2010	ALS	GPS	20 - 42	0.25	100 - 41 000	38 - 134	--

Debris-flows rheological properties can be characterized with grain-size distribution and shape of debris-flow levees and lobes (Ancey, 1999). Shapes of cross-sections on lobe deposits for granular flows (frictional) have a smoother surface and are more cohesive (when dry) than muddy flows (viscoplastic) (Bardou et al., 2003). A very practical means for estimating the yield strength of the debris-flow material is measuring the thickness and slope of overbank lobes (Johnson, 1984; Tecca and Genevois, 2009). In the canton of Wallis, Switzerland, debris-flow deposits were measured for classification in 35 catchments (Bardou et al., 2003). There was a distinct difference of grain-size distributions. Granular flows were found to be well sorted with a D_{50} of gravel and muddy flows were poorly sorted with a D_{50} of medium to coarse sand.

Important field observations were also obtained from high-frequency monitoring stations of debris-flow channels. Typically, ultra-sonic sensors and/or radar and geophones are used to measure the flow heights and velocities at frequencies generally higher than 1 Hz (eg. Marchi et al., 2002; Arattano et al., 2012a). Monitoring cameras (video and photo) are used to validate instrumental readings and to characterize flow behavior and particle velocities on the flow surface (eg. Imaizumi et al., 2005). Pore-water pressure or moisture sensors installed in the banks and channel bed monitor the antecedent conditions and response to passing flows (e.g., McArdell et al., 2007; McCoy et al., 2010; Iverson et al., 2011). Recently, researchers have been able to directly measure the shear stress of debris-flows with force plate and erosion rates with scour sensors during a flow event (Berger et al., 2011a). Many monitoring catchments have one or two stations which limits the spatial coverage of the debris-flow monitoring. By increasing the number of instruments along the channel, the dynamics of surge propagation can be observed (Hürlimann et al., 2003; Navratil et al., in press).

Numerous field studies were also dedicated to the reconstruction of past debris-flow activity by using dating techniques applied to debris-flow deposits. Dendrogeomorphology is the reconstruction of past geomorphic activity inferred from tree ring information (Stoffel et al., 2006; Bollschweiler et al., 2007). On debris-flow fans, scarred tree rings or growth rate decline give dates of debris-flow events (Jakob and Friele, 2010; Stoffel et al., 2006; Pelfini and Santilli, 2008). For lichenometry, a local growth curve of lichen near a given study site is used to give an age of the largest lichens found on debris-flow deposits which gives an approximate age of a debris-flow event (Helsen et al., 2002). These dating methods can be used to study climatic forcings on debris-flow activity and to construct magnitude-frequency relationships for a given catchment (eg. Stoffel et al., 2006; Jakob and Friele, 2010; Lopez Saez et al., 2011).

1.2.2 Experimental laboratory studies

It is notoriously difficult to study in the field the effect of single controls (e.g. channel slope, pore-water pressure, grain-size distribution) on debris-flow processes. Laboratory experiments can provide

interesting observations on such processes. Tilting flumes (inclined planes) experiments showed that the sediment size of the erodible bed and the sediment concentration of the flow influence erosion rates (Papa et al., 2004). The travel distance of the granular flow can be controlled by the erodible bed thickness and the slope of the inclined plane (Mangeny et al., 2010). The travel distance can also be controlled by the initial volume input and sediment concentration (D'Agostino et al., 2010). Large-scale debris-flow experiments are performed by the U.S. Geological Survey with a 95m long and 2m wide debris-flow flume (Iverson et al., 1992). The role of pore-fluid pressures and total bed-normal stresses provides insights on how debris-flows are deposited (Major and Iverson, 1999). On erodible beds, the influence of the pore pressure of the erodible bed on flow momentum and velocity was recently studied (Iverson et al., 2011). Data obtained during these experiments revealed that the flow momentum increases as a power function of the erodible bed's water content. This highlights the importance of antecedent conditions on debris-flow interactions with channel.

1.2.3 Debris-flow modeling

Important efforts have been made during the last decades in the field of debris-flow modeling at different spatial scales. In the Italian Alps, 40 debris-flow catchments were used to derive statistical relationships between debris-flow magnitude, the planimetric deposition area, and the cross-sectional inundated area at the alluvial fan apex (Berti and Simoni, 2007). These relationships were combined with a digital elevation model using an automated code (DFLOWZ) for predicting inundated areas from debris-flows. A similar approach was recently proposed for the prediction of the potential runout area covered by debris-flow deposits (Scheidl and Rickenmann, 2010). An energy line approach was used to predict debris-flow velocity and dynamic pressures in Sarno, Italy, where in May 1998, ten debris-flows occurred (Toyos et al., 2008). Regression models were found with empirical and field-measured peak velocity and peak discharge related to the vertical distance from the energy line and the surface. The probability of occurrence for debris-flows and shallow landslides can be simulated by using the spatial distribution of hydrology, geomorphology, and geomechanics (Simoni et al., 2008).

Regional-scale modeling of debris-flows generally makes use of DEMs and remote sensing imagery for determining susceptible areas for debris-flow initiation and runout. This provides a preliminary investigation of debris-flow hazard analysis. In the Oregon Coast Range, USA, 10m DEMs and 25m satellite images are readily available from which we can produce flow paths, topographic attributes (eg. slope, aspect, roughness, and flow area accumulation) and landcover data. This information allows application of empirical probabilities for debris-flow runout paths calibrated by field mapped debris-flow tracks (Miller and Burnett, 2008).

2 SEDIMENT TRANSFER BY DEBRIS-FLOWS

2.1 Catchment-scale sediment cascade

2.1.1 *Sediment supply from hillslopes*

In steep catchments, sediment is transferred in pulses from hillslopes down to channels where debris-flow and bedload transport occur. The sediment sources in the Alps typically originate from rockfall, landslides, and hillslope debris-flows (eg. Schlunegger et al., 2009). Other mountain ranges such as the Oregon Coast Range have sediment budgets dominated by mass wasting (Benda and Dunne, 1997). Gully erosion is an important sediment source in the Te Weraroa Stream catchment, New Zealand, which supplies considerable volumes of material into the river (Gomez et al., 2003). The sediment production from the gullies was dramatically reduced by reforestation on the hillslopes, but most of the sediment generated by gully erosion was stored in the torrent channel and still contribute to the sediment transport during flow events.

Lithology and bedding configuration are prominent controls for developing erosional landforms which influence the sediment dynamics of a catchment. In two debris-flow catchments in the French and Swiss Alps (Manival and Saxé-Métin, respectively), relationships were developed between structural properties of the bedrock and active geomorphic features (Loye et al., 2011). It was notably established that the anisotropy of the rock strength controls the spatial pattern of the gully network, and then of the sediment sources.

Active hillslope processes need to be connected to the channel for providing sediment to the stream network. The degree of hillslope-channel coupling is a primary control of the geomorphic sensitivity of upland catchments. In the Illgraben torrent catchment, Switzerland, sediment yields from subcatchments with active hillslope-channel coupling are one to two orders of magnitude larger than those obtained from subcatchments with disconnected hillslopes (Schlunegger et al., 2009). A 30-yr monitoring program of geomorphic activity in a Scottish upland catchment revealed that downstream of the most effective hillslope-channel coupling areas, an increase of channel instability is observed (Harvey, 2001).

Catchment-scale sediment dynamics of torrents may also be dramatically influenced for long periods of time by catastrophic events. An illustrative example was provided by the Wenjia Gully in Sichuan (China) after the Wenchuan earthquake in 2008 described by Ni et al. (2012). Before the earthquake, the catchment was stable with a dense forest cover, but then the earthquake triggered a major landslide in the upper catchment depositing in the gully beds (Figure 5). Within two years after the landslide, rainfall triggered five debris-flows with magnitudes over $1.5 \times 10^5 \text{ m}^3$. The Illgraben in Switzerland is another good example of the importance of the recent history for understanding the present

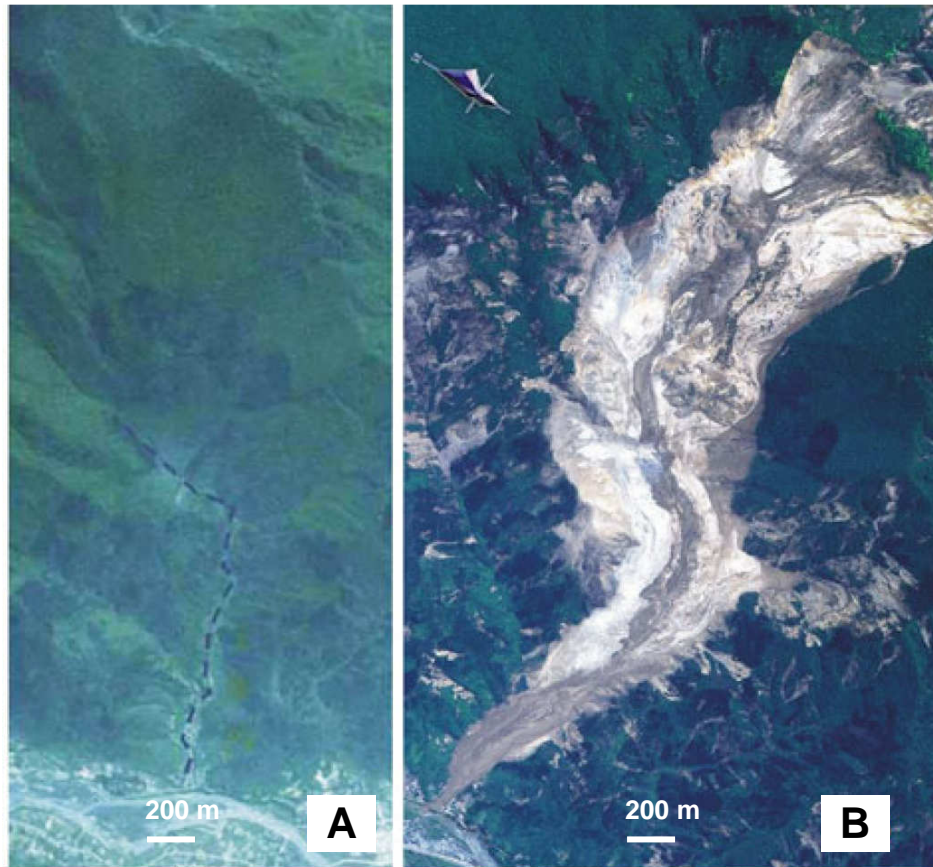


Figure 5 The Wenjia gully (A) before Wenchuan 2008 earthquake showing a stable highly vegetated catchment, and (B) after the earthquake that triggered a major landslide that transforms downstream into debris-flows (from Ni et al., 2012).

geomorphic activity of upland catchments. A catastrophic rock avalanche occurred in 1961 and supplied $5 \times 10^6 \text{ m}^3$ of sediment to the upstream channel. The present debris-flow activity of the torrent is still influenced by the sediment influx provided by the rock avalanche (Schlunegger et al 2009).

2.1.2 Sediment yields

Upland catchments are characterized by an extreme variability of sediment yields, for any considered time interval. A compilation of data from literature revealed that for drainage areas of the same size, the maximum recorded debris-flow volumes in the Alps fluctuate over 2 to 3 orders of magnitude (Liébault et al., in press). Important efforts have been deployed during the last decades to empirically predict debris-flow volumes flowing out of catchments.

During summer of 1987 in Switzerland, an intense rainstorm triggered 600 debris-flow events with volumes ranging from 1 000 - 200 000 m^3 (Rickenmann and Zimmermann, 1993). The larger events

occurred in periglacial zones where large amounts of loose and unconsolidated material were located. Based on analysis of these events, three predictive empirical formulas for debris-flow volumes were developed including several predictors: (1) active channel length and fan slope, (2) erosion constant, catchment area, and mean channel slope, (3) runoff coefficient, 24h rainfall, and catchment area. These equations had a similar performance with a decreasing scatter as the volumes increase, yet the predictions are still considered a general estimate.

In Colorado, Utah, and California, 53 burnt debris-flow prone catchments were characterized with 25 indicators (catchment morphometry, soil properties, rock types, rainfall properties, and burnt severity) that were used to predict volumes of eroded material (debris-flow volumes) (Gartner et al., 2008). Multiple regression analysis was used to propose a predictive model for debris-flow volume which included the best performing indicators: (1) catchment area with slopes greater than 30%, (2) catchment area with moderate to high burnt severity, and (3) total storm rainfall. The developed model explained 83% of the variability in the volumes of debris-flows. Other databases were inputted to validate the model, 87% of the predicted values were within two residual standards of error.

Historical data of debris-flows from 130 basins in the eastern Italian Alps were collected to compare volumes with morphometric and geological characteristics (D'Agostino and Marchi, 2001). The three independent variables used in the predictive model are catchment area, mean channel slope and geological index (GI). The GI corresponds to the erodibility of the lithology in the catchment feeding the channel. Fractures and alterations can also influence the index value. A relationship was found between volume and catchment area which its envelope becomes larger as the area increases. The model had an accuracy of 87 500 m³ which could be explained by heterogeneity of geologic and hydroclimatic conditions. This type of predictive model gives a general estimate of magnitude; however field investigations, detailed geomorphic conditions, and event frequencies are needed for a more practical assessment.

Sediment flowing out of upland catchments may be transported as bedload or debris-flows. The respective contribution of each process in the sediment yield of small mountain streams is of primary importance for the prediction of catchment responses to rainfall events. Sediment transport by bedload and debris-flow processes were assessed throughout Switzerland during the catastrophic August 2005 floods (Rickenmann and Koschni, 2010). Bedload transport volumes were found to be related to runoff volumes and channel slope, but debris-flow volumes were much more variable and could not be predicted by these two variables. The study found that empirical predictions using catchments metrics were more powerful for debris-flows. Another recent study proposed an interesting comparison of bedload transport and debris-flow volumes based on long-term data from two monitoring catchments in the Eastern Italian Alps (Mao et al., 2009). This revealed that for equivalent return periods, debris-flow volumes were 2 to 3 orders of magnitude larger than bedload transport volumes.

2.2 Interactions with the channel

2.2.1 Channel scouring

Channel scouring is known to have an important influence on debris-flows' magnitude and behaviour. Not only does erosion increase the debris-flow's volume, it can also increase the debris-flow's momentum and speed which increases the travel distance (Iverson et al., 2011; Mangeney et al., 2010). At the Chemolgan test site in Kazakhstan, field experiments released water surges from a lake into a channel composed of an ancient moraine and bedrock (Rickenmann et al., 2003). As the channel scoured, the water surge grew into a debris-flow with 100% sediment volume originating from the channel bed (total eroded volumes for each experiment ranged from 26 000 to 127 000 m³). Another example of volume growth is provided by a rainfall-induced debris-flow in the Faucon torrent (Southern French Alps) that started as a hillslope debris-flow in the source area (5000 m³) which grew 10 times in volume from channel scouring and attains a total volume of 50 000 m³ in the fan (Figure 6A) (Remaître et al., 2005). This volume growth from channel erosion is consistently found among other field investigations which include debris-flows in Hong Kong (Hungri et al., 2005), Victoria, Australia (Nyman et al., 2011), and the Queen Charlotte Islands, British Columbia (Fannin and Wise, 2001) (Figure 6B-D). In the case of the Illgraben, Switzerland, landslides stopped on hillslopes or in channels with volumes of 500-4400 m³ (Berger et al., 2011b). Debris-flows occurred afterwards with volumes of one magnitude larger.

The eroded volume per length of channel segment (m³ m⁻¹) is referred as "yield rate" (Hungri et al., 1984). In the Queen Charlotte Island (British Columbia), 174 debris-flow and debris-avalanche events had a large range of yield rates (0 to 40 m³ m⁻¹) with scour depths reaching 3 m and sometimes up to 5 m (Hungri et al., 2005). In the Eastern Italian Alps, 127 basins were studied showing the highest frequency of yield rates being approximately 10 m³ m⁻¹ with an extreme value of 125 m³ m⁻¹ (Marchi and D'Agostino, 2004). Channel scouring by debris-flows can be viewed as a supply-limited process since it is generally constrained by the depth of the erodible bed. This is not the case for scouring induced by bedload transport, which is controlled by the shear stress (Haschenburger, 1999).

Little is known about the timing of erosion by debris-flows. A flume experiment with an erodible bed shows that the most significant erosion occurs behind the flow front (Rickenmann 2003). The front destabilizes the channel banks and the tail with higher water content erodes (mobilizes) the material. In the Illgraben torrent, erosion rates were measured in the channel by erosion sensor columns (Berger et al., 2011b). The largest observed debris-flow progressively scoured the bed before the front reached maximum height. After the front passes, erosion continues at a lower rate with a longer duration.

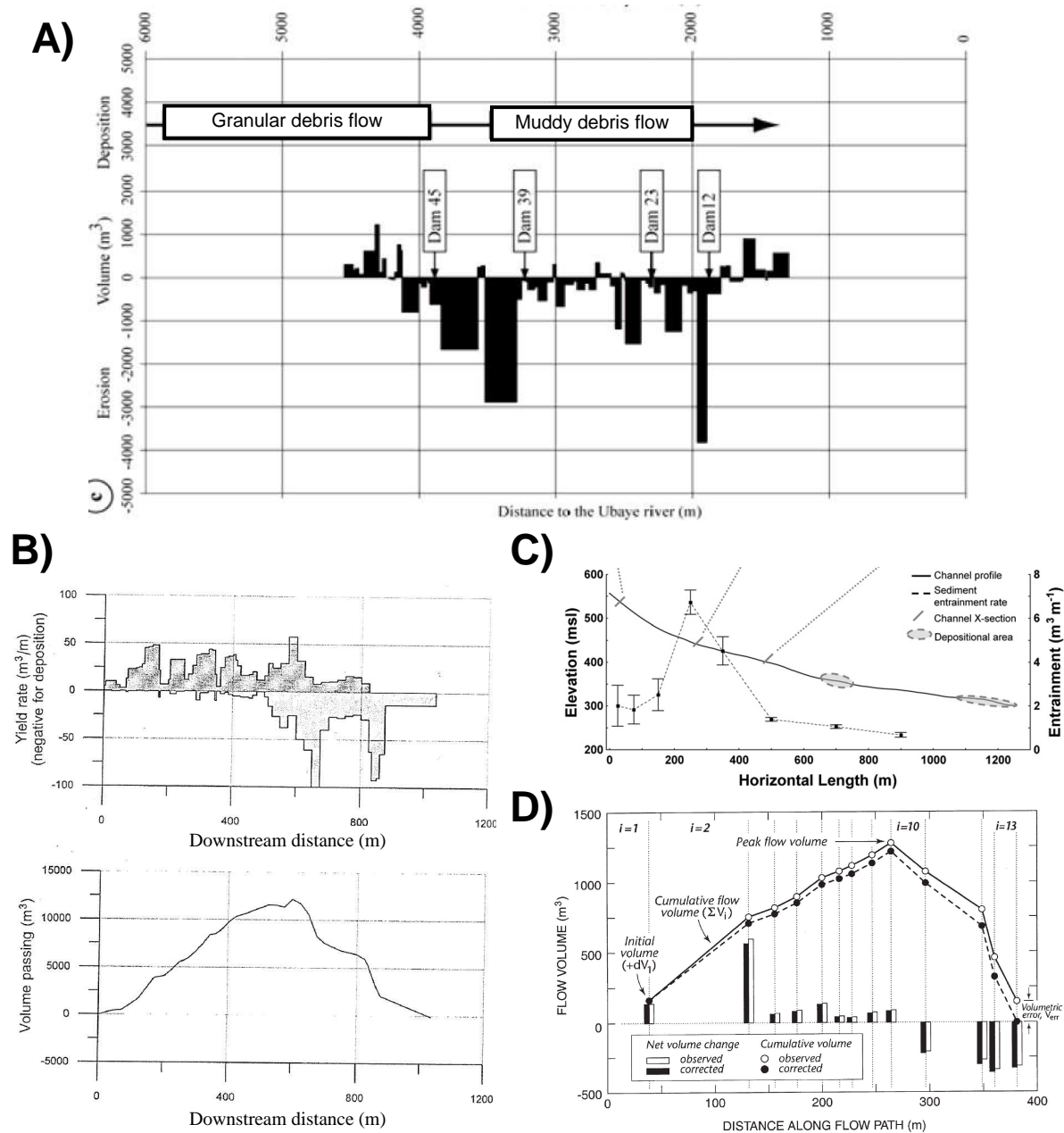


Figure 6 Examples of channel scouring contributions to debris-flow bulking: (A) Erosion and deposition along a channel after the passage of a debris-flow in the Faucon Torrent, French Alps (from Remaître et al., 2005), (B) longitudinal patterns of yield rates and volume passing for a debris-flow in Hong Kong (from Hungr et al., 2005), (C) yield rates (entrainment) for a debris-flow in Victoria, Australia (from Nyman et al., 2011) and (D) cumulative volume of a debris-flow in the Queen Charlotte Island, Canada (Fannin and Wise, 2001).

A smaller debris-flow also scoured at the head of the flow. Consistent measurements were difficult to obtain because of the deposition between events and the reworking of the bed during the events (scour/fill). There is still little known about the variability of erosion rates from debris-flows because of limited field observations.

2.2.2 Controlling factors

Channel scouring is controlled by both the debris-flow properties and the channel bed conditions. Hungr et al. (2005) lists the important channel factors for controlling yield rates as slope angle, channel width and depth, bed material, bank angle, bank height, bank material, bank stability, and tributary drainage area or discharge. Rickenmann and Zimmermann (1993) limited the list to two important factors for erosion, (1) erodible storage depth and (2) channel slope.

Field experiments at the Chemolgan site in Kazakhstan showed that channel scouring increases linearly with the water runoff volume (Rickenmann et al., 2003), although data shows a high scattering. Observed yield rates along the scouring channel were also controlled by the hydraulic load of the flowing mixture, defined as a function of the mixture volume, the mixture density, and the channel slope. Similar conclusions were found from the monitoring debris-flow catchment of the Réal in the French Alps, where a good correlation was obtained between the magnitude of rainfall bursts and the volume of debris-flow surges (eg. Navratil et al., in press).

Sediment concentration of debris-flows is another important control of channel scouring. In field experiments at Chemolgan, erosion rates increased until the sediment concentration of the flowing mixture reached 0.4, then it decreased as the sediment concentration kept increasing up to 0.7 (Rickenmann et al., 2003). These observations were confirmed by laboratory experiments showing decreasing erosion efficiency with sediment concentration by volume (Rickenmann et al., 2007). However small scale experimental tests showed that the effect of sediment concentration on erosion rate was less significant than the effect of grain-size of the erodible bed (Egashira et al., 2001). This was also observed in other experiments, where the increase of bed grain-size monotonically decreases the erosion rate (Papa et al., 2004).

Laboratory experiments also demonstrated that pore-water pressure in an erodible bed increases the erosion rate of a debris-flow (Iverson et al., 2011). The large scale experiment released saturated material from the gate onto partially saturated beds. The manipulated variable in the test was the volumetric water content in the erodible bed on a fixed slope of 31°. It was found that the increase of pore-pressure facilitates progressive scour of the bed and reduces basal friction. The added mass to the flow from scouring increases the flow's momentum, speed, and travel distance. Therefore, antecedent rainfall and storm durations can influence the volume of erosion and the magnitude of a debris-flow. However, saturated beds are not a requirement for debris-flow scouring, the bed material and slope are found to be just as important (Mangeny, 2011).

Channel scour is limited by the slope of the bed. Small scale laboratory experiments on dry erodible beds show that erosion begins at the angle of repose of the bed material which normally corresponds to talus slope angles of the source area (Mangeny et al., 2010). This experiment also showed that erosion increases the momentum of the debris-flow until the channel slope is less than half the repose

angle of the bed material. Field observations of debris-flow scouring for different conditions of channel slope produced variety of results. Compiled data in the Queen Charlotte Islands, British Columbia show a large scatter on yield rate vs. slope diagrams (Hungry et al., 2005). The confined reaches in the database revealed a limiting slope of 10° for channel scouring. A larger compiled database covering Queens Island and Vancouver Island, British Columbia showed that unconfined reaches scour above 10° and confined reaches scour above 5° (Guthrie et al., 2010). Hillslope debris-flows in Iceland revealed at a limit of 19° for channel scouring (Conway et al., 2010). The confinement of a reach can therefore be seen as an increasing factor of scouring.

2.3 Channel storage changes over time

Since debris-flow scouring is controlled by channel storage, debris-flow occurrence is dependent on the formation and mobilization of in-channel sediment reservoirs. The spatial and temporal patterns of channel storage were studied in the field in different contexts along the stream network. A presentation of key findings from low- to high-order channels is proposed here.

First-order channels generally experience seasonal cycles of cut-and-fill which are directly influenced by hillslope processes and debris-flow occurrence. Thirty-nine debris-flows were monitored during a 6 year period in a first-order channel of the Ohya landslide, central Japan (Imaizumi et al., 2006). It was observed that important infilling from freeze-thaw and dry raveling from hillslopes during the winter resulted in the largest deposits in the spring. Debris-flows in this headwater depleted the infill during the summer, providing important sediment recharge to the downstream reaches. The smallest channel storage occurred typically during autumn. Another monitoring program in a first-order channel in the Chalk Cliffs, Colorado, allows for observing several debris-flows in one year (McCoy et al., 2010). Smaller debris-flows tend to have shorter travel distance depositing within the first-order channel while larger debris-flows scoured the channel down to the bedrock. The residence time of storage in these reaches depends on the frequency of large-magnitude rainfall events that trigger the largest debris-flows (normally occurring during summer convective storms).

In the Oregon Coast Range, it is found that storage is built up in first- and second-order channels supplied by mass wasting (Benda, 1990). The sediment size of bed-material supplied by mass wasting is generally too coarse to be entrained by water runoff. Only debris-flows triggered by landslides in hollows are able to remobilize these sediments (Figure 7). Investigations on the frequency of debris-flows in the Oregon Coast Range from the dating of sediment deposition in hollows revealed a recurrence interval of 750 yrs in first-order channels and 1500 yrs for second-order channels (Benda and Dunne, 1987). Contrary to the observations from active alpine environments, debris-flow in the forested mountain range of Oregon appears as a very infrequent phenomenon.

In the Illgraben debris-flow catchment, the transfer of storage has been monitored through the entire catchment seasonally and annually (Berger et al., 2011b). Landslide deposition in first-order reaches have a residence time less than one year. This storage mobilizes to the torrent channel and is again stored for less than one year. The trunk stream where debris-flows propagate was characterized by very active cycles of erosion and deposition over the monitoring period, emphasizing a short residence time of sediment. The Manival torrent (French Alps) also shows frequent cycles of cut-and-fill along the main channel, which is fed by very active rockfall and rockslides in the upper catchment (Veyrat-Charvillon and Memier, 2006). This shows that steep catchments are highly responsive to sediment pulses from the source area with little residence time of storage.

Since 1983, biannual cross-section surveying on the alluvial fan of the Waipaoa catchment, New Zealand revealed seasonal cycles of aggradation and incision (Fuller and Marden, 2010). More recent sequential DEMs revealed that scour and fill involves 47 000 tonnes of sediment within 3 months. Landslides and debris-flows from the gully complexes enhance the storage development in the fan during wet weather periods and large rainstorms. Dry periods limited the activity in the gullies and therefore water runoff incised the storage in the fan. These examples highlight the significance of sediment supply and climate for the development and depletion of channel storage in the steep catchments.

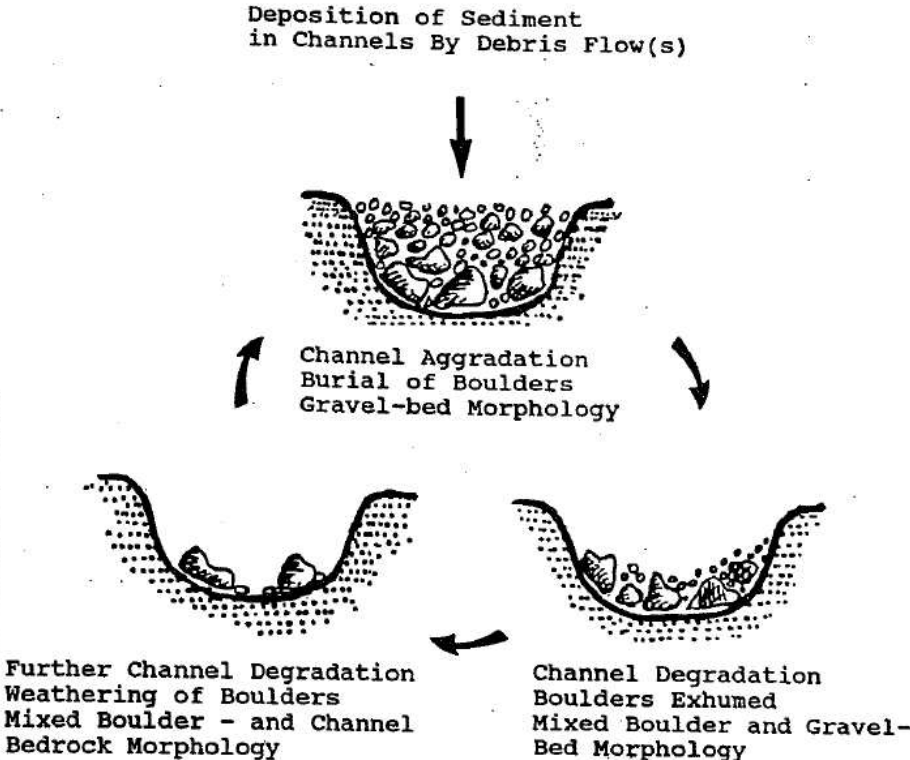


Figure 7 Typical evolution of a debris-flow channel over time (from Benda, 1990)

3 THESIS OBJECTIVES

This study focuses on an intensive field-based geomorphic monitoring to quantitatively analyze flow events in active debris-flow catchments. Two study sites were selected in the French Alps, the Manival and Réal torrent catchments which frequently experience debris-flows and bedload transport.

Objective 1: Sediment transfer in debris-flow catchments at a seasonal time scale

The first objective (Chapter 3) is to characterize and understand how sediment transfers through an active debris-flow catchment at a seasonal time scale. Several studies have acknowledged the necessity for obtaining a short enough timescale for observing sediment transfers in steep catchments. In addition, full spatial coverage of a debris-flow catchment is needed to identify the scour-fill patterns that are known to exist from hillslopes to high-order reaches. This was accomplished by a complete sediment budget of the catchment derived by multi-date topographic measurements between important flow events. This detailed sediment budget monitoring took place in the Manival torrent catchment from 2009 to 2011. The channel scouring by debris-flows was quantified as well as the channel responses during autumn water runoff events. Both debris-flow and bedload transport contributions were quantitatively compared which identifies their significance and function in the catchment.

Objective 2: Debris-flow propagation and channel interactions

Post-event topographic surveys and high-frequency monitoring stations in the Réal Torrent are used to compare accuracies of transport volumes, velocities, and discharge of flow event (Chapter 4). The compiled database provides an opportunity to accomplish two objectives 1) to characterize trends of sediment transport for debris-flow and bedload transport processes and 2) quantify and the changing properties of a debris-flow front (heights, velocities, discharge, volumes, and flow resistance) and analyze how they interact with the channel. Topographic surveys were measured from April 2010 to October 2011 and three monitoring stations began operation in September 2010. Six flow events with revealed how sediment is transferred through the channel according to flow types. One large debris-flow was studied in detail which revealed surge growths in volume, surge coalescence, yield rates and debris-flow front dynamics (decreasing shear stress, flow resistance, velocity and heights).

Objective 3: Spatial variability of channel erosion by debris-flows

The final objective (Chapter 5) was to analyze the spatial variability of channel scouring, analyze the effect of slope on channel scouring, and propose a method for mapping sensitive reaches to erosion.

Channel storage and channel slope have important influences on debris-flow scouring, and in turn, the scouring influences the debris-flow magnitude and travel distance. These relationships have been found in laboratory experiments but have not been extensively quantified and compared in the field. Both the Manival and Réal torrents were compared in this chapter which introduces global relationships in debris-flow catchments. The distribution and significance of debris-flow scouring in the torrent catchments are identified with multi-date cross-sections distributed throughout the two catchments. Standardized measurements of scour (normalized by active width) and channel slope (upstream from cross-section and 6 times the channel width) allow for a realistic multi-catchment analysis. Detailed TLS multi-date scans between debris-flows and floods allow for scour/fill to be correlated with roughness. This chapter presents a scour/slope relationship and a roughness classification for available storage which can easily be developed into hazard models.

This thesis contributes to the need of quantitative field observations in the realm of debris-flow research. Complete and thorough databases were obtained by integrating multi-date cross-section surveys, multi-date laser scans, and high-frequency monitoring stations. Quantified evidence revealing sediment transfers, channel interactions/controls, debris-flow dynamics, and storage characterizations in two different catchments provides a strong basis in development of physical models. These observations also highlight the significant field parameters that have an influence on debris-flows and steep catchment systems.

Chapter 2: STUDY SITES

1 STUDY SITES OVERVIEW

The two study sites, the Manival and Réal, are very active debris-flow catchments located in the French Alps (Figure 8). We have conducted intensive field monitoring of morphologic change in these catchments between important flow events during the spring, summer and autumn. The Manival catchment was the most practical field site because of its close proximity to Grenoble. The Réal catchment was more difficult to manage, however the site was very important to study because it experiences multiple debris-flows each year.

2 THE MANIVAL TORRENT CATCHMENT

The Manival is a very active debris-flow torrent near Grenoble in the Chartreuse Mountains of the Northern French Prealps, located at $45^{\circ} 17' N$, $5^{\circ} 49.75' E$ (Figure 9). It flows intermittently into the Isère River in the Grésivaudan valley. The high frequency of debris-flow events (once every year since 2008), easy access throughout the main channel and presence of a large sediment trap ($25\ 000\ m^3$) in the channel (protecting the urbanized alluvial fan against debris-flows) makes the Manival site suitable for implementing a monitoring program of sediment transfer associated with debris-flows. The 3.6-km^2 catchment above the sediment trap has 1130 m of relief with a mean catchment slope of 81% (Table 1) and the 1.8-km study reach extends from the apex of the alluvial fan to the sediment trap (Figure 9A and F).

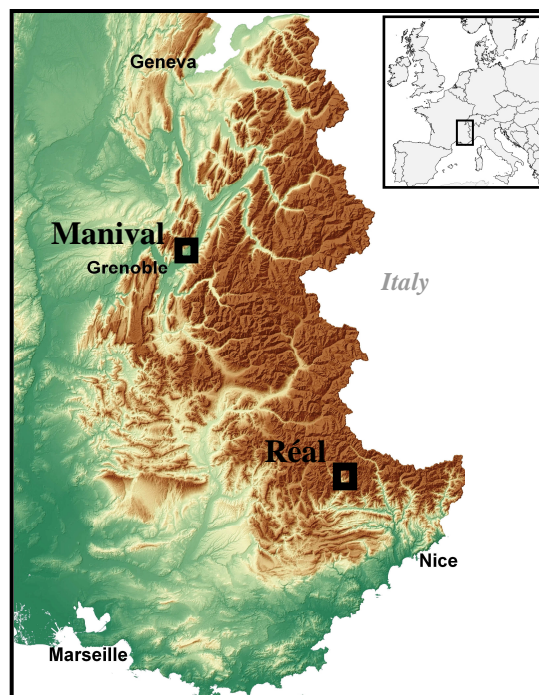


Figure 8 Location of the two study sites in the French Alps, the Manival and Réal torrent catchments.

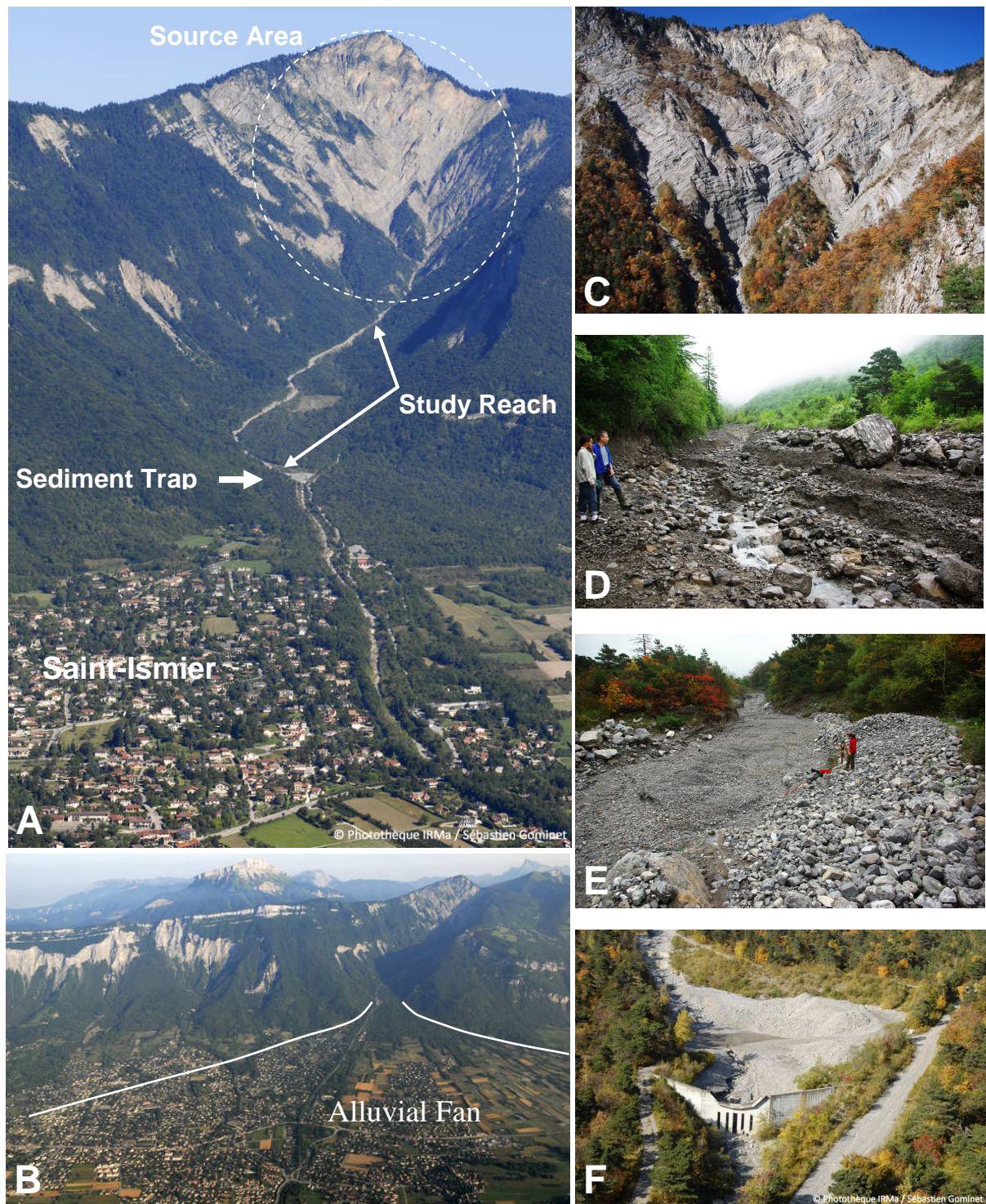


Figure 9 View of (A) the Manival torrent and its source area (B) Manival’s urbanized alluvial fan (C) sediment source area (D) debris-flow scoured reach (E) debris-flow levee and gravel wedge from bedload transport (F) sediment trap (Photos A, B, and F were taken from Sébastien Gominet, Photothèque IRMa)

Table 2 General features of the Manival Torrent

Drainage area (km ²)	3.6
Minimum elevation (m a.s.l.)	570
Maximum elevation (m a.s.l.)	1738
Mean catchment slope (%)	81
Length of the study reach (km)	1.8
Mean slope of the study reach (%)	16
Mean active channel width (m)	15
Monitoring period	07/2009 – 12/2010
Number of topographic surveys	9
Number of check-dams along the study reach (whole catchment)	19 (+180)
Sediment trap capacity (m ³)	25000

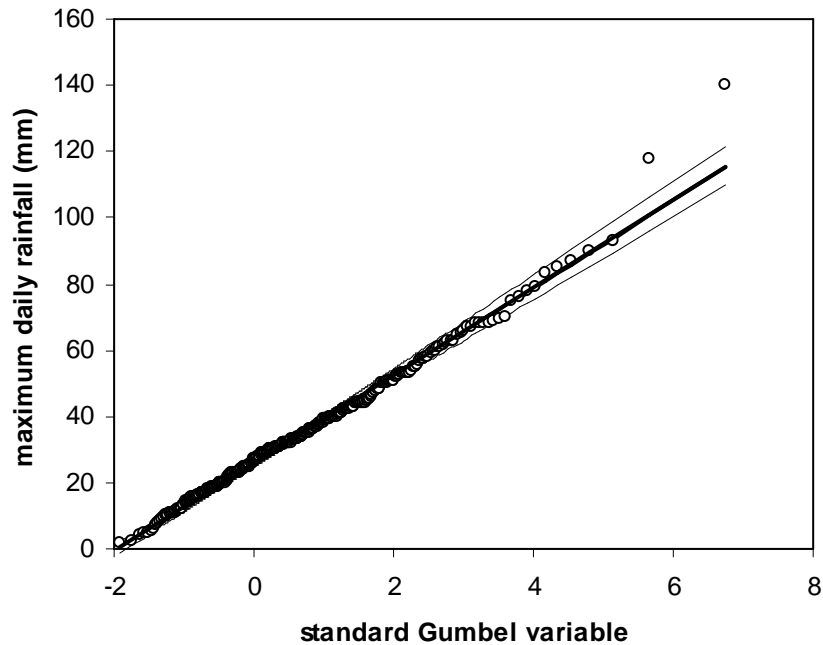


Figure 10 The Gumbel frequency distribution of the maximum daily rainfall observed in the Météo France station of Saint-Hilaire-du-Touvet, from 1964 to 2010, located 5 km from the Manival.

The nearest meteorological station (Saint-Hilaire-du-Touvet, located 5 km from the Manival, on the same mountain side) has a mean annual precipitation of 1450 mm and a 10-yr daily rainfall of 88 mm (Figure 10). Spring and summer (May to September) experiences intense rainfall from convective storms which typically trigger debris-flows. During autumn (September to December), steady long-duration rainfall are common which produce bedload transport. During winter (January to March), snow typically covers the catchment and the channel becomes dormant.

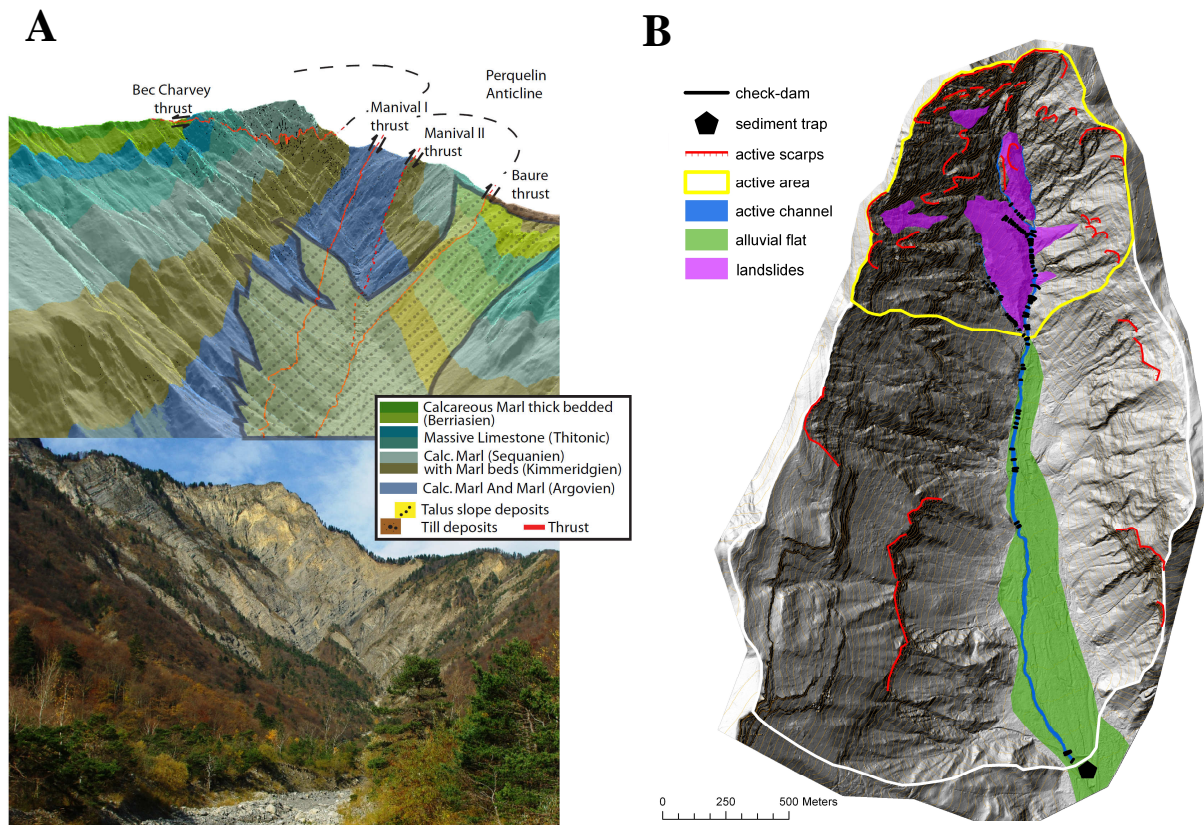


Figure 11 A) 3D view of the geologic structures of the Manival (from Loye et al., 2012) B) general process map of the Manival indicating active erosion and the active channel, the yellow zone is the most important sediment source of the catchment.

The catchment is located in the northern Prealps (Chartreuse Range), which corresponds to the Mesozoic cover of the external alpine crystalline belt. The bedrock is composed of highly fractured, alternating sequences of marls and limestone from the upper Jurassic to early Cretaceous (Figure 11A) with a bedding thickness ranging from decimeters to meters (Charollais et al., 1986). The catchment has been formed along the axis of an anticline with secondary Miocene folding and continuous overthrust faults (Gidon, 1991). Sets of inverse and reverse faults cuts across the hinge of the upper catchment.

Geomorphic processes in the Manival are typical of upland prealpine catchments (Figure 11B). Thick colluvial deposits below the cliffs and hillside were formed by shallow landslides, hillslope debris-flows and snow avalanches. Limestone rock faces are prone to active rockfall which supplies debris to talus slopes. During the snowmelt season, gullies located below rock faces can experience one rockfall every 5 to 10 minutes (according to the authors' field experiences).

Upstream from the sediment trap, which is located at the distal limit of the upper third of the alluvial fan, the mean channel slope is 16% over 1.8 km to the apex of the alluvial fan. This steep channel has

a mean active width of ~15 m (range: 10-20 m) and presents a typical morphology of a debris-flow scoured channel with levees, boulder fronts and coarse lags (Figure 9D). It is entrenched into the wide alluvial fan (40 to 250-m wide, increasing downstream). Macroforms related to bedload transport are observed along the main channel. They can be defined as gravel wedges with well sorted grain-size distributions (Figure 9E). These macroforms partly or totally fill the debris-flow scoured cross-sections and reveal that bedload transport is an important component of the torrent sediment budget. Further geomorphic descriptions can be found in previous works (Veyrat-Charvillon and Memier, 2006; Peteuil et al., 2008).

Approximately 180 check-dams were constructed since the 1890s throughout the main channel and small gullies. They are managed by the French forest and torrent-control service of the Isère Department (ONF-RTM38). Nineteen concrete check-dams are present along the upper part of the study reach. Before the 1970s, debris-flows propagated in the upper fan through several active channels, but to avoid the maintenance of check-dams along secondary channels, the ONF-RTM38 decided to concentrate debris-flows along one single channel constrained in the right-side of the fan by embankment works (gravel levees). This work was motivated because of the urbanization on the alluvial fan (Figure 12). Archive analysis of the Manival flood history during the last two centuries showed that the torrent can produce large debris-flows ranging from 10 000 to 60 000 m³ (Peteuil et al., 2008). Lopez Saez et al. (2011) presents further details on the debris-flow history of the Manival with these archives and the reconstruction of past debris-flow events using dendrogeomorphology. Since 2008, the Manival has produced one debris-flow each year depositing into the 25 000-m³ sediment trap. The trap is a 40-m wide and 130-m long sediment retention basin built in 1926 and was closed since 1991 by a 5-m high concrete dam with sluice openings allowing water and fine sediment to pass through the dam, trapping only the coarse fraction of the sediment transport.

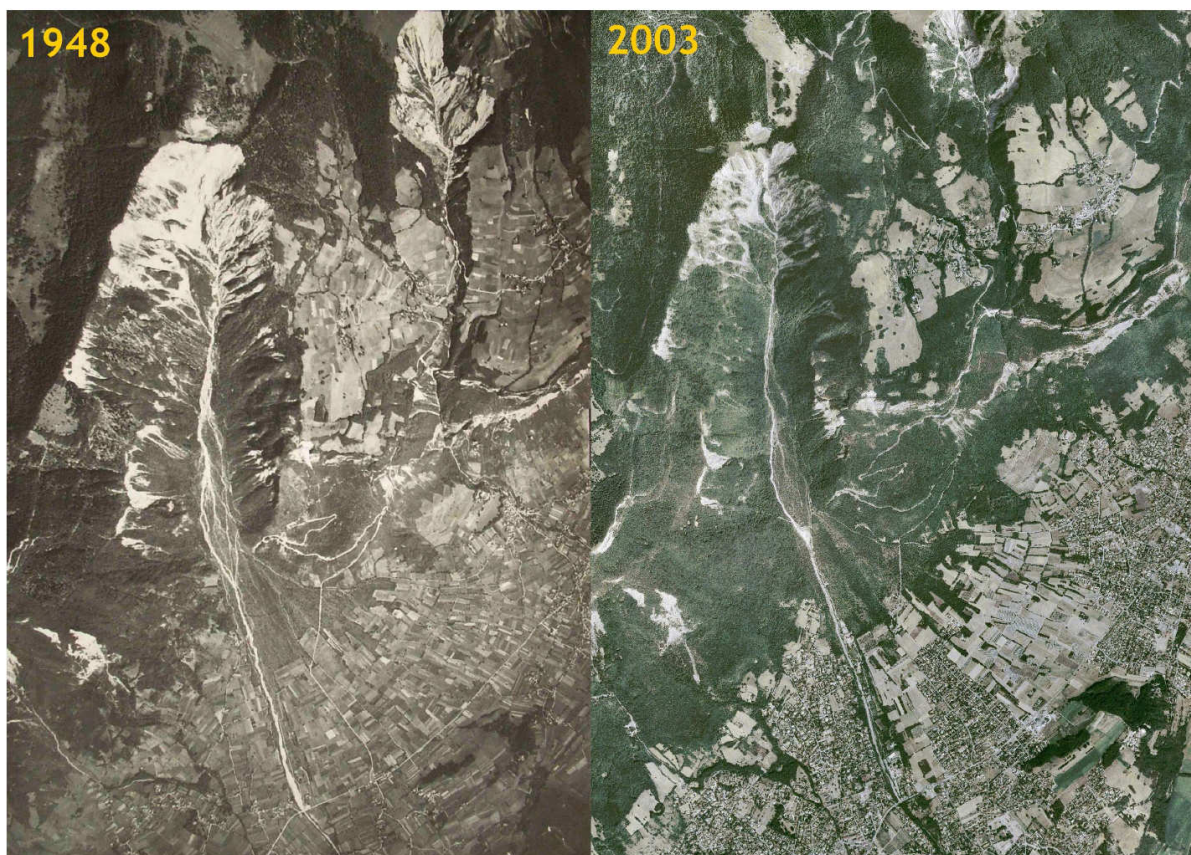


Figure 12 Air photos from 1948 and 2003 show the increase of urbanization on the alluvial fan. The torrent is less active in 2003 because of the engineering works of the last century (from Peteuil et al., 2008)

3 THE REAL TORRENT CATCHMENT

The Réal torrent is a very active debris-flow torrent located in the upper Var River catchment of the Southern French Prealps, located $06^{\circ} 54.5' E$, $44^{\circ} 07' N$ (Figure 13). It flows intermittently into the Tuébi River, a tributary to the Var River, near the small village of Péone. Debris-flows occur 2-3 times every year and interacts with bedload transport processes which makes this catchment ideal for morphological monitoring. The 2.3-km^2 catchment has 800 m of relief with a mean catchment slope of 58% (Table 3).

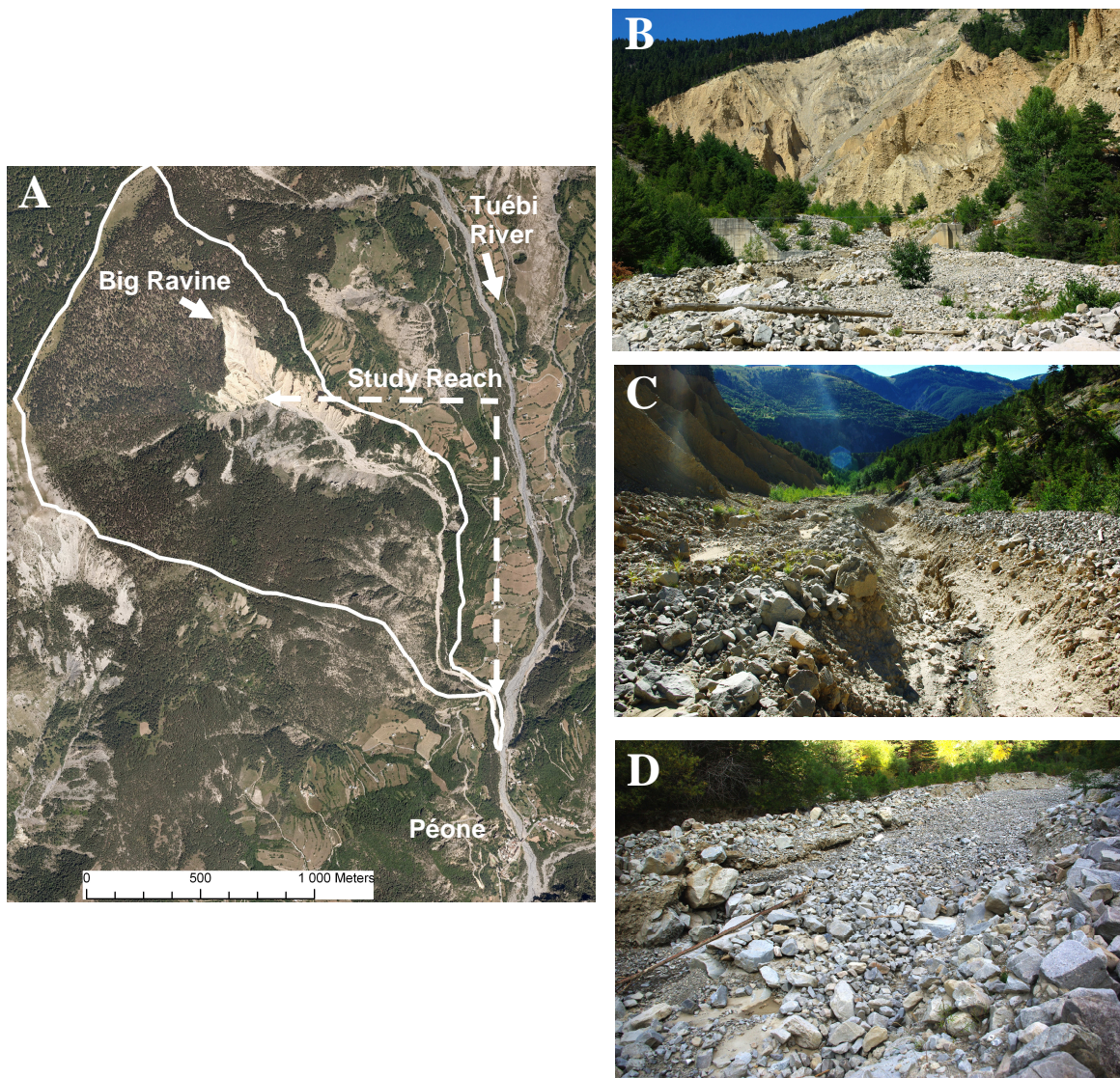


Figure 13 View of (A) the Réal torrent, its source area the “Big Ravine”, and the confluence to the Tuébi River (B) the source area (C) debris-flow scoured channel (D) gravel wedge formed from bedload transport and debris-flow levees on the banks

Table 3 General features of the Réal Torrent

Drainage area (km ²)	2.3
Minimum elevation (m a.s.l.)	1254
Maximum elevation (m a.s.l.)	2048
Mean catchment slope (%)	58
Length of the study reach (km)	1.8
Mean slope of the study reach (%)	16
Mean active channel width (m)	25
Monitoring period	04/2010 – 09/2011
Number of topographic surveys	7
Number of check-dams along the study reach	8

The catchment is in the mountainous Mediterranean climate with a mean annual rainfall of 1050 mm and a 10-yr daily rainfall of 102 mm (Météo France station of Péone from 1951-2010) (Figure 14). Spring and summer (May to September) typically have convective storms which trigger debris-flows. During autumn (September to December); steady and long duration rainfall generates bedload transport. The catchment is typically covered by snow in the winter (January to March), thereby having a dormant channel.

Bedrock geology is composed of Paleogene sandstones and alternating sequences of Cretaceous and Jurassic marls and limestone (Figure 15). Quaternary deposits cover approximately 70% of the catchment. Most of the sediment transported during flow events comes from spectacular alluvial fills related to the obstruction of the valley by a glacier during the Würm period. These 100-m thick unconsolidated alluvial constructions are prone to intense gullyng and landslides which provide an unlimited sediment supply to the torrent. They are composed of a stratified mixture of coarse gravels and boulders with a fine sandy clay matrix. An active deep-seated landslide affecting Jurassic black marls since the 1920s located on the right bank of the main channel also contributes to the sediment recharge. However field observations reveal that the most important sediment source comes from a very active gully entrenched into the fluvio glacial deposits (Chambon and Richard, 2004); we call this gully the “Big Ravine”.

The 1.8-km study reach extends from the confluence of the Tuébi to the proximal limit of the alluvial flat (Figure 13A). The mean channel slope is 16% and the mean active width is ~25 m (range: 15-55 m). The channel morphology is a complex assemblage of erosional and depositional forms resulting from both debris-flow (Figure 13C) and bedload transport processes (Figure 13D). In the upstream part of the study reach, the active channel is wider and occupies the entire valley floor. An isolated vegetated alluvial terrace is observed in the middle part of the study reach, on the left bank of the torrent. This terrace tread is continuous along the last 800 m of the study reach, and creates a buffer zone between the active channel and the hillslopes. Between the exit of the hillslope-confined valley and the confluence with the Tuébi, the Réal flows along a short 250-m reach entrenched into the recent terraces of the Tuébi. Sediments coming from the Réal are incorporated into the wide (55 m) and steep-slope (0.09) active channel of the Tuébi, mostly by bank erosion from debris-flows, which prevents the formation of a large alluvial fan.

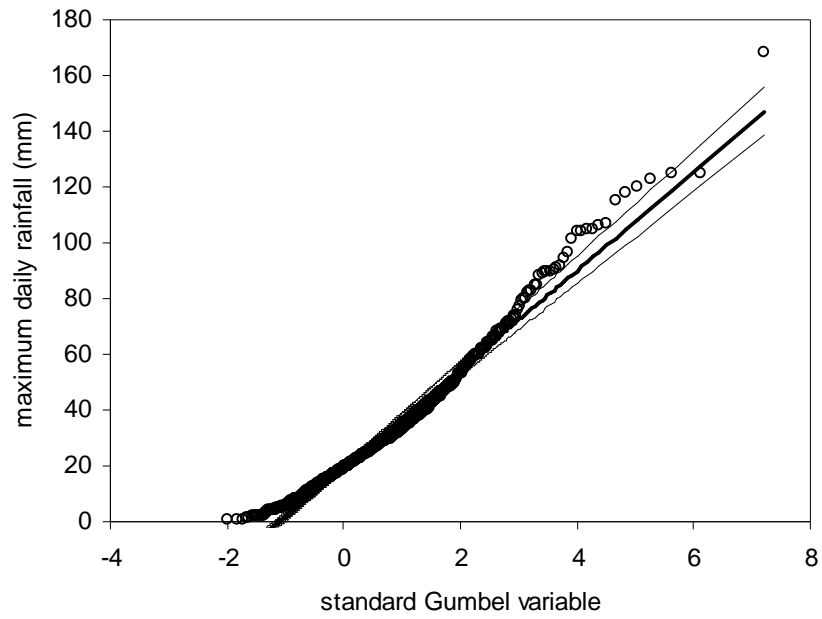


Figure 14 The Gumbel frequency distribution of the maximum daily rainfall observed in the Météo France station of Péone, from 1951 to 2010.

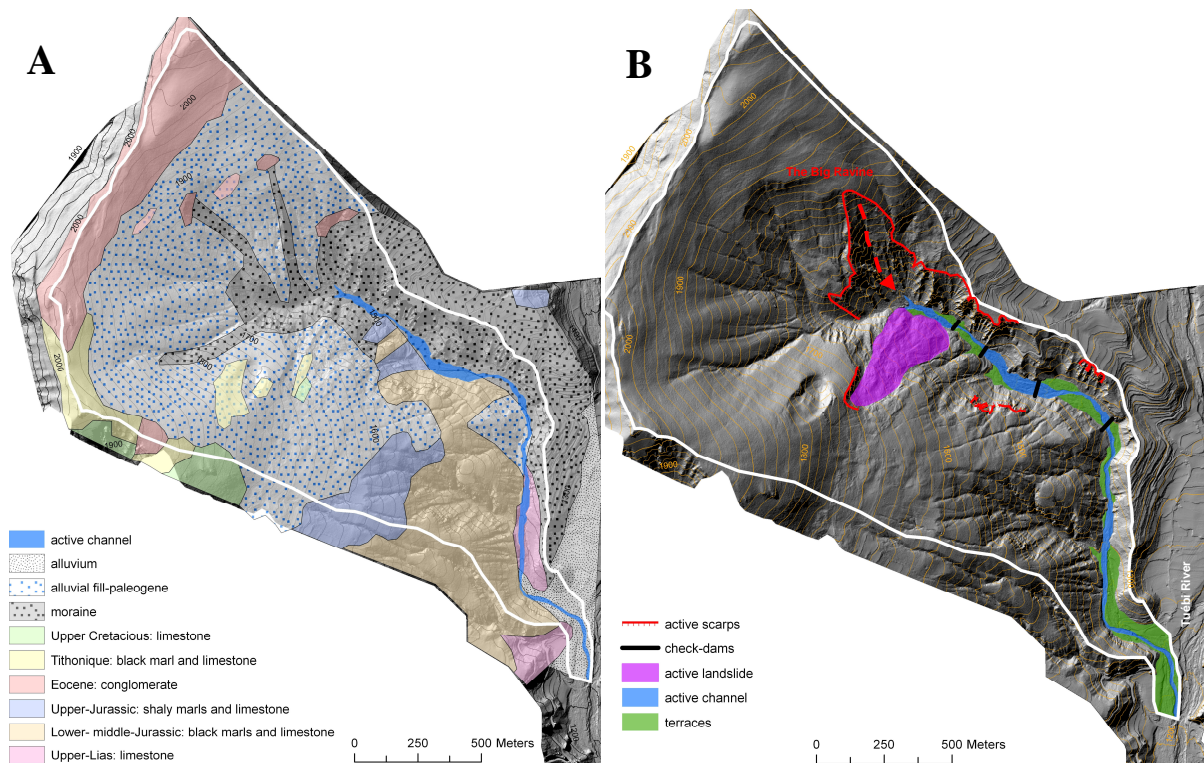


Figure 15 The Réal catchment's general (A) geology (modified from Quélenec and Rouire, 1981; Jomard, 2003) and (B) surficial processes indicating active erosion and active channels

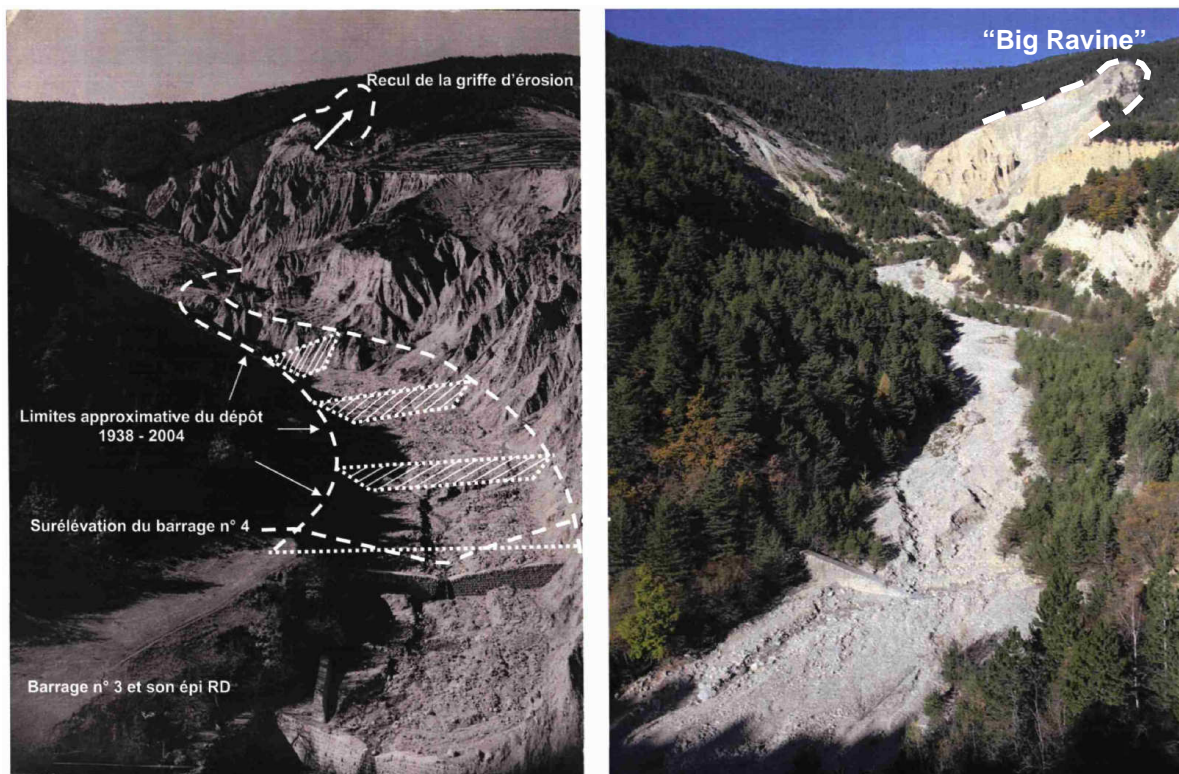


Figure 16 View of the Réal torrent from the third check-dam up to the “Big Ravine”. The left photo is from 1938 and the right is from 2004. Large aggradation occurred, filling and burying the check-dams, and the “Big Ravine” has been deeply incised. (from Chambon and Richard, 2004)

The study reach of the Réal is controlled by eight check-dams constructed between 1933 and 1983 and managed by the forest and torrent-control service of the Alpes-Maritimes Department (ONF-RTM06). Five of these check-dams are cut-stone dams constructed between 1933 and 1935, and all of them are now totally or partially buried by debris-flow deposits. The archives of ONF-RTM06 revealed that cut-stone check-dams of the Réal were regularly heightened after their construction, attesting channel aggradation of the Réal during the 20th century (Figure 16). The three other check-dams are concrete dams deployed between 1976 and 1983. One of them is now partially buried by sediment. Clearly, the most important hillslope contribution comes from the “Big Ravine” which shows considerable incision during the past century (Figure 10). Historical data about debris-flows of the Réal are scarce in comparison with the Manival’s. The only reported debris-flow volume concerns an event of 20 000 m³ that occurred at the end of the 19th century.

Chapter 3:
**SEDIMENT BUDGET MONITORING OF DEBRIS-
FLOW AND BEDLOAD TRANSPORT IN THE
MANIVAL TORRENT**

1 INTRODUCTION

The volume of channelized debris-flows have frequently been identified as influenced by channel scouring along the flow path (see Hungr et al., 2005 for a recent review). Several case studies of debris-flows triggered by slope failures reported that the volume of initial failures were insignificant as compared to the total volume of the event (Benda and Dunne, 1987; Remaître et al., 2005; Berger et al., 2011b). Debris-flows incorporate in-channel sediment as they move down slope. This is known as debris-flow bulking and the rate at which debris-flows scour the channel is referred as the yield rate (expressed in m^3 per unit length of channel). Therefore, the presence of erodible sediment in headwater channels is recognized as a primary control on the timing and magnitude of debris-flows (Jakob et al., 2005). Some authors proposed to discriminate supply- and transport-limited debris-flow catchments as a function of the sediment recharge rate for low-order channels, this being defined as the rate at which colluvium fills the scoured channel after the passage of a debris-flow (Bovis and Jakob, 1999). The higher the recharge rate, the higher is the susceptibility of the catchment to produce a debris-flow during high-intensity rainfall events.

Temporal fluctuations and spatial distributions of channel storage are therefore key controls of debris-flow occurrence and magnitude. In steepland catchments, these fluctuations are influenced by both debris-flows and bedload transport, but the respective influence of both can be very different between investigated sites. Field studies of sediment transfer in Oregon's steepland catchments revealed that low-order channels accumulate sediment input from hillslopes for thousands of years until a slope failure occurs and transforms into a debris-flow which scours the sediment of first- to second-order channels (Benda and Dunne, 1987; Benda, 1990). Given the nature of coarse sediments delivered to headwaters, common runoff events are unable to mobilize them as bedload and therefore sediments are accumulated for very long periods of time. Similar sequences of scour and fill were reported in other regions, but over much shorter timescales. A recent study of an alluvial fan in New Zealand revealed seasonal cut-and-fill sequences driven by successive wet and dry periods (Fuller and Marden, 2010). In this case, aggradation phases of the fan are related to large sediment influx from debris-flows during wet periods, when failures are triggered in the upper catchment. Degradation phases are related to bedload transport events during autumn. Observations of a first-order channel in Japan showed sediment accumulation during winter freeze-thaw cycles, and channel scouring during summer convective storms (Imaizumi et al., 2006). Most of the sediment flushing was driven by debris-flows while bedload transport was considered as a minor sediment transport process. Annual sediment transfer investigations in the Illgraben catchment (Switzerland) also revealed the importance of alternating scour and fill of the channel in the understanding of sediment transfer in complex debris-flow catchments (Berger et al., 2011b), however interactions between debris-flow and bedload transport were not emphasized.

Intensive seasonal field observations of the sediment cascade in steepland catchments prone to debris-flows are still lacking in the alpine environment and notably in catchments where sediment transfer is driven by both debris-flow and bedload transport. These two processes may occur during the same flow event, but some events do not produce debris-flows when bed material is entrained only by shear stress exerted from water flow. We refer the latter case as a bedload transport event. This chapter presents observations from frequent field surveys of sediment transfer in the Manival debris-flow torrent in the French Alps (Figure 17), where sequences of scour and fill were studied at a seasonal timescale from first to fourth-order channels. These observations allowed us to (1) quantify the relative contribution of channel scouring for debris-flow volumes, and to (2) characterize the seasonal cycles of scour and fill from low- to high-order channels with respect to the driving processes (debris-flow vs. bedload).

2 MATERIAL AND METHODS

2.1 Sediment budget

2.1.1 Channel storage changes

Multidate topographic surveying of cross-sections were used for monitoring channel storage change in the study reach of the Manival torrent. Cross-sections were regularly spaced along the study reach, paying special attention to sample sections where channel deformation (scour and fill) was expected to be active. Thirty-nine cross-sections were deployed along the 1.8-km study reach of the Manival, giving a mean cross-section spacing of 46 m (3 times the mean active channel width) (Figure 17). Wooden stakes on top of the channel banks were installed for cross-section benchmarking. Points were surveyed along transverse lines at each break of slope, and each measurement point was marked with spray paint. This saved time during subsequent surveys by only measuring the active portion of the cross-section (the portion where paint marks were no longer visible). The mean point spacing was 1.3 pts/m. Two days were required for surveying all of the cross-sections. Topographic surveys were measured with a total station (Leica Flexline TS02). The manufacturer's electronic distance measurement precision is 1.5 mm +/-2 ppm, and the angular resolution is 7'' or 3.4 mm of precision at a distance of 100 m. The total station was benchmarked on permanent points of alluvial terraces.

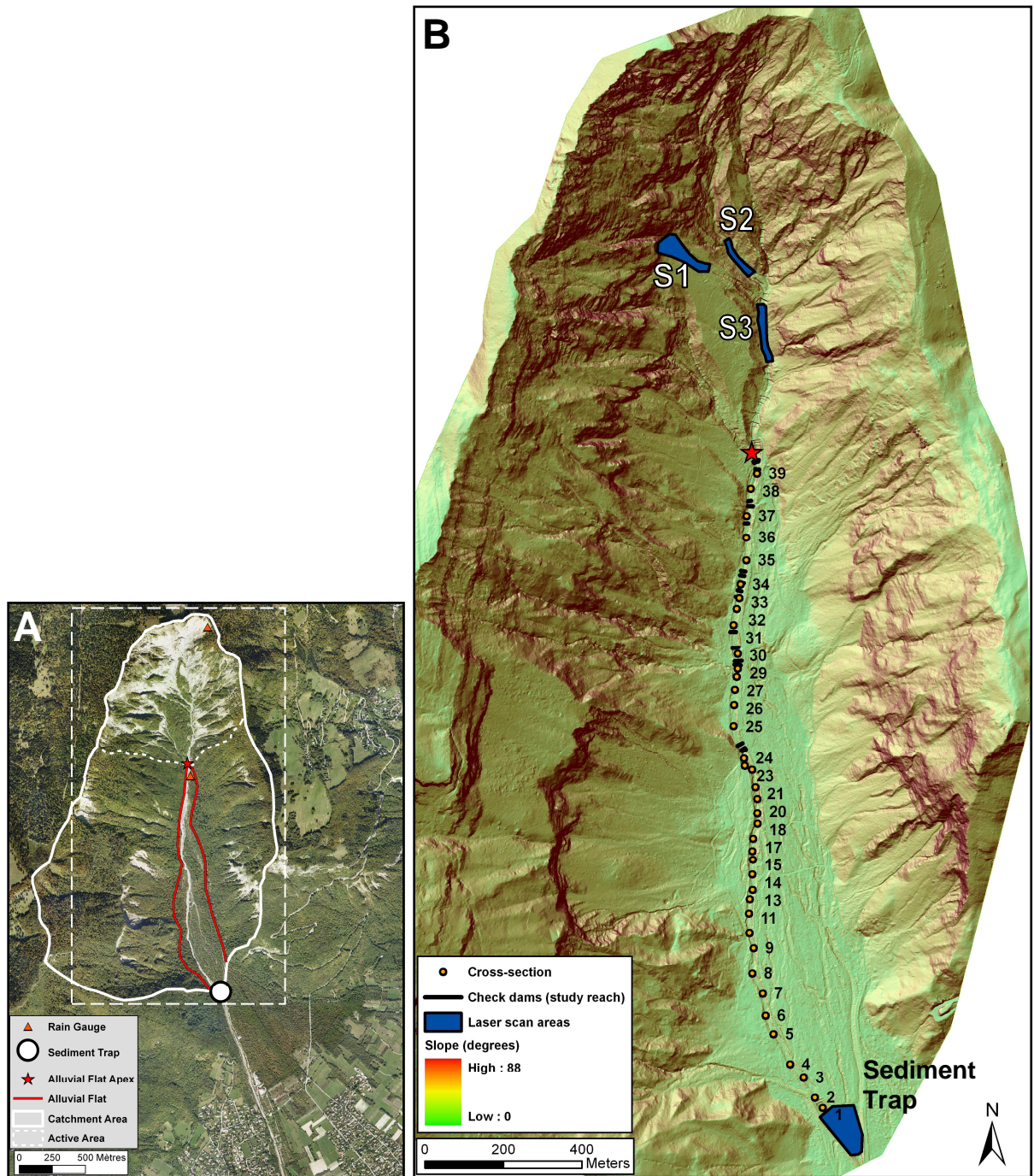


Figure 17 (A) Orthophoto view of the Manival catchment (image @ Aerodata International Surveys) located at $45^{\circ} 17' N$, $5^{\circ} 49.75' E$; (B) Shaded relief map of the Manival study reach derived from airborne LiDAR surveys, displaying locations of cross-sections, check-dams, and laser scanned areas; Sites S1-S3 refer to multi-scanned headwater reaches (Figure 28)

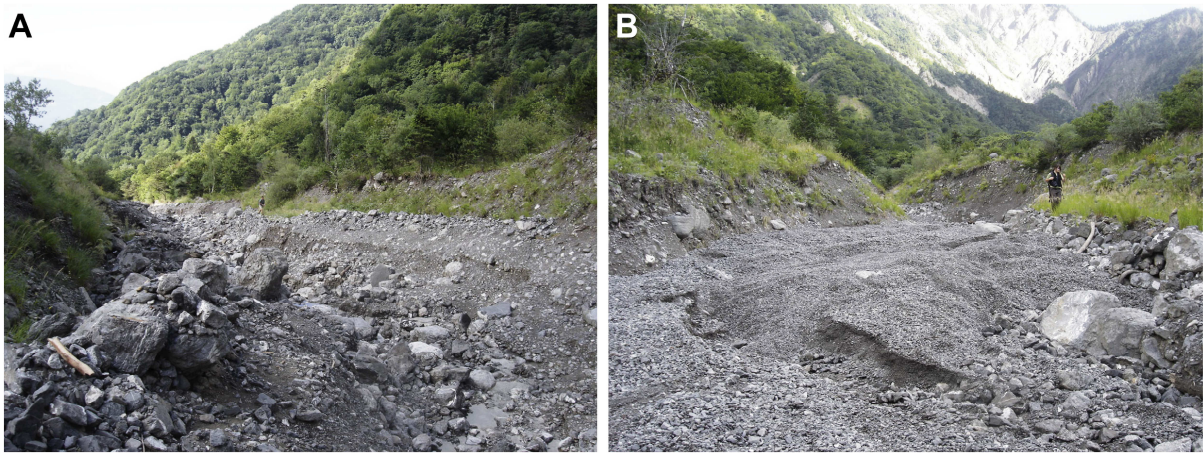


Figure 18 Views looking downstream and upstream from XS 19 (Figure 17) in the Manival study reach showing (A) debris-flow levees and coarse lags and (B) gravel wedges filling the U-shape debris-flow channel

The time frequency of topographic surveys was controlled by the occurrence of competent flow events (flow events that induce a morphological response of the channel), but the time-lapse between two successive events was sometimes too short to permit a perfect match between events and surveys. Eight post-event surveys were measured since spring 2009, two surveys being done after debris-flow events of moderate intensity. It is important to mention that the debris-flows in this torrent are often in the form of multiple surges (eye witness reported 4 surges with 10 minute intervals for one debris-flow). Therefore topographic surveys capture the time-integrated volume change of the torrent during the event. For this paper, the two types of events are characterized:

- A debris-flow event consisting of multiple surges, also including secondary bedload transport. Typical field indicators are unsorted levee, lobe, lag, and terminal deposits with a fine sediment matrix (eg. Figure 18A). The secondary bedload transport can sometimes deposit sorted unconsolidated gravels in the thalweg.
- Bedload transport events refers to bedload processes occurring without debris-flows which regularly occur during intermittent flows and floods from low intensity rainfall and snowmelt. Typical field indicators are sorted unconsolidated gravel deposits which sometimes develop into large wedges reaching bankfull (eg. Figure 18B). No debris-flow field indicators are present.

Cross-sections (Figure 19) were used for quantifying volumes of erosion and deposition in the channel and back-calculating bed-material sediment transport using the morphological method (Ashmore and Church, 1998), widely applied for balancing sediment budgets in gravel-bed rivers (Ferguson and Ashworth, 1992; Martin and Church, 1995; Reid et al., 2007; Raven et al., 2009). Volumes of deposition (V_D) and erosion (V_E) between cross-sections are obtained by the following:

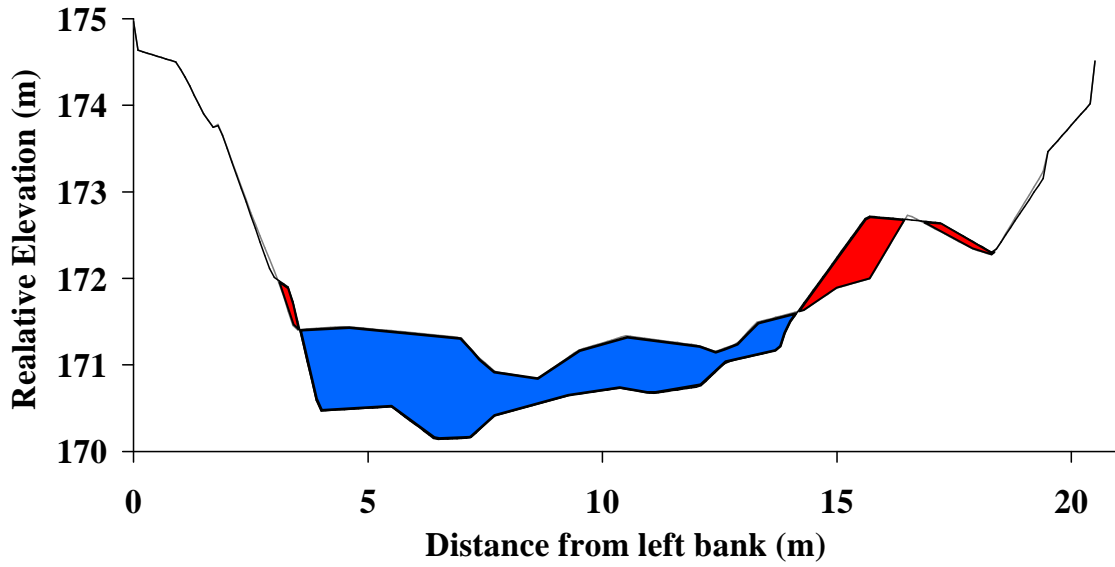


Figure 19 Example of two Manival cross-section surveys (XS29) with channel deposition (blue) and an eroded bank and levee (red) during the P2 period in autumn 2009.

$$V_E = \frac{A_{E(n)} + A_{E(n+1)}}{2} L_{(n,n+1)} \quad (1)$$

$$V_D = \frac{A_{D(n)} + A_{D(n+1)}}{2} L_{(n,n+1)} \quad (2)$$

with L , the streamwise distance between the two cross-sections n and $n+1$, and A_E and A_D the cross-sectional area of erosion and deposition, respectively. The net storage change δV between two surveys for the channel reach between two cross-sections is determined by the difference of the two volumes V_D and V_E . The principle of mass conservation is used to determine the coarse sediment transport for each reach with:

$$V_o = V_i - \delta V \quad (3)$$

with V_o the sediment output and V_i the sediment input. Through monitoring sediment outputs at the downstream end of the study reach, the sediment transport and the sediment input can be determined for each sub-reach comprised between two cross-sections.

Uncertainties of erosion or deposition volume estimates for each sub-reach, σ_V , were calculated according to the propagation of uncertainty's law of Taylor (see Reid et al., 2007 for details):

$$\sigma_V = \sqrt{\left(\sigma_{A_n} \left[\frac{\partial V}{\partial A_n} \right] \right)^2 + \left(\sigma_{A_{n+1}} \left[\frac{\partial V}{\partial A_{n+1}} \right] \right)^2 + \left(\sigma_{L_{n,n+1}} \left[\frac{\partial V}{\partial L_{n,n+1}} \right] \right)^2} \quad (4)$$

The terms σ_{A_n} and $\sigma_{A_{n+1}}$ refers respectively to errors associated with cross-sectional area of erosion or deposition at cross-sections n and $n+1$, respectively, and $\sigma_{L_{n,n+1}}$ refers to the error associated with the distance between cross-sections n and $n+1$. Cross-sectional areas of erosion (A_E) or deposition (A_D) were calculated by the following:

$$A_E = \sum_{i=1}^n \left(\frac{e_i + e_{i+1}}{2} \right) d_{i,i+1} \quad (5)$$

$$A_D = \sum_{i=1}^n \left(\frac{f_i + f_{i+1}}{2} \right) d_{i,i+1} \quad (6)$$

with e_i , the erosion depth at point i , f_i , the deposition depth at point i , and $d_{i,i+1}$ the distance between points i and $i+1$. Therefore, σ_A used in Equation (4) can be calculated using the Taylor's propagation of uncertainty with individual errors associated with e_i , f_i , and $d_{i,i+1}$. Erosion and deposition depths were calculated as elevation differences between two successive surveys. We assumed that the uncertainty of elevation measurements was equivalent to the D_{84} of the bed surface grain-size distribution of the channel, which is approximately 5 cm for the Manival (measured by Wolman's pebble counts on 100+ particles). A similar value was attributed to the error associated with the distance between two successive points, since the position of the prism during surveys is influenced by the roughness of the bed. The error associated with the curvilinear distance between two successive cross-sections was measured on a high-resolution digital terrain model (DTM) derived from an airborne laser scan (ALS) and was attributed a value of 1 m, corresponding to the pixel size of the DTM.

2.1.2 Sediment output

The 25 000-m³ sediment trap was used for reconstructing sediment output by post-event topographic surveys. The trap is a 40-m wide and 130-m long sediment retention basin built in 1926 and was closed since 1991 by a 5-m high concrete dam with sluice openings allowing water and fine sediment to pass through the dam, trapping only the coarse fraction of the sediment transport (Figure 20). Since it can be expected that the trapping efficiency of the check-dam is not 100%, resurveys of the sediment trap may only give a lower-bound estimate of the sediment output. Nevertheless, several observations lead us to consider sediment losses as negligible during the monitoring period. We observed that bedload deposits never reached the distal end of the trap during the recorded events. We also observed that debris-flows were slowly moving in the trap and they progressively reached the dam with a boulder front obstructing the sluice openings. The strong channel incision observed downstream from the dam, which indicates sediment starvation, also suggests a high trapping efficiency.



Figure 20 View of the sediment trap after a debris-flow with (A) the dam blocked by the boulder front with tree debris and (B) the rest of the trap filled with finer sediment.

Most surveys of deposition in the sediment trap (4 of 5) were measured with the Leica TS02 total station. These surveys were subtracted from a terrestrial laser scan (TLS) of the empty sediment trap surveyed at the onset of the monitoring program. TLS surveys were measured with an ILRIS-3D (Optech Inc.) terrestrial laser scanner, with a 1535 nm laser giving a minimum footprint of 22 mm at 100 m. This TLS has a laser repetition rate of 2000 Hz, with a maximum range of about 1200 m for 80% reflectivity surfaces. The manufacturer's precisions of the TLS are 7 mm for distance, 8 mm for position, and 80 μ rad for angle. The minimum point spacing is 2 cm at 1000 m.

Overall point densities of the total station surveys were comprised between 0.08 to 0.23 pts/m². The deposition surface was smooth and conical, however, to get a more reliable representation of the deposition surface, we increased the density of surveyed points in areas with irregular topography and each break of slope was carefully sampled during the survey. Total station measurements were manually aligned with the previous TLS survey using 7 to 10 tie points (check-dams corners and edges) by using IM Align module on the software PolyworksTM of InnovMetric. The uncertainty associated with deposition volume estimates was assessed by calculating the propagated uncertainty related to two parameters: (i) the surface roughness which was attributed a value corresponding to the D_{75} of the surface grain-size distribution for debris-flow deposits (0.07 m) and bedload deposits (0.05 m), and (ii) the standard deviation of alignment error of the tie points which ranges from 0.05 to 0.10 m.

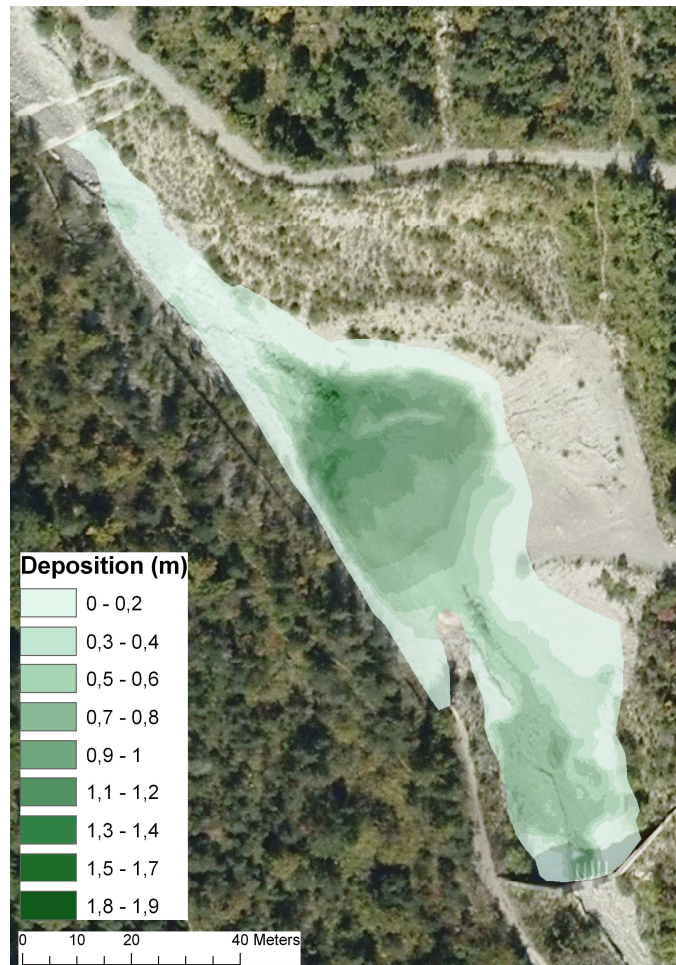


Figure 21 Example of DEM of Difference (DoD) with TLS in the sediment trap before and after the first observed debris-flow event

One post-event survey was done with the TLS (Figure 21). For the sediment trap, TLS surveys required less than one hour with a final point spacing less than 2 cm and a maximum root mean square error (RMS) between the multi-date cloud points of ± 0.02 m (detailed TLS methods are presented in Section 2.3).

Sediment trap surveys were measured during the cross-section survey campaign, except when sediment deposition was not visible in the sediment trap or when a substantial part of the deposit was removed by dredging operations. The sediment trap is managed by a private company in charge of dredging operations to maintain a full capacity over time. Generally, the time lapse between the flow event and the dredging works was long enough to implement a topographic survey. For three out of eight times, the trap was disturbed after small floods. The outputs in these situations had to be estimated according to sediment yields determined from cross-section surveys.

Table 4 General features of the three headwaters in the Manival catchment dedicated to the monitoring of sediment supply from hillslopes by LiDAR resurveys

	S1	S2	S3
Length of the surveyed reach (m)	140	95	170
Drainage area (km ²)	0.03	0.17	0.52
Channel slope (%)	67	55	45
Stream order*	1	2	3
Scanned surface (m ²)	1600 - 1900	660	840
Number of check-dams	0	5	11

*based on LiDAR-derived DTM stream network

2.2 Sediment supply from low-order headwaters

The sediment supply from headwaters was monitored by TLS resurveys and an airborne laser scan survey (ALS) for three study areas (Figure 17): a small active first-order headwater entrenched into a talus slope below a limestone cliff with 400 m relief (denoted as S1), and two upstream second- and third-order steep-slope channel reaches confined between eroding hillslopes directly delivering sediments to the channel by shallow landsliding and hillslope debris-flows initiated on talus slopes (denoted respectively as S2 and S3). General characteristics of these 3 areas are presented in Table 4. The S1 site was accessible on a trail and can be seen from a view point with optimal angle and coverage. S2 and S3 sites were chosen because of having safe viewable locations and they are reaches between the first-order to the main torrent channel.

The TLS data were collected on a seasonal basis during 2009 (April, July, August, and November). Scanning positions for S1 were taken both within the channel and across the upper catchment using 2 to 8 locations with distances ranging from 2 to 600 m. S2 required two to three scanning positions with distances of 20 to 450 m. S3 required one position at a maximum distance of 250 m. In order to save time in the field, long range scans had a maximum point spacing of 0.1 m which can vary according to shadow effects (channel areas hidden by terrain obstructions from the laser).

The ALS survey for the entire catchment was flown by helicopter in June 2009 by a private company (Sintegra) using a 200 kHz Riegl LMS Q560 laser scanner. The flight elevation fluctuated between 450 and 650 m above ground, with a maximum instantaneous scan angle of 25 degrees, giving a laser footprint range between 0.16 and 0.24 m for flat terrains. The mean density of the filtered point cloud was 6.9 pts/m² and the altimetric and planimetric errors were 0.10 and 0.15 m, respectively. However, with the raw LiDAR data for the 3 sites, sparse vegetation cover was manually cleaned preserving a point density up to 30 pts/m². Manually cleaning refers to identifying and selecting the backscattering from vegetation in the scan's point cloud and deleting it rather than using automatic filters.

The multi-date scans (ALS and TLS) were merged and aligned on IM Align module on the software PolyworksTM of InnovMetric. With the IM Align, identifiable permanent structures such as check-

dams can be selected as tie points for different scans, the point clouds of these features can then be aligned with the Automatic Iterative Closest Point algorithm (Besl and McKay, 1992). Digital Elevation Models (DEMs) with 0.1 m resolution were created by ordinary kriging interpolation for the TLS data. This interpolation method was chosen because the resulting relief representation was qualitatively identified as the most reliable to the field morphology. The DEM from the ALS data was created with a linear drift kriging for smoothing high density linear swaths of points in the airborne scans. These DEM layers were used to create classical DEM of differences (DoD) for calculating volumes of erosion and deposition. The uncertainty associated with volume estimates was assessed by using IM Align to find the maximum RMS of alignments between the multi-date point clouds (± 0.08 m) covering areas with permanent structures (Iavarone and Vagners, 2003; Rabatel et al., 2008).

2.3 Initial channel storage quantification

The volume of sediment storage in the main channel of the torrent was estimated at the onset of the monitoring. The objective was to determine the boundary conditions of the captured storage changes over the monitoring period and to evaluate the fraction of the total alluvial sediment reservoir that is remobilised during debris-flows. The Manival torrent has limited lateral migration with well defined channel banks where the susceptible areas are controlled by the engineering works of the RTM services. This provides realistic estimations of connected channel storage to the sediment trap.

Channel storage at t_0 (July 6, 2009) was obtained by the “sloping local base level” (SLBL) method (Jaboyedoff and Derron, 2005). The SLBL has been initially defined as a surface above which rocks are assumed to be erodible by landsliding (Jaboyedoff et al., 2004) and the method was adapted to estimate the sediment infilling of glacial U-shape valleys (Jaboyedoff and Derron, 2005; Otto et al., 2009). The general principle is to deepen DTM pixels included in the alluvial fill by an iterative routine until an assumed bedrock surface shape is reconstructed. The surface geometry was determined by quadratic equations. Cross-sections in the Manival are located in the main channel of the alluvial flat where a U-shape is most likely to form (validated with multi-date cross-section overlays). Therefore it seemed relevant to use the SLBL method for quantifying the volume of erodible sediment by debris-flows along the main channel of the Manival. In this case, the maximum scour surface is not controlled by bedrock because the thickness of alluvial fill is much greater than the maximum potential scouring depth of debris-flows (which we estimated around 4 to 5 meters). The main channel is entrenched in the alluvial fan with a general range of thickness from 10 to 30 meters.

ALS-derived DTMs were used with a grid size of one meter to run the SLBL routine (Jaboyedoff and Derron, 2005). The first step was to edit manually the limits of in-channel depositional landforms. This was done by mapping the spatial extent of the active channel using both 12.5-cm resolution

digital orthophoto (Aerodata International Surveys) and a hillshade representation of unfiltered DTMs with vegetation manually cleaned. The second step was to assign values for two user-defined parameters of the SLBL routine which constrain the shape of the reconstructed parabola. The first is the maximum depth of the alluvial storage and the second is the maximum curvature of the debris-flow scour surface. These two parameters were determined from the interpretation of the cross-section shapes of the torrent. For each cross-section surveyed in the field with the total station, we interpolated the maximum debris-flow scour surface by fitting a polynomial curve to the bank slopes on each side of the active channel, assuming that the bank profile is controlled by debris-flow erosion. We also constrained the best-fit polynomial with the lowest elevation observed at each cross-section during the monitoring period, providing that this lowest elevation corresponds to the presence of older highly consolidated coarse lag (similar in strength to soft bedrock) preventing deeper scour during subsequent flows (Figure 22). This procedure allowed for calculating the sediment storage in the main channel and controlling the SLBL-derived sediment volume.

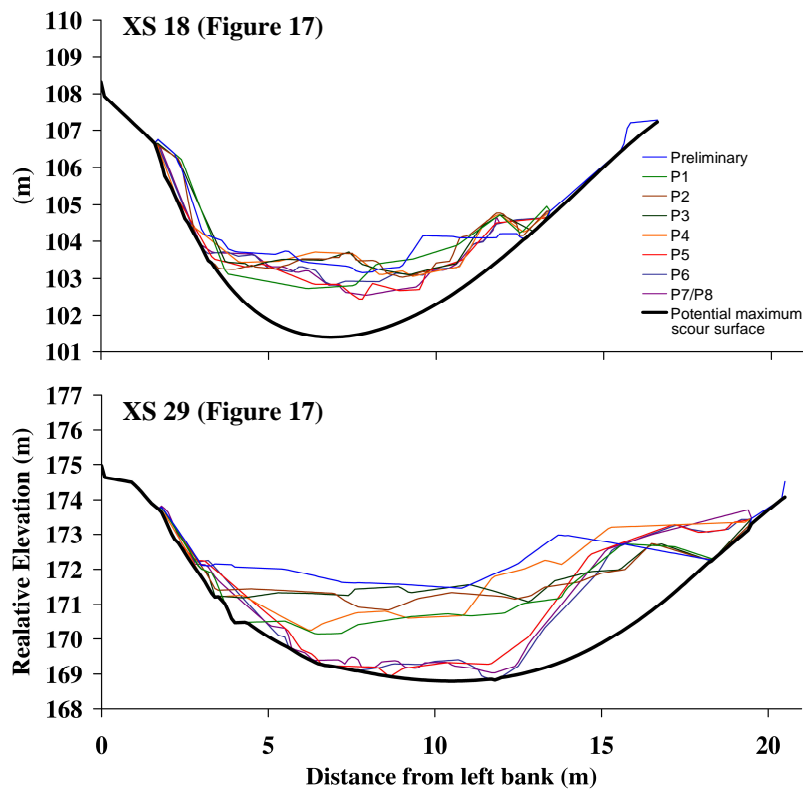


Figure 22 Examples of Manival cross-section interpretations for determining the maximum debris-flow scour surface from best-fit polynomial curves; the XS 18 shows a maximum scour surface constrained only by the bank slopes since the lowest elevation reached over the monitoring period did not excavate the channel up to the coarse lag layer; XS 29 shows a polynomial fit constrained by the lowest elevation over the monitoring period, since the presence of a coarse lag formation suggests that the channel will not deepen any further; thin coloured lines: cross-section resurveys over the monitoring period (P1-P8); thick black line: maximum debris-flow scour surface derived from polynomial fit.

2.4 Rainfall monitoring

Two tipping bucket rain gauges (Rainwise Inc.) with a 196-mm diameter and resolutions of 0.12 and 0.16 mm were used for rainfall monitoring in the catchment. The rain gauges are connected to a data logger recording instantaneous time of tips and allowing computation of rainfall intensity at varying time intervals. The first was installed in October 2008 at the apex of the alluvial fan (Figure 17), at an elevation of 860 m a.s.l. The second was installed on the catchment ridge in July 2010 at an elevation of 1490 m a.s.l. We chose open sites easily accessible from the road to facilitate regular visits of the instrument for maintenance and data collecting. The two rain gauges are spaced 1.1 km apart, and they both generally showed similar rainfall readings in the Manival during the summer (Figure 23). From autumn to spring the upper rain gauge is susceptible to snow cover and melt. Therefore the lower rain gauge was used for analysis because of its continuous recording from the beginning of the monitoring program.

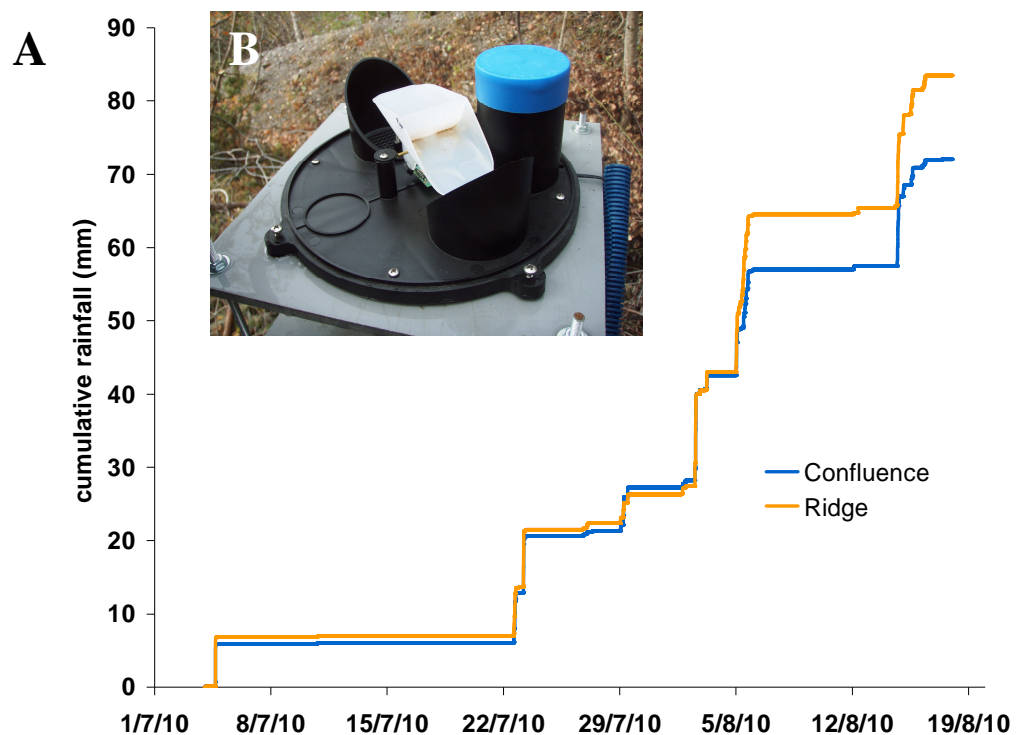


Figure 23 A) Variation of cumulative rainfall between the two rain gauges during the summer 2010 with convective storms. Only one storm does not have comparable volumes (August 5, 2010); B) Interior view of the tipping bucket rain gauge (Rainwise Inc.) with a 196-mm diameter and a 0.12 mm resolution.

3 RESULTS

3.1 Rainfall and channel responses

Despite rainfall of low to moderate intensity during the monitoring period (less than one to two year return period) (Figure 24, Table 5), considerable channel responses were observed along the torrent. Eight periods of significant geomorphic activity were observed along the study reach between July 2009 and December 2010 (denoted as P1 to P8), two of these periods being characterized by the occurrence of a debris-flow (August 2009 and June 2010). The maximum daily rainfall was observed during P1, with a value of 34.7 mm. A frequency analysis of maximum daily rainfall based on the nearest long-term rainfall time series (Météo France station of Saint-Hilaire-du-Touvet, 1964-2010, elevation of 970 m a.s.l, located 5 km from the Manival, on the same mountain side) gave a 10-yr daily rainfall of 88 mm (90% confidence interval : 83-94 mm). This calculation was based on a monthly sampling of maximum daily rainfall to increase the size of the sample and to provide a more accurate estimate of extreme rainfall (Djrboua, 2001; Djrboua and Lang, 2007). According to the fitted probability law, the return period of the maximum 24h rainfall observed during the monitoring period was 1.0 yr. The maximum 5-minute rainfall intensity was recorded during P6, with a value of 79 mm hr⁻¹. This high-intensity storm event did not initiate any debris-flow in the catchment. Debris-flows occurred during P1 and P5, when maximum rainfall intensities were 49 and 25 mm hr⁻¹, respectively. The minimum rainfall intensity associated with an observable channel response was 7 mm hr⁻¹ during P3 and P8.

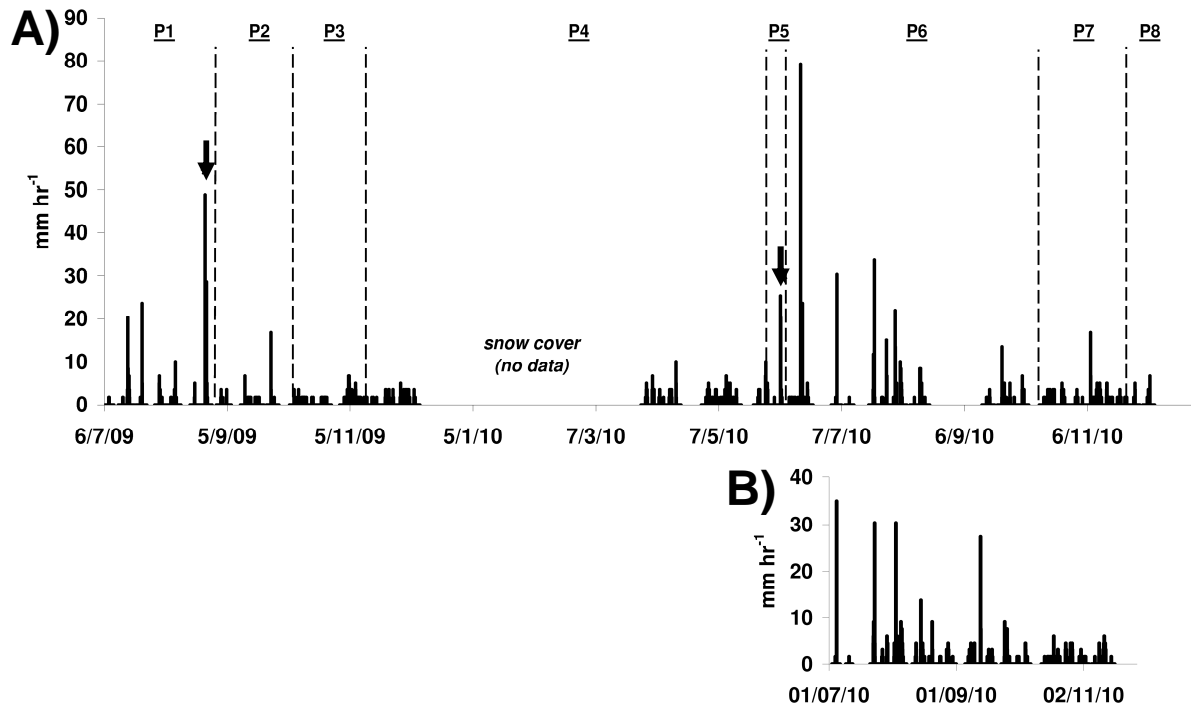


Figure 24 Maximum rainfall intensity (five-minute resolution) observed for the Manival from A) the lower study site rain gauge and B) the upper study site rain gauge; cross-section surveys are indicated by dotted lines; the arrows indicate debris-flow occurrence

Table 5 Summary values of rainfall for each monitoring period of channel storage changes; mean and maximum intensities are calculated for a 5 minutes time-interval; rainfall data from the rain gauge at the Manival ridge are indicated in brackets and showed similar values to the rain gauge located near the main channel

Survey time period	Period ID	Total rainfall (mm)	Maximum 24h rainfall (mm)	Mean storm intensity (mm hr ⁻¹)	Maximum burst intensity (mm hr ⁻¹)	Debris-flow
06/07/09 – 28/08/09	P1	93	34.7	3.2	49	25/08/2009
30/08/09 – 07/10/09	P2	24	14.5	2.8	17	
08/10/09 – 12/11/09	P3	101	16.6	1.9	7	
13/11/09 – 01/06/10	P4	239	32.2	2.1	10	
02/06/10 – 08/06/10	P5	26	24.4	6.2	25	06/06/2010
09/06/10 – 08/10/10	P6	174	21.3	3.0	79	
04/07/10 – 08/10/10*	P6*	135 (170)	21.3 (21.0)	2.9 (2.7)	34 (35)	
14/10/10 – 25/11/10	P7	150	22.3	2.2	17	
14/10/10 – 15/11/10*	P7*	115 (76)	22.3 (23.0)	2.3 (2.0)	17 (6)	
25/11/10 – 10/12/10	P8	33	19.4	2.0	7	

*Time period with available data from the Manival ridge rain gauge

3.2 Torrent sediment budgets

Sediment budgets reconstructed for the Manival during the eight investigated periods are summarized in Table 6. Unit volume changes (including yield rates) for these periods are reconstructed from the cross-section resurveys (Figure 25). The high yield rates from the debris-flows (P1 and P5) identifies the extent of entrainment which can divide the torrent channel into two sections, the proximal and distal reach in reference to the apex of the alluvial fan. Sediment transport volumes were computed by first cumulating the unit volume change, and then they are readjusted so that the output volumes match the sediment trap volumes (Figure 25).

During P1, a debris-flow occurred. The geomorphic activity of the main channel was only driven by a short-duration convective storm which occurred on 25th August 2009. With the storm burst defined as a continuous rainfall according to a 5-minute time step, the duration was 45 minutes with a total of 11 mm and a maximum 5-minute intensity of 49 mm hr⁻¹. Considerable channel erosion was observed (Figure 26) in the proximal part of the study reach from the apex of the alluvial fan, while the distal part was characterized by net deposition. Maximum local scour reached 2.9 m. A net storage loss of 2034 m³ +/-199 was obtained, which was equivalent to the sediment output captured by the TLS survey of the sediment trap (1873 m³ +/- 62). Therefore, sediment input from the upper catchment could be considered as very low (not greater than 63 m³ given uncertainties of storage changes and output) and most of the sediment yield was supplied by channel scouring along the main channel. There were no signs of a debris-flow upstream from the proximal reach. This suggests that the debris-flow initiated in the proximal reach of the main channel.

Table 6 Sediment budget for the Manival Torrent obtained from cross-section and sediment trap resurveys; sediment inputs were back-calculated from storage changes and outputs; uncertainties of channel erosion and deposition are calculated from the Taylor's law of uncertainty propagation; storage change uncertainty is the sum of erosion and deposition uncertainties; sediment output uncertainty is calculated from individual errors associated with topographic surveys; ranges of values proposed for sediment output (when a topographic survey of the sediment trap is not available) or input are derived from storage change uncertainty

Study period	Period ID	Sediment Input (m ³)	Storage Change (m ³)	Channel Erosion (m ³)	Channel Deposition (m ³)	Sediment Output (m ³)
06/07/2009 - 28/08/2009	P1	0-63	-2034 (±199)	5232 (±136)	3199 (±63)	1873 (±62)
30/08/2009 - 07/10/2009	P2	736-842	789 (±84)	1409 (±31)	2197 (±53)	0
08/10/2009 - 12/11/2009	P3	198-260	-73 (±66)	1546 (±36)	1473 (±31)	266-338
13/11/2009 - 01/06/2010	P4	0-36	-580 (±81)	1961 (±45)	1372 (±36)	535-625
02/06/2010 - 08/06/2010	P5	0-537	-3052 (±272)	7658 (±178)	4605 (±93)	3320 (±176)
09/06/2010 - 08/10/2010	P6	174-246	-608 (±82)	2246 (±46)	1637 (±36)	773-865
14/10/2010 - 25/11/2010	P7	0-49	-267 (±35)	921 (±20)	685 (±15)	226 (±34)
25/11/2010 - 10/12/2010	P8	0-76	-306 (±51)	1351 (±29)	1056 (±23)	515 (±41)
06/07/2009 - 10/12/2010		1108-2109	-6147 (±870)			7195-8075

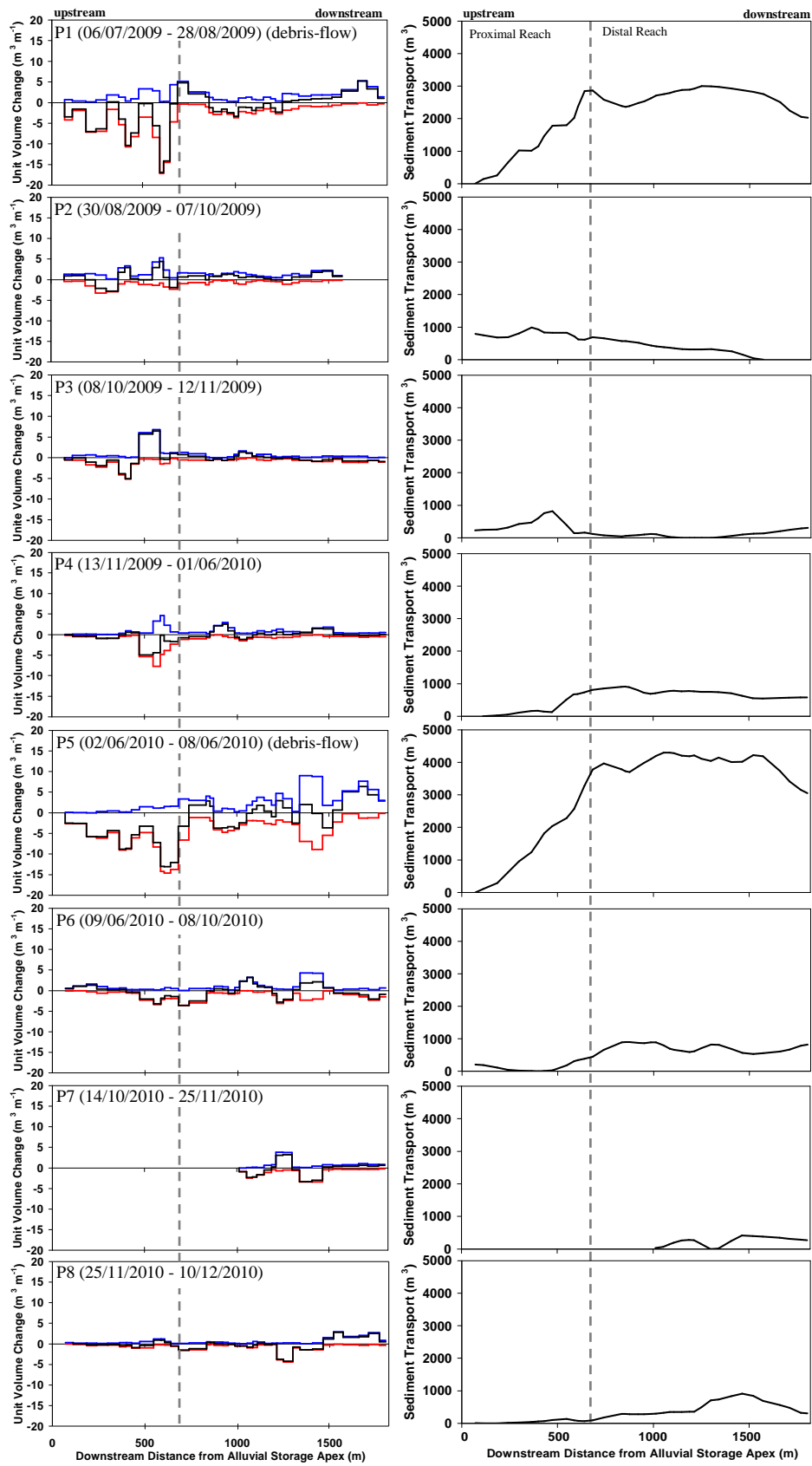


Figure 25 In-channel storage changes per unit length and sediment transport in the Manival Torrent for each time period investigated by cross-section and sediment trap resurveys; the general debris-flow entrainment extent (proximal reach) is indicated by the dashed grey line; blue line: deposition; red line: erosion; black line: net storage change



Figure 26 Photo sequence displaying channel scouring of the August 2009 debris-flow in the main channel of the Manival; views looking downstream

During P2 period (August 30 to October 7, 2009), a succession of small rainfall events with a maximum intensity of 17 mm h^{-1} induced moderate channel changes related to bedload transport, with a general storage gain of $789 \text{ m}^3 \pm 84$, homogeneously distributed along the study reach. A substantial part of the sediment loss from the August 2009 debris-flow was recharged during P2 (Figure 25) by the deposition of gravel wedges (the storage recharge was estimated to be between 33 and 41% given the uncertainty of the volume calculation). The sediment trap stayed empty during this period, meaning that an important amount of sediment had been delivered by the upper catchment (calculated between 736 and 842 m^3), despite the low rainfall. The main channel functioned as a sediment trap, capturing gravels coming from the upper catchment. A similar pattern of rainfall was observed during P3, with long duration and low intensity rainfall events, typical of the autumn season. A net storage loss of $89 \text{ m}^3 \pm 66$ was obtained. The sediment trap was disturbed by dredging operations; however, assuming zero input, the output could be estimated from the sediment transport trend to be $266\text{-}338 \text{ m}^3$ and a recharge from the upper catchment of $198\text{-}260 \text{ m}^3$. Channel responses were not very important, except in a small proximal reach where considerable gravel wedges accumulated in the channel, generating 1.2 m of deposition locally. Those gravel deposits were supplied by both channel scouring in the proximal main channel and sediment supply from the upper catchment. The P4 period (November 13, 2009 to June 1, 2010) included small rainfall events with low intensity (maximum of 10 mm hr^{-1}) during the early spring. A net storage loss of $580 \text{ m}^3 \pm 81$ was captured, without any sign of debris-flow activity. Again, the sediment trap was disturbed by dredging operations; however, assuming zero sediment input, the output could be estimated from the sediment transport trend to be $535\text{-}625 \text{ m}^3$ and a recharge from the upper catchment of $0\text{-}36 \text{ m}^3$. The most remarkable channel response was observed in the proximal reach, where a considerable remobilisation of the gravel wedges deposited during the P3 period was observed. It is possible that

those gravels were transported down to the sediment trap since no significant channel deposition was observed in the distal reach.

The most important debris-flow of the monitoring period occurred during P5 period which was initiated by a short duration convective storm that occurred the 6th June 2010. With the storm burst defined as a continuous rainfall according to a 5-minute time step, the duration was 2.3 hours with a total of 21 mm and a maximum 5-minute intensity of 25 mm hr⁻¹. The general pattern of erosion and deposition along the main channel was very similar to the one of the August 2009 debris-flow (Figure 25). A net storage loss of 3052 m³ +/-272 was obtained, which is equivalent to the sediment deposition in the trap, measured at 3320 m³ +/-176. Channel scouring of the proximal reach supplied most of the sediment output and the direct contribution of the upper catchment to the sediment yield was negligible. The debris-flow grew in volume along a reach of 600 m length and 18% slope, contributing ~4000 m³ to the distal reach and sediment trap. Despite the high intensity of the rainfall, the sediment supply from the upper catchment was low (higher-bound estimate of 537 m³). However, mud marks were observed upstream from the scoured reaches indicating that fine sediments were already present. They most likely originated from hillslope runoff and bank erosion.

The channel response after the June 2010 debris-flow was different than what was observed after the August 2009 event. The debris-flow occurred in early summer; for the rest of the summer (P6), a series of high intensity rainfall (range: 20-79 mm hr⁻¹) did not produce any debris-flows. The P6 period was the most active in terms of rainfall, but not the most sensitive in terms of geomorphic response. The proximal reach continued to scour, whereas some thin gravel wedges were deposited in the distal reach (Figure 25). A net storage loss of 608 m³ +/-82 was obtained. The sediment trap was disturbed; however, the output was estimated to be 773-865 m³ and a recharge from the upper catchment of 174-246 m³ was obtained. The August 2009 debris-flow lag and levee deposits were eroded during this period and accumulated into gravel wedges along the distal reach. Throughout autumn 2010 (P7 and P8), these gravel wedges gradually mobilized downstream into the sediment trap without substantial sediment supply from the upper catchment (Figure 25).

3.3 Sediment supply from first-order headwaters

Seasonal repeat TLS surveys of Manival headwaters from April to November 2009 revealed important elevation changes over time. At site S1, located in Figure 1, four DEMs of difference (the subtraction of a post and prior DEM) were produced during the period. From April to June and from June to August, the most striking change was a strong decrease of elevation in the proximal part of the gully, which had reached 3 to 5 m locally (Figure 27A and B). The loss in elevation was most dramatic between June and August even with rockfall deposits occurring just upslope. During this period, no convective storms occurred and no geomorphic activity was observed along the main channel of the

Manival. Moreover, no gain of elevation was observed in the distal part of the gully (confirmed with painted field marks), and it is difficult to imagine long travel distances of sediment without any significant rainfall. Therefore, the captured elevation changes in the proximal part of the gully should have been driven by the melting of buried snow accumulations of the winter which were mixed and recovered by rockfall deposits coming from the active rock wall (Figure 27C and D). Snow accumulations in shaded gullies resulted partly from snow avalanches, which are very frequent in the upper catchment of the Manival. The resulting DEMs of difference could not be integrated in the sediment budget analysis since most of the lost volume concerned snow (total volume loss: $754 \text{ m}^3 \pm 145$).

TLS resurvey of the S1 site during August (corresponding with P1) showed that a talus slope failure occurred in the proximal zone (Figure 28A). An erosion of 266 m^3 took place at the talus slope with 268 m^3 depositing 40 to 80 m down the gully. The net deposition of $2 \text{ m}^3 \pm 87$ shows very little input from the rock wall. No morphological change was observed further downstream in the gully. There were not any rainstorms or sustained rainfall throughout August 2009 until the debris-flow event. The small talus slope failure was most likely initiated during the storm event of August 2009 that generated a debris-flow in the main channel of the Manival. The remobilized sediments remained in the distal part of the headwater channel and for the rest of the monitoring period. Even though the S1 site was disconnected from the channel, other first-order headwaters were active and connected to the channel and the S2 and S3 site (locations in Figure 17).

TLS resurveys of S2 and S3 sites during August 2009 (P1 period) showed net erosion in the upper reach (S2, Figure 28C) and net deposition in the lower reach (S3, Figure 28E). No signs of a debris-flow were observed along these two reaches, and the morphological changes were induced by bedload transport. The confluences of the numerous left-bank (east-bank) gullies of the S3 site stayed unchanged, without any fan formation related to the deposition of hillslope debris-flows in the main channel. Laser scan observations for the following period (from August to November 2009, P2 and P3) showed the inverse situation, with net deposition in the upper reach (Figure 28D) and net erosion in the lower reach (Figure 28F). As for the previous period, these responses were related to bedload transport. During 2010, little geomorphic activity was observed in the 3 sites and no TLS surveys were implemented.

We acknowledge the fact that there may be an influence of check-dams (visible in Figure 28C-F) on sediment transfer. There were not any second- or third-order uncontrolled reaches available at the study site to make any comparisons. Furthermore, observations showed that erosion and deposition takes place at varying check-dam spacing for both debris-flow and bedload transport. Therefore, with the observed complexity and limited information we cannot make a detailed analysis on the effect of check-dams.

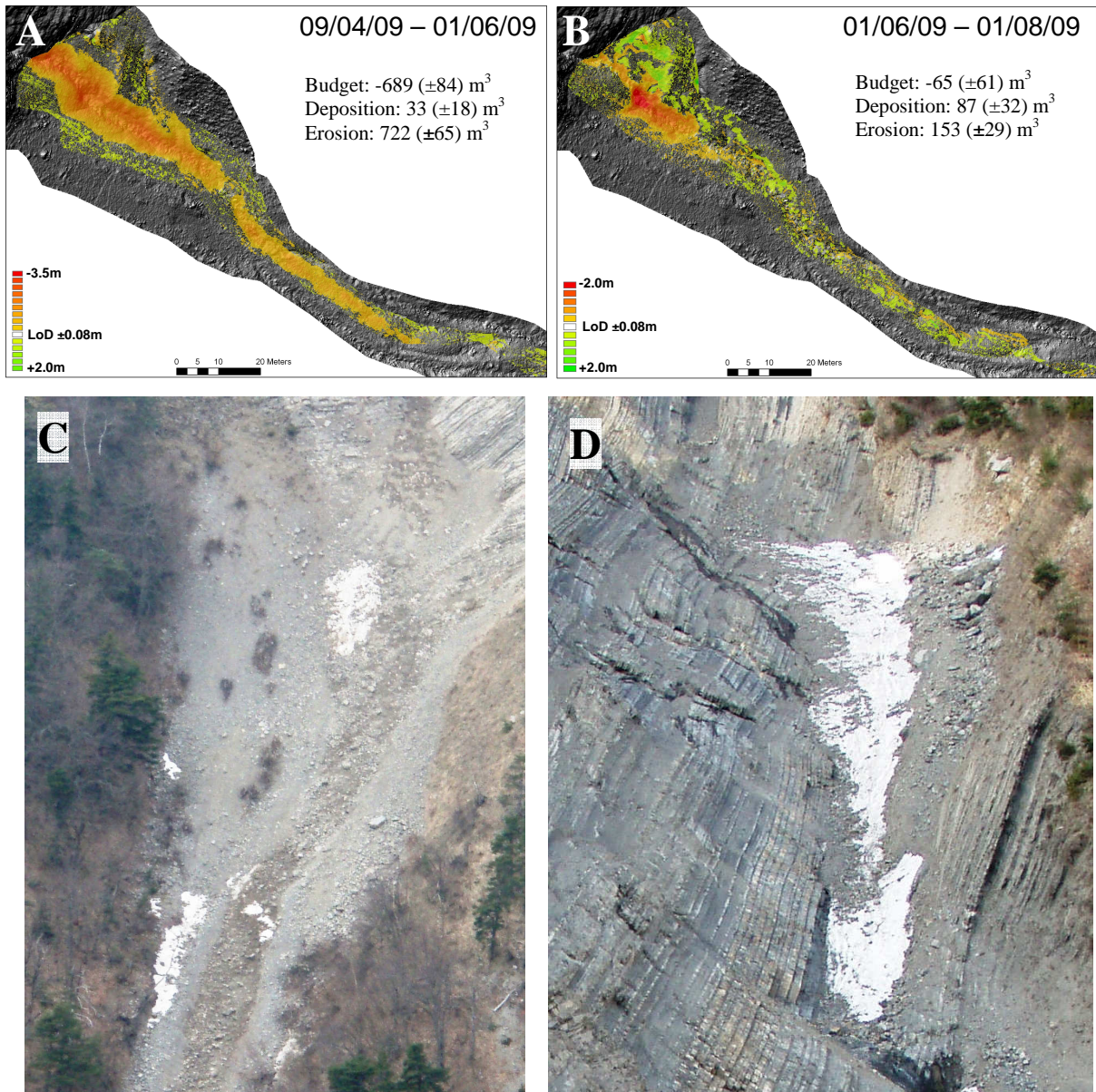


Figure 27 Snowmelt indicated by DEM of differences derived from TLS and ALS resurveys of the S1 site on the Manival from April to June 2009 (A) and June to August 2009 (B); LoD: level of detection of significant elevation change based on the RMSE of the merging process. View (C) is of the proximal zone of the S1 site where snow was mostly mixed in the deposits; view (D) is of the proximal zone of a typical first-order gully of the Manival showing snow accumulation partially covered by rockfall deposits

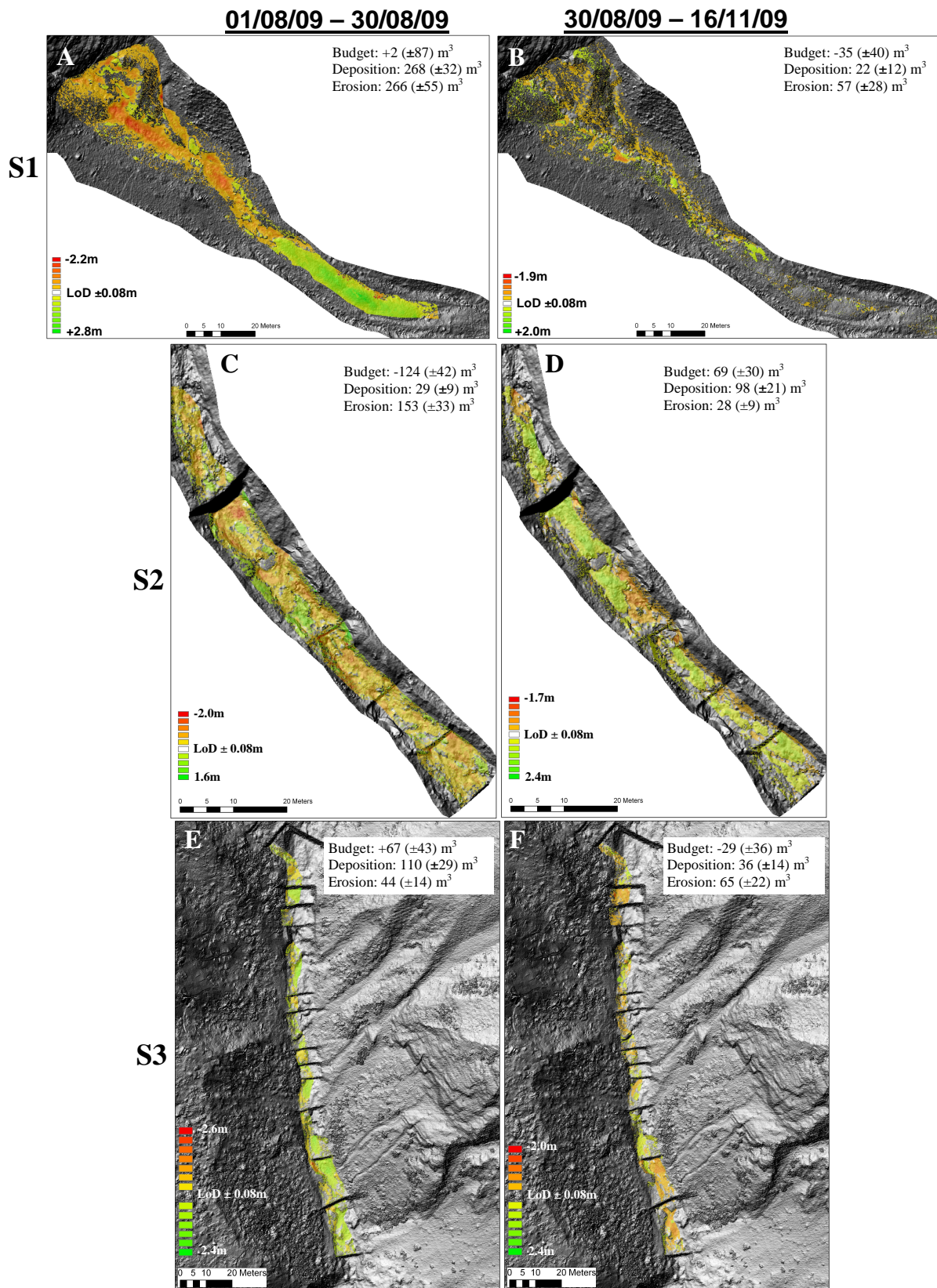


Figure 28 DEM of differences derived from TLS resurveys of the S1 (A and B), S2 (C and D) and S3 (E and F) sites on the Manival between August and November 2009; LoD: level of detection of significant elevation changes based on the RMSE of the merging process

3.4 Fluctuating channel storage over time

The initial channel storage for the main channel of the Manival torrent at the onset of the monitoring estimated to be 35 500 m³ according to the SLBL method. This value is in good agreement with the storage volume estimated by cross-section interpretation of the maximum debris-flow scouring surface, which gave a total volume of 31 500 m³. The storage estimates were subdivided in 3 functional reaches according to the geomorphic responses observed during the monitoring period: the proximal reach where maximum channel scouring was observed, holds an initial storage of 13 500 m³, the transport reach where an equilibrium was observed between erosion and deposition, with 13 800 m³ of storage, and the lower reach where deposition was higher than erosion, with a storage of 4 200 m³. After two years of monitoring, the total sediment storage decreased to 25 400 m³ (Figure 29) with the proximal reach losing 7 600 m³, the transport reach losing 700 m³, and the lower reach gaining 1 400 m³ (Figure 30). Most of the storage loss was induced by the two debris-flows, which remobilised 14% of the in-channel sediment reservoir. If only the proximal reach is considered, the two debris-flows evacuated 56% of the available storage.

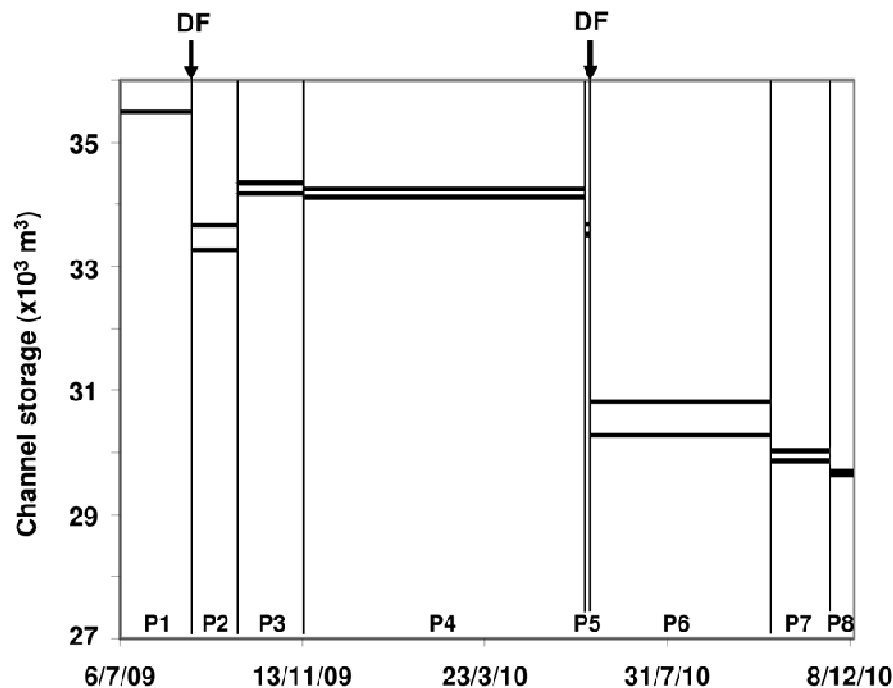


Figure 29 Evolution of in-channel sediment storage during the monitoring period along the Manival study reach. Upper and lower limits are plotted according to the calculated uncertainty. DF denoted debris-flow occurrences

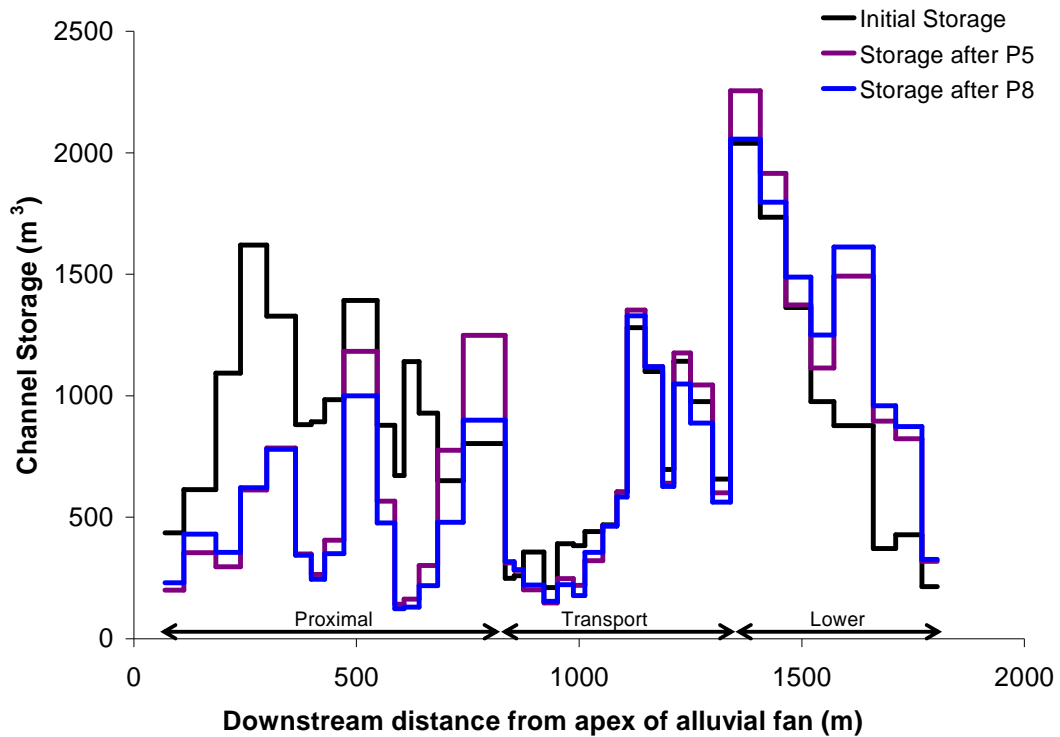


Figure 30 The distribution of the channel storage change during the monitoring period derived from cross-section interpretation of the maximum debris-flow scouring surface. Within the monitoring period, the proximal reach had a large storage loss, the transport reach had little change, and the lower reach gained in storage.

4 DISCUSSION

Gregoretti and Fontana, 2008) found that debris-flows in the Dolomites (Italian Alps) formed due to the scouring effect of critical discharge from peak runoff. They also found that the triggering areas are located where sediment is available and where overland flow can occur. Observations in the Manival Torrent are consistent with these findings; channelized debris-flows were initiated in the proximal reach of the main channel where most sediment storage is present. Triggering occurred during high intensity rainfalls. For the two debris-flow events, clear field observations upstream from the main channel showed that surface water runoff was initiated in the upper catchment producing water surges (indicated by high water marks). Morphological signatures of bedload transport were clearly detected in these upper reaches (sorted unconsolidated gravel deposits), without any signs of debris-flow propagation (unsorted levee, lobe, lag, and terminal deposits with a fine sediment matrix). Multiple surges occur in the Manival which we do not know when it transports sediment in the headwaters (before, during or after the main channel debris-flow). However, the sediment budgets indicate that

there was little sediment transfer between the channel and the upper catchment for all the surges combined.

Sediment budget reconstitutions showed that debris-flow volumes at the downstream end of the study reach are equivalent to net erosion along the main channel (Figure 25, Table 6). The direct contribution of hillslope erosion to debris-flow volume was insignificant, despite the occurrence of talus slope failures during storm events (Figure 28). Sediment transfer along the stream network was characterized by important spatial discontinuities during summer storms. Sediment coming from talus slope failures or gully stores stayed captured in the distal reaches of headwaters and did not propagate down to the main channel (Figure 28). A similar observation of sediment retention after a debris-flow in a second-order steep-slope channel was made at the Chalk Cliffs experimental site in Colorado (McCoy et al., 2010). These temporary storages in the Manival headwaters were released during long duration and low intensity rainfall events in autumn and were deposited as gravel wedges along the main channel, partly refilling the previous debris-flow scoured channel. The retention of sediment in headwaters during the summer induced the formation of low sediment concentration water surges in the proximal main channel, with a high erosive “hydraulic load” (Rickenmann et al., 2003). When these water surges entered the main channel, they rapidly scoured the channel and transformed into debris-flows.

The morphological responses to debris-flows along the main channel of the Manival torrent showed that debris-flow volumes increased by more than 3 orders of magnitude over streamwise distances of several hundreds of meters. Field observations reported for the Faucon Torrent in the French Alps revealed a similar increase of debris-flow volume by an incorporation of channel sediments, with scoured volumes of $\sim 10\,000\text{ m}^3$ along short reaches of 600 m (Remaître et al., 2005). Sediment budget analysis of debris-flow events reported for the Illgraben in the Swiss Alps showed that the debris-flow volume at the exit of the catchment were one order of magnitude higher than typical landslide volumes observed in the production zone (Berger et al., 2011b). The normalization of scoured volumes by reach length for the Manival gave mean yield rates in the proximal reaches of $5\text{ to }7\text{ m}^3\text{ m}^{-1}$, with maximum values of $17\text{ m}^3\text{ m}^{-1}$. These values are close to the $10\text{ m}^3\text{ m}^{-1}$ reported in the Eastern Italian Alps (Marchi and D'Agostino, 2004) and within the range of $3.6\text{ to }30\text{ m}^3\text{ m}^{-1}$ from the recent compilation of yield rates for confined debris-flows (Hungr et al., 2005).

The respective influence of debris-flow and bedload transport on channel deformations during flow events is of crucial importance for the understanding of mountain stream morphodynamics. Field observations of morphological responses to these two types of flows in a same channel are not very common. The intensive topographic monitoring of the Manival Torrent gave a unique opportunity to characterize sediment budgets for both flow types. Even though it was easy to determine if a debris-flow occurs during each monitoring period and then to compare morphological responses of periods with and without debris-flows, it was much more difficult to discriminate the effects of the two flow

types for the periods characterized by a debris-flow occurrence. In this latter case, channel deformations integrate the effects of both types since bedload transport is generally active during flow recession and between debris-flow surges. Our monitoring strategy was not designed to detect the variability of the flow properties during events and to cross-correlate with a high-frequency morphological signal. Without such information, it is not possible to unambiguously attribute scouring and filling phases to specific flow conditions. However, other field (Berger et al., 2011a) and experimental evidences (Mangeney et al., 2010) identify that the maximum scouring is related to the passage of the debris-flow front.

The influence of sediment recharge on debris-flows is quite evident in the Manival. Figure 29 and Figure 30 show a large decrease in channel storage after the June 2010 debris-flow (P5). This affected the channel's response to rainfall for the rest of the year. In Figure 31, rainfall burst intensity versus duration is plotted (bursts defined as a continuous rainfall, according to a 5-minute time interval). These bursts are identified to when the channel had storage (before June 2010 debris-flow), when the channel was without storage (after June 2010 debris-flow), and when a debris-flow occurred. The mean burst intensity and duration corresponds well with triggering thresholds from other monitoring sites (bursts defined with a 10-minute time interval) (Badoux et al., 2008; Coe et al., 2008). However, when the channel was without storage, there were rainfall bursts similar to ones which triggered debris-flows. If storage was available, these bursts could have triggered debris-flows and therefore changing the threshold. This is clearly shown with the maximum burst intensities in Figure 31. Unfortunately there is not enough data for calculating the different triggering thresholds; however a general range can still be observed (interpreted threshold range). The threshold range was approximately drawn to fit a line at the maximum extent for bursts with channel storage (lower-limit), and then a parallel line is drawn along the bursts which triggered debris-flows (upper-limit). This shows that the presence of storage controls the sensitivity of channel response to rainfall.

The general patterns of spatial and temporal variability of geomorphic responses in the Manival catchment is consistent with other recent reported monitoring studies on sediment dynamic in debris-flow channels (Remaître et al., 2005; Imaizumi et al., 2006; Fuller and Marden, 2010; McCoy et al., 2010; Berger et al., 2011b). The pulses of sediment supply from hillslopes during the winter accumulated in first-order channels and are transferred to their next higher order reaches during spring and summer storms by debris-flows. These observations can be summarized by a conceptual model of seasonal cycles of sediment routing from low to high-order channels (Figure 32).

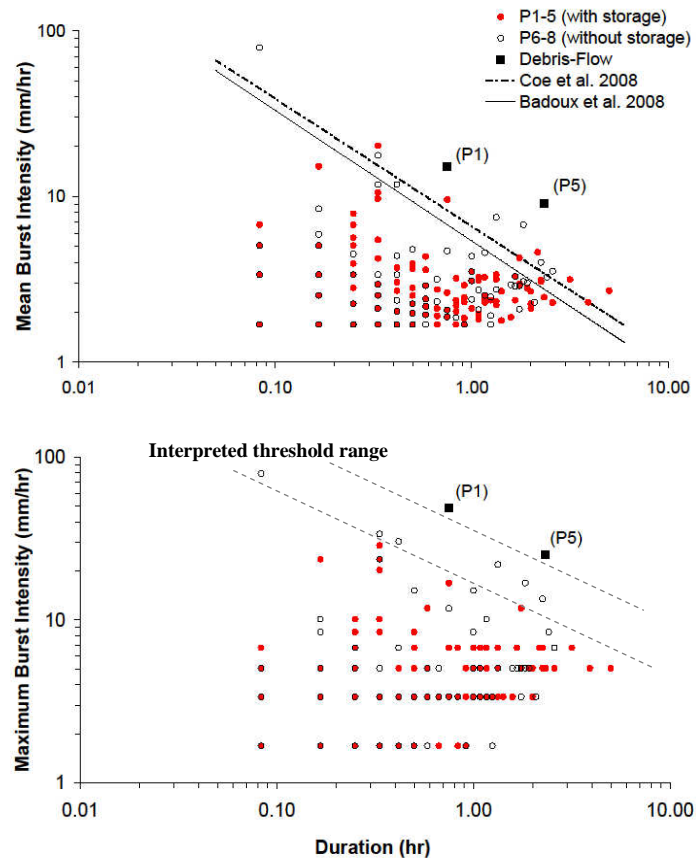


Figure 31 Mean and maximum rainfall burst intensities against burst duration. Bursts are grouped according to available storage (before P6 debris-flow) (filled-red) and the channel with minimal storage (after P6 debris-flow) (empty-black). Debris-flows (solid-black) correspond well with thresholds from other sites with burst calculations; however the presence of storage can influence the threshold line (interpreted threshold range).

The model incorporates different event intensities:

- (1) Low rainfall intensity events during spring and summer (1-2 yr return period) remobilizes sediment from first-order channels which have been recharged with debris during winter by slope processes (rockfall and snow avalanches). The debris may be entrained by slope failures generating short-travelling debris-flows, as observed by TLS survey of the S1 site during summer 2009 (Figure 28). We can also easily imagine that fine-grained debris may be mobilised as bedload by surface runoff and transported over short distances to second- or third-order channels. The net deposition observed for the third-order S3 site during summer 2009 is consistent with this scenario (Figure 28E). Even if the expected general trend for intermediate channels is deposition of debris coming from headwaters, it is possible to observe local channel scouring (Figure 28C). The stochastic nature of the sediment supply from

hillslopes during winter can explain heterogeneous conditions of debris coverage in first-order channels, and then variable conditions of sediment supply to intermediate channels during summer.

In high-order channels, the expected response during the summer is channel scouring by debris-flow entrainment of loose sediment accumulated during the preceding autumn. These debris-flows are formed by the sediment concentration increase of surface runoff when the flow starts to entrain sediment from the main channel. This has been consistently observed in the Manival during summer 2009 and 2010 (Figure 25), where the volume of the two debris-flows obtained in the sediment trap was equivalent to net erosion along the main channel. During autumn, high-order channels are expected to receive sediment coming from debris in intermediate channels that accumulated during the summer. These sediment transfers are governed by bedload transport, with rainfall intensities being generally insufficient to initiate debris-flows. Net deposition in the main channel during autumn 2009 confirmed this scenario (Figure 29). Qualitative observations made by the ONF-RTM38 after a small flow event in September 2008 (Peteuil et al., 2008) confirmed net deposition during autumn in the main channel of the Manival. It was not the case in autumn 2010, where net erosion was observed (Figure 29). This may be attributed to a low sediment supply from hillslopes during winter, which may explain low sediment availability in intermediate channels.

- (2) Intermediate rainfall intensity in the summer was not observed during the monitoring periods. However it can be assumed that the storage in the main channel is still evacuated out as a debris-flow. In the headwaters, longer travel distances would be observed with more continuity in the sediment routing. The headwater material could potentially contribute to the main channel debris-flow as well as depositing material in the main channel. In autumn, this new material would then continue to mobilize out of the channel in the form of gravel wedges.
- (3) Extreme rainfall intensity in the summer flushes sediment from first- to fourth-order channels out of the catchment system. An illustration of this is provided by the recent debris-flow history of the Manival. A large landslide occurred in the upper catchment during winter 1991, with a volume of 26 000 m³ estimated from ALS data (Figure 33). The archives of ONF-RTM38 revealed that during the summer of 1991, two important debris-flows occurred and deposited a cumulative volume of 25 000 m³ in the sediment trap. The large hillslope pulse depositing in the headwaters in the winter was essentially flushed out of the catchment during rainfall events in the summer.

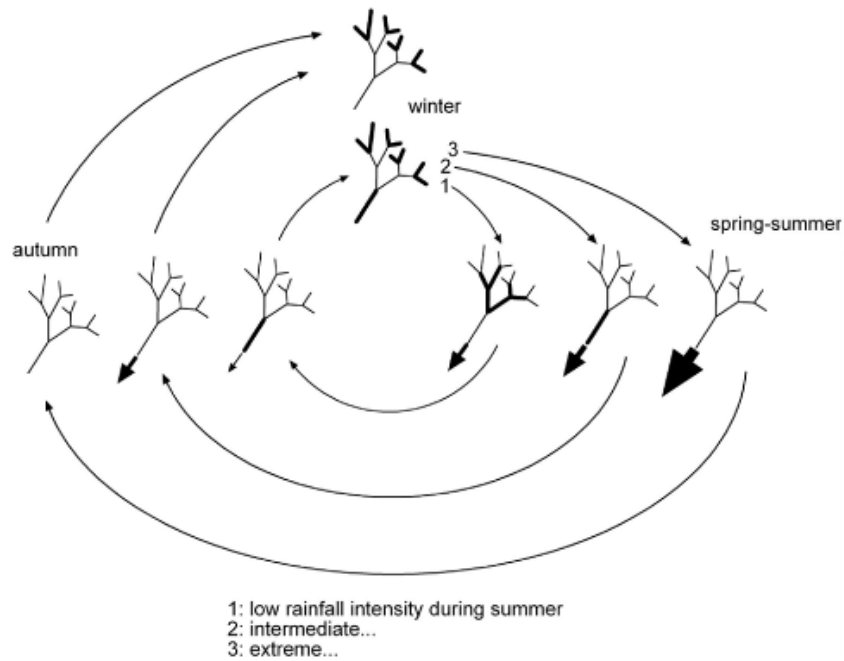


Figure 32 Conceptual model of seasonal cycles of channel scour and fill from first-order to high-order debris-flow channels according to level of storm intensity. Thickness of lines indicates the importance of storage. Seasonal cycles with low summer rainfall intensities have downstream progressing sediment waves initiated by pulses of sediment supply from hillslopes during winter. The cycle with intermediate summer storms has a summer flushing from the headwaters but large lag deposits continue to flush out in autumn. The extreme summer events have longer sediment routings which flush out most of the channels with minimal lag deposits during the summer storms.



Figure 33 View of a landslide ($26\,000\text{ m}^3$) in the upper catchment of the Manival which failed in the winter of 1991; during the summer of the same year, two channel-debris flows deposited a sum of $25\,000\text{ m}^3$ in the sediment trap

In the upper catchment of the Manival, a parallel study has been made by monitoring the sediment production for the cliffs and gullies using TLS (Loye, 2012). The seasonal variability of sediment supply from hillslope confirms the proposed conceptual model (Table 7, Figure 34, Figure 35, and Figure 36). Large amounts of rockfall have been observed during the P4-5 periods in which most were concentrated in the winter time (Figure 36). This season holds the most important recharge in the headwaters with 3 425 m³ of rockfall production.

The calculated sediment input of the torrent channel from cross-section surveys can be compared with the upper catchment production from TLS surveys (Table 7). The budgets are similar for the shortest time period P2-3 in the autumn which confirms the autumn recharge with bedload transport. However, volume comparisons for the P1 and P4-5 periods do not agree. This could be explained by the long periods (5-8 months) between scans where sediment transport may have been undetectable. Some important second- and third-order reaches were difficult to scan because of the ruggedness of the upper catchment. These reaches may have experienced important erosion and deposition which could not be measured (indicated as yellow in Figure 34, Figure 35, and Figure 36). Despite the rigorous field work involved with the main channel and upper catchment in both studies, there still needs to be a better scanning coverage in the channels and more correspondence of scans/surveys within each season.

Table 7 Overall headwater sediment budget recorded during the three survey periods and net sediment balance of the 16 months of monitoring. Back-calculated sediment input from cross-section surveys of the main channel and sediment trap are compared.

Survey periods	TLS survey of the upper catchment				XS survey of the main channel
	Rockfall (m ³)	Erosion (m ³)	Deposition (m ³)	Net budget (m ³)	Sediment input (m ³)
P1	99 (±6)	1184 (±93)	557 (±46)	-726 (±104)	0-63
P2-P3	50 (±3)	1162 (±46)	309 (±21)	-904 (±51)	934-1102
P4-P5	3425 (±21)	2592 (±92)	4269 (±176)	-1748 (±199)	0-573
Total	3575 (±30)	4938 (±241)	5135 (±251)	-3378 (±361)	934-1734

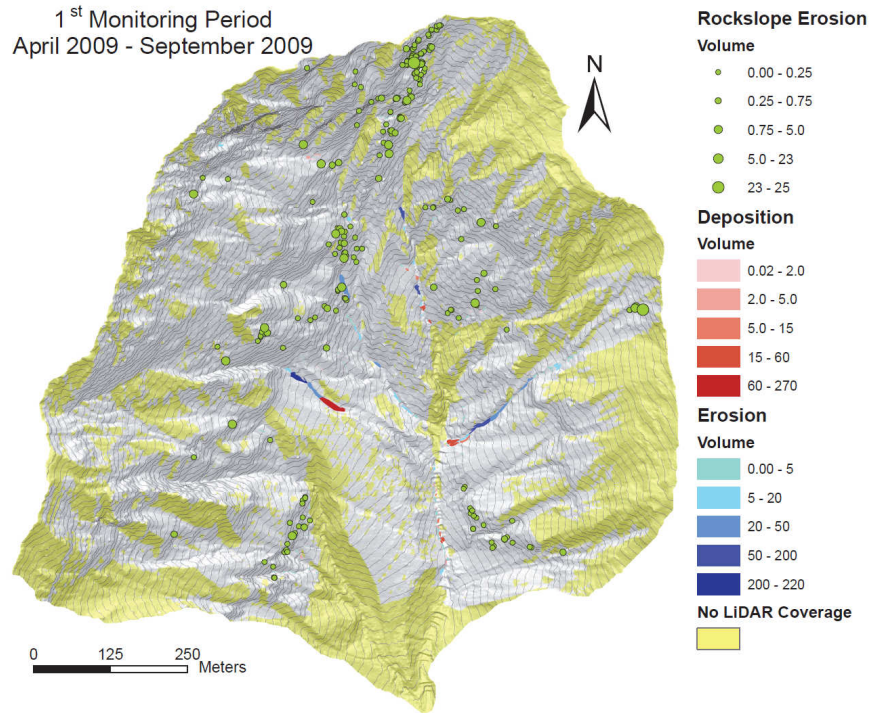


Figure 34 Geomorphic activity revealed by comparing the topographic differences of the two successive TLS surveys operated in April and August 2009 (from Loye, 2012).

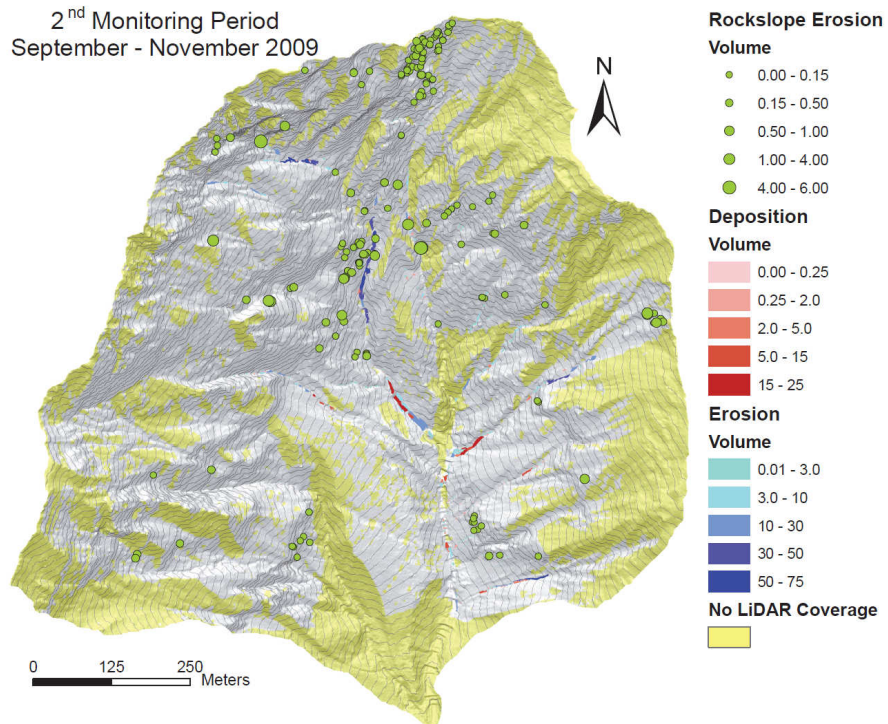


Figure 35 Geomorphic activity revealed by comparing the topographic differences of the two successive TLS surveys operated in August and November 2009 (from Loye, 2012).

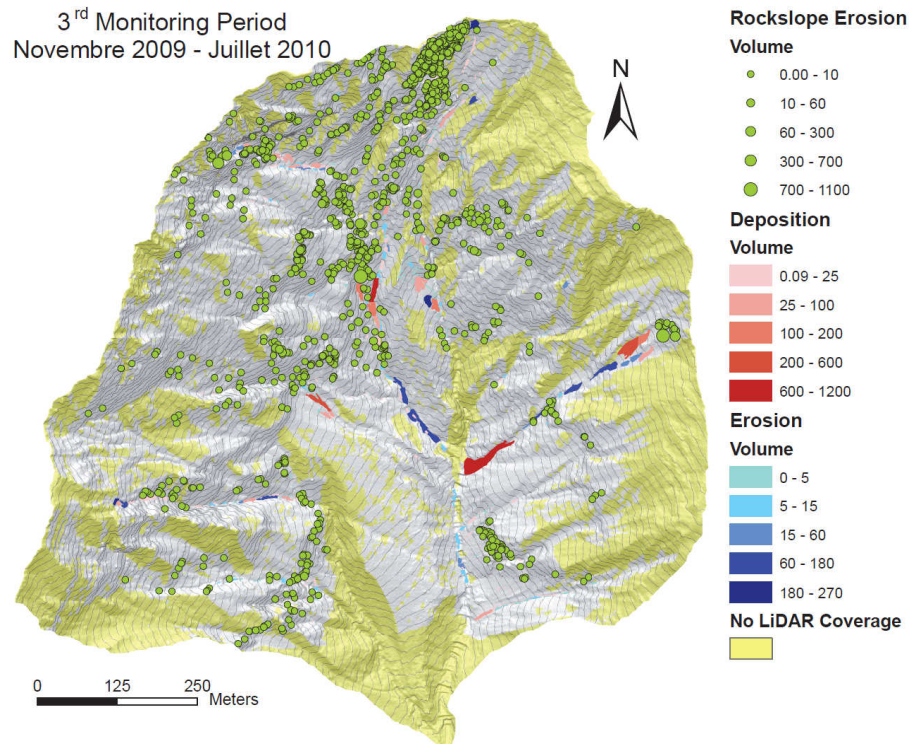


Figure 36 Geomorphic activity revealed by comparing the topographic differences of the two successive TLS surveys operated in November 2009 and July 2010 (from Loye, 2012).

5 CONCLUSIONS

This study revealed the importance of detailed catchment-scale field monitoring to understand debris-flow and bedload sediment transfer. Longer monitoring periods is needed for a more complete understanding of the proposed conceptual model. However, this study reveals important time shifts in scour- and fill-sequences in this active torrent catchment for common flow events. The two important processes, bedload (channel recharge) and debris-flow (channel scouring), are identified to be the seasonal forcings for sediment transfer in the torrent catchment. Finally, sediment pulses from hillslopes are the original control for these processes where further research is still needed.

The conceptual model provides a better understanding on seasonal cycles of scour and fill. Some authors provide similar sediment routing schemes but at a much longer timescale (Benda, 1990). The presented model provides valuable input for assessing current and potential hazards (seasonal and extreme). The determination of where and when important storages occur allows for more effective management in these catchments.

Chapter 4:
DEBRIS-FLOW PROPAGATION AND CHANNEL
INTERACTIONS: THE CASE OF THE REAL
TORRENT

1 INTRODUCTION

Debris-flows are known to have changing conditions during propagation. They entrain channels which gives an important volume growth to the flow (review from Hungr et al., 2005). Multiple surges often occur during one event which can coalesce into bigger and more mature surges (Zanuttigh and Lamberti, 2007). Sediment concentrations are known to be able to significantly increase and decrease during the propagation of the flow (eg. Pierson and Scott, 1985; Rickenmann et al., 2003). These changing characteristics of the flow can influence a varying height, velocity, discharge, and flow resistance of the material. For understanding these dynamic flow conditions and channel interactions, two typical methods are used 1) post-event surveying and 2) high-frequency monitoring stations.

Post-event surveys have been a widely used method for measuring channel morphology, sediment transport, debris-flow velocities, discharge, and even flow resistance. Traditional cross-section surveys have shown to be able to characterize yield and deposition rates which then characterizes the volumes and extents of debris-flows and bedload transport (Chapter 3, Fannin and Wise, 2001; Nyman et al., 2011). Debris-flow velocities and discharge are normally backcalculated from surveyed channel bends with superelevated flow heights using the forced vortex equation (eg. Hungr et al., 1984; Chen, 1987; Prochaska et al., 2008). Measured flow heights, velocity, and slope from the post-event survey are commonly used to backcalculate flow resistance coefficients to understand the viscosity and sediment concentrations of the debris-flows (eg. Rickenmann, 1999). For debris-flow channels, the accuracies of post-event survey are usually not compared with results from high-frequency monitoring stations, which are known to be the most accurate measurements of debris-flows (Arattano et al., 2012).

High-frequency monitoring of debris-flows is a difficult project to setup and maintain, however research groups are increasing these monitoring programs because of their capability for observing several parameters of the complex process (eg. Marchi et al., 2002; Arattano et al., 2012; Navratil et al., in press). Typical monitoring stations consist of geophones, ultrasonic sensors (or radar), and video cameras which satisfy the basic measurements of velocity, height, discharge, and visual validation. Only few monitored catchments have multiple stations distributed throughout the debris-flow channel and most of these are located only in headwater channels (Berti et al., 2000; Marchi et al., 2002; Hürlimann et al., 2003; McCoy et al., 2010; Arattano et al., 2012).

There are few studies that integrate post-event surveying and high-frequency monitoring together for observing debris-flows. Some studies have integrated topographic surveys of flow heights and superelevations at channel bends with high-frequency monitoring stations to increase the spatial resolution for observing the dynamic front of a debris-flow (Berti et al., 1999; Hürlimann et al., 2003; Tecca and Genevois, 2009). Other studies have integrated multi-date elevation models with the monitoring stations which were located in only one or two reaches (eg. Imaizumi et al., 2005; Schürch et al., 2011b; Staley et al., 2011). A pre- and post-event topographic survey of a whole channel length,

integrated with multiple monitoring stations is a unique study which will allow for observing downstream changes of debris-flow characteristics (eg. height, velocity, discharge, and flow resistance) and their interactions with the channel. The link between the channel morphology and the dynamics of the debris-flow has not been well observed. These important observations require detailed measurements spatially and temporally in the field which is very difficult to obtain with this unpredictable phenomenon.

This chapter presents the capability and reliability of post-event surveys for 1) measuring volumes of debris-flows and bedload transport from cross-sections and 2) backcalculating velocity and discharge from superelevated channel bends. The study is located in the Réal Torrent where both debris-flows and bedload transport occur every year. The topographic results are evaluated by direct comparisons with three high-frequency monitoring stations distributed throughout the torrent (each station equipped with three geophones, an ultrasonic sensor, and a rain gauge) (Navratil et al., 2012; Navratil et al., in press). With the two methods, a compiled dataset can be created with an unusual amount of information distributed throughout a whole debris-flow channel. The first objective is to characterize and analyze the sediment transport trends for debris-flows and bedload transport processes. The second objective is to quantify the changing properties of a debris-flow front (heights, velocities, discharge, volumes, and flow resistance) and analyze their interactions with the channel and with other surges (coalescence).

2 MATERIAL AND METHODS

2.1 Post-event field surveys

2.1.1 *Cross-section surveying*

Multi-date topographic surveying of cross-sections began on April 15, 2010 for monitoring channel erosion, deposition, and sediment transport in the study reach of the Réal torrent. Fifteen cross-sections were deployed along the 1.8-km study reach (Figure 37), at places expected to show high and representative morphological responses to flow events and giving a mean-cross section spacing of 120 m (5 times the mean active channel width). The remote character of the site induces costly and time-expensive field surveys. Therefore, we reduced the number of cross-sections to be able to complete a survey in one day. Wooden stakes on top of the channel banks were installed for cross-section benchmarking. Points were surveyed along transverse lines at each break of slope, and each measured point was marked with spray paint (10-30 points per cross-section). This saved time during subsequent surveys by only measuring the active portion of the cross-section (the portion where paint marks were

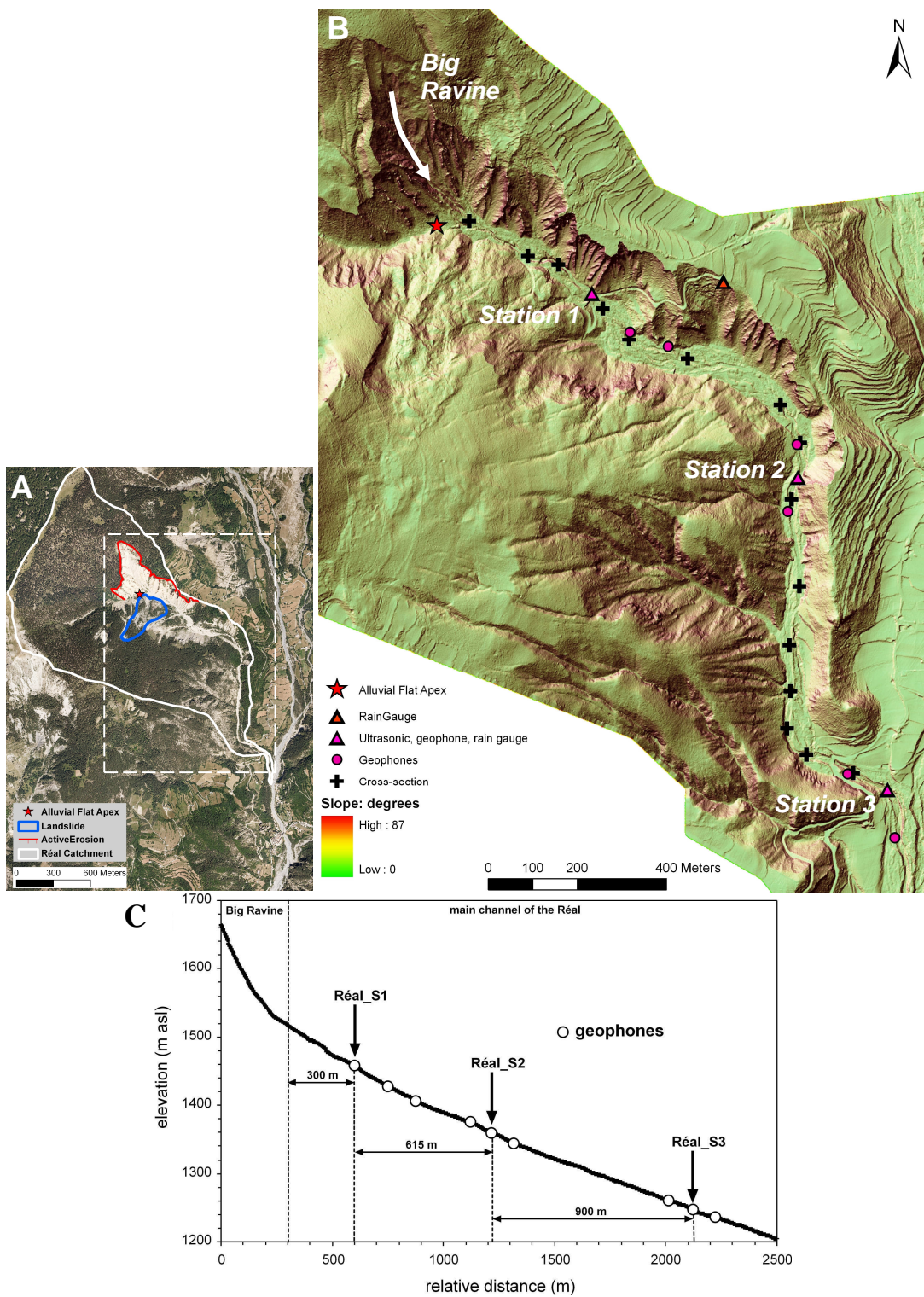


Figure 37 Réal torrent catchment (A); hillshade view of the torrent with cross-section and monitoring instrument locations (B); long profile from the sediment source “Big Ravine” to the confluence of the Tuébi River (C).

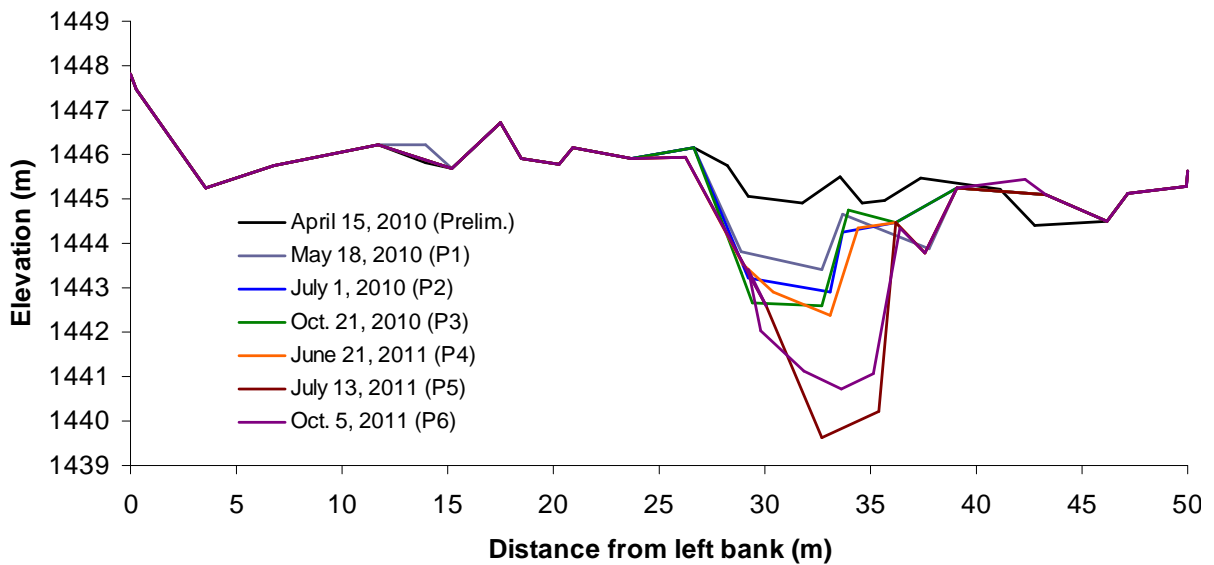


Figure 38 Example of the surveyed events for a cross-section 625 m downstream from the alluvial apex and 40 m downstream from the monitoring station Réal_S1. This cross-section has the highest yield rates for large torrent debris-flows. The preliminary surface of the active channel was full of sediment and was gradually eroded to almost 6 m during the monitoring period.

no longer visible). The mean point spacing was 0.6 pts/m. At least one day was required for surveying all the cross-sections. Topographic surveys were measured with a total station (Leica Flexline TS02). The ONF-RTM06 Forest Service overtook the cross-section surveying halfway through the monitoring program using a rangefinder and measuring staff..

The timing of topographic surveys was driven by the occurrence of flow events that were able to modify the torrent channel morphology. Figure 38 shows an example of a multi-surveyed cross-section for the entire monitoring period. However, the time-lapse between two successive events was sometimes too short to allow a perfect match between flow events and field surveys. It is important to mention that the debris-flows in these torrents are often in the form of multiple surges, whereas topographic surveys capture the time-integrated volume change of the torrent.

Cross-sections were used for quantifying volumes of erosion and deposition in the channel and back-calculating bed-material sediment transport using the method presented in Chapter 3 for the Manival torrent. The same method for calculating volume uncertainties is also used. After the installation of the monitoring stations, the cross-section volumes can be readjusted to match the station's volumes, which provide a more accurate estimate of sediment input.

2.1.2 Backcalculating debris-flow velocity

The largest debris-flow in the monitoring program which occurred on June 29, 2011 had multiple channel bends topographically surveyed. The debris-flow revealed large amounts of scouring and clear distinct mud marks throughout most of the torrent channel. The reflectorless laser from the total station was used to survey flow heights, profiles, and cross-sections located at 7 reaches (80-160 m lengths) where channel bends and high-frequency monitoring stations are both located. Velocities can be backcalculated using superelevations with the forced vortex equation (Prochaska et al., 2008) with the mean velocity (m s^{-1}) as:

$$v = \sqrt{\frac{R_c g \Delta h}{k b}} \quad (7)$$

where g is the gravitational acceleration (9.81 m s^{-2}), Δh superelevation height (m), k is the correction factor for viscosity and vertical sorting, and b is the flow width (m). R_c is the channel's radius of curvature (m):

$$R_c = \frac{360L}{2\pi\theta} \quad (8)$$

where θ is the angular difference (degrees) between two cross-section azimuths, and L is the measured arc length which is measured from three points in the channel bend (typically 15 to 20 m spacing).

Prochaska et al. (2008) shows that the scale of measurement for curvature influences the calculated velocities. However, little is known about the sensitivity of the correction coefficient k . This topic has not been thoroughly investigated in previous studies where k varies from 1-10 and in many cases, or the k is not used (ie. $k=1$). The coefficient can vary according to viscosity and vertical sorting which effects the superelevation (Hungri et al., 1984). This method has been identified to have approximately 20% uncertainty (Iverson et al., 1994) where in most cases the velocity estimates are too high (Jakob et al., 1997). The true k (Equation 7) and its sensitivity are determined in this study by comparing 16 velocity back-calculations to the velocities measured from geophones distributed within 1.5 km. The longitudinal distribution throughout the channel will also show the variation and trends of the debris-flow front conditions.

2.2 High-frequency debris-flow monitoring stations

Three high-frequency monitoring stations installed in October 2010 (detailed description in Navratil et al., in press) were used for comparing the results of the multi-date cross-section volumes and the back-calculated debris-flow velocities and discharges. For each station (Figure 39), an environmental datalogger CR1000 (Campbell®) was chosen for its very low energy consumption. The stations are powered by a battery (100 Ah) and a solar panel (55 Wc) providing their complete autonomy. Rainfalls were recorded with a 5 min. time step. Ultrasonic sensors and radar sensors (Paratronic®)

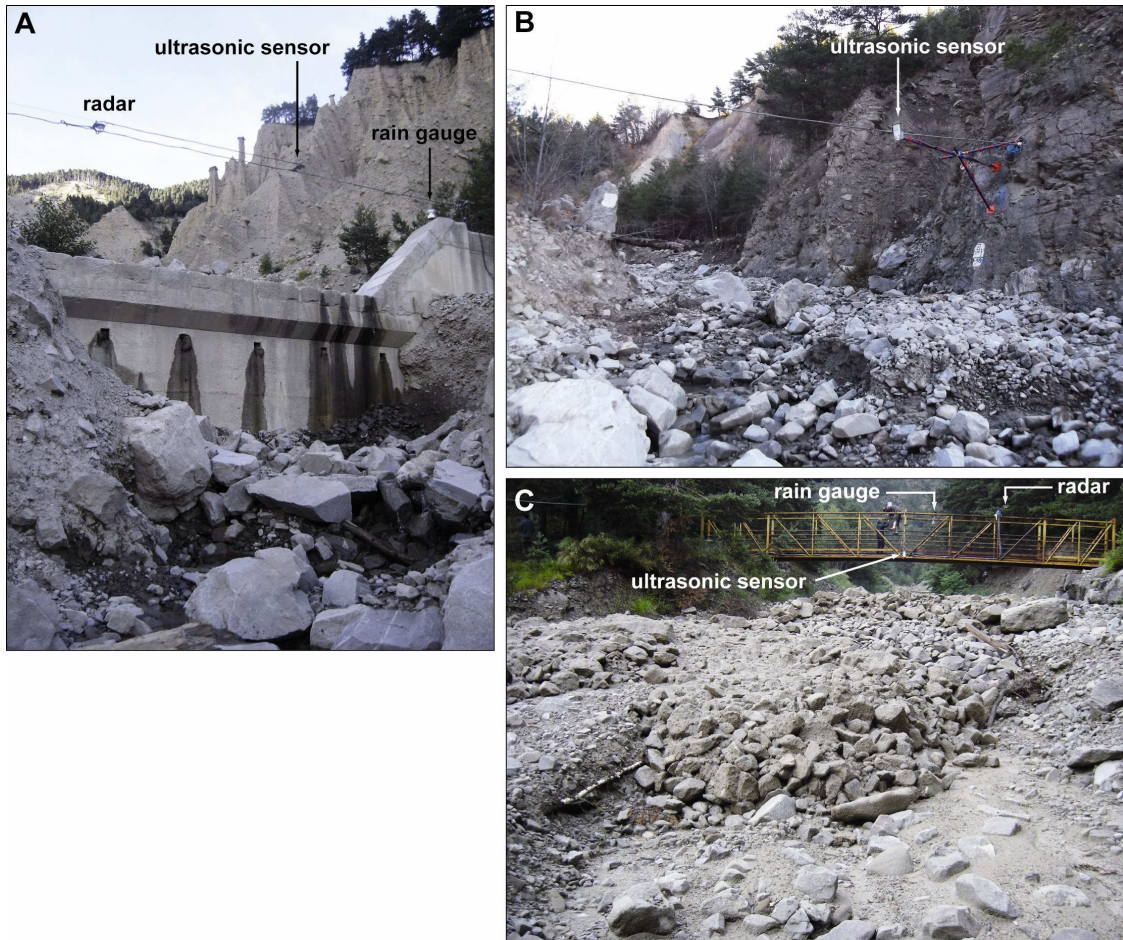


Figure 39 View of monitoring station 1 (A), station 2 (B), and station 3 (C) with additionally three geophones distributed 100 m apart along the channel (from Navratil et al., in press)

Table 8 Characteristics of the monitoring stations (from Navratil et al., in press)

Station Id.	Drainage Area (A_d km ²)	Elevation (m)	Eroded area (%)**	Channel slope (S)
Réal_S1	1.3	1450	30	0.195
Réal_S2	1.7	1340	20	0.123
Réal_S3	2.0	1254	18	0.095

* the remaining % corresponds to vegetated area

provide the flow level at the monitoring cross-section with high-frequency recordings (200 ms recording time-step). These elevations were used to compute the wetted surface area at each gauging cross-section. At the Réal_S1 (station 1), the gauging cross-section is located in a section controlled by a check-dam to guarantee morphological stability of the flow section. At the two other remaining sites, no check-dams were available; so flow section topography was regularly checked by the RTM service after each cross-section change. The passage of the front of the debris-flow generates significant soil vibrations at the vicinity of the torrent which can be recorded with geophones (e.g.

Marchi et al., 2002; Hürlimann et al., 2003; Itakura et al., 2005). In this study, at each site, we deployed sequentially three vertical geophones GS20DX0 Geospace® (natural frequency, 8Hz) near the flow section to record the front velocity of debris flows (distance interval of approximately 100 m; Table 8; Figure 39). They were used to estimate the surge velocity to compute the discharge and total volume of the water-sediment mixture. The monitoring stations were visited at least every 3 weeks and systematically after large flood events. A GSM communication was installed at each station in order to send a SMS alert when a heavy rainfall occurs, and to collect data samples each day to the office (5 min. time step recordings). This procedure allows also for checking regularly the status of the monitoring stations from the laboratory to avoid missing data.

3 RESULTS

3.1 Flow records

3.1.1 *Rainfall conditions and flow occurrence*

During the period of April 2010 to October 2011, six periods of recognizable geomorphic activity in the main channel were observed in the Réal torrent (denoted as P1 to P6 in Figure 40), three of these being characterized by the occurrence of debris-flows (E1, E2, and E6 events during P1, P2, and P5 respectively) (Figure 40, Table 9 and Table 10,). Events E3, E4, E5, and E6 are characterized as two processes, hillslope debris-flows in the upper reaches and water runoff in the lower reaches.

The 10-yr daily rainfall in the vicinity of the Réal was calculated using the rainfall time series of Péone (Météo France station of Péone, 1951-2010, elevation of 1659 m a.s.l, located at 4 km from the Réal, on the opposite hillside) and we obtained a value of 102 mm (90% confidence interval : 97-108 mm). The frequency analysis was based on a monthly sampling of maximum 24h rainfalls. The calculated return period of the maximum daily rainfall observed during the monitoring period was 1.0 yr. The maximum rainfall intensity (based on 5 min. time step recording) was observed during P5, with a value of 79 mm hr⁻¹. During P1, a maximum rainfall intensity of 21 mm h⁻¹ was sufficient to produce a debris-flow.

Rainfall conditions corresponding to individual flow events in the torrent are summarized in Table 10 (denoted as E1 to E7). The debris-flow events distinctly have a larger rainfall burst (Figure 41); however they are not always consistent with runout distances. Antecedent conditions are characterized by the total rainfall from the preceding week. However, there are not enough events to analyze the rainfall intensities, durations, and antecedent conditions with flow types and runout distances.

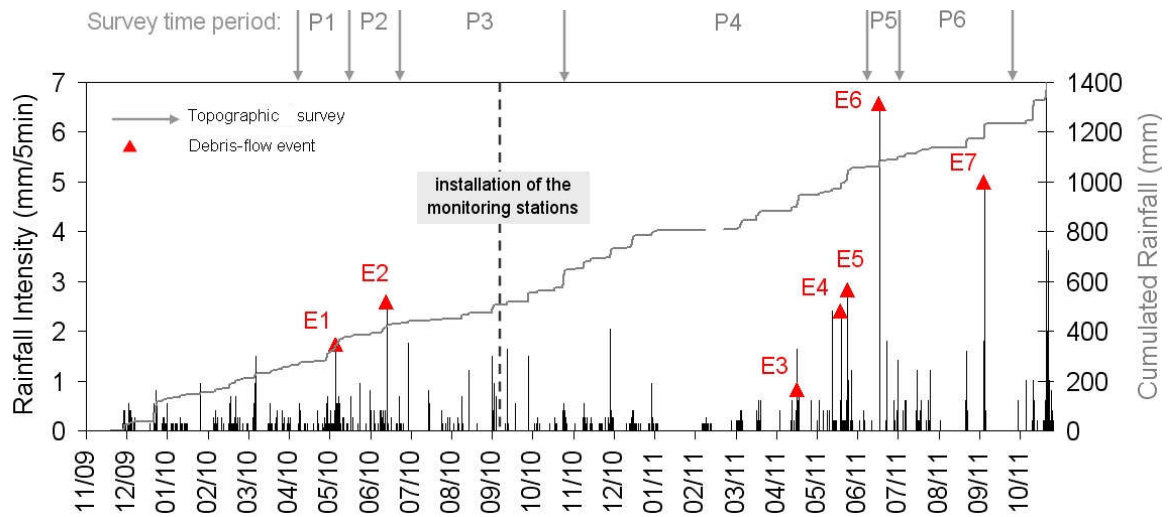


Figure 40 Rainfall characteristics during the 2009 – 2011 period. Rainfall intensity/volume, and occurrence of the main debris-flow events (red plots, E1 – E7; see Table 9) and the cross-section surveys (survey time periods P1 – P6; see Table 10).

Table 9 Survey time period of channel storage changes with total rainfall, maximum/mean intensities (with 5 min. recording) and flow observations. Events E1-E7 are described in Table 10.

Period Id.	Survey time period	Total rainfall (mm)	Maximum intensity (mm hr ⁻¹)	Mean intensity (mm hr ⁻¹)	Debris-flow/water run-off observation or monitoring
P1	15/04/10 – 18/05/10	100	21	3.0	E1
P2	18/05/10 – 01/07/10	57	31	1.3	E2
P3	01/07/10 – 21/10/10	130	21	1.1	5 rainfall events with $I_{max} > 12 \text{ mm hr}^{-1}$
P4	21/10/10 – 21/06/11	499	34	2.2	E3, E4, E5
P5	21/06/11 – 13/07/11	41	79	1.9	E6
P6	13/07/11 – 05/10/11	143	60	1.8	E7

Table 10 Debris-flow events observed during the 2010-2011 period and rainfall characteristics. For several events, debris-flow was observed only in the upstream part (*upper*) of the torrent, with no flow or only water-runoff in the lower part (*lower*) of the catchment (i.e. E3, E4, E5, E7).

Event Id.	Date	Type of flow		Rainfall Volume R_v (mm)	Rainfall Duration D (hr)	Maximum Intensity I_{max} (mm hr ⁻¹)	Rainfall volume during the preceding week (mm)
		Debris flow	Water runoff				
E1	10/05/2010	✓		6	1	21	48
E2	18/06/2010	✓		6	0	31	24
E3	28/04/2011	✓ <i>upper</i>	✓ <i>lower</i>	47	28	10	30
E4	31/05/2011	✓ <i>upper</i>	✓ <i>lower</i>	18	4	29	10
E5	05/06/2011	✓ <i>upper</i>	✓ <i>lower</i>	40	12	34	37
E6	29/06/2011	✓		39	1	79	1
E7	17/09/2011	✓ <i>upper</i>	✓ <i>lower</i>	45	5	60	0

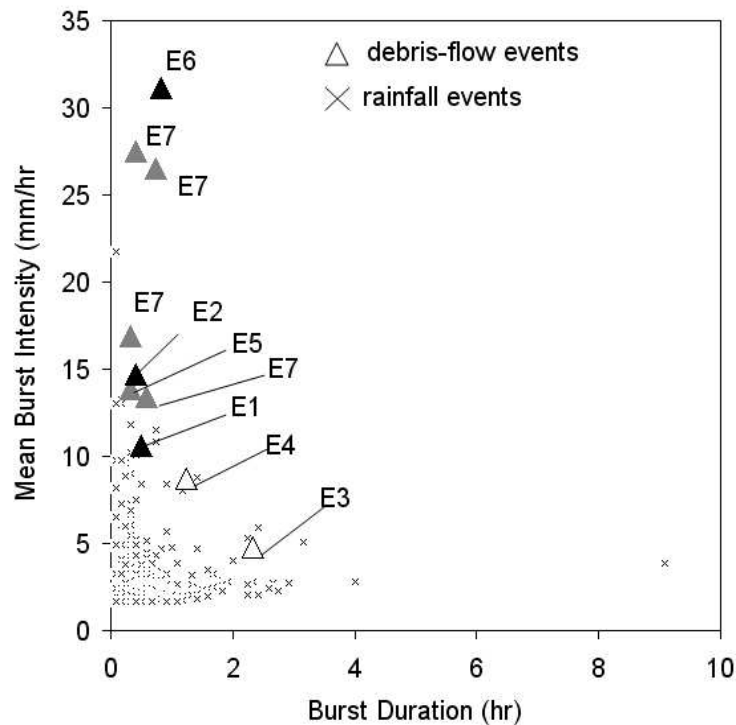


Figure 41 Mean burst intensity vs. duration of the rainfall burst; the mean burst intensity is associated only with the rainfall that triggered each debris-flow surge. E1 – E7 referred to Table 9. The runout distance was shown with a grey-scale: in black, the debris-surge propagated up to Réal_S3; in grey, up to Réal_S2; in white, up to Réal_S1. E7 was composed by four individual bursts (for details see Navratil et al., in press).

3.1.2 Event descriptions and results (P1-P6)

The channel response and sediment budget are reconstructed for the Réal during six investigated periods summarized in Figure 42. Yield and deposition rates are given with their budgets distributed downstream from the apex of the alluvial flat (very similar distance from the “Big Ravine”). The cumulative budget travelling downstream composes the volume passing for each given flow event. For P1 to P3, monitoring stations have not been installed yet and therefore the sediment inputs and outputs of the channel could not accurately be determined. Therefore these values give the minimum volume estimates since all volumes passing must be above zero. For P4 to P6, the topographically measured volumes are corrected by adding an offset volume so that they will match the most accurately measured volume from the monitoring stations. This allows for giving a proper estimate of the sediment input and output of the channel.

Proximal, intermediate, and distal reaches are divided according to the monitoring station locations which also distributes the different geomorphic responses appropriately (Figure 42). Transport volume in each reach is characterized by interpreted flow processes with black (debris-flow) and grey (bedload transport, or hyperconcentrated flow). Debris-flows have a sharp distinct increase of height in the

hydrographs, with a triangular-tail (Navratil et al., in press). Hyperconcentrated flows have an elongated front and tail with typically smaller flow heights than debris-flows. Morphologically, it is more difficult to distinguish event types. Typically, if there are no debris-flow features (levees, lobes, unsorted channel deposits with sandy-clay matrix) distributed throughout the channel, then we say that there were no debris-flow pulses. In this case, mostly unconsolidated well sorted gravels are found in the channel.

P1: April 15, 2010 – May 18, 2010

During P1, a small convective storm initiated a debris flow on the 10th of May 2010 (E1). The storm surge duration was 20 minutes with a total precipitation of 5 mm and a burst intensity of 21 mm hr⁻¹. In the proximal reach, the debris-flow volume grew by approximately ~2 000 m³ and continued to grow in the intermediate reach through channel scouring to at least 5 200 m³. The flow diverged into two channels and converged into one channel in the intermediate and distal reach indicating that there were multiple surges during the event. Large levees and lobes are typical in these locations as well. The total channel contributed 4 100 ±110 m³ which most of the sediment transported through the distal reach and into the Tuébi River. The input was determined to be insignificant according to field observation of a small hillslope debris-flow featuring terminal lobes just upstream of the proximal reach (Figure 43).

P2: May 18, 2010 – July 01, 2010

One month later, 18th of June 2010, another debris-flow occurred during P2. A 20-minute duration convective storm surge triggered the event with a total precipitation of 6 mm and a burst intensity of 31 mm hr⁻¹. The trends of proximal and intermediate reach erosion and distal reach transport and deposition were similar to P1. The local channel scouring in the proximal reach had a maximum scour depth of 3.9 m. Despite the short time interval between events, there was a significant sediment output which estimated to be 4 300-4 500 m³ (similar to P1). A net storage loss of 3 100 ±120 m³ was obtained, and a sediment input comprised between 1 250 and 1 350 m³. In the field another hillslope debris-flow was observed from the same gully as during P1, where this time scouring and deposition extended further into the proximal reach (Figure 43).

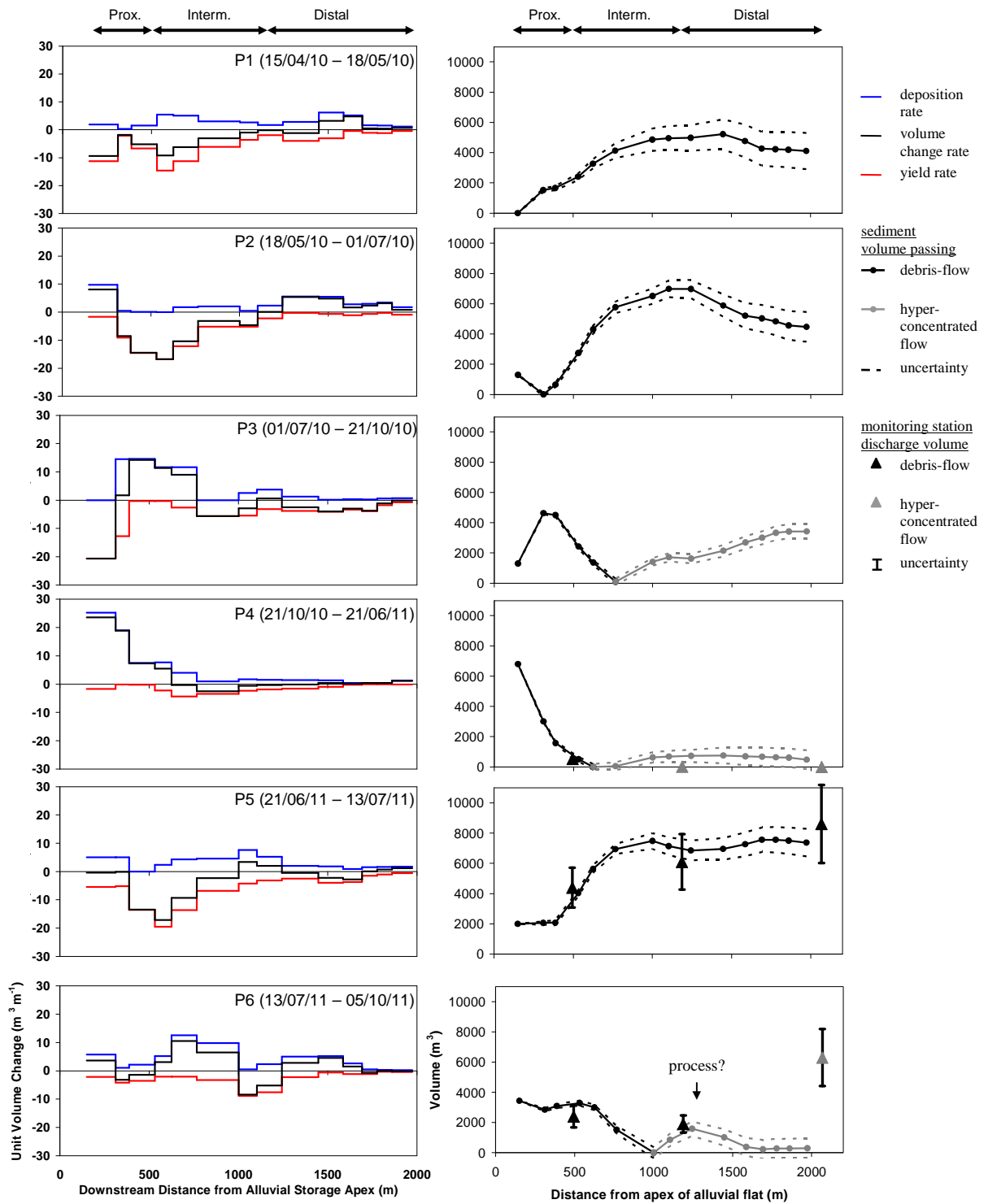


Figure 42 Yield (red), deposition (blue), and unit volume change (black) rates from measured cross-sections for all events (P1-6). Total volumes of events passing through for all monitored periods are presented with comparisons from the monitoring stations (P4-6); processes types are indicated by black (debris-flow) and grey (water-runoff or hyperconcentrated flow). Stations without marked uncertainties are too small to display.

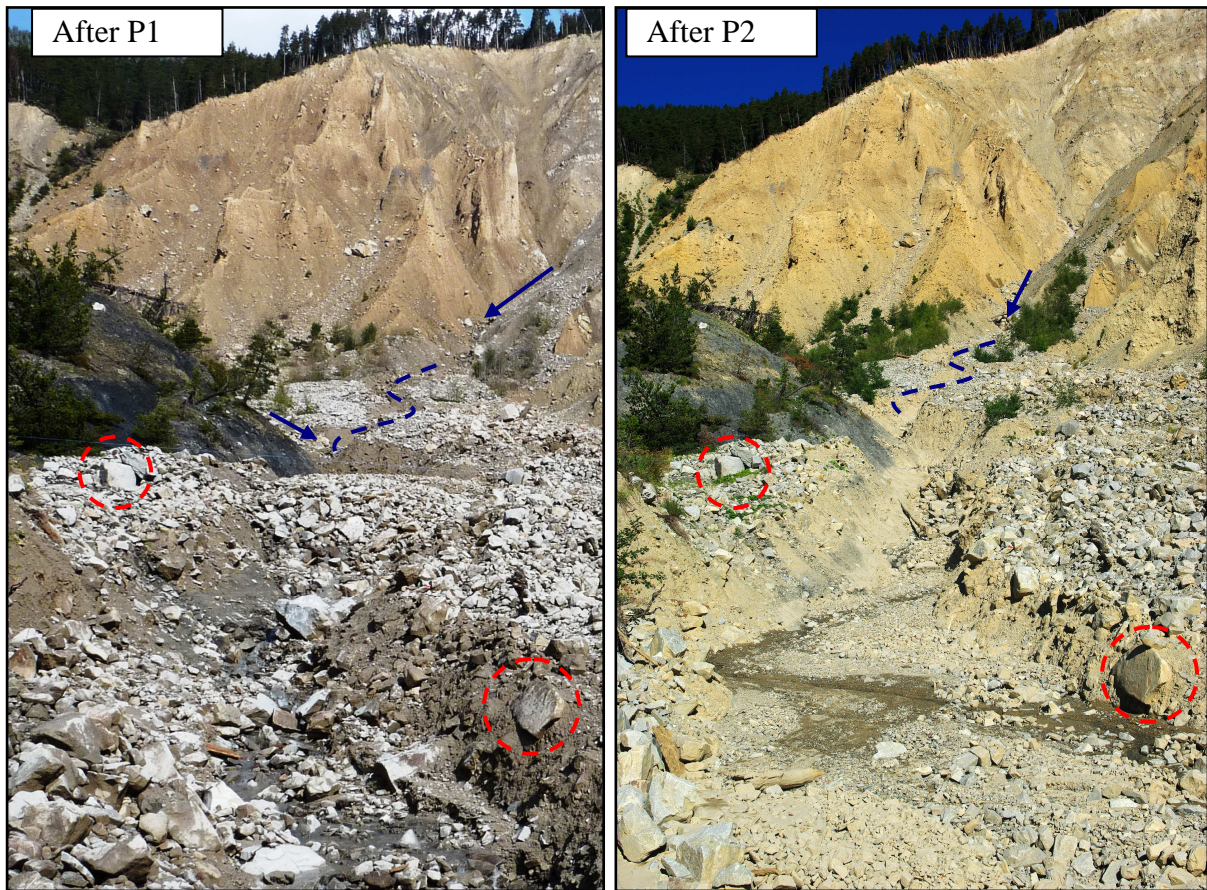


Figure 43 Photographs taken after P1 and P2 looking upstream at the alluvial storage apex and the Big Ravine. Hillslope debris-flows can deposit and erode material when entering the torrent.

P3: July1, 2010 – October 21, 2010

During P3 in the late summer and autumn of 2010, we observed the propagation of gravel wedges along the main channel. This period was characterized by long duration rainfalls with a comparatively high maximum intensity of 21 mm hr^{-1} . Sediment input of $1\,200\text{--}1\,400 \text{ m}^3$ was deposited into the proximal reach. It is not sure whether hillslope debris-flows deposited material in the proximal reach and the beginning of the intermediate reach, during the four month period of P3. However, the bedload transport occurrence was quite apparent at the end of the period with unconsolidated sorted gravels. In the lower part of the intermediate reach and the distal reach, channel storage (mostly from the previous debris-flow deposits) was gradually transported out into the Tuébi River with $3\,400 \pm 500 \text{ m}^3$ of sediment output. Here significant gravel wedges of approximately $4\,600 \text{ m}^3$ were developed according to the magnitude of the sediment transport trend of erosion and deposition. The net storage loss of the channel was measured with $2\,200 \pm 140 \text{ m}^3$.

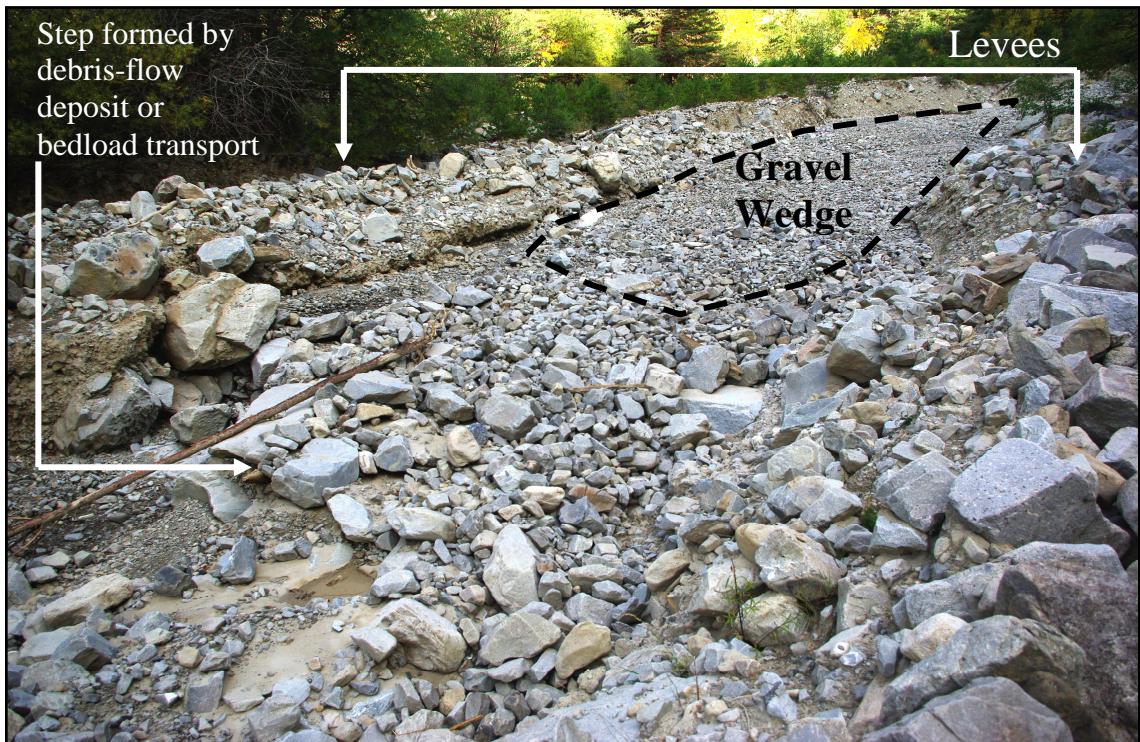


Figure 44 Photograph of the torrent (after P3) showing the multiple processes; debris-flow levees, debris-flow channel deposit (or a developed step from bedload transport) with the build-up of a gravel wedge behind it from bedload transport

P4: October 21, 2010 – June 21, 2011

The P4 period carried through the winter and spring of 2011 where activity has not been observed until April 28 to June 5, 2011. This period was characterized by long duration rainfalls with a comparatively high maximum intensity of 34 mm hr^{-1} . Monitoring stations were in operation during this period and the next two periods providing more detailed surge descriptions including time, flow type, maximum flow height, front velocity, peak discharge, and volumes (Table 11).

A 28-hour rainstorm with a maximum burst intensity of 10 mm hr^{-1} triggered the E3 event (28/04/2011). Two debris-flow surges were observed only in Station 1 (Table 11). Three days later a four hour rainstorm with a maximum burst intensities of 29 mm hr^{-1} triggered the E4 event (31/05/2011). Observations were again located only in Station 1 with one debris-flow surge.

In the next week another rainfall (12 hr) with maximum burst intensity of 34 mm hr^{-1} triggered the E5 event (05/06/2011). Station 1 observed 4 pulses of one debris-flow and three hyperconcentrated flows with one minute intervals. The first pulse was a debris-flow with the most significant magnitude. Station 2 observed only one hyperconcentrated flow and Station 3 had no observations.

P4 topographic surveys represent the combined events E3-E5. The proximal reach gained 6 800 m³ of material from the active gully as mostly hillslope debris-flows which were verified in Station 1. The intermediate reach experienced moderate channel scouring of 690 m³ in the form of bedload processes (hyperconcentrated flows according to Station 2). Almost all of this scoured material continued to propagate through the distal reach and into the Tuébi River in undetectable magnitudes at Station 3.

P5: June 21, 2011 – July 7, 2011

The most intense rainstorm for the entire monitoring period (max. burst 79 mm hr⁻¹, 1 hour storm) triggered the largest debris-flow (E6) on June 29, 2011. The back-calculated volumes from the topographic surveys indicate that 2 000 m³ of material from the gully was transported into the proximal reach. Scouring and levees were distributed throughout the reaches. The volume grew into 4 000 m³ passing through Station 1. This station observed 8 pulses of 2 debris-flows and 6 hyperconcentrated flows with intervals ranging from 1-10 minutes (Table 11). The sixth pulse is a debris-flow having the most significant magnitude and 2.5 minutes later the next important and faster surge (HF) passed through. The combined surge volume accumulates to 4 400 m³.

Topographic surveys in the intermediate reach between Station 1 and Station 2 indicate very large scouring of 3 500 m³ with 6 900 m³ passing through Station 2. Levees and lobes were also distributed throughout the reach. The channel diverges into two different flow paths and then converges in the intermediate reach indicating that multiple pulses occurred. Station 2 observed four pulses which two were debris-flows and two hyperconcentrated flows with intervals ranging 1.5 – 6 minutes (Table 11). The fourth pulse is the only significant surge (DF) with a large peak discharge.

Topographic surveys in the distal reach, between Station 2 and Station 3 indicate a small channel loss of approximately 500 m³ with a total volume 7 400 m³ passing through Station 3. Levees and lobes were again distributed throughout the reaches with distinct high mud marks on trees and channel bends. Station 3 observed one large debris-flow pulse for the entire event (Table 11). This single pulse volume is larger than the combined pulses at Station 2 which suggests that the pulses coalesced.

P6: July 13, 2011 – October 5, 2011

A five-hour storm occurred with a maximum burst intensity of 60 mm hr⁻¹ triggering event E7 (17/09/2011). A large sediment pulse of 3 400 m³, mostly from the “Big Ravine”, deposited into the proximal and intermediate reaches (according to the back-calculated topographic surveys). Station 1 observed five pulses with two debris-flows and three hyperconcentrated flows with intervals ranging from 2 – 40 minutes (Table 11). The most significant pulse was the fourth (DF). The combined pulses accumulates to 2 400 m³ passing through Station 1.

Table 11 Physical properties of flow events in the Réal Torrent measured from the three monitoring stations. (modified from Navratil et al., in press)

Survey Period	Event Id./ Date	Station	Surge Id.	Flow Type*	Time (UTC) (hh:mm:ss)	Max. Height H (m)	Front Vel. v (m s ⁻¹)	Peak Disch. Q (m ³ s ⁻¹)	Total Volume V (m ³)	
P4	E3 28/04/2011	S1	1	DF	22:33:57	0.3	0.7	0.8	100	
		S1	2	DF	22:38:38	0.2	0.7	0.6	80	
		S2	---	---	---	---	---	---	~0	
		S3	---	---	---	---	---	---	~0	
	E4 31/05/2011	S1	1	DF	17:48:11	0.3	0.7	0.8	70	
		S2	---	---	---	---	---	---	~0	
		S3	---	---	---	---	---	---	~0	
	E5 05/06/2011	S1	1	DF	07:37:17	0.3	1.4	1.8	100	
		S1	2	HF	07:39:40	0.2	1.2	1.1	40	
		S1	3	HF	07:40:26	0.3	1.3	1.6	70	
		S1	4	HF	07:41:52	0.3	1.2	1.4	60	
		S2	1	DF	07:50:41	0.5	0.6	1.2	60	
		S3	---	---	---	---	---	---	~0	
	P5	E6 29/06/2011	S1	1	DF	13:02:12	0.7	1.6	3.5	190
			S1	2	HF	13:05:30	0.4	1.7	2.3	110
S1			3	HF	13:06:42	0.5	0.2	2.6	60	
S1			4	HF	13:08:33	0.6	1.4	2.9	200	
S1			5	HF	13:18:08	0.6	0.3	0.7	10	
S1			6	DF	13:19:26	1.9	4.2	32.3	1,900	
S1			7	HF	13:23:00	1.3	4.5	22.1	1,200	
S1			8	HF	13:23:54	1.0	2.3	12.5	730	
S2			1	HF	13:16:55	0.6	0.9	1.9	170	
S2			2	DF	13:18:24	1.1	1.1	6.4	420	
S2			3	DF	13:22:57	2.0	3.5	50.0	3,000	
S2			4	HF	13:29:16	1.2	1.2	8.0	2,500	
S3			1	DF	13:28:43	2.0	2.7	33.4	8,600	
P6	E7 17/09/2011	S1	1	DF	15:54:25	0.5	1.4	2.4	450	
		S1	2	HF	16:10:42	0.5	0.4	0.7	300	
		S1	3	HF	17:20:30	0.4	1.3	1.8	40	
		S1	4	DF	17:22:08	1.2	1.5	6.5	1,400	
		S1	5	HF	18:02:15	0.6	0.5	0.8	230	
		S2	1	HF	16:06:25	0.4	1.5	1.7	420	
		S2	1	DF	17:27:17	1.2	1.3	8.4	850	
		S2	2	DF	17:32:29	0.7	1.4	3.7	650	
		S3	1	HF	17:32:59	1.6	2.5	18.2	6,300	

* Flow patterns' definition is based on the maximum water level gradient during the rising of the flow elevation: the surge corresponds either to a debris-flow (DF) with a rapid rising stage (<1 s.) or a hyperconcentrated flow (HF; >1s.).

** Total volume of water and sediment

Topographic surveys in the lower part of the intermediate reach indicate that channel scouring occurred with an accumulation of ~1 000m³ passing through Station 2. This station observed three pulses of which two were debris-flows with intervals of 21 and 5.2 minutes. The second pulse (DF) is the most significant in discharge. The combined pulse volume accumulates to 1 900 m³ passing through Station 2.

The topographic surveys in the distal reach show a sequence of scouring and redeposition of 1 600 m³ which is typical for the development of gravel wedges in the torrent channels. This indicates that there was bedload transport from Station 2 to Station 3 with very little sediment output (~300 m³). Station 3 observed only one pulse which was a hyperconcentrated flow of 6 300 m³. The important difference between the calculated volumes can be explained by the limitations of the monitoring station for quantifying sediment volume for surface water runoff processes.

3.1.3 Debris-flow volume measurement comparisons

Multi-date cross-section surveying and high-frequency monitoring stations have variable comparisons of volume measurements for sediment transport (Table 12). It should be mentioned again that the cross-section measurements for sediment transport volumes had a corrected volume from the monitoring stations to account for sediment input. Therefore, measurement comparisons are general and just the consistencies of errors or large anomalous errors should be examined. Interestingly, volumes are comparable for debris-flow processes, but very different for hyperconcentrated flows or water flows. Volumes from high-frequency monitoring stations measure both the sediment and water which makes the highly concentrated debris-flow a more accurate measurement. These debris-flow volume measurements are very similar to the multi-date topographic surveys with differences ranging from 4-27% of the measured volume.

The largest percent difference (2 069%) was located at Station 3 during the P6 period with little bedload transport. During this period, large channel response was measured in the proximal reach from a hillslope debris-flow. In the intermediate reach, large deposition occurred with a mixture of debris-flow and bedload deposits. Very little sediment traveled through the distal reach. Therefore, the hydrograph readings, with a maximum flow height of 1.6 m, were most likely measurements of water discharge.

3.1.4 Surge dynamics for June 29, 2011 debris-flow

The June 29, 2011 debris-flow (P5) is the largest event and has the most detailed and complete measurements from the monitoring stations and topographic surveys which provides further insight on the dynamics of the surges during the event. The volume change of surges and their coalescence for the event is shown in Figure 45. Hydrographs for the three monitoring stations show the magnitude and timing of discharge for each surge during the event. The surges with significant magnitudes have volumes (sediment + water) indicated in red (debris-flow) and blue (hyperconcentrated flow). The total sediment transport volume of the event is measured from the multi-date cross-section surveys indicating the sediment input from the channel between stations.

Station 1 (Figure 45A) has 8 surges (details in Table) which the 6th surge is the debris-flow ($1\,900\text{ m}^3 \pm 30\%$) traveling at 4.2 m s^{-1} . A distinct pulse (7th surge) at the end of the debris-flow tail indicates a hyperconcentrated flow ($1\,200\text{ m}^3 \pm 30\%$) with a higher velocity of 4.5 m s^{-1} . The last surge (8th) is a smaller and slower hyperconcentrated flow ($730\text{ m}^3 \pm 30\%$, 2.3 m s^{-1}). According to the velocity of the surges, the 7th surge (hyperconcentrated flow) will converge with the debris-flow while the last surge will separate.

Table 12 Differences of sediment transport volumes calculated from cross-section surveys and high-frequency monitoring stations (Volume Difference and % Difference) with their indicated process types DF (debris-flows) and HF (hyperconcentrated flows or water flow).

Survey Period	Station Id.	Process Type	Vol. Diff. (m ³)	% Diff.
P4	S1	DF	20	4
	S2	HF	700	99
	S3	HF	480	100
P5	S1	DF	-370	9
	S2	DF	900	13
	S3	DF	-1200	16
P6	S1	DF	890	27
	S2	HF/DF	-700	57
	S3	HF	-6000	2069

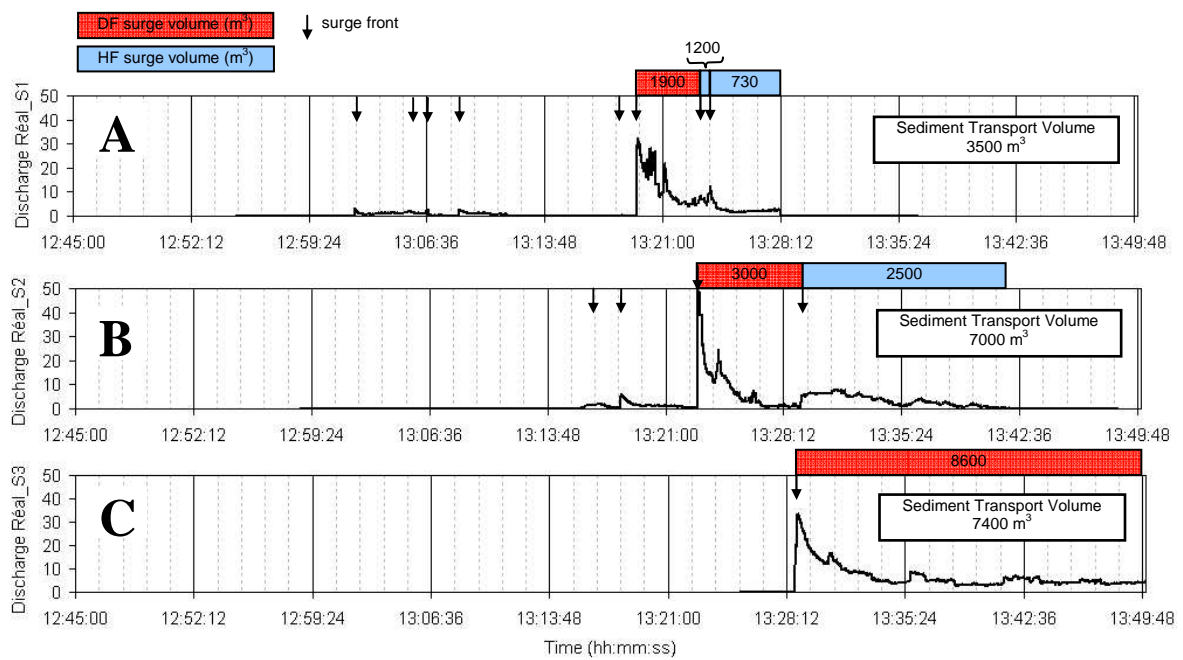


Figure 45 Hydrographs of the 29 June 2011 debris-flow (P5) measuring discharge at station 1 (A), station 2 (B) and station 3 (C) (discharge in m³ s⁻¹). Surge fronts are indicated with arrows and the ones with important volumes are indicated in red (debris-flow) and blue (hyperconcentrated flow). Sediment transport volumes are for the whole event calculated from multi-date cross-section surveys. It also indicates the volume growth (channel input) between stations. (modified from Navratil et al., in press)

Station 2 (Figure 45B) has 4 surges which the 3rd surge is the debris-flow ($3\,000\text{ m}^3 \pm 30\%$) traveling at 3.2 m s^{-1} . The debris-flow grew in height and has a volume similar to the combined 6th and 7th surge volumes at Station 1 which confirms that they coalesced. Several minutes behind the debris-flow is the last hyperconcentrated surge which grew to $2\,500\text{ m}^3 \pm 30\%$ traveling approximately 1.2 m s^{-1} . Topographic surveys indicate that $3\,500 \pm 420\text{ m}^3$ has been entrained between Station 1 and 2. The only surge that had an important volume growth without coalescence was the last hyperconcentrated surge with $+1\,770\text{ m}^3 \pm 30\%$. This indicates that the hyperconcentrated flow entrains more material than the debris-flow.

Station 3 (Figure 45C) has one surge with a volume of $8\,600\text{ m}^3 \pm 30\%$ traveling at a decreased velocity of 2.4 m s^{-1} . This volume is a little larger than the topographic volume $7\,400 \pm 900\text{ m}^3$ and shows a decreased maximum flow height. The large increase of the debris-flow tail and the little geomorphic response between the two stations ($+400\text{ m}^3$) indicates that the hyperconcentrated flow must have accelerated and coalesced with the debris-flow.

3.2 June 29, 2011 debris-flow velocity and discharge

3.2.1 Reach-scale comparison (Station 3)

Several days after the June 29, 2011 debris-flow (P5), a total station was used to survey flow heights, channel profiles, and cross-sections in seven reaches (16 bends) covering most of the torrent (Figure 46A). The superelevation in these bends was used for calculating velocities and discharge. Two reaches directly overlap monitoring stations 2 and 3 which allow us to directly compare and analyze the post-event topographic results.

A detailed comparison is made in the reach of Station 3 (Figure 46B) showing all the surveyed points and channel bends with superelevations (cross-sections A-D). The left bank (LB) of cross-section A is used as an example of measurements. It has three white points (15 m spacing) used for determining the curvature resulting in a R_c of 94 m and a dH of 0.57 m. Prochaska et al. (2008) describes that the variations of R_c is influenced by the scale of measurement. In Figure 46C, we test the scale of R_c measurements and the k coefficient in the velocity calculations. Mean velocities for the left bank (LB) and right bank (RB) were calculated from varying 3 point spacings (5-40 m) and a range of k (1-10) is used. The sensitivity of the scale for measurement is insignificant in comparison to the sensitivity of k where velocities range from 2.9 to 11.2 m s^{-1} . We were able to accurately determine k as 10, in accordance to the mean velocities derived from the geophones (2.7 m s^{-1}).

In Figure 47, velocities ($k = 10$) and its parameters are shown for cross-sections A-D with curvatures R_c (range of 37 to 220 m) and superelevations Δh (range of 0.11 to 0.77 m). The mean of the right and

left bank velocities are used for representing the cross-section velocity. These velocities for A-D average 2.3 m s^{-1} which is a little less than the measured geophone mean velocity 2.7 m s^{-1} . However, cross-section B has a significantly lower velocity which could have been caused by a disturbed bank of a large debris-flow lobe (observed in the field). By excluding cross-section B, the mean velocity becomes 2.8 m s^{-1} which is very similar to the geophone calculations. The ultra-sonic sensor measured a maximum flow height of 2.0 m , in the same range than the surveyed maximum flow height 1.82 m at the same cross-sections. The two methods seem to have good agreement with each other within the reach.

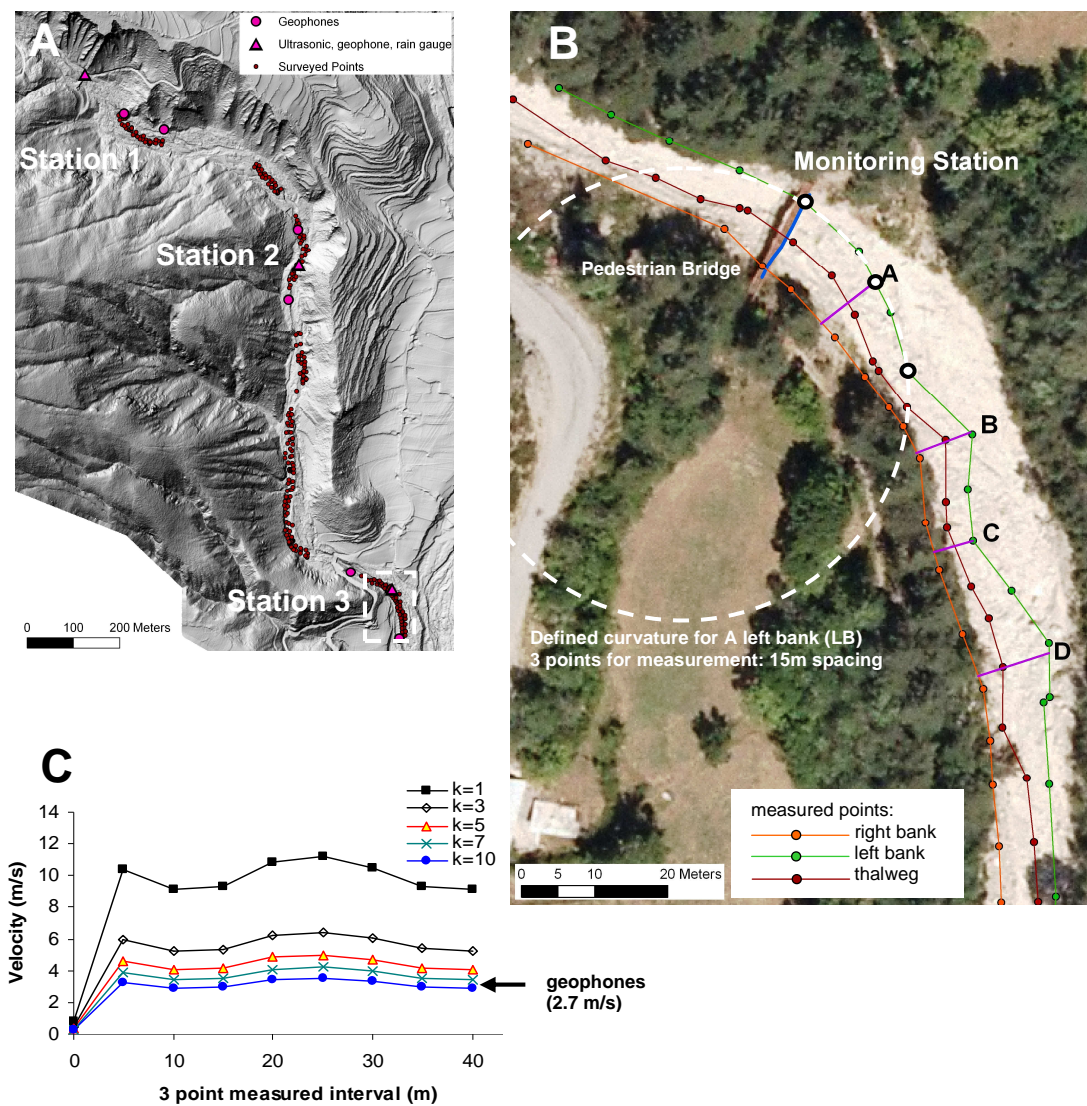


Figure 46 A) locations of surveyed debris-flow marks and profiles for P5. B) Example of one surveyed reach where Station 3 is located, which allows for detailed measurement comparisons for flow height and velocity calculations. Four cross-sections (A-D) are found to have good curvatures and super-elevations for back-calculating velocities which are presented in the next figure. C) Velocity calculations for cross-section A showing large variations with k , where $k=10$ has the best velocity to match the geophone calculations (2.7 m/s).

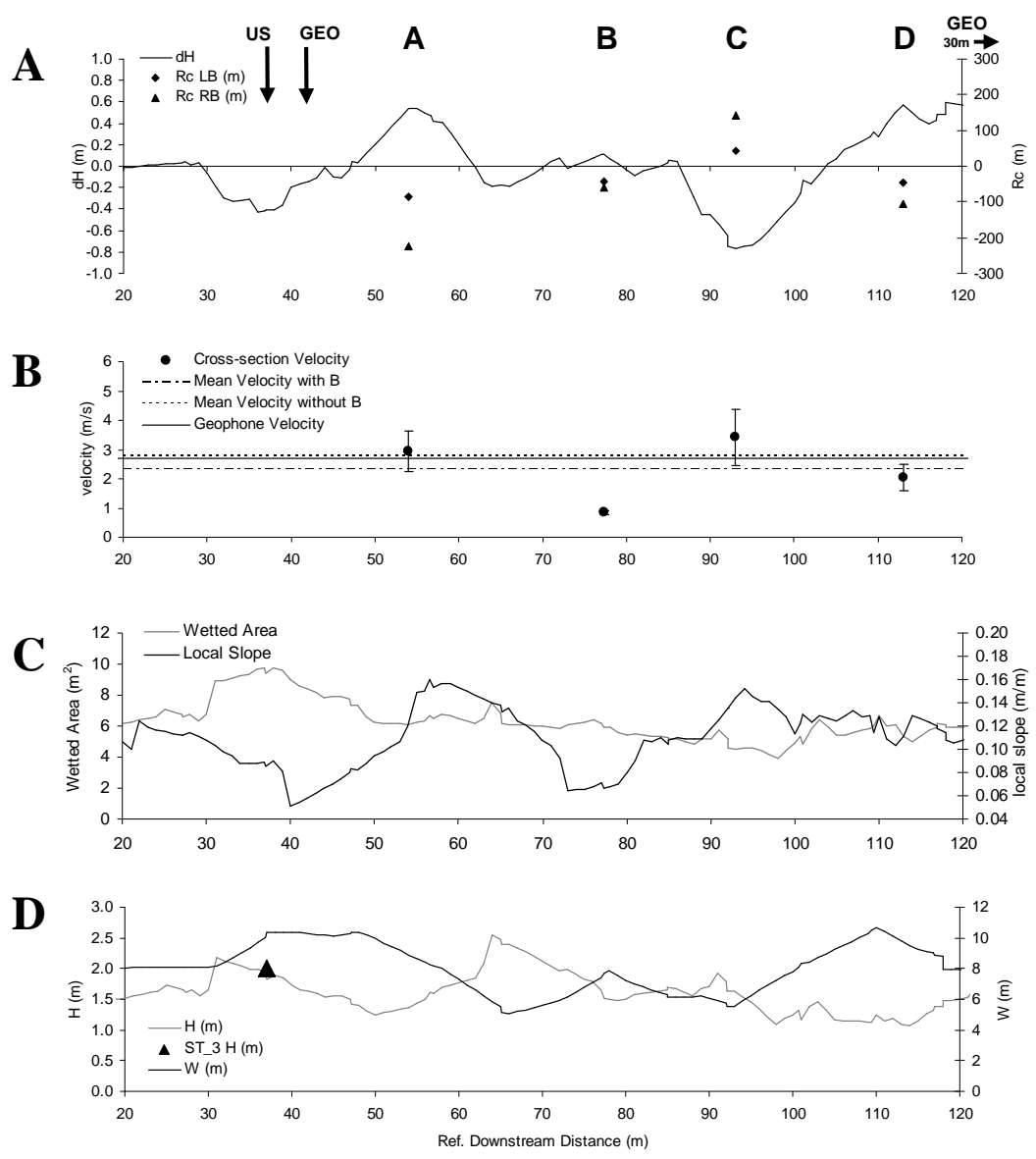


Figure 47 Survey measurements for the reach located at Station 3 after E6 event. Channel bend locations A-D are indicated with A) curvature (Rc) and super-elevation (dH), B) calculated velocities, C) wetted area and local slope and D) flow width (W) and height (H). Calculated velocities obtain a mean velocity similar to the velocity obtained from the geophones (GEO). Measured flow heights also correspond with the ultrasonic sensor (US).

3.2.2 Full channel comparison

For all the surveyed reaches covering most of the torrent, velocities for 16 channel bends were calculated for the same debris-flow using the same method (Table 13). These results show that the coefficient k can change at different stages in the torrent (Figure 48A). Again k can be calibrated according to the velocity measured between geophones which results in a coefficient k varying from 5 to 10. The final calibrated velocities appear to have large variations within short distances which could indicate its uncertainty (Figure 48B). However, the trend of the local slope appears to correspond strongly with the velocities' variation, and furthermore, the velocities derived from the geophones also show large variations within the reach of Station 2. Therefore, we are comfortable with analyzing these velocity calculations which have a gradual decrease downstream in parallel with the local slope. A strong linear relationship was found between the debris-flow velocity and local slope with an R^2 of 0.69 (Figure 49).

Table 13 Surveyed debris-flow features at channel bends and their back-calculated velocities, and discharges

Distance from alluvial apex (m)	Slope (m/m)	Flow Width (m)	Flow Height (m)	dH (m)	Rc (outer bank)	Rc (inner bank)	Wetted Area (m ²)	V* (m s ⁻¹)	Q (m ³ s ⁻¹)
663**	0.16	8.6	2.6	1.1	75	93	9.2	3.8	35
698	0.16	7.0	3.6	1.4	55	40	10.5	3.6	38
951	0.08	8.2	2.5	0.7	36	35	9.2	2.1	19
966	0.11	8.8	2.2	0.5	-68	-65	8.8	2.2	19
1104	0.16	9.2	1.9	0.2	--	335	11.5	3.6	41
1159	0.10	8.4	2.0	0.1	-198	-171	11.2	2.4	27
1162**	0.08	7.5	1.9	0.1	-394	-138	9.4	2.6	25
1410	0.09	9.5	2.4	0.4	-91	-95	15.5	2.3	36
1572	0.09	10.0	1.7	0.2	187	167	10.2	2.3	24
1621	0.11	13.4	1.7	0.6	106	242	13.5	3.2	44
1789	0.11	9.3	2.2	0.4	125	213.4	12.9	3.3	42
1827	0.07	9.3	1.8	0.7	58	55.4	10.3	2.5	26
2085**	0.12	8.9	1.4	0.5	-85	-223	7.2	2.9	21
2108	0.07	7.7	1.5	0.1	-42	-59	6.9	0.8	6
2124	0.14	5.5	1.6	0.8	44	141	5.3	3.4	18
2144	0.11	9.8	1.1	0.6	-45	-107	6.3	2.0	13

* Calibrated by the selected k according to mean velocities from geophones

** Closest channel bend to each monitoring station

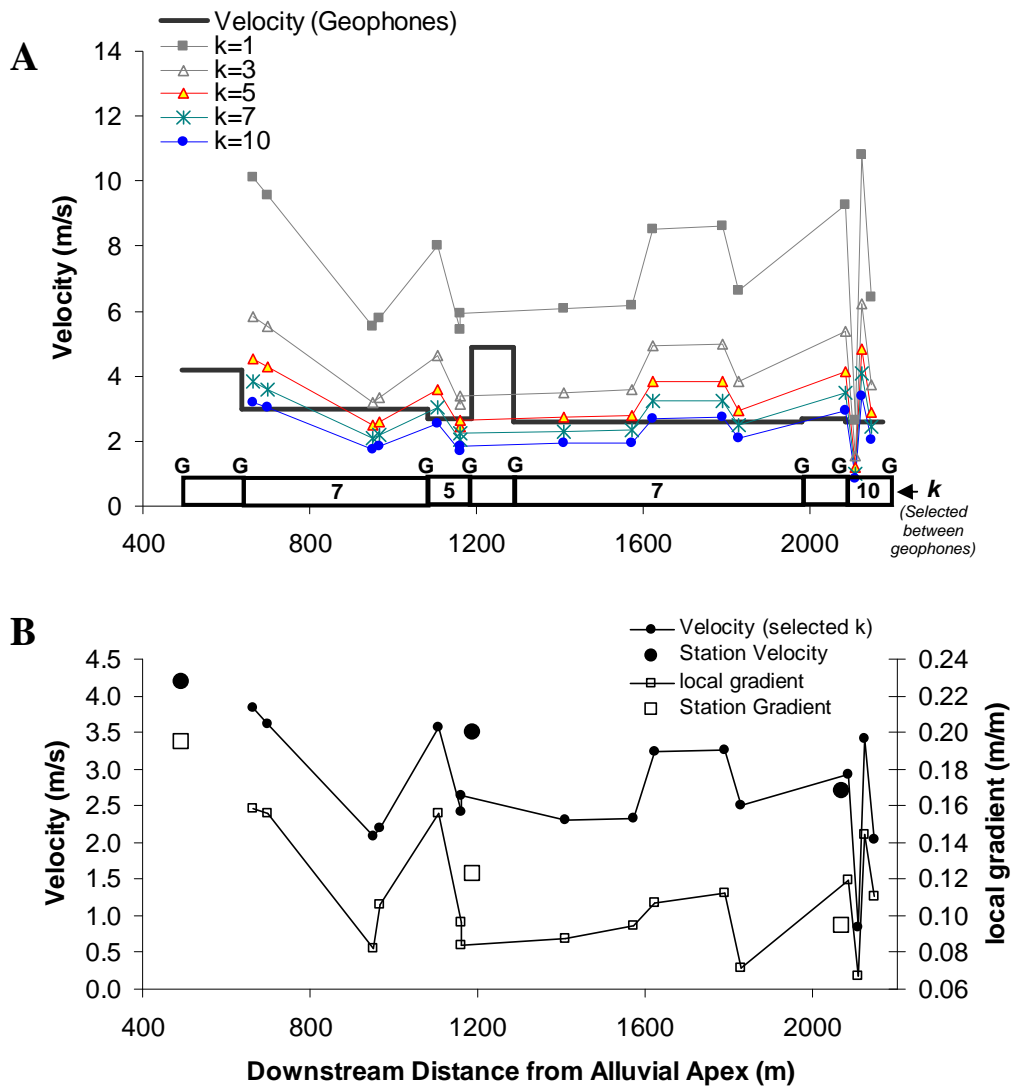


Figure 48 (A) Range of velocities for k is shown along the torrent, the best-fit k can be approximately chosen according to the mean velocities derived from the geophones “G” in the same reaches. (B) The calibrated velocities (with the correct k) at the channel bends has a gradual downstream decrease with a similar trend with the local slope, the upstream monitoring station does not correspond well.

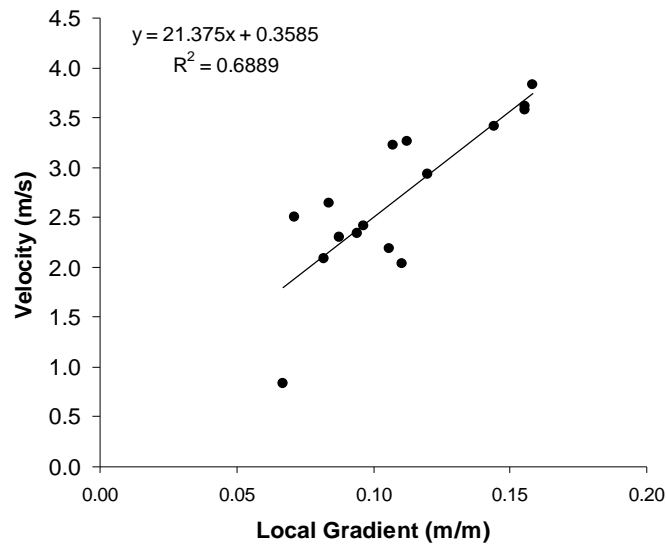


Figure 49 The backcalculated front velocity for the June 29, 2011 debris-flow related to slope

The maximum flow heights, flow width, wetted area and local slope are distributed downstream at an average 20 m interval in Figure 50. The maximum flow height (ranging from 1.1-3.6 m) has a strong downstream decrease where as the flow width (ranging from 5.5-13.4 m) has no apparent trend. The wetted area is calculated by multiplying the maximum flow height with width. This is then normalized by a shape coefficient which corresponds to the nearest pre-event surveyed cross-section. This wetted area also has a strong decrease traveling downstream where as the local slope has a more gradual decrease. For each reach through the torrent, slopes can vary to at least 0.1 m m^{-1} .

The wetted perimeter multiplied by velocity calculates the discharge of the measured channel bends with an average of $21 \text{ m}^3 \text{ s}^{-1}$ (from 6 to $44 \text{ m}^3 \text{ s}^{-1}$) (Figure 51). These measurements are generally less than the peak discharges derived from the monitoring stations which has an average of $39 \text{ m}^3 \text{ s}^{-1}$ (from 32 to $50 \text{ m}^3 \text{ s}^{-1}$). The back-calculated discharge values also have a local variation as the debris-flow travels downstream. We are not able to determine their uncertainties; we can just assume that they are higher than the velocity measurements. The monitoring station uncertainty is 30% creating a limitation for finding any clear trends. Visually, the discharge is the highest around the middle station (station 2), and traveling downstream the discharge decreases.

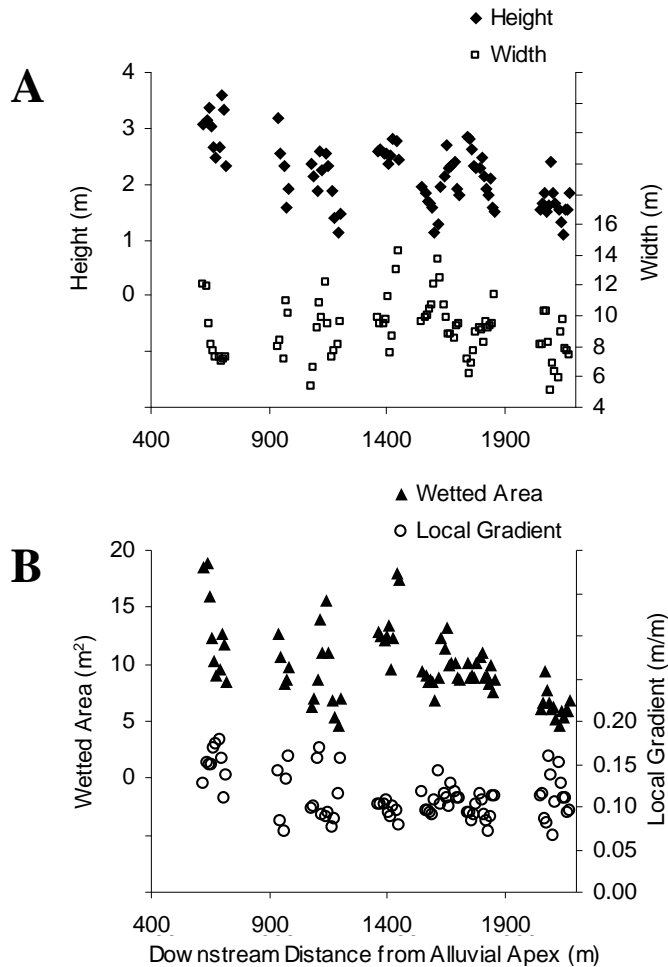


Figure 50 Longitudinal distribution of A) maximum flow height and flow width, and B) local slope and wetted area, measured after the P5 event.

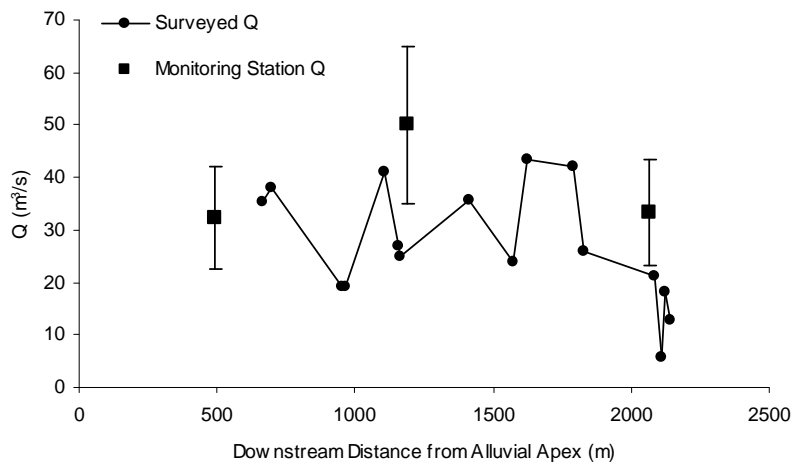


Figure 51 Discharge values from back-calculated velocities and wetted areas; monitoring station discharges are also compared showing local variations and a settle dissipation downstream.

4 DISCUSSION

4.1 Reliability of post-event surveys

4.1.1 *Sediment transport volumes*

Multi-date cross-section surveys are found to have similar observations and calculations as the high-frequency monitoring stations. Debris-flow volumes derived from both methods have approximately 4-27% difference in volume. Topographic surveying gives a more accurate sediment volume estimate for bedload transport because the ultra-sonic sensors are limited by measuring the bulk volume (water + sediment). There are however other monitoring instruments, such as the piezoelectric bedload impact sensors (PBIS), that are a much more accurate method for the measuring bedload transport volumes (Rickenmann and McArdell, 2007).

The fifteen cross-sections have a better spatial coverage than the three monitoring stations, which allows for characterizing the spatial variability of transport volumes and channel interactions. In the Manival torrent, 39 cross-sections provided accurate volumes which matched the sediment trap volumes (Chapter 3). With only fifteen cross-sections in the Réal torrent, the volumes still agree with the monitoring stations as long as the cross-section volumes are calibrated with one of the stations.

An important limitation with cross-section surveying is the need for a sediment input or output volume measurement typically from either a sediment trap or high-frequency monitoring station. In the Réal, we required to add 2 000 m³ to the largest event (P5) in order to match the volumes to the best-measured monitoring station. The P4 and P6 events did not require any added volume because the processes had short travel distances. Another important limitation with topographic measurements is its inability to measure individual surges of an event which was observed during the June 29, 2011 debris-flow. Several individual headwater debris-flows were also identified from the monitoring stations during bedload transport events. We have also shown with the monitoring stations that hyperconcentrated surges can transport just as much sediment than debris-flows during the same event.

4.1.2 *Backcalculation of velocities*

Back-calculating superelevations in channels bends with the forced vortex equation have shown to be very effective in this study. These velocities differ from geophone measurements by 0.1 to 0.4 m/s. In order to achieve such accuracies, the correct k coefficient must be used. We use a k coefficient between 5 and 10 which can vary the velocity by approximately 1 m/s. However many debris-flow

studies do not use a k coefficient (or $k=1$) for their velocity calculations, which in the case of the Réal torrent, it gives a velocity three times greater than the true value (plus 4 to 7 m/s).

Hungr et al. (1984) suggests that the k is probably controlled by the viscosity and vertical sorting of the front. As the viscosity increases, the k coefficient should increase as well. We have observed that the k coefficient has an approximate downstream increase. However, we identify (in the next section) that the flow resistance coefficients including viscosity have a downstream decrease. Therefore other factors must have a stronger influence on the k coefficient such as the vertical sorting of the front, bend geometry, and other material properties (Hungr et al., 1984; Chen, 1987).

4.2 Influence of channel interaction and surge coalescence

For the June 29, 2011 debris-flow, multi-date cross-section surveys, post-event channel bend surveys, and high-frequency monitoring stations provide a very interesting combination of results. The monitoring stations reveal that hyperconcentrated surges coalesce with the debris-flow surge. Interestingly, between station 1 and station 2, the hyperconcentrated flow had the most important volume growth and not the debris-flow ahead of it (Figure 45). This intermediate reach is where the highest yield rates of the torrent occur (Figure 52A). The debris-flow front has been a prominent surge throughout the whole monitored torrent with a downstream decrease of height observed by both the monitoring stations and the post-event surveys. With the post-event survey of channel bends, we can estimate the maximum shear stress τ (N m^{-1}) of the debris-flow front defined as:

$$\tau = \rho gH \sin(S) \quad (9)$$

The water-sediment density (ρ) is estimated to be 2300 kg m^{-3} (measurements of earlier deposits at the same torrent from Chambon et al., 2010). The shear stress has a strong downstream decrease in parallel with the yield rate (calculated from multi-date cross-sections) (Figure 52A). The yield rate represents the erosion for the total event which consequently has a linear relationship with the debris-flow front's shear stress (Figure 52B). Other debris-flow monitoring sites have observed important erosion at the debris-flow front (Berger et al., 2011a). The longitudinal sorting of the debris-flow distributes the highest sediment concentration to the front creating a steep slope with a high shear stress which creates the most erosive force of the flow. However, a very high sediment concentration in the front can inhibit the transport capability of the eroded material. During laboratory experiments on erodible beds, debris-flow fronts have been observed to destabilize the banks and the more fluid like tail entrained the material (Rickenmann et al., 2003). Field experiments at the Chemolgan site in Kazakhstan (Rickenmann et al., 2003) showed little growth in the debris-flow front which indicates

that the large channel erosion was entrained in the tail of the flow. We can assume a similar situation in the Réal; the well defined debris-flow front scoured the channel bed and destabilized the banks. The tail of the debris-flow was originally short and had little growth which must have had a high sediment concentration. Therefore, the debris-flow left loose saturated material in the channel which was then entrained by the following hyperconcentrated flow. The hyperconcentrated flow grew in volume and coalesced with the tail of the decelerating debris-flow. This indicates that both the debris-flow front and the tailing surges both play a role in the scouring and sediment transport of the material. The front acts as the plow and the following hyperconcentrated surge acts as the truck carrying the material.

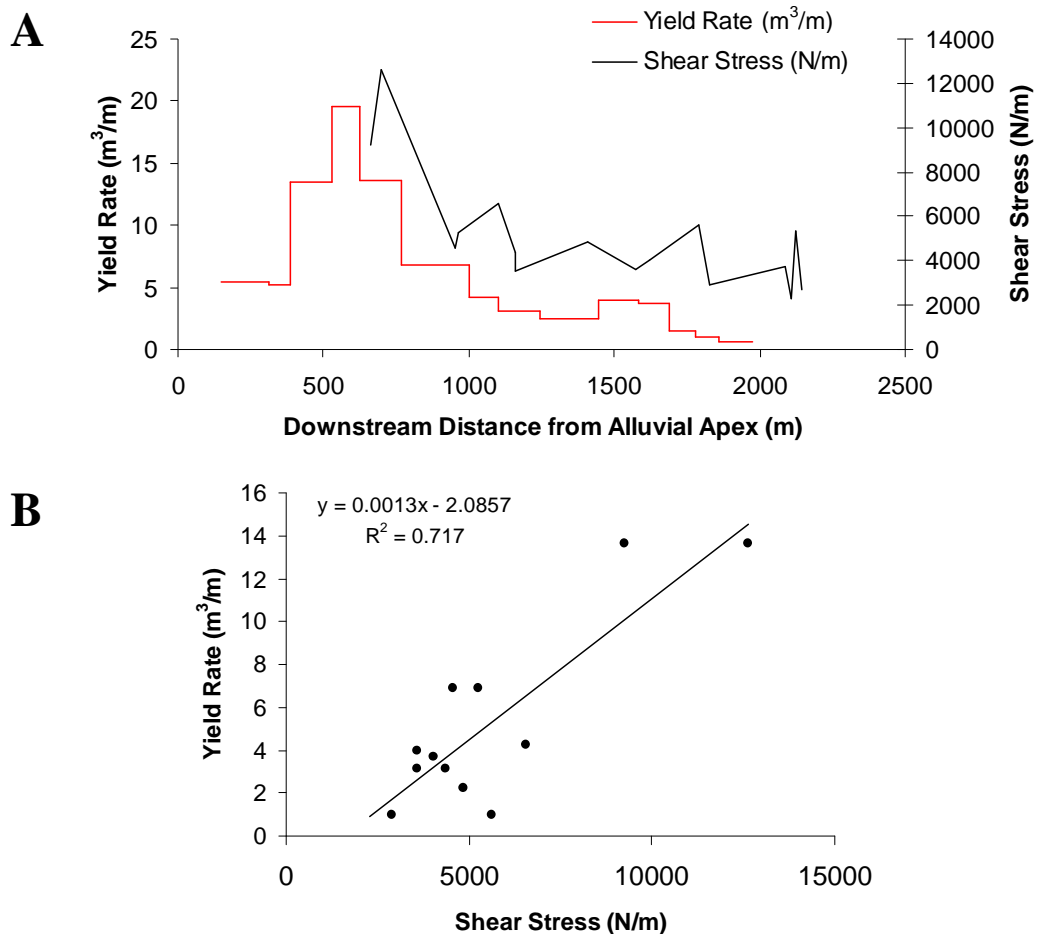


Figure 52 A) Longitudinal distribution of yield rate derived from resurveyed cross-sections and shear stress derived from post-event survey for the June 29 debris-flow. B) It appears that shear stress of the debris-flow front influences the total event yield rate of the flow event.

4.3 Flow resistance characterization

The downstream decrease of the front’s shear stress and velocity, the increasing sediment volume and coalescence of surges indicate that the June 29, 2011 debris-flow may have a changing flow resistance. We would like to accurately characterize the flow resistance of the debris-flow front and relate it to the calculated velocity and shear stress. Several equations (which assume a steady uniform regime) have been used to characterize flow resistance for debris-flows (Table 14). The flow resistance coefficient for these equations have been backcalculated using the field measurements of flow height, slope, and velocity for over 200 debris-flow observations Rickenmann (1999). Large scattering of two magnitudes was observed for viscosity (μ) where as only one magnitude of scattering was observed for Manning’s coefficient (n) and Chezy’s coefficient (C_{chezy}).

The June 29, 2011 debris-flow post-event surveys were used to compare the performance of Equations 10-13 for predicting velocity (Figure 53). The flow resistance coefficients were backcalculated and their mean were applied to the equations. We find that the Manning-Strickler (Equation 11), Chezy (Equation 12), and an empirical equation from (Koch, 1998) (Equation 13) are very similar and with the best results. The Newtonian laminar flow (Equation 10) is largely overestimated with large scattering because of its high sensitivity to height. We have observed that velocity is more correlated with slope rather than height which make the turbulent flow equations more appropriate.

Table 14 Equations used for estimating debris-flow surge velocities (v) using flow resistance coefficients μ , n , C_{chezy} , and C_1 . Table modified from Rickenmann (1999)

	Formulas	Eq.	Defined variables
Newtonian laminar flow	$v = \frac{\rho g H^2 \sin(S)}{B\mu}$	10	v : front velocity ($m\ s^{-1}$) H : maximum flow height (m) S : channel slope ($m\ m^{-1}$) ρ : water-sediment density $\sim 2300\ kg\ m^{-3}$ (measurements of previous deposits from Chambon et al., 2010) g : acceleration due to gravity ($m\ s^{-2}$) B : equals 7 for channels between a U- and trapezoid shape (Hungur et al., 1984)
Newtonian turbulent flow: Manning–Strickler equation	$v = \frac{H^{2/3} \sin(S)^{1/2}}{n}$	11	g : acceleration due to gravity ($m\ s^{-2}$) B : equals 7 for channels between a U- and trapezoid shape (Hungur et al., 1984)
Newtonian turbulent flow: Chézy equation	$v = C_{chezy} H^{0.5} \sin(S)^{0.5}$	12	<u>flow resistance coefficients :</u> μ (Pa. s), n ($s\ m^{-1/3}$), C_{chezy} ($m^{0.5}\ s^{-1}$), and C_1 ($m^{0.7}\ s^{-1}$)
Empirical equation (Koch, 1998)	$v = C_1 H^{0.3} \sin(S)^{0.5}$	13	

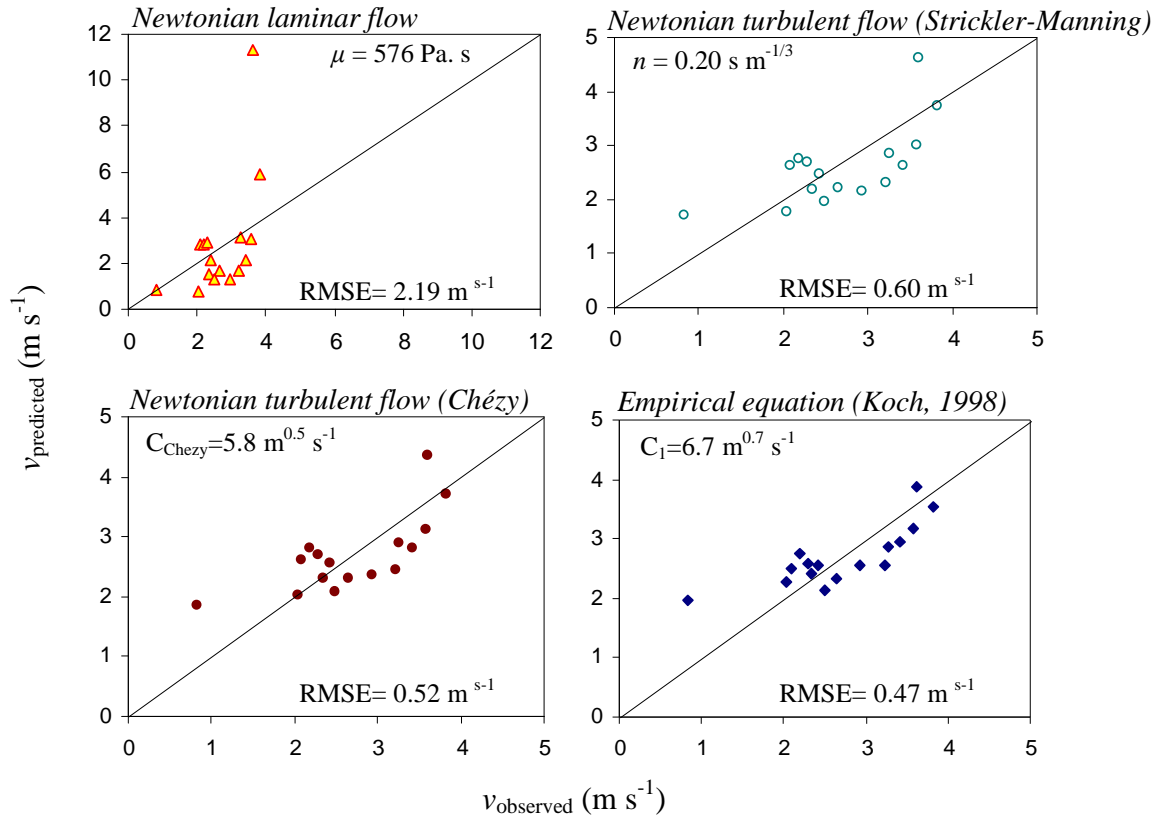


Figure 53 Predicted velocities (v) from Equations 10-13 are compared with the observed v for the June 29, 2011 debris-flow. Flow resistance coefficients are the backcalculated means from the observations.

The downstream distribution of the backcalculated flow resistance coefficients for the June 29, 2011 debris-flow has a large variation (Figure 54). The scattering can be influenced by the unsteady flow regime of debris-flows. The calculated viscosity (μ) can range from 200 to 1800 Pa. s with a mean of 576 Pa. s. For one event in the Acquabona torrent, Italy (Berti et al., 1999), backcalculated apparent viscosities also had a large scatter with a range from 524 to 1609 Pa. s. Other apparent viscosities of debris-flows have been reported to be approximately 3000 Pa. s (Hungr et al., 1984).

Manning's coefficient (n) in the Réal event ranges from 0.14 to 0.41 $\text{s m}^{-1/3}$ with a mean of 0.20 $\text{s m}^{-1/3}$. This corresponds to observed granular debris-flows which have a mean of 0.16 $\text{s m}^{-1/3}$ for small scale events and 0.18 $\text{s m}^{-1/3}$ for large scale events; where as fine-grained large scale debris-flows have a mean of 0.05 to 0.08 $\text{s m}^{-1/3}$ (Rickenmann, 1999; Rickenmann and Weber, 2000). Clear water flows in gravel bed channels have the lowest mean value of 0.067 $\text{s m}^{-1/3}$ (Rickenmann, 1994; Rickenmann, 1999).

Chezy's coefficient (C_{chezy}) ranges from 2.6 to 7.7 $\text{m}^{0.5} \text{s}^{-1}$ with a mean of 5.8 $\text{m}^{0.5} \text{s}^{-1}$ for the Réal event. Our observations are very similar to an event in the Schipfenbach catchment, Switzerland with

the C_{chezy} ranging from 3.3 to 9.1 $\text{m}^{0.5} \text{s}^{-1}$ but without a downstream trend (Hürlimann et al., 2003). Other observations observed a mean C_{chezy} of 11 $\text{m}^{0.5} \text{s}^{-1}$ (Rickenmann and Koch, 1997), 17 to 22 $\text{m}^{0.5} \text{s}^{-1}$ (Ayotte and Hungr, 2000), and 14 $\text{m}^{0.5} \text{s}^{-1}$ (Jakob et al., 2000). In general, these estimates are in the lower end of large datasets ranging from 3 to 56 $\text{m}^{0.5} \text{s}^{-1}$ (DeLeon and Jeppson, 1982; Rickenmann, 1990).

Previous rheological studies have identified debris-flows in the Réal to be muddy flows (visco-plastic fluid) despite their granular appearance (Chambon et al., 2010). However, our backcalculated n corresponds to a granular flow behavior according to Rickenmann and Weber (2000). The observed range of C_{chezy} also indicates that the flow was more resistant in comparison to large debris-flow datasets. Unfortunately, we do not have rheological measurements for the June 29, 2011 debris-flow. However, we can question the characterization of these flow types between the two studies. “Granular flows” according Rickenmann and Weber (2000) may include “granular flows with a visco-plastic fluid” which for Chambon et al. (2010) is considered a “muddy flow” with a granular appearance. If this is the case, granular flows with or without visco-plastic fluid have a similar flow resistance.

All of the presented flow resistance coefficients suggest that the debris-flow has a downstream decrease in flow resistance. High yield rates observed in the main channel would have provided enough sediment for an increasing flow resistance. Therefore, the debris-flow front may have been diluted by either the small preliminary surges before the front, water input from secondary tributaries, or the hyperconcentrated flow which coalesced with the debris-flow tail. However, we do not have any more information for further analysis.

The shear stress of the debris-flow is related to yield rate (Figure 52) and the velocity is correlated with slope (Figure 49), therefore we made a comparison of the depth-slope product ($H \sin S$) with velocity which is equivalent to the Chézy equation (Table 14). The June 29, 2011 debris-flow (Figure 55) results were compared with several events and study sites including: 1) debris-flow surges during the P4-P6 periods measured from the monitoring stations in the Réal, 2) several debris-flow events in coastal British Columbia which were determined from post-event surveys and eye-witness reports (Hungr et al., 1984), and 3) another debris-flow event with post-event surveys and monitoring stations in the Schipfenbach catchment, Switzerland (Hürlimann et al., 2003).

The depth-slope product ($H \sin S$) is found to have a strong relationship with velocity as a power-function (R^2 of 0.81) for all of the events (Figure 55). The exponent is a little higher than the Chezy equation but the difference appears to be insignificant according to the envelope of the results. The compiled events have a C_{chezy} ranging from 2.6 to 10.5 $\text{m}^{0.5} \text{s}^{-1}$. All of the events in the Réal (large and small) are shown to be consistent with this relationship. The depth-slope product for the June 29, 2011 debris-flow has almost a one magnitude range and the velocities almost have half a magnitude range. Predicting velocities and shear stress for a debris-flow event requires a better understanding of the

control of the flow resistance coefficients. It is quite evident that these coefficients cannot be considered constant for one event; however we do see an envelope of almost half a magnitude for the C_{chezy} coefficient.

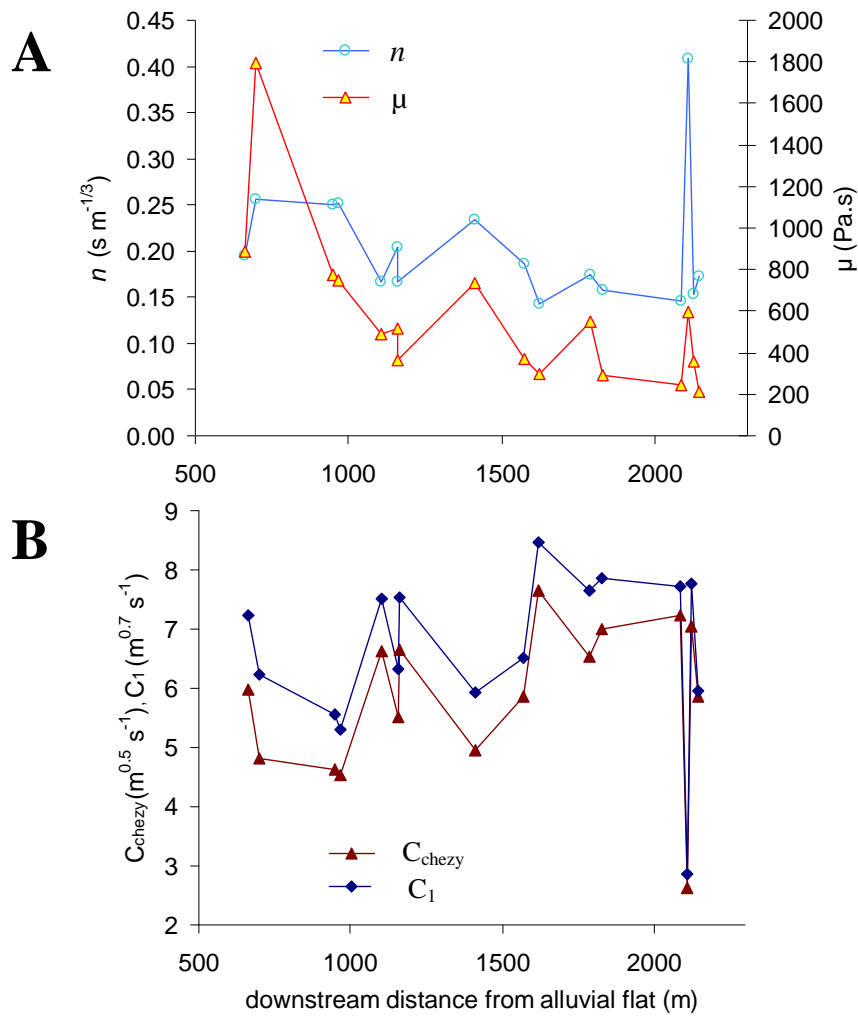


Figure 54 Backcalculations of flow resistance coefficients including (A) μ and n and (B) C_{chezy} and C_1 for the June 29, 2011 debris-flow with post-event survey data. Coefficients are plotted along the downstream distance of the torrent showing a high variation for one flow front and a decreasing trend for flow resistance.

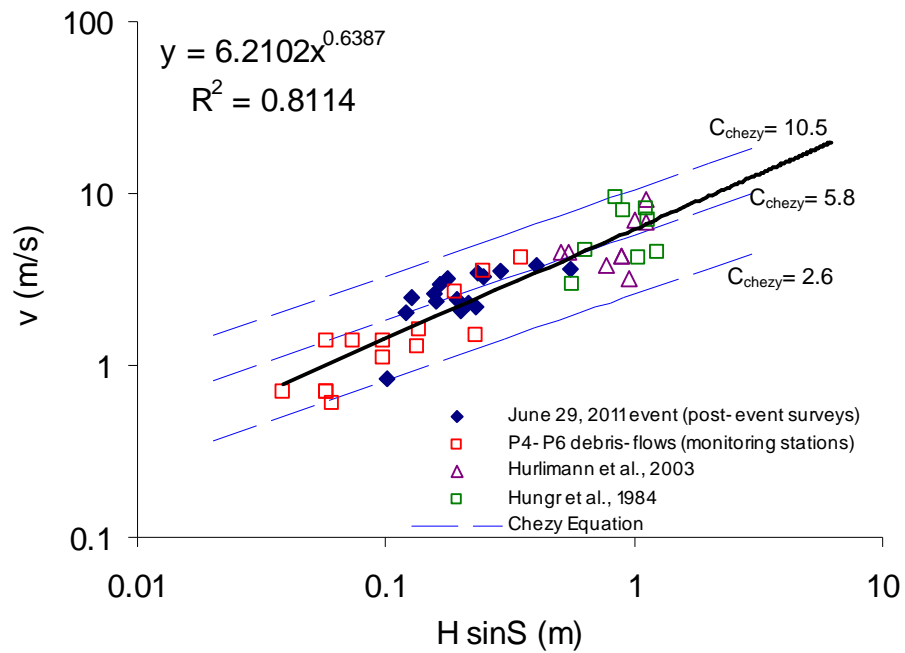


Figure 55 Velocity related to depth-slope product ($H \sin S$) (m) with compiled field observations from the June 29, 2011 debris-flow, debris-flow surges during the periods P4-P6 from the monitoring stations, debris-flows in coastal British Columbia (Hungr et al., 1984), and one debris-flow event in the Swiss Alps (Hurlimann et al., 2003).

4.4 Sediment transport trends by process type

For flow events during the survey periods (P1-6), multi-date cross-section surveys in the Réal have been able to observe two distinct trends of sediment transport volumes (Figure 56A). These two trends are separated by the different types of events: 1) torrent debris-flows (red) and 2) headwater debris-flows/bedload transport events (black). Their envelopes have an inverse trend indicating a sequence of storage transport through the catchment. Sediment pulses from the gullies (mostly the Big Ravine) deposit in the proximal and upper-intermediate reach from short traveled headwater debris-flows (survey periods P3, P4, and P6). The torrent debris-flows are larger ($5\ 200 - 7\ 600\ m^3$) and have longer travel distances which removes the material out of the catchment leaving tail and levee deposits throughout the reaches (survey periods P1, P2, and P5). These tail and levee deposits are then eroded by bedload transport in the intermediate and distal reaches (maximum of $3\ 400\ m^3$), and during this period the proximal reach is recharged again (survey periods P3, P4, and P6).

The rainfall conditions that trigger the two types of events generally have different characteristics. Torrent debris-flows (P1, P2, and P5) are triggered with short-high intensity rainfall bursts ($21, 31,$ and $79\ mm\ hr^{-1}$). The largest debris-flow (P5) has the longest duration of the three events with 1 hour of continuous rainfall. Headwater debris-flow/bedload transport events (P3, P4, and P6) typically have

longer duration rainfalls of 4 to 28 hours. However, their maximum rainfall intensities can sometimes be as large as the torrent debris-flow's intensities (29, 34, and 60 mm hr⁻¹). In this situation, there may not be enough sediment recharge in the main torrent to produce a torrent debris-flow. This has been the case in the Manival torrent where the channel's sediment budget was very low, and even the largest observed rainfall intensities did not trigger any torrent debris-flows (Chapter 3).

Multi-date cross-section surveys in the Manival torrent have similar trends of sediment transport for torrent debris-flows (indicated as red in Figure 56B). Most of the debris-flow volumes in both torrents come from the entrainment in the proximal reach with high yield rates of up to 15 – 19 m³ m⁻¹. Channel erosion typically occurs in loose unconsolidated gravel wedges formed by bedload transport. Torrent debris-flow events in both the Réal and Manival are very dependant on this storage and on high rainfall intensities.

The sediment transfer from the source to the channel is different for the Manival and Réal. The Réal torrent has a sediment source in a very active gully directly connected to the torrent on the alluvial flat (The Big Ravine). This gully is incising weak fluvio glacial deposits which provide an unlimited supply of material influencing a short cycle of sediment routing. The recharge is quite evident (Figure 56A) showing gully debris-flows depositing into the proximal reaches. The hillslope pulses are of the same magnitude to the torrent debris-flow volumes. For the Manival torrent, the sediment source from the headwater channels produces less material and is not directly connected to the main torrent on the alluvial flat (Figure 56B). Therefore, the sediment depends on bedload transport to continue the transfer of storage into the main torrent during long duration low intensity rainfall.

The most channel response for the Réal and Manival are located in the proximal reach on the alluvial flat with local slopes of 0.15-0.24. This is a reach which stores the hillslope production. This storage grows until a large flow event entrains the material becoming most of the debris-flow volume. The debris-flows transport the material for at least 1-2 km downstream.

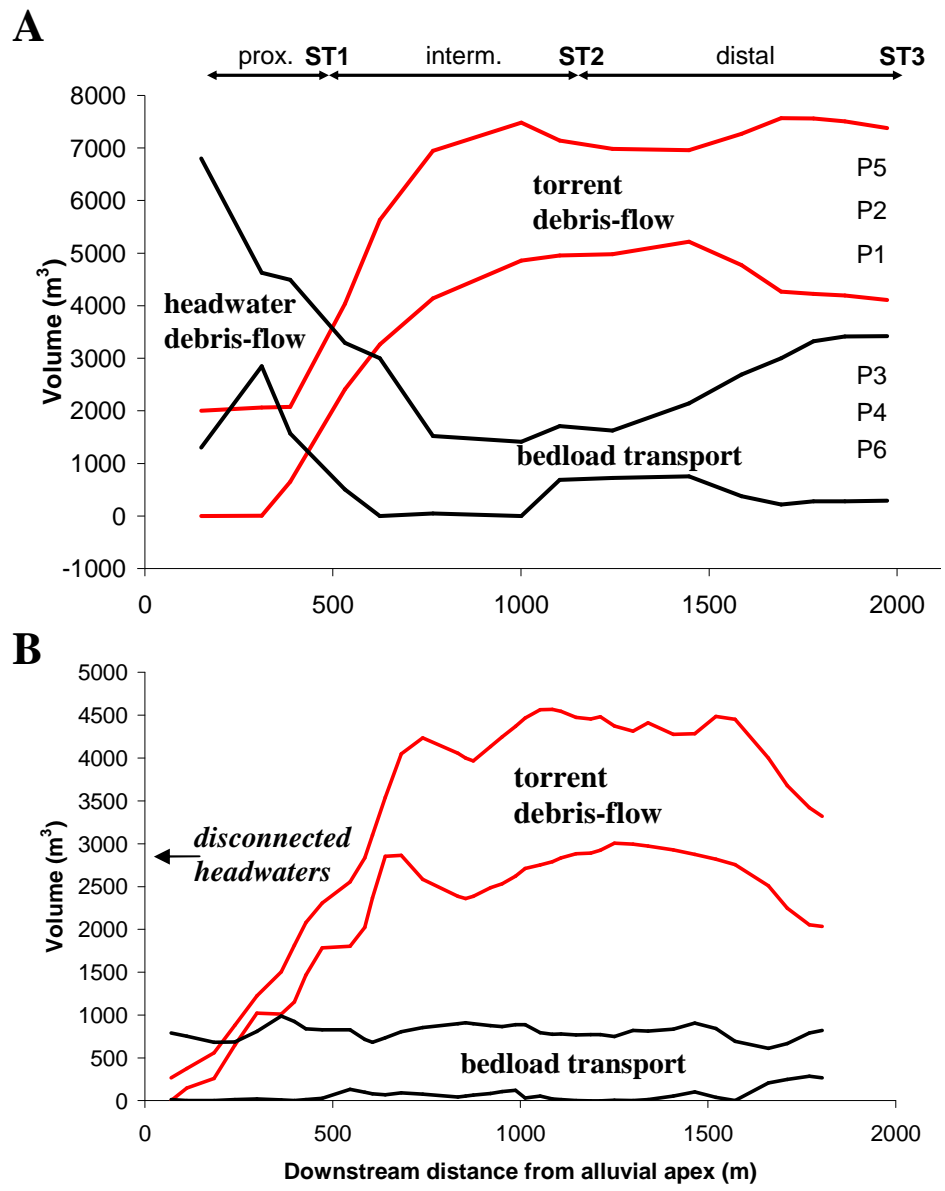


Figure 56 Envelopes of sediment transport volumes according for torrent debris-flows (red) and headwater debris-flows/ bedload transport (black). The Réal (A) and the Manival (B) torrent have very similar torrent debris-flow entrainment and transport. The Réal has a very active connected headwater increasing the rate of recharge where both the Manival and Réal experience the same bedload transport.

5 CONCLUSIONS

Post-event surveys in the Réal torrent have effectively and accurately measured sediment transport volumes of six flow events within 1½ years. For the largest debris-flow on June 29, 2011, channel-bend surveys also accurately measured front velocities, discharge, and flow resistance. Multi-date cross-section surveys and monitoring station volume measurements were comparable for debris-flows and less comparable for bedload transport. Front velocities backcalculated by superelevations at channel bends is found to be highly sensitive to the correction coefficient k . For the June 29, 2011 debris-flow, the velocities measured from the geophones corresponded with the backcalculated velocities when k ranged from 5 to 10. As the debris-flow travels downstream, k can vary, which does not correspond with the flow resistance of the debris-flow front.

Predicted debris-flow velocities using the Chezy and Strickler-Manning equations for Newtonian turbulent flow are well correlated with observed velocities. The June 29, 2011 debris-flow in general has a high flow resistance which may be considered as a granular flow with a visco-plastic fluid. It is observed however that the backcalculated flow resistance coefficients decrease downstream. For all of the debris-flows in the Réal and other sites including the Swiss Alps and coastal British Columbia, the Chezy coefficient is shown to have a well defined envelope of less than one magnitude.

The June 29, 2011 debris-flow observations are summarized below:

- 1) The debris-flow has a distinct sharp front with heights varying from 1.1 to 3.6 m with a downstream decrease.
- 2) The shear stress of the debris-flow front corresponds with the total event yield rate.
- 3) The hyperconcentrated surge behind the debris-flow has a significant volume growth rather than the debris-flow itself.
- 4) The hyperconcentrated flow coalesces with the debris-flow tail in the distal reach
- 5) Flow resistance of the debris-flow front decreases travelling downstream

We hypothesized that the debris-flow front scoured and destabilized the channel, but it could not grow because of its high sediment concentration. The saturated unstable material remaining in the channel was remobilized by the trailing hyperconcentrated flow; this surge grew in volume and then coalesced with the decelerating debris-flow. It is difficult to explain the decreasing flow resistance of the front; it may be influenced by preliminary water flow in the channel (Navratil et al., in press).

For all of the flow events monitored in the Réal torrent from April 2010 to October 2011, two distinct event types are observed: 1) torrent debris-flows which have large channel scouring and long travel distances and 2) headwater debris-flows which scour and deposit in the torrent at short travel

distances, with bedload transport occurring downstream. The Réal has distinct sediment routing of material in an event-based cycle from gully to proximal/intermediate reach and to the end of the distal reach. The entrainment and transport trends for the torrent debris-flows are very consistent in the Réal and the Manival torrents. More events are needed with the integration of topographic surveying and high-frequency monitoring distributed along whole torrents to find consistencies of the surges and their longitudinal dynamics.

This chapter has presented the variability of a debris-flow during propagation. Despite their complexities, these debris-flow events have consistent trends of sediment transport volumes with high yield rates. The combination of post-event surveying and high-frequency monitoring stations needs to become a standard approach to accurately describe the varying propagation of debris-flow events and their important interactions with the channel.

Chapter 5:
SPATIAL VARIABILITY OF CHANNEL EROSION
BY DEBRIS-FLOWS

1 INTRODUCTION

For several decades, the volume of a debris-flow has been found to originate mostly from channel scouring (described in Chapter 3). Large scouring (high yield rates) is typically observed where channel storage is present. Yet, there have been little advances for understanding channel scouring and its influence on the dynamics of debris-flows.

Channel storage encompasses many influences on debris-flows. The growth of the debris-volume increases the flow's momentum which then increases the runout distances (Iverson et al., 2011). In retrospect, for debris-flows initiated by water surges (from runoff or glacial lake outbursts floods) the entrainment increases the sediment concentration which creates changing flow conditions (described in Chapter 4). The sediment concentration increase of the flow decreases erosion rates in the erodible bed. Also larger grain-sizes in the storage decreases the erosion rates (Egashira et al., 2001). Experimental studies showed that the growth of momentum from scouring becomes insignificant when the erodible beds are below half the repose angle (Mangeney et al., 2010). This shows that channel slope has a strong influence on channel erosion by debris-flows

The relationship between scour and slope is difficult to determine because in the field many spatial and environmental conditions are present. Maximum scouring of the 1987 debris-flows in Switzerland revealed a broad linear relationship with slope (Rickenmann and Zimmermann, 1993). Debris-flow yield rates in the Queen Charlotte Islands, British Columbia were highly scattered in relation with slope (Hungri et al., 2005). The database consisted of 174 debris-flows and avalanches compiled from different practitioners and researchers. There was a high variability of channel conditions (confinement, grain-size, slope, and channel width) and observation errors, especially the erosion measurements because the pre-event geometry of the channel was not known (Hungri et al., 2008). Detailed airborne laser scanning (ALS) and differential GPS surveys for several debris-flows in Iceland showed that detailed multi-date field measurements at several sites can be used to study the effect of slope on channel scour by debris-flows (Conway et al., 2010). More multi-date field studies are needed in debris-flow research for providing field-based observations of channel responses to debris-flows.

There are three main objectives in this chapter which uses multi-date field measurements for analyzing (1) channel storage and (2) channel deformation. First, spatial variability of channel scouring is analyzed for debris-flow and bedload transport processes. Second, the effect of slope on channel scouring during debris-flows is analyzed. Third, a method for mapping sensitive reaches to erosion is proposed by correlating roughness with scour and fill. The study sites include both the Manival (Chapter 3) and the Réal (Chapter 4) torrent catchments which experiences frequent debris-flows and bedload transport. The influence of slope and storage on scouring is quantitatively determined with detailed pre- and post-event topographic surveying. The characterization of channel storage and its

influence on debris-flow scouring is analyzed in detail with multi-date terrestrial laser scanning in a selected reach of the Manival torrent.

2 METHODS

2.1 Channel observations from cross-section surveying

Scour and fill in the Manival and Réal torrents were quantified by topographic resurveys of cross-sections (described in Chapter 3). Along the 1.8-km study reach of the Manival, 39 cross-sections are distributed with a mean spacing of 40 m (3 times the mean active channel width). For the Réal, only 15 cross-sections were deployed along the 1.8-km study reach, giving a mean-cross section spacing of 120 m (5 times the mean active channel width). Cross-section locations are found in Chapter 3, Figure 17 for the Manival and Chapter 5, Figure 37 for the Réal.

Eight post-event surveys were done in the Manival since spring 2009, with two being after debris-flow events of moderate intensity. The monitoring period in the Réal was from spring 2010 to autumn 2011; six post-flow surveys were measured, with three being after debris-flows of moderate intensity. The level-of-detection for significant elevation change between pre- and post-event surveys is determined from the D_{84} of the bed surface grain-size distribution, which for the Manival and Réal are approximately 5 cm. It is important to mention that the debris-flows in these torrents are often in the form of multiple surges. The topographic surveys capture the time-integrated elevation change of the torrent and not the individual surges. An eye witness reported 4 surges for an event in the Manival, and high-frequency monitoring stations in the Réal observe a variation of one to four surges depending on the downstream distance from the source area (Navratil et al., in press). In many cases for individual surges, the front of the debris-flow scours the bed and the tail reworks the material where deposition can occur (eg. Berger et al., 2011a). The tail deposit of the debris-flow is measured in the post-event topographic survey; this gives a lower bound estimate of scour depth.

Determining a standard method for measuring channel scour in a debris-flow channel is difficult. Distinguishing debris-flow scour rather than bank failure or scouring from hillslope processes requires careful interpretation. Analysis needs to be made from available data and field observations. An example of a surveyed cross-section before and after an event (Figure 57) helps to define metrics that were derived from cross-section resurveys. We use the maximum scour depth (d_{\max}) for analysis in order to have the closest true measurement of debris-flow scour. The maximum scour depth is the greatest negative elevation change within the active channel of the resurveyed cross-section. Bank erosion is not included as channel scouring, because this is not directly controlled by the shear stress of the debris-flow acting normal to the channel surface.

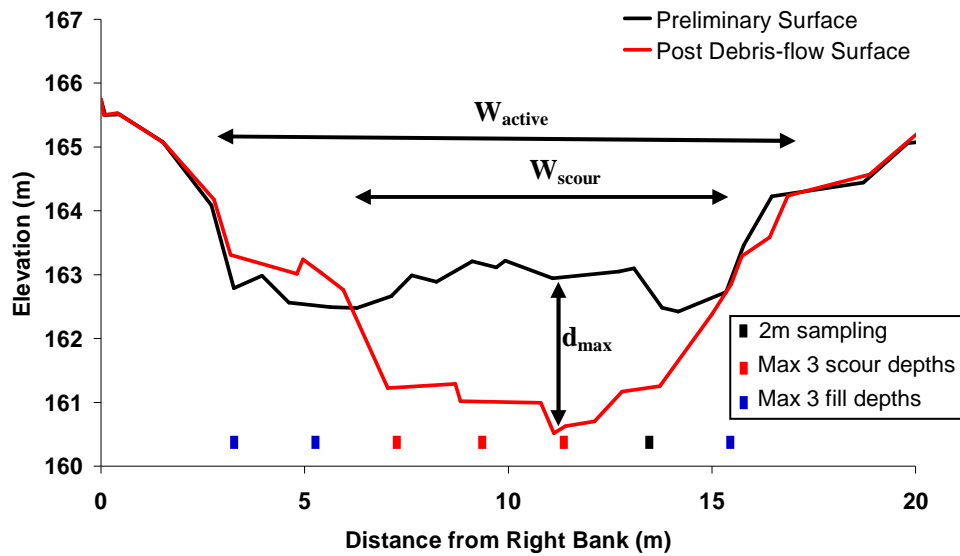


Figure 57 Cross-section view before and after a debris-flow. Active channel width and maximum scour depth (d_{max}) are used for finding statistical correlations with slope. The 2 meter sampling of scour and fill depths are found within the total active width. The maximum three scour samples (red dash) and maximum three fill samples (blue dash) are used for frequency distribution analysis.

For comparing debris-flow scouring in multiple sites, we normalize the maximum scour by (what we call) the channel scour width (W_{scour}). This width, according to the flow dynamics, is measured from the top edge of each bank where the flow occurred (Figure 57). The overbank deposition such as levees and lobes are not included in the width because they are separated from the actual flow in the channel. These debris-flow channels can have several different bank heights from previous debris-flows. Therefore careful field and data interpretation is required to match the closest bank to the observed flow height.

For analyzing frequency distribution of scour and fill, multiple samples in each cross-section are needed to increase the data population. Therefore a 2-meter sampling interval is taken for the active width (W_{active}) (Figure 57). Active widths can be determined from pre- and post-event surveys by delineated significant elevation changes of the bed (Liébault and Laronne, 2008). This width includes the levee and lobe deposits on the channel banks in order to include important debris-flow deposition. Channel width varies throughout the channel where wider sections have higher sampling numbers. In order to have an even sampling distribution along the channel profile, the maximum three samples for scour and fill are selected (Figure 57). This also limits the zero population in the wide channels where inactive patches occur within the active width.

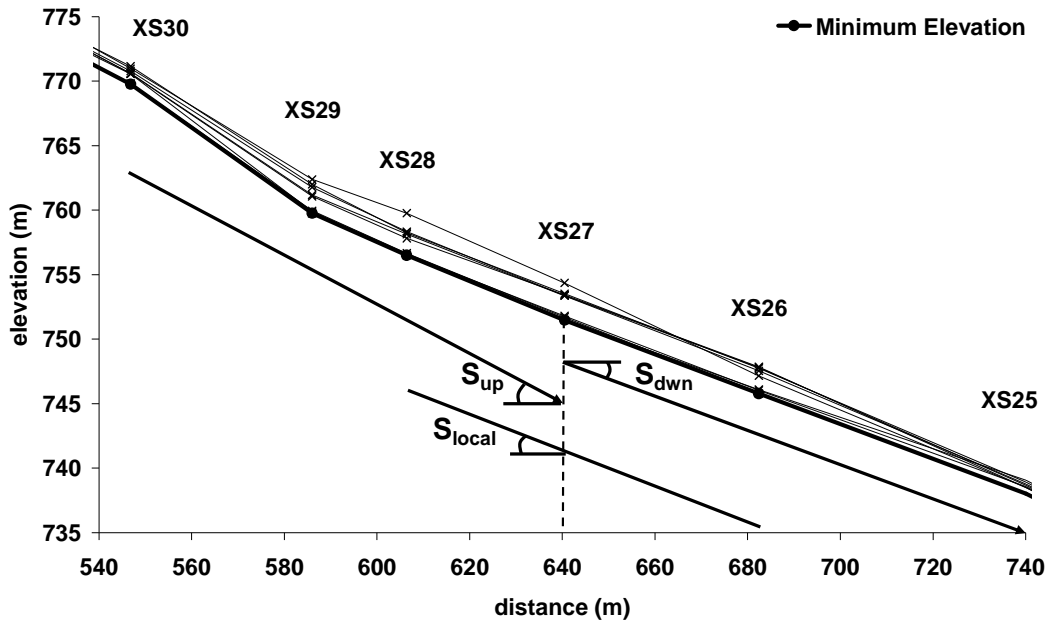


Figure 58 Multi-date profile of a reach in the Manival torrent derived from cross-section surveys. Minimum surface used for slope calculations is indicated by the thick thin with solid dot. Different slope measurements for XS 27 are S_{up} (upstream slope), S_{local} (local slope), and S_{down} (downstream slope).

Defining the method for measuring channel slope is very important. In debris-flow channels, the channel bed elevation can vary through time changing the local slope. However, the scale and location of measurement is even more important. Figure 58 shows an example of a very active reach in the Manival torrent. Throughout the survey periods the elevation can vary up to 4 meters. The minimum elevation measured throughout the monitoring program was used representing the stable channel bottom. Different measurements for slope were taken upstream (S_{up}), locally (S_{local}), and downstream (S_{down}). These slopes at different scales are tested for their correlation with channel scouring.

2.2 Data compilation from literature

For developing a global relationship between debris-flow scouring and channel slope, data from the literature have been compiled for a more thorough analysis. Maximum debris-flow scour depths, widths, and upstream slope need to be obtained from detailed topographic measurements of channel cross-sections. Three previous studies have matched these requirements for debris-flows triggered by water surges:

- 1) The Chalk Cliffs in Colorado, USA (Staley et al., 2011) have a small debris-flow catchment (0.3 km²) with multiple debris-flows occurring every year induced by runoff from high intensity rainfall (Figure 59A). The channels (slopes ranging from 0.15 to 0.56) are supplied by very active cliffs with rockfall, rockslides, and hillslope debris-flows. The site was resurveyed by TLS for debris-flow events and the largest event (820 m³) is used for comparison in this study (Staley et al., 2011).
- 2) Eastern Victoria, Australia (Nyman et al., 2011) has multiple sites with burnt areas where debris-flows were triggered by runoff from high intensity rainfall (Figure 59B). Catchments (with cross-section surveys) ranged in areas from 0.1 to 2.0 km² with channel slopes of approximately 0.2 to 0.8. Material originated from exposed hillslope material and loose colluvial and alluvial channel storage which produced debris-flow magnitudes of 2 900 – 6 000 m³. Three debris-flows from different catchments were compared with three cross-sections each. Pre-event surface was interpolated according to cross-section features from the post-event field surveys.
- 3) Fjaerland, western Norway (Breien et al., 2008) experienced a large glacial lake outburst flood (GLOF) in the spring of 2004 which initiated a debris-flow (Figure 59C). The initial glacial lake area was 10 000 m² and the channel slope below varied from 0.07 to 1.73 (average of 0.31). Some breached moraine material and mostly channel storage composed a debris-flow volume of 250 000 m³. This is a less active torrent where only two other debris-flows occurred in the last century. Cross-sections were extracted from DEMs derived from aerial photos before and after the event.

The upper catchment of the Manival was also compared by using transects from multi-date TLS data in first- to third-order reaches (Chapter 3). The first-order reach consisted of a runoff generated granular flow on a talus slope. The second- and third-order reaches experienced runoff generated water surges not yet at a debris-flow state because of low sediment concentration (the debris-flow was developed further downstream).

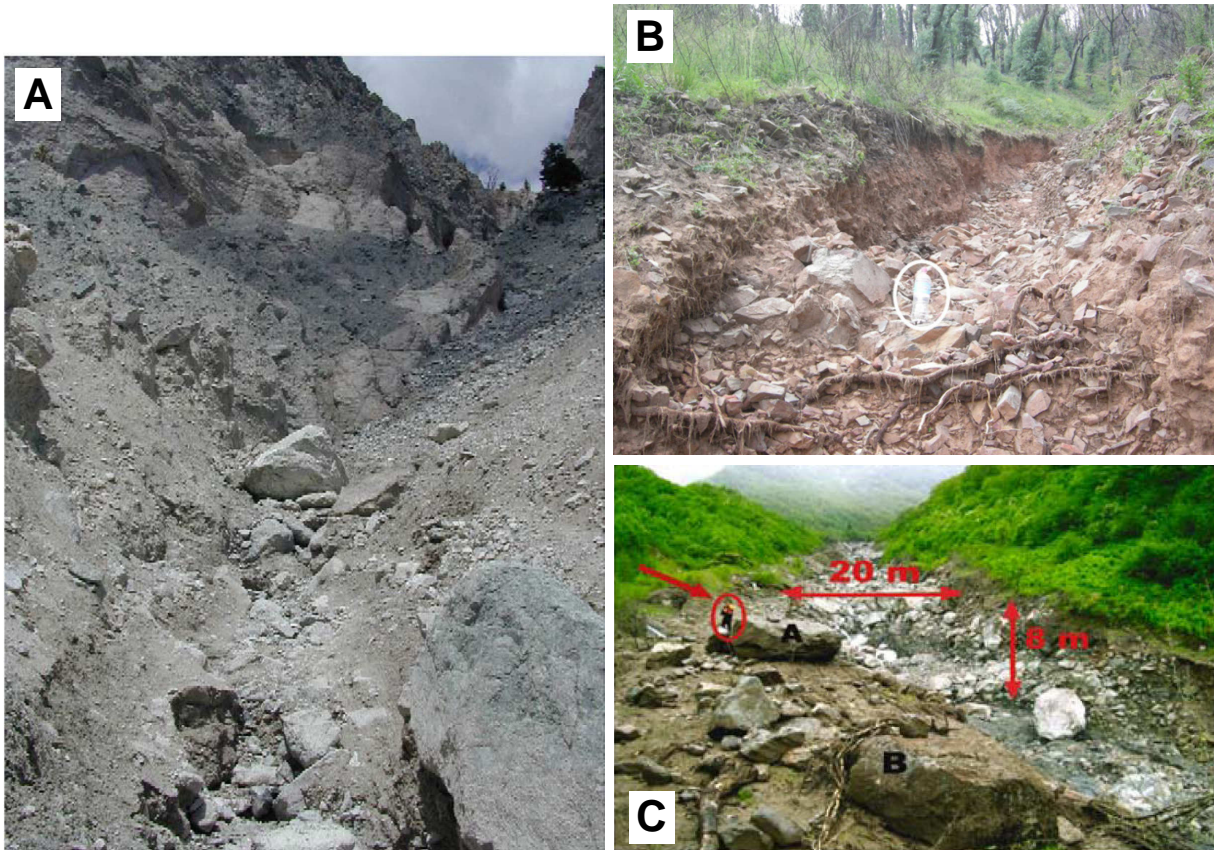


Figure 59 Channel views of the compared study sites from literature; (A) the Chalk Cliffs in Colorado, USA (from Coe et al., 2008), (B) Eastern Victoria, Australia (from Nyman et al., 2011), and (C) Fjaerland, western Norway (from Breien et al., 2008).

2.3 Laser scanning for the characterization of erodible material

Channel scour, deposition, and roughness were measured from multi-date terrestrial laser scans (TLS). The focus of this study was to make detailed observations in one reach (test reach) with a resolution that can be applied throughout a channel or river network. The test reach is located in the Manival torrent, a very active reach 190 m long 17 m wide (Figure 60A).

The reach was scanned before and after three events (debris-flow / bedload transport / debris-flow) with an ILRIS-3D (Optech Inc.) terrestrial laser scanner (first and last hillshades of the monitoring program shown in Figure 60B-C). Several scanning positions from different viewing angles were always used for obtaining the maximum point coverage, thereby minimizing the most important source of error (Schürch et al., 2011a). The multiple scans for each survey campaign were merged together using Polyworks™ which calculated a root mean square error (RMSE) ranging from 0.6 to 1.0 cm. The final point density after data processing for each campaign ranged from 22 to 55 points per 20-cm grid cell (Table 15). Merging the multi-date scans together by selecting permanent features

as reference points produced a RMSE range of 1 to 3 cm. According to a 20 cm resolution, overlapping data between survey campaigns covered 52 to 59% of the study reach. Further details on instrumentation and measuring techniques are found in Chapter 3.

DEMs with a 20cm resolution were developed by taking the mean elevation of points within each 20cm cell. Cells with at least five points were used for analysis; this limits any noisy data that does not accurately represent the surface. Interpolation methods were not used for developing the DEMs. We only used non-interpolated overlapping data. The 20cm resolution allows for quantifying erosion and deposition in narrow channels which are typical in steep catchments; it also allows a more efficient computing time for large scale applications. Elevation differences were then directly calculated from the post- and pre-event 20-cm grids.

For characterizing the nature of the channel sediment, we apply a method proposed by Cavalli et al. (2008) who identifies channel features using roughness from airborne LiDAR. Step-pools and riffle-pools were distinguished with the standard deviation of residual elevations with a 0.5 m grid and a 2.5 m search window (1:5 ratio). With the TLS data in the test reach of the Manival, we used the same ratio with the 20 cm grid and a 1-m diameter search window. The kernel-cell in the search window is kept for analysis only if there are at least five cells in its window. This filters out poorly covered areas which are usually found on the vegetated banks of the channel.

Similar methods with higher resolutions (within centimeters) have been used with TLS data for characterizing grain size in gravel bed rivers (Heritage and Milan, 2009). The large grain size distribution in debris-flow channels makes this analysis complex, and the high resolutions create inefficient computations. Therefore, our 20 cm grids are applied for characterizing the channel features instead. The final characterizations of sensitive material from roughness were then tested on airborne laser scan data in the Manival at the same resolutions. The characterized sensitive material was validated with the surveyed cross-sections.

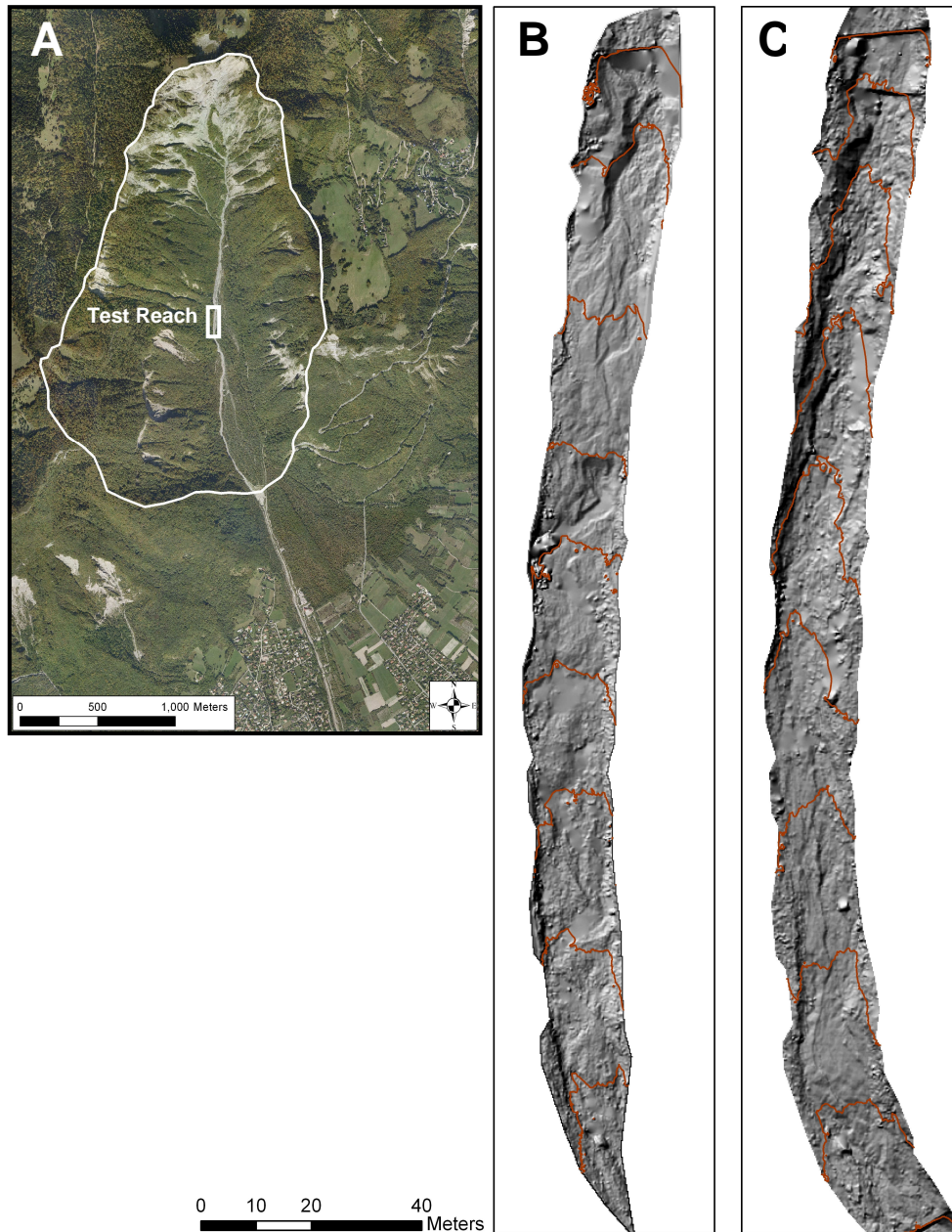


Figure 60 (A) location of the test reach in the Manival catchment; hillshades derived from 20 cm TLS scans when the test reach was full of sediment in July 2009 (B) and when it was empty in July 2010 (C); 4 meter contour interval.

Table 15 Test reach TLS scan periods with measurement coverage and errors.

Date	Points per 20cm cell	Multi-date RMSE (cm)	Multi-date data coverage (%)
July 2009	28	--	--
August 2009	22	1	57
November 2009	25	3	52
July 2010	55	1	59

3 RESULTS

3.1 Spatial variability of scour and fill

3.1.1 *Scour and fill for the Manival*

During the monitoring program in the Manival torrent, eight events have been observed between survey periods P1-8. Two debris-flows (P1 with 1 900 m³ and P5 with 3 300 m³) were triggered during short intense rainfalls during summer convective storms. The intense runoff develops into water surges which scour channel storages; these surges develop into debris-flows which continue to propagate down the channel with even more scouring. These events usually have multiple surges (4 observed from eye witness). The bedload transport events (P2-4 and P6-8) normally occurred during long duration rainfalls in autumn and during snowmelt in spring. Detailed descriptions, sediment budgets, and yield rates for these events are found in Chapter 3.

Large spatial variability of scour and fill has been observed after the events in the Manival (Figure 61). Debris-flows (P1 and P5) have significant scouring (up to 2.4 and 2.9 m) in the upper reaches of the study site. The average maximum scours are 0.8 (P1) and 1.0 m (P5), and the fills are 0.6 (P1) and 0.7 m (P5). Bedload transport events (P2-4 and P6-8) relatively have little scour and fill distributed throughout the entire study site. The average maximum scour is less, ranging from 0.4 to 0.6 m, and for fills from 0.3 to 0.5 m.

The large debris-flow scoured areas located in the upper reaches are distributed between long spaced check-dams. The scoured material is normally loose unconsolidated gravel wedges which have been deposited by bedload transport. They typically deposit in low slopes reaches downstream from steeper reaches. Little fill was observed in the upper reaches after the debris-flow events and the lower reaches also had little scour and fill.

Even with generally less scour and fill during bedload transport, there was still large scouring (1.1 to 2.1 m) and fill (1.2 to 2.6 m) in one or two reaches. This large localized scour and fill occur where gravel wedges are developed and mobilized. In 2009, more bedload transport occurred, especially in the upper reaches, due to a more important sediment supply from the headwaters. In 2010, there was still bedload transport in the lower reaches. This was due to the gradual scouring of the previous debris-flow deposits in the channel and levees. This material accumulates into gravel wedges and gradually mobilizes out of the channel.

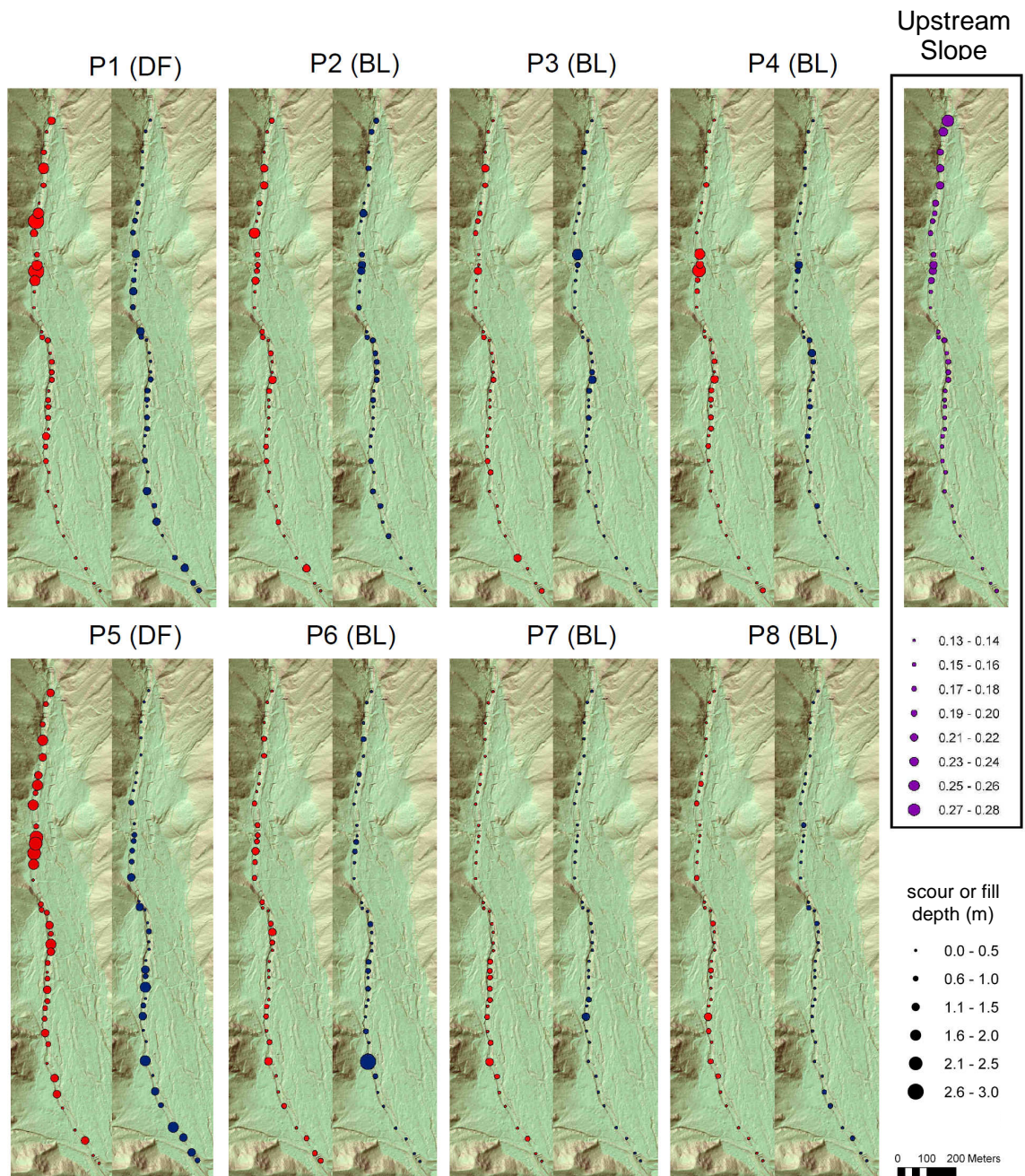


Figure 61 Map view of maximum scour (red) and fill (blue) in the Manival for measured events and upstream slope (magenta). (DF refers to debris-flow and BL refers to bedload transport)

3.1.2 *Scour and fill for the Réal*

During the monitoring program in the Réal torrent, six events have been observed between survey periods P1-6. Three main channel debris-flows (P1: 5 200 m³, P2: 7 000m³, and P5: 7 600m³) were triggered during short intense rainfalls during the summer convective storms. Small hillslope debris-flows and bedload transport (P3, P4, and P6) occurred during long duration low intensity rainfalls. Detailed descriptions, volumes, velocities, and discharge rates for these events in the Réal are found in Chapter 4.

Large spatial variability of scour and fill was also observed in the Réal torrent (Figure 62). The debris-flows significantly scoured the upper reaches with maximum depths of 2.0 m (P1), 3.8 m (P2), and 4.8 m (P5). The event average of maximum scours ranged from 1.0 to 1.3 m and fills ranged from 0.7 to 0.8 m. Events during P3, P4 and P6 have a higher variability because of the multiple processes involved (hillslope debris-flows and bedload transport). The event average of maximum scours ranges from 0.6 to 1.3 m, and for fills from 0.7 to 1.2 m.

Debris-flows consistently have a large scouring in the upper reaches because of the large filling of the hillslope debris-flows. The upper reach has very little fill as well as the lower reaches for both scour and fill. During bedload transport events, hillslope debris-flows interact with the upper reaches with deep scours (maximums from 1.8 to 4.5 m) and fills (maximums from 2.0 to 5.8 m). The lower reaches have relatively little scour and fill except where gravel wedges are developed and mobilized. There is not enough information to characterize the hillslope debris-flows, thereby excluding their effected cross-sections for analysis. Only the bedload processes in the lower reaches are used where gravel wedges are developed and mobilized.

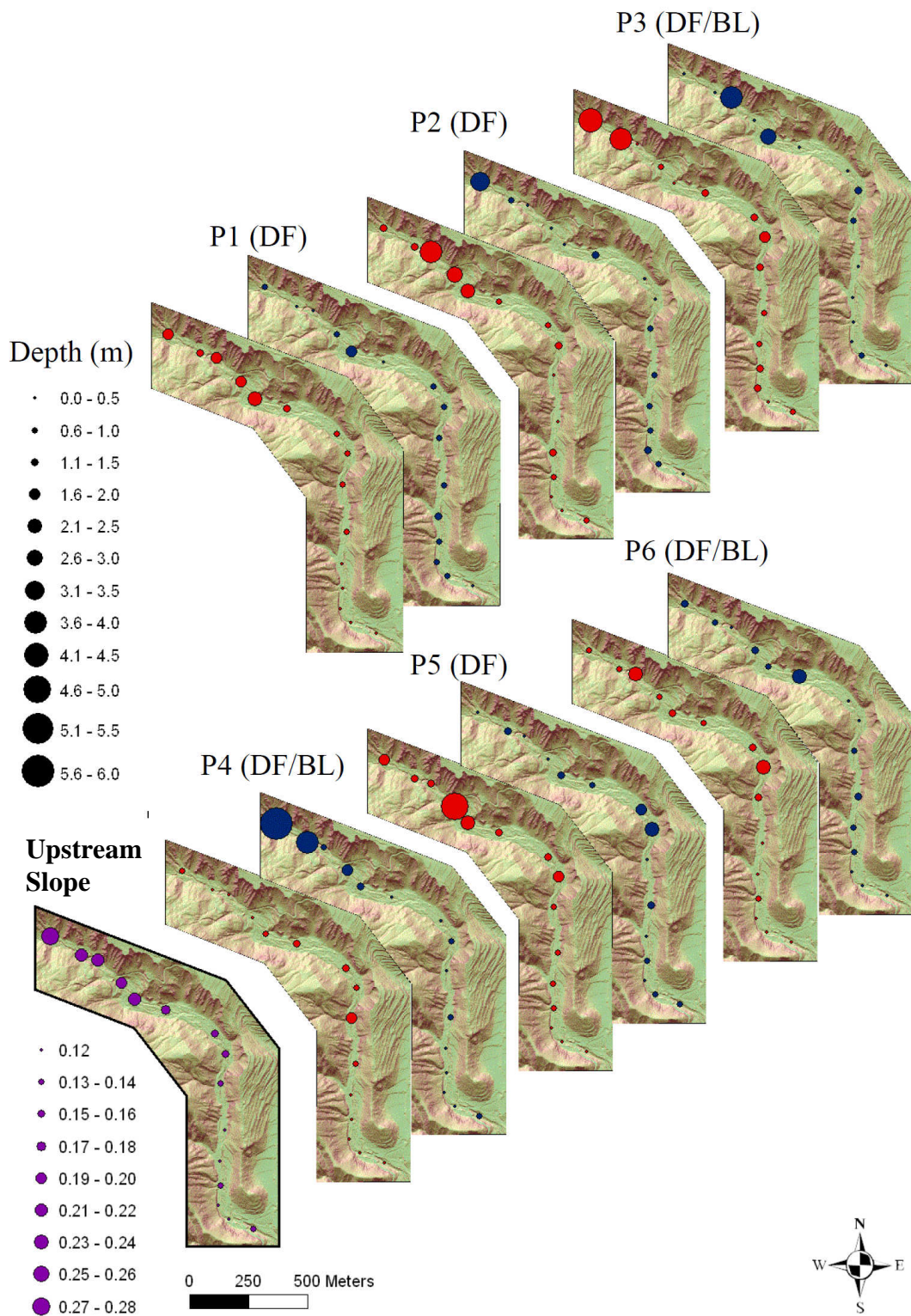


Figure 62 Map view of maximum scour (red) and fill (blue) in the Réal for measured events and upstream slope (magenta). (DF refers to debris-flow and BL refers to bedload transport)

3.1.3 Comparison between debris-flow and bedload transport

As observed in Figure 61 and Figure 62, debris-flows and bedload transport had distinct behaviors for both the Manival and Réal torrents. A general comparison of mean elevation change between debris-flow and bedload transport is made with notched box plots for the Manival (Figure 63). Debris-flows had 78 samples and bedload transport had 211 for analysis. Not enough data was available in the Réal to make an accurate comparison which consisted of 45 samples for debris-flows and bedload transport.

The t-test was used for assessing whether the normally distributed independent variable (mean elevation change) for debris-flows and bedload transport in the Manival significantly differed from equilibrium. According to the null hypothesis that the mean value of elevation change is zero, debris-flows could be rejected but bedload transport could not be rejected at a 5% confidence level. Mean elevation changes for debris-flows have a p-value less than 0.001 and the 95% confidence interval for the mean ranges from -0.23 to -0.06 m. Mean elevation changes for bedload transport have a p-value of 0.36 and the 95% confidence interval for the mean ranges from -0.04 to 0.02 m. Debris-flows had a large variation of elevation changes with a median value of -0.10 m and bedload transport had a median of 0.00 m and with much less variation. This statistical test and results clearly indicate that debris-flows are a scouring process and bedload transport is at equilibrium.

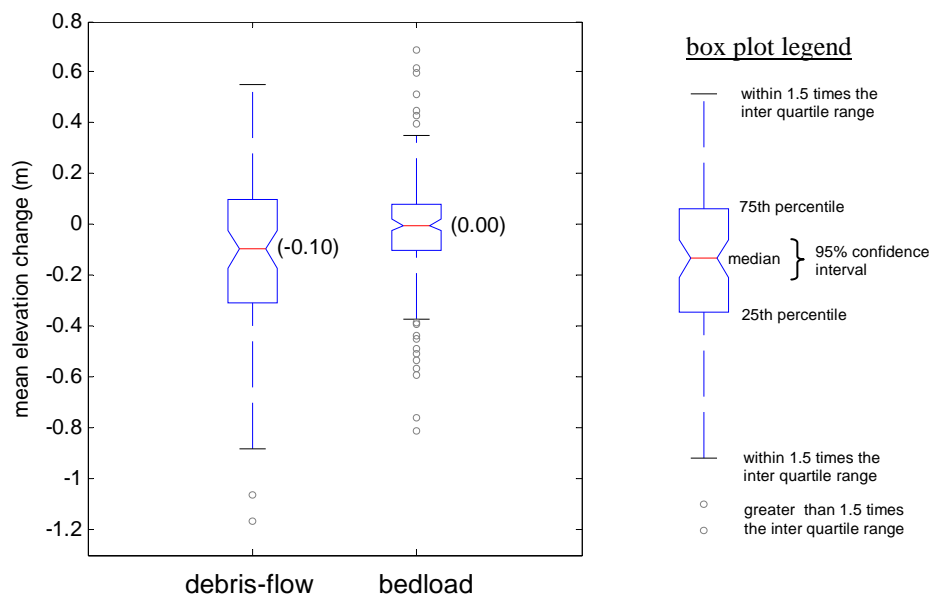


Figure 63 Notched box plot of the mean elevation changes for each cross-section in the Manival torrent indicate significant difference between debris-flow and bedload transport. Box plots indicate the median, 25th and 75th percentiles, data extents within 1.5 times the inter quartile range and the outliers larger than 1.5 times the inter quartile range. Notches indicate the 95% confidence range of the median value.

For comparing scour and fill between bedload transport and debris-flows in both the Réal and Manival, the maximum three samples of each cross-section were used (Figure 64). In the Manival, there are 234 samples for debris-flows and 633 samples for bedload transport. Réal has 135 samples for debris-flows and 127 samples for bedload transport.

The Mann-Whitney U test was used to assess whether the non-normally distributed independent variables (scour and fill) are statistically different. According to the null hypothesis (medians between scour and fill are equal) debris-flows for the Manival and Réal could be rejected at a 5% confidence level (Figure 64). The hypothesis for the bedload transport in the Manival could also be rejected, but not for the Réal. The Manival has more samples creating low p-values of 0.003 for debris-flows and 0.001 for bedload transport. The Réal has fewer samples with p-values of 0.023 for debris-flows and 0.339 for bedload transport.

According to Figure 64, both torrents indicate that scouring during debris-flows is the most important channel response. Debris-flows in the Manival have a median scour of 0.31 m and fill of 0.12 m. This is larger than the bedload transport which has a median scour of 0.07 m and fill of 0.06 m. The Réal has a larger channel response with a median debris-flow scour of 0.44 m and fill of 0.28 m. Its bedload transport has a median scour of 0.20 m and fill of 0.19 m. Debris-flow scouring is significantly larger than its fill and has the greatest variation. Bedload transport for both catchments has little difference between scour and fill. The large variation of scour and fill for the Réal's bedload transport is influenced by the hillslope debris-flows entering the upper reaches.

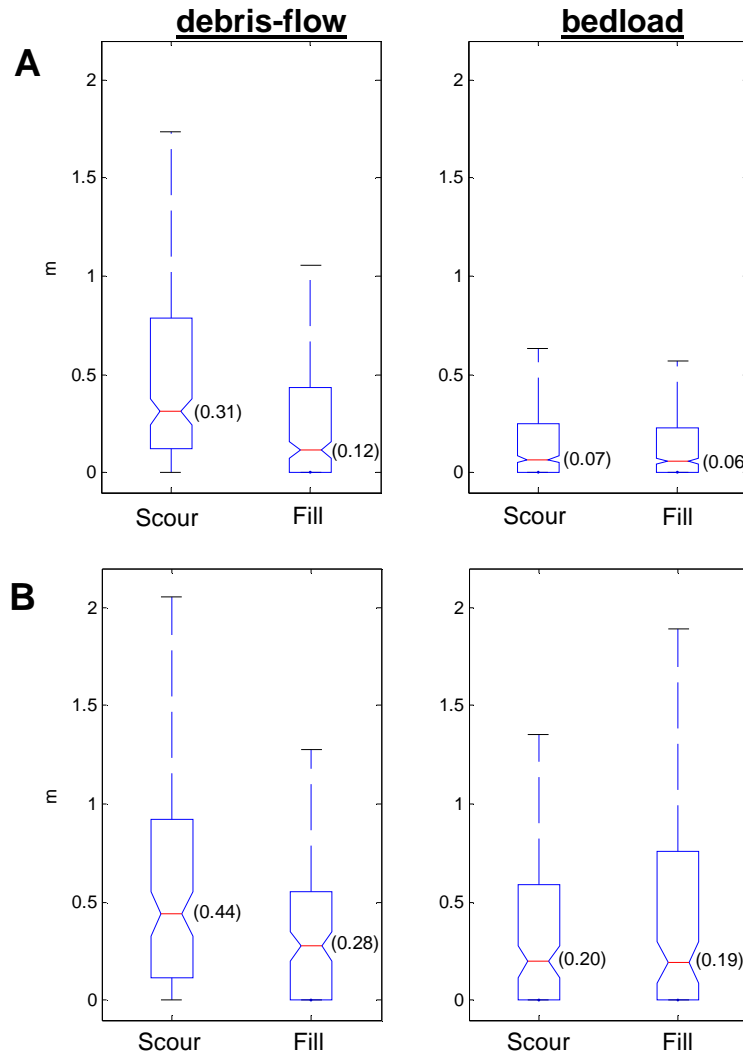


Figure 64 Notched box plots of the maximum three samples for scour and fill at each cross-section. Both (A) the Manival and (B) the Réal show that the most scouring occurs during debris-flows. Box plots indicate the median, 25th and 75th percentiles, data extents within 1.5 times the inter quartile range and the outliers are larger than 1.5 times the inter quartile range. Notches indicate the 95% confidence range of the median value.

The spatial distribution of debris-flow scour and fill can be influenced by the upstream slope (seen in Figure 65). Only results from the Manival were used for comparison because of its larger database. The upstream slope (S_{up}) was compared with the maximum three random samples of scour and fill for both bedload transport and debris-flows. Debris-flow scour strongly decreases as the slope decreases down to 0.16. Debris-flow fill gently increases as the slope decreases, however the study site does not include the important depositional reach for debris-flows. For bedload transport, both scour and fill do not have any trend with slope. Either the scale of the measured slope is too large or the time resolution is too long for flood measurements. Nevertheless, these results indicate that upstream slope (S_{up}) has an important influence on debris-flow scouring in the Manival.

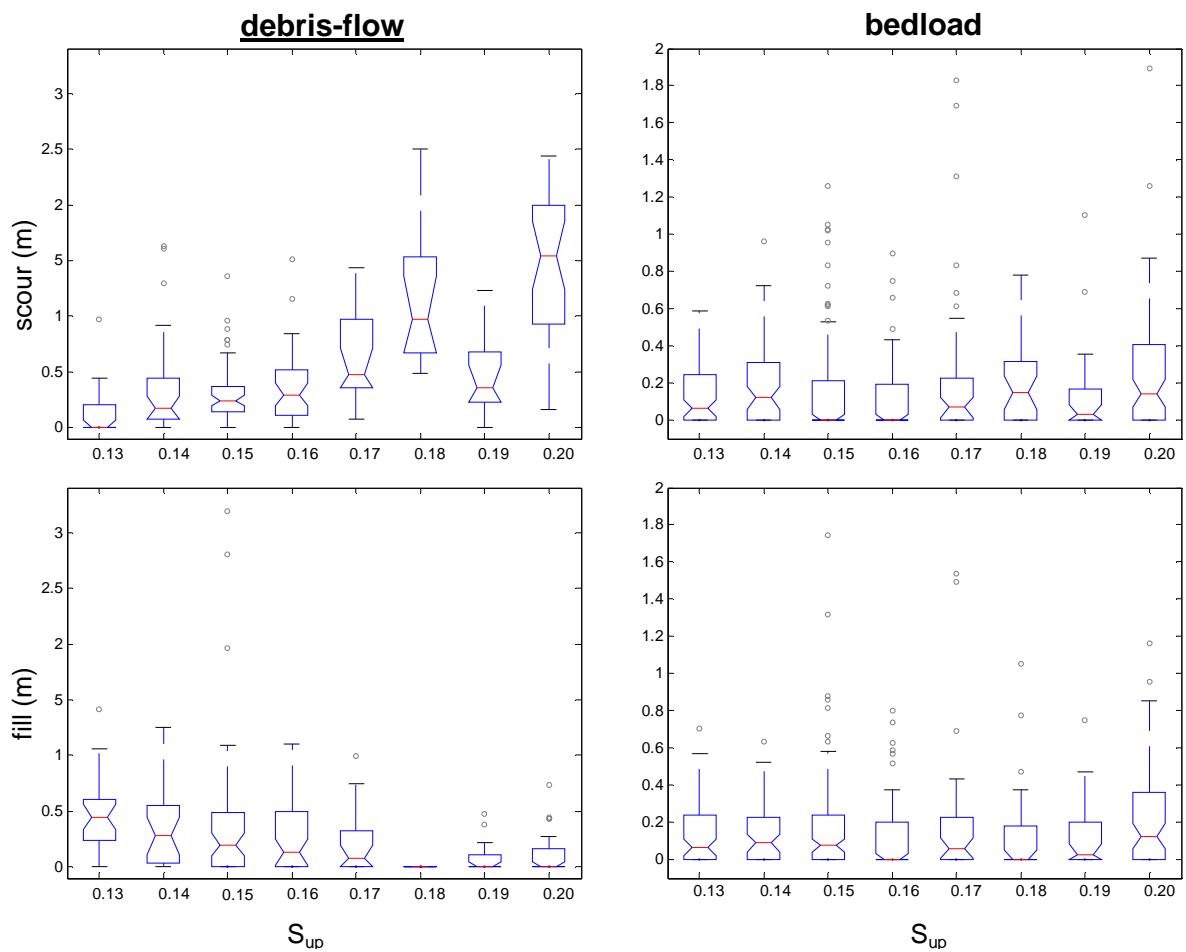


Figure 65 Notched box plots of the maximum 3 sampled scour and fill for each cross-section in the Manival related with upstream slope (S_{up}). Debris-flow scour and fill relates to slope where as bedload transport shows no relation. Not enough data is available for comparing the Réal torrent. Labeled slope values are the center values of the bins. Box plots indicate the median, 25th and 75th percentiles, data extents within 1.5 times the inter quartile range and the outliers are larger than 1.5 times the inter quartile range. Notches indicate the 95% confidence range of the median value.

3.2 Global relation of debris-flow scour and channel slope

With the Manival cross-sections, the three slopes (S_{up} , S_{local} , and S_{dwn}) were measured at different scales. These measurements were correlated with mean scouring from two debris-flow events (Figure 66). The correlation coefficients indicate that the upstream slope S_{up} has the most influence on erosion. Another important observation is that the correlations dramatically increase when the scale increases up to 6-8 times the channel width or 10 times the channel scour width (W_{scour}). Therefore, the S_{up} at this scale is used for analysis in this study. This slope controls the debris-flow condition before entering the cross-section.

The mean W_{scour} for the Manival torrent during two debris-flows was 10.1 m (range of 5.1 m to 18.7 m). The defined S_{up} in the Manival ranges from 0.13 to 0.28 (mean 0.16). In the Réal torrent for three debris-flows, the mean W_{scour} was 11 m (range of 3.8 m to 20.2 m). The defined S_{up} in the Réal has a range of 0.12 to 0.27 (mean 0.16).

A global database of debris-flow scour (d_{max}), scour width (W_{scour}), and upstream slope (S_{up}) were compiled with 144 cross-section measurements from the Manival torrent (and its upper catchment), Réal torrent, Fjaerland, Norway (Breien et al., 2008), Eastern Victoria, Australia (Nyman et al., 2011), and the Chalk Cliffs, Colorado, USA (Staley et al., 2011). The S_{up} ranges from 0.12 to 0.84, d_{max} from 0.1 to 8.8 m, and W_{scour} from 1 to 49 m.

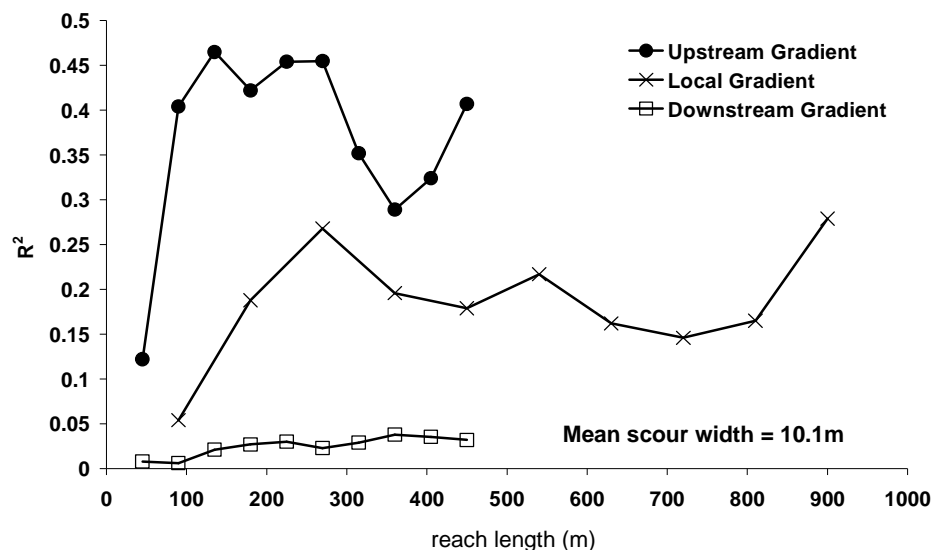


Figure 66 Correlation between mean scour and slope for the debris-flows in the Manival torrent measured at different scales. Upstream slope with measured length of 10 times the scour width shows the best correlation with debris-flow scour.

A logarithmic relationship (R^2 of 0.50) was found between the normalized maximum erosion ($d_{\max} / W_{\text{scour}}$) and S_{up} (Figure 67). Scouring decreases rapidly below an upstream slope of approximately 0.15. As the slope increases above 0.15, the increase of scouring becomes gradual which could be influenced by supply-limited reaches. The steepest measurements are in the range of repose angles of gravels and cobbles which are typically found on talus slopes (slopes of 0.61-0.73).

The envelope between the D_{95} and the D_5 of the erosion/slope distribution is approximately half an order magnitude. This distribution can be explained mostly by the available storage. Scour depths can range from the upper- to lower-envelope for the same cross-sections in both the Manival and Réal which depends on whether there is storage present in the channel. Other similar sites, such as the upper catchment of Manival and the Chalk Cliffs also correspond well with the envelope boundaries and presence of storage. The steepest two reaches of the Manival upper-catchment are talus slope failures where the channels were completely filled with sediment. The next lower reaches are found below the envelope, these reaches experienced more of a hyper-concentrated flow because of little sediment availability. The Chalk Cliffs with a similar S_{up} , experienced debris-flows which had deeper erosion with the presence of storage.

Nyman et al. (2011) found that the debris-flow scouring in the burnt areas also depend on the channel storage. The cross-sections before the events were mostly full of storage with reaches scouring down to bedrock afterwards. These channel conditions explains why they are in the upper-envelope. However, some of the cross-sections for the glacial lake outburst flood (GLOF) induced debris-flow in Norway were almost full of storage and they are within the lower-envelope of erosion. Most of the reaches were originally V-shaped and were scoured into rectangular trenches with vertical sides (Breien et al., 2008). The changing of the channel shape at this large magnitude influences the normalization of debris-flow scour by width.

Outlying points above the envelope are cross-sections with a deep, narrow active width, U-shape form. The channels are filled with loose colluvial and alluvial material that are easily washed away. The cross-section shape is unusually deeper than the other cross-sections. Outlying points under the envelope are mostly reaches without storage except for the GLOF induced debris-flow reach.

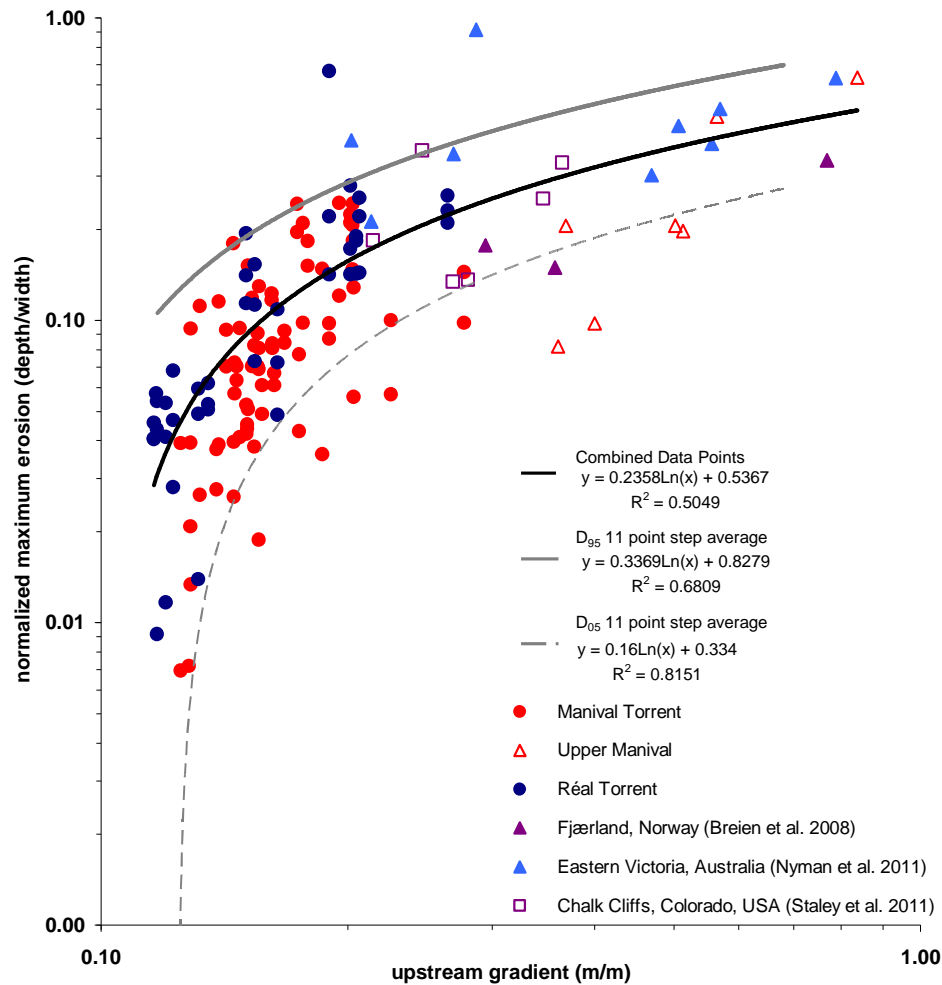


Figure 67 Relationship of maximum erosion (normalized by width) and upstream slope measured by resurveyed cross-sections. Three debris-flows for Réal (blue) and two for Manival (red) show the variation of erosion for each cross-section. Other sites are compared revealing a global relationship.

3.3 Characterizing erodible material with TLS

3.3.1 Sequence of events and topographic descriptions

Erodible storage was characterized in a very active reach of the Manival torrent with a terrestrial laser scanner. The TLS results for the multi-date surveying in the test reach includes an event sequence of debris-flow (P1), bedload transport (flooding) (P2-3) and debris-flow (P5) (Figure 68). These periods correspond with the monitored channel responses observed from the cross-section resurveys (Figure 61). The P4 period is within the TLS scanning period of the P5, however it had little change in the test reach and therefore it is not grouped with the P5 event.

Initially (end of July 2009) the reach was full of unconsolidated sorted gravels (gravel wedges) which created the highest elevation long profile (Figure 68C). These gravel wedges have the smoothest

roughness in the reach ($D_{50} = 0.039$ m), which also makes the reach the smoothest for the entire monitoring period (Figure 68B).

On August 25 2009, a debris-flow (P1) passed through the reach. Scans with the TLS were taken several days after showing significant scouring (Figure 68A). However, the long profile shows that the debris-flow did not scour the entire gravel wedge (Figure 68C). The reach had a mean elevation change of -0.41 m. The reach lost 786 m³ of material which is 41% of the debris-flow volume measured at the outlet of the catchment. The post-surface is a little rougher (Figure 68B) with a D_{50} of 0.042 m but still contains smooth material (gravel wedges deposited at the lower end of the reach).

From the end of August to November 2009 (P2 and P3), bedload transport occurred during low intensity, long duration rainfalls. Several flow events eroded the previous debris-flow tail deposits and levees which formed new gravel wedges. These gravel wedges were likely mobilized from the source area into the test reach with net deposition (Figure 68A). The reach had a mean elevation change of 0.12 m with a relatively normal distribution. Elevation in the profile increases on the upstream and downstream extent of the gravel wedge (Figure 68C). The reach gained 226 m³ of material which is 29% recharge from the previous debris-flow scouring. The test reach becomes smoother where deposition took place ($D_{50} = 0.039$ m).

The last debris-flow (P5) scoured down to the channel bottom (highly consolidated old debris-flow deposits) (Figure 69). The highly consolidated material's scour was insignificant compared to the large scour depths of the unconsolidated gravels. The minimum long flat profile after the event shows that it is at channel bottom (Figure 68C). The elevation change again has an asymmetric distribution (mean of -0.46 m). The reach lost $1\ 013$ m³ of material which is 31% of the debris-flow volume. After this event, the test reach had the highest roughness for the entire monitoring period ($D_{50} = 0.049$ m). There were smooth deposits in the lower end of the reach which were likely formed during the recession limb, but they quickly eroded away later by bedload transport. Since this event, there has not been any recharge from the source area for the rest of the year. Without unconsolidated storage in these reaches, no events occurred, even during high rainfall intensities observed from June-July 2010 (maximum 79 mm hr⁻¹).

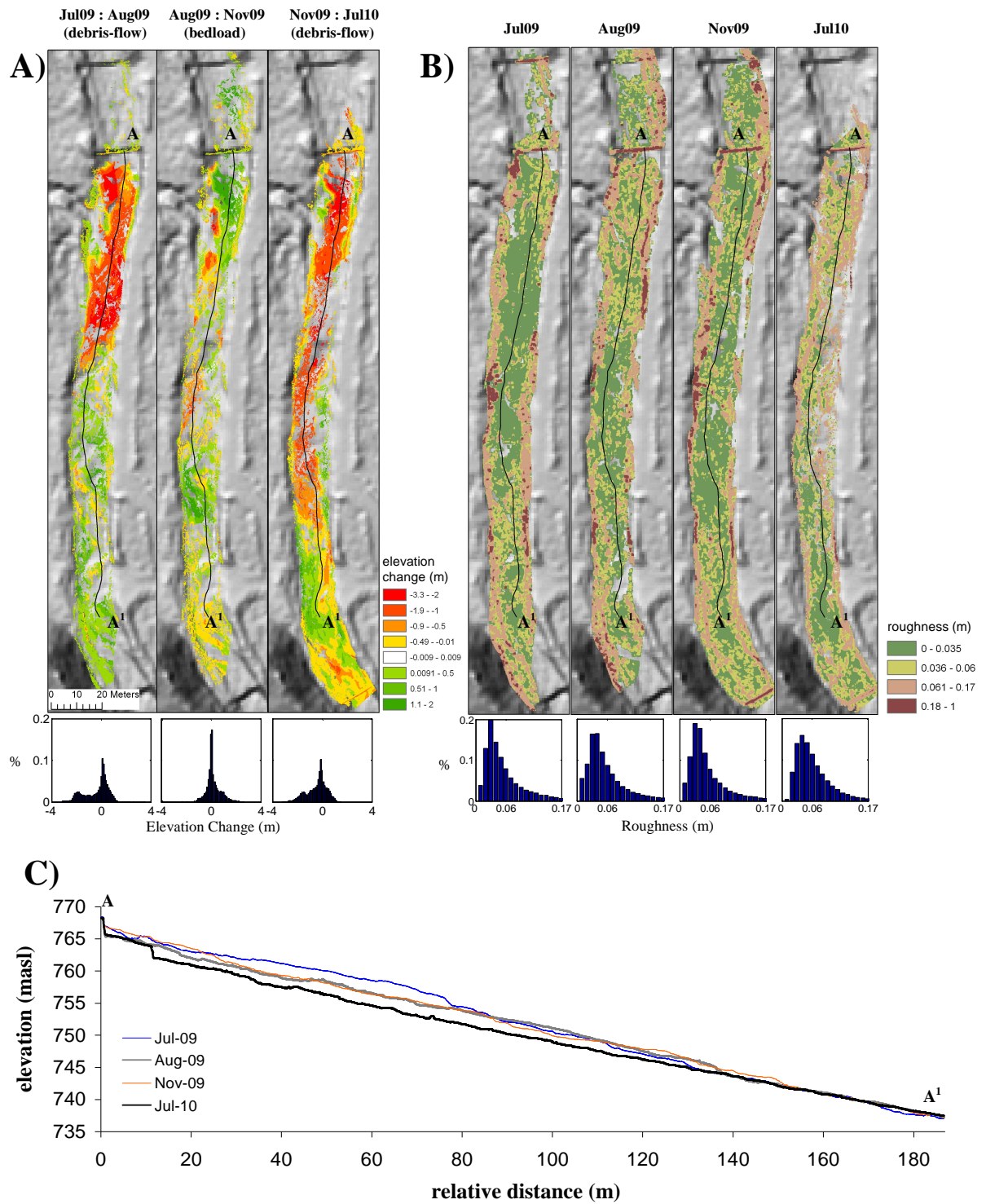


Figure 68 Results of TLS scans in the test reach of the Manival torrent showing the relationship between debris-flow scour and roughness. A) Elevation differences between survey dates with frequency distribution of scour and fill. B) Roughness derived from the TLS for each survey date with their frequency distributions in the reach below the D_{95} (roughness above the D_{95} is considered noise from steep features such as banks and check-dams). The classes are defined according to the roughness/scour relationship; dark green (median), light green and rose (defined in Figure 71), and red (above the roughness D_{95}). C) Channel profile of each TLS survey with July 2010 revealing channel bottom.



Figure 69 View looking upstream of the scoured test reach in the Manival torrent after the July 2010 debris-flow. The reach before the event was almost bank full of a gravel wedge (A). The wedge was scoured down to the highly consolidated coarse-lag deposit (C) and debris-flow levees (D) are deposited. Remnants of smaller terraces can be found (B) which are sequences of fill and scour during or after the debris-flow event.

The effect of the check-dam upstream of the test reach can also be seen in Figure 68. The greatest debris-flow scouring occurred closest to the check-dam and progressively decreased downstream. The largest bedload deposits are also closest to the check-dam where the gravel wedge is formed. Check-dam analysis is difficult, because of the difficulty to obtain enough information to discriminate the effect of the step-profile, the presence of channel storage and the debris-flow condition. The check-dams are known to disrupt the debris-flow momentum (Remaître et al., 2008), where the loss of the energy can be reflected with the channel scouring observed downstream of the check-dam. However, throughout the channels of the Réal and Manival, significant scouring only occurs below the check-dams when storage is present.

3.3.2 *Classifying erodible material with roughness*

In the maps of Figure 11A-B, it can be seen that debris-flows preferentially scour on smooth surfaces. This can be quantified by using the TLS data for grouping cells which have been scoured and not scoured by debris-flows. These groups are then related to pre- and post-event roughness (Figure 70). The Mann-Whitney U test showed that the non-normally distributed independent variable (roughness) have statistically different medians for scoured cells and non-scoured cells with a 5% confidence level and p-values less than 0.001.

Scoured cells have a median pre-roughness surface of 0.035 m which is significantly less than the non-scoured cells (0.043 m) and the post-roughness scoured cells (0.047 m) and non-scoured cells (0.043 m). The pre-roughness scoured cells represent the gravel wedges which have broad smooth convex surfaces. The non-scoured surfaces typically represent boulders, channel banks, and check-dams. The post-roughness scoured-cells represents the remaining material after the scouring, this can be the tail deposits of the debris-flow surge, or old debris-flow deposits (highly consolidated and unsorted) which forms the channel bottom.

Scour depths are correlated with the pre-roughness surface which is distributed in 1 cm bins (Figure 71). The distribution is plotted below the D_{95} of roughness (17 cm). Any higher roughness is considered noise in the distribution such as steep boundaries where little horizontal erosion is calculated as large inaccurate channel scouring. The roughness of 2-3 cm is the highest frequency for scoured cells. There is a linear relation between the scour depth and roughness with the bins statistically different from one another. This trend extends to the roughness 6 cm which indicates the extent of the sensitive gravel storage. The linear relationship could be caused by the outside surface of the gravel wedge which is included in the 1-m window roughness calculation along the limit of the gravel wedge. We do not have information for actually predicting depths of scour; we can only identify the scourable material.

With the 20-cm grid, the gravel deposits can be automatically mapped (Figure 68C) according to the calculated roughness. Gravel wedges are two classes, 0-0.35 m and 0.35-0.6 m, which marks the median and extent of roughness relating to scouring. The next class, 0.6-0.17 m, covers areas that might be scoured but with little contribution, such as channel banks, large cobbles and boulders that are embedded in a matrix (debris-flow deposits). Roughness greater than 0.17 m covers areas mostly permanent structures such as check-dams and steep channel banks. The search radius of 1 m is sometimes problematic for capturing the roughness for entire boulders (their tops appear to have smooth roughness). However, the more sensitive areas (the gravel wedges) are mapped accurately which is of most concern in active debris-flow channels.

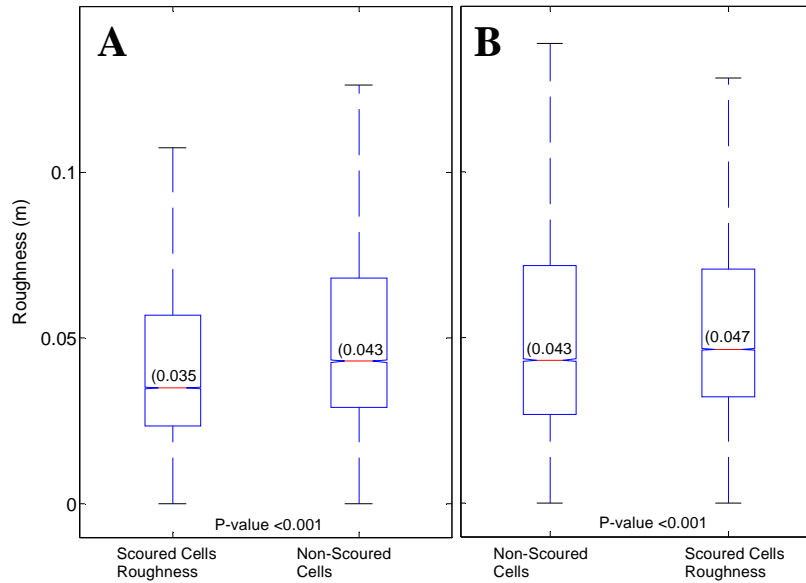


Figure 70 Notched box plots for precondition surfaces (A) show that debris-flow scouring occurs on a smoother roughness with a 95% confidence level. Post-condition surfaces (B) are rougher because of the eroded gravel wedges and the deposition of debris-flow levees. Over 207×10^3 samples were used for analysis. Box plots indicate the median, 25th and 75th percentiles, data extents within 1.5 times the inter quartile range. Notches indicate the 95% confidence range of the median value.

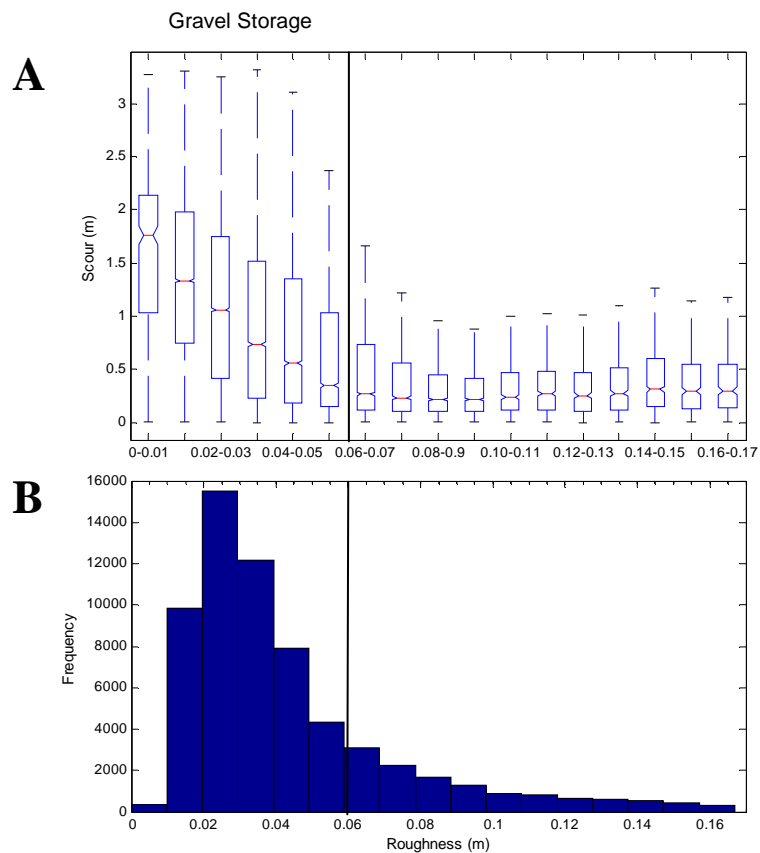


Figure 71 A) The roughness relation with scour reveals a linear trend ending at 0.06m roughness indicating the extent of the gravel storage. B) Roughness is binned at 1cm with the highest frequency between 0.02-0.03m. The plots extend to the D_{95} of the roughness calculations; any larger roughness is considered noise and is normally located on channel banks and check-dams.

3.4 Reach-scale roughness

The sensitive gravel wedges can also be mapped using airborne laser scanning (ALS). The raw ALS data was treated manually along the channel with approximately 30 pts/m² which was normally filtered automatically producing 6 pts/m² (see Chapter 3 for further details). A 20 cm grid was used to apply the roughness methods used in the test reach of the Manival.

ALS data in the Manival catchment was surveyed June 1, 2009 which represents the channel conditions before the first debris-flow in August 25, 2009 (P1). The roughness is consistent with the test reach output which was surveyed during the same channel surface condition. The storage in the test reach is the largest storage in the whole torrent. This corresponds to the largest scouring which is verified with the surveyed cross-sections (Figure 72). Channel storage (determined from roughness) covers 52% of the torrent.

We were not able to perform the same analysis with the ALS in the Réal torrent. The point densities varied throughout the catchment. The upper reaches where large scouring occurs have the poorest quality with laser swaths of large band spacings. This could be caused by the variable flight elevation or the flight speed of the aircraft. The lower reaches have a better quality point spacing which shows good channel feature correspondence with the same roughness values as the Manival, however there is not enough quality data for analysis.

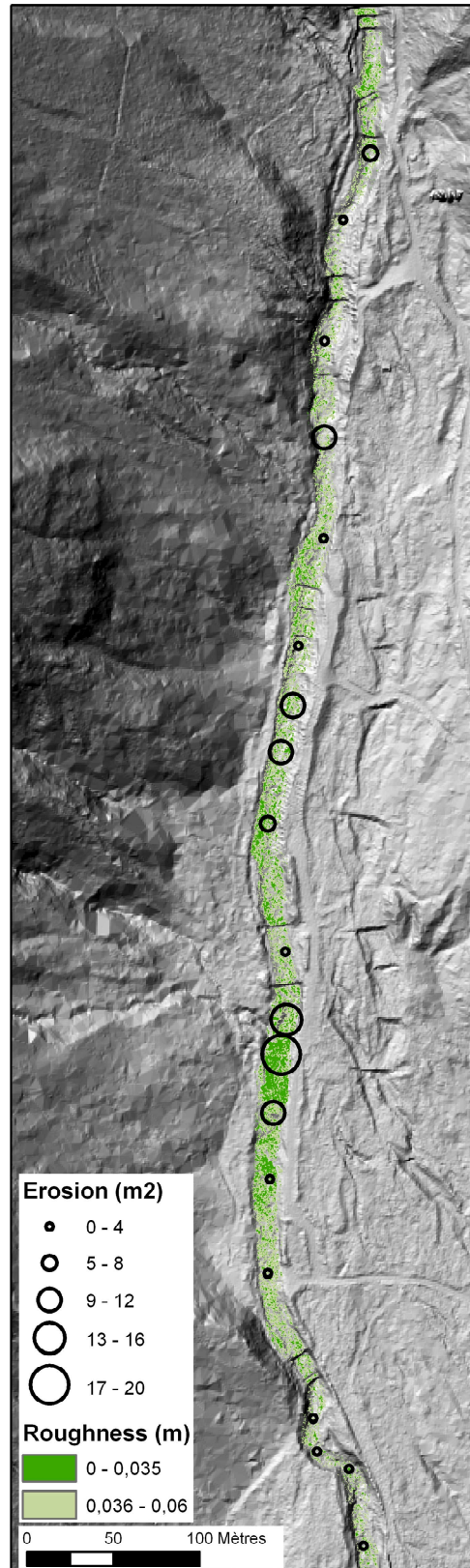


Figure 72 Storage mapping using roughness calculations derived from ALS with a 20cm grid (treated within the torrent channel). The storage before the August 2009 debris-flow is related to the erosion (m²) from the surveyed cross-sections.

4 DISCUSSION

4.1 Comparing debris-flow and bedload scouring

Scouring was observed to have a large spatial variability in the Manival and Réal torrents. Debris-flows are a significant scouring process with a large variation of scour depths. In contrast, bedload transport is at equilibrium with small variation of scouring. Debris-flows tend to have important scouring (up to 2-5 m) where gravel wedges were located. Because of the large discharge of the debris-flow events, this scouring accumulates to large volumes (2 000 to 8 000 m³) and transported out of the catchment. During bedload transport, important scouring (up to 1-2 m) occurs in localized reaches where gravel wedges were mobilized from reach to reach which does not play an important role on the catchment's sediment production. In the Eastern Italian Alps, long-term field data of an active debris-flow catchment and an active bedload transport catchment with equivalent return periods revealed that debris-flow volumes were 2 to 3 orders of magnitude larger than bedload transport volumes (Mao et al., 2009). We have observed in one debris-flow catchment that debris-flows produce 2-10 times more sediment than bedload transport within one year.

The spatial variation of scour and fill in gravel bed rivers during bedload transport can be modeled with an exponential density function (Haschenburger, 1999). As the discharge increases, the distribution of scour and fill becomes stretched with an increase of depth (Powell et al., 2005). These characteristics are seen in Figure 63 for both the Manival and Réal torrents with small magnitude and variation of scouring during bedload transport and large magnitude and variation of scouring during debris-flow processes. This indicates that scouring for bedload transport depends on the shear stress of the flow whereas the debris-flows depend more on the erodible depth.

4.2 Influence of slope and storage on debris-flow scouring

Defining a proper slope was found to be very important for characterizing the channel response in debris-flow channels. Rather than local slope S_{local} , the upstream slope S_{up} (scale of 10 times the scour width) was found to be more significant for controlling channel scouring. It better characterizes the condition of the debris-flow front entering a given channel cross-section.

The Manival and Réal torrents independently showed a relationship between debris-flow scour and upstream slope S_{up} . With the comparison of multiple study sites, a logarithmic trend revealed that S_{up} has a high influence in many torrent catchments which can be developed as a statistical model (Figure 73). The general potential scour depths is controlled by the storage level (erodible thickness) indicated

by the upper- and lower-envelope. A transport-limited and supply-limited regime can be established from the empirical data collected from the field. The transport limited-regime has a strong increase of erosion with slope because storage is usually not a limiting factor. The supply-limited-regime (steeper than 0.15) has a small increase of erosion with slope because the thickness of the erodible bed becomes thinner.

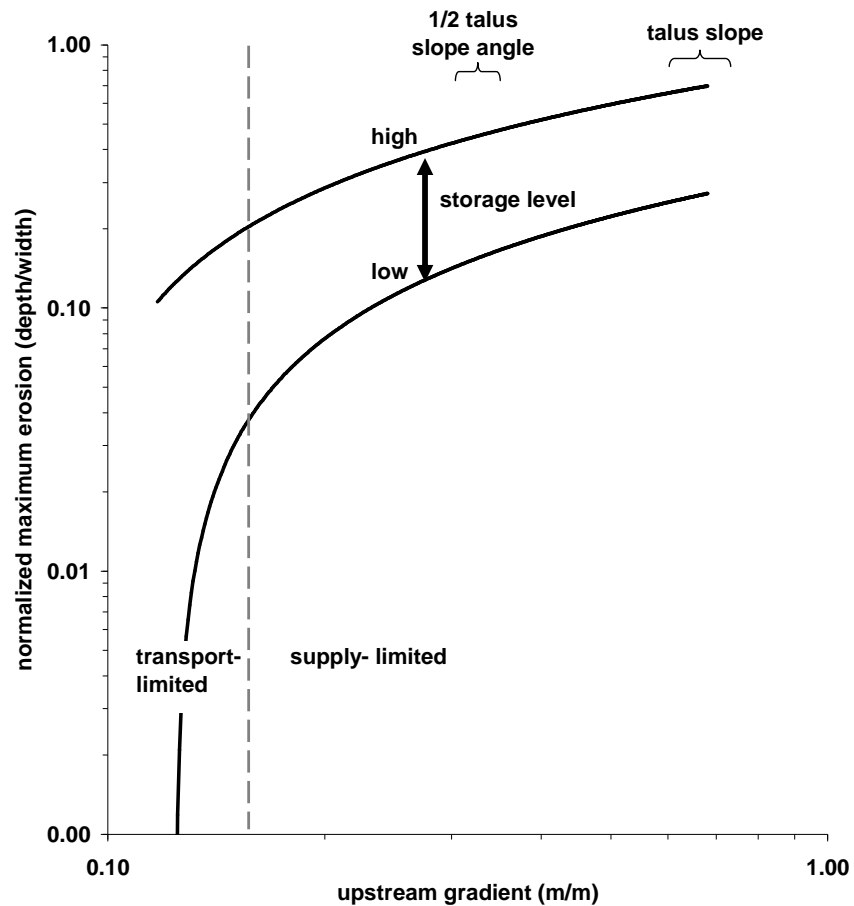


Figure 73 Statistical model of normalized debris-flow erosion controlled by upstream slope and storage level. The logarithmic envelope is the upper- and lower-limits from Figure 67. Transport-limited and supply-limited regimes are divided according to the critical slope for erosion (0.15). Experimental results from Mangeney et al. (2010) suggests that dry erodible beds have little influence on debris-flow travel distance below half the repose angle. Our critical slope is much less than half the talus slope angle (pore-water pressures could be a contributing factor).

Laboratory experiments showed that the presence of an erodible bed increases granular flow travel distance by 40% (Mangeny et al., 2010). Linear relationships exist between the travel distance and thickness of the erodible beds for a given slope angle. This represents the positive energy exchange from channel erosion to the passing flow. Mangeny et al. (2010) showed that below a critical slope (which corresponds to half the repose angle of the material), erosion does not have any influence on the travel distance. Above this critical slope, the influence of erosion on travel distance increases exponentially as the slope increases. The compilation of field data show contrasting results. The critical slope above which channel erosion has a strong effect on debris-flow volumes (and then runout distances) corresponds to the transition between previously defined transport- and supply-limited regimes. Empirical observations revealed that this critical slope is around 0.15. This value is significantly lower than half the repose angle of bed sediment of the Manival and Réal, which can be roughly estimated from talus slopes in the upper catchments (0.6). This can be explained by the effect of pore-water pressure which likely decreases the critical slope above which channel erosion influence granular flow dynamics (experiments from Mangeny et al., 2010 were done with dry beds).

The envelope of erosion in Figure 73 represents the relative thickness of the erodible bed (or the relative storage level), which according to Mangeny et al. (2010), also represents the potential increase of travel distance. This emphasizes the importance of storage; it is an important control on the occurrence of a debris-flow, its magnitude, and its runout distance. The positive energy exchange from erodible beds to the flow was also revealed by large scale experiments (Iverson et al., 2011). These experiments were performed on a constant slope (0.60) with varying pore-water pressures, which was found to increase the erosion efficiency and therefore the mobility of the debris-flow. However, experiments from Mangeny et al. (2010) were performed on dry erodible beds which had large increases of travel distances controlled by slope and thickness of the bed. The increase of pore-water pressure can change the erodible thickness of the bed, but the erosive capability mostly depends on the material of the bed. Debris-flows in the Manival and Réal can experience debris-flows without antecedent conditions because of the unconsolidated gravel storages which are typically found in these steep active catchments.

It should be noted that the erosion also depends on the condition of the passing debris-flow such as the sediment concentration of the passing flow (Egashira et al., 2001). Within one debris-flow event, a reach can experience deposition because of high sediment concentration and then it can be eroded by a proceeding surge with a lower sediment concentration (Imaizumi et al., 2005). Field laboratory tests in the Chemolgan site in Kazakhstan showed that debris-flow scouring increases linearly with water runoff volume (Rickenmann et al., 2003). This indicates that even with large channel storage, there still needs to be a large enough water surge to mobilize the erodible bed. We do not include the flow condition in the statistical model but it should be acknowledged as a contributing factor.

4.3 Mapping potential debris-flow scour and volume

An effective way to determine locations of potential debris-flow scour is by identifying the loose gravel wedges on steep slopes in torrent catchments. The TLS results showed that they are smooth macroforms which have a distinct roughness from the rugged debris-flow channels. A digital terrain model with a 20 cm grid can effectively characterize these potential scour areas by using roughness characterization from Cavalli et al. (2008). It has been shown that even ALS can be used with careful processing to produce a 20 cm elevation grid which then automatically maps the most sensitive and contributive material to debris-flows covering whole torrent reaches.

Debris-flow erosion can also be quantified by a long profile of a torrent by using the logarithmic relationship of normalized erosion versus upstream channel slope S_{up} (Figure 73). The potential scour widths need to be interpreted as well as the relative storage level of the channel. Maximum and minimum debris-flow scour can be determined according to the logarithmic envelope and their cumulative volumes can estimate potential debris-flow volumes. The benefit of this method is that low resolution calculations (ten times the potential scour width) can be used for determining different magnitudes of scouring and volume. A simple application of this model was made in the Manival torrent from the headwaters down to the extent of the study reach (sediment trap) (Figure 74). A long profile was made from a 1-m DEM and the upstream slope S_{up} was calculated at one meter intervals with measurement lengths of 110 m (10 times the mean scour width). The potential scour depths were determined from the mean, D_{05} (lower limit), and D_{95} (upper limit) logarithmic equations from Figure 67. The highest potential scouring was found above the study reach (Figure 74A), however seasonal debris-flows typically began at the upper end of the study reach because of larger storage development. The upper-catchment is too steep for regular storage to develop in the channel; if there is large storage, it is from an infrequent large landslide which can produce catastrophic debris-flow events.

The potential volume growth of a debris-flow can be determined by the cumulative downstream calculation (one meter interval) of the normalized scour depth multiplied by the estimated scour width (Figure 74B). For potential scour widths in the lower and mean erosion limits, we use the mean scour widths which were observed during the monitoring program (10.1 m) for a general estimate. For the maximum scour width, we use the average full channel width (14 m), the widths are variable but with very little downstream trend. The average potential volumes of typical debris-flows in the study reach are of course similar to the measured volumes (2 000 – 3 000 m³). The model provides a potential scour volume of 8 000 m³ when the study reach is full of sediment. In the scenario when the upper catchment is full of sediment from a landslide deposit, the maximum potential debris-flow volume growth of the entire catchment is 19 000 m³. As mentioned before in Chapter 3, a large landslide occurred in the headwaters in the winter of 1991 with 26 000 m³ of material. In the next summer, this volume of material was remobilized as not just one massive debris-flow but two individual events of

10 000 m³ and approximately 15 000 m³ which is still less than the potential maximum. This model still needs to be tested on other sites for accuracy, resolution, and variations of storage situations in steep catchments. However with it being derived from several sites, it already provides a strong basis for application in multiple areas.

It should be noted that the Manival and Réal had large variations of scouring because of local storage conditions; therefore the lower- and upper-limits of erosion vary from reach to reach. For assessing the storage conditions, if a 20 cm DEM is available, the roughness corresponding to storage can identify the upper-limits of erosion in each reach. The integration of the roughness and the logarithmic model still needs to be made in future studies where high resolution laser scanning is available.

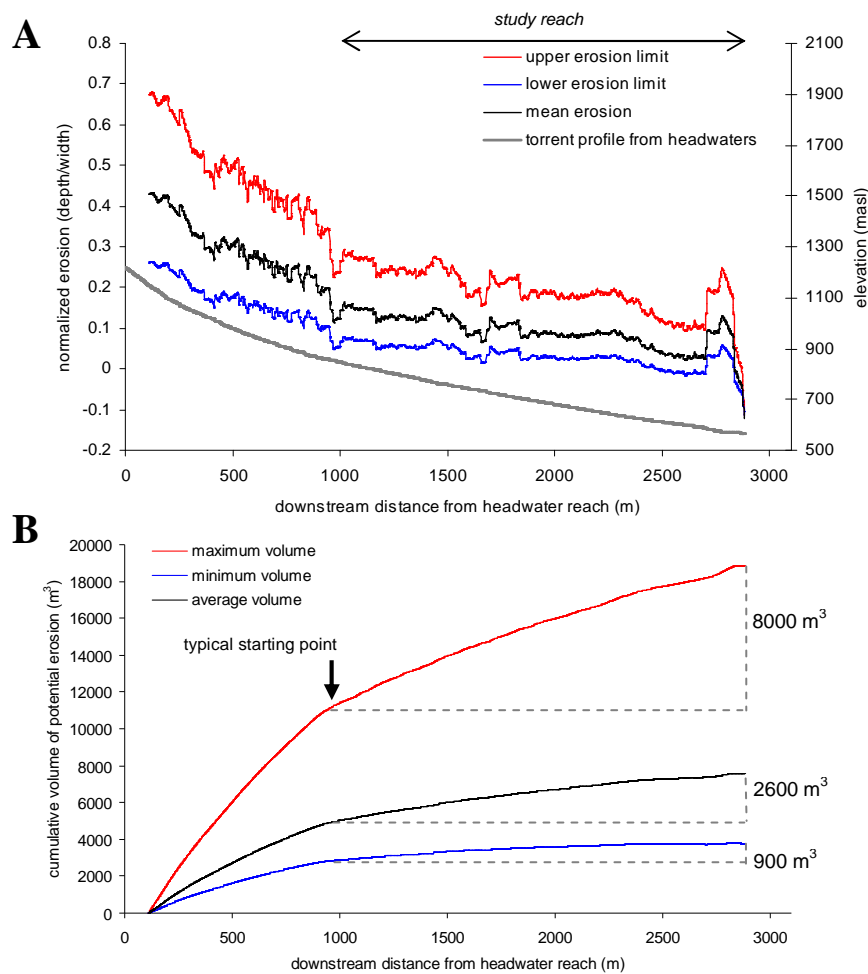


Figure 74 Example of the statistical model applied in the Manival torrent from the headwater to the end of the study reach derived from a one meter DEM. A) The normalized erosion logarithmic equation for the mean, D₉₅, and D₀₅ were calculated at one meter intervals by using the upstream slope (110 m length measurements). B) The cumulative volumes of the calculated erosions show the potential debris-flow volumes of the catchment. Observed seasonal debris-flows occur downstream from the typical starting point, their maximum potential volumes are 8 000 m³. The total potential maximum of the catchment is 19 000 m³ which is greater than the largest historical debris-flow (approximately 15 000 m³).

5 CONCLUSIONS

Multi-date cross-sections in both the Manival and Réal have clearly shown that debris-flows have significant scouring with large spatial variability. Bedload transport was found to be at equilibrium with less activity. Within the same catchment, debris-flows produce 2-10 times more sediment than bedload transport within a year.

Field observations of channel deformations show that debris-flow scouring is strongly controlled by upstream slope and storage conditions. A logarithmic relationship is proposed as an empirical fit for the prediction of channel erosion. Two regimes have been observed: 1) the transport-limited regime, which has a large increase of erosion with slope until the critical slope (0.15), the regime then switches to 2) the supply-limited regime, where the increasing erosion becomes more gradual with slope because the erodible beds become thinner.

The most susceptible materials for erosion in the Manival are the unconsolidated gravel wedges developed from bedload transport. This material has a smooth surface within the rugged channel which can be automatically mapped with a 20 cm DEM from either TLS or ALS by calculating roughness with a one meter window. This provides an automatic assessment of erodible areas in a channel at the time of the laser scan survey.

We have defined standard measurements for a dimensionless scour depth and upstream slope which can be used for predicting debris-flow volumes. The envelope of the logarithmic relationship still needs to be better understood. We suspect that the thickness of the erodible bed and the pore-water pressures must be important contributing factors. These parameters at varying slopes need to be further explored in both laboratory experiments and field monitoring of debris-flows. Multi-date cross-section surveying has shown to be very useful for measuring scour depths. They are cost and time efficient for measuring and data processing. Pore-water pressures are more difficult which require monitoring stations located in the erodible beds.

Chapter 6:

GENERAL CONCLUSIONS

1 SUMMARY OF CONCLUSIONS

The purpose of this research was to investigate the coarse sediment transport through torrent catchments and how this sediment can influence debris-flows. This required intensive field-based geomorphic monitoring of flow events in the Manival and Réal torrent catchments which frequently experience debris-flows and bedload transport. In the Manival Torrent, the sediment transfers were characterized at a seasonal time scale by a complete sediment budget of the catchment derived from multi-date topographic measurements (cross-section surveying and terrestrial laser scanning) between important flow events (Chapter 3). In the Réal Torrent, post-event surveying and high-frequency monitoring stations were used to compare and compile measurements for important flow events (Chapter 4). This extensive monitoring allowed us to compare sediment transport volumes between debris-flow and bedload transport processes and it also allowed us to characterize a debris-flow's propagation and interaction with the channel. For both study sites, the spatial variability of channel scouring was analyzed and correlated with channel slope (Chapter 5). The surface of the eroded material from debris-flows was also characterized by roughness with airborne and terrestrial laser scans.

Field monitoring at a detailed catchment-scale has been deemed very important for understanding debris-flow and bedload sediment transfers. The two important processes, bedload (channel recharge) and debris-flow (channel scouring), were identified to be the seasonal forcings for sediment transfer in the torrent catchment. The sediment budget reconstitution of two debris-flows revealed that most of the debris-flow volumes (more than 92%) were supplied by channel scouring. The influence of sediment recharge on debris-flows was quite evident. Bedload transport during autumn contributed to the sediment recharge of high-order channels by the deposition of large gravel wedges. During the monitoring period, high rainfall intensities triggered debris-flows only when these gravel wedges were present in the entrainment zone. During the monitoring period, the sediment budget has been decreasing because of little sediment supply which limits the activity of the torrent. Historically, large sediment supplies created large channel response within the same year with large debris-flows. We developed a conceptual model of seasonal cycles of sediment routing from low- to high-order channels for three levels of rainfall intensities. For low levels of intensity (observed annually), the pulses of sediment supply from hillslopes during the winter accumulated in first-order channels and were transferred to their next higher order reaches during spring and summer storms by debris-flows. The high level of intensity (catastrophic) produces a long continuous sediment transfer through the entire catchment.

Post-event surveys were found to accurately measure sediment transport volumes and debris-flow velocities in the Réal Torrent according to comparisons with high-frequency monitoring stations. The

backcalculated front velocities using the forced vortex equation was highly sensitive to the correction coefficient k . For the June 29, 2011 debris-flow, the velocities measured from the geophones corresponded with the backcalculated velocities when k ranged from 5 to 10. The flow resistance of the debris-flow front could be effectively backcalculated using the Chezy and Strickler-Manning equations for Newtonian turbulent flow. Their coefficients decreased traveling downstream with large variations. For all of the debris-flows in the Réal and other sites including the Swiss Alps and coastal British Columbia, the Chezy coefficients are within a one magnitude envelope when comparing velocities and depth-slope products.

Key observations for the June 29, 2011 debris-flow are: 1) the debris-flow has a distinct sharp front with heights varying from 1.1 to 3.6 m with a downstream decrease 2) the shear stress of the debris-flow front is correlated with the pre-/post-event yield rate 3) the hyperconcentrated surge behind the debris-flow grows significantly (rather than the debris-flow itself) 4) this hyperconcentrated surge then coalesces with the decelerating debris-flow in the distal reach and 5) the flow resistance of the debris-flow front decreases travelling downstream. From these observations we hypothesize that the debris-flow front scoured and destabilized the channel. However the front could not grow in material because of its high sediment concentration. The saturated unstable material that remained in the channel was remobilized by the trailing hyperconcentrated flow. This surge grew in volume and then coalesced with the decelerating debris-flow. It is difficult to explain the decreasing flow resistance of the front; it may be influenced by preliminary water flow in the channel (Navratil et al., in press). These findings indicate that the debris-flow front and the following surges play an integral role for net channel erosion of the event.

For all of the flow events monitored in the Réal torrent from April 2010 to October 2011, two distinct event types were observed: 1) torrent debris-flows which have large channel scouring and long travel distance and 2) headwater debris-flows which scour and deposit in the torrent at short travel distances, with bedload transport occurring downstream. The proximal/intermediate reach of the main torrent is the most responsive reach of the catchment because of the large depositions from the headwater debris-flows and the large scouring from the large torrent debris-flows. The large yield rates and sediment transport volume trends for the torrent debris-flows are very similar between the Réal and Manival torrents. The geomorphic monitoring in both catchments has shown that debris-flows highly depend on channel storage in the steep proximal reaches.

Multi-date cross-sections in both the Manival and Réal have clearly shown that debris-flows have significant scouring with large spatial variability whereas bedload transport was found to be at equilibrium with less variability. In fact, debris-flows produce 2-10 times more sediment than bedload transport within one year. Field observations of channel deformations show that debris-flow scouring is strongly controlled by upstream slope and storage conditions. A logarithmic relationship is proposed as an empirical fit for the prediction of channel erosion. Two regimes have been observed: 1) the

transport-limited regime, which has a large increase of erosion with slope until the critical slope (0.15), the regime then switches to 2) the supply-limited regime, where the increasing erosion becomes more gradual with slope because the erodible beds become thinner. This empirical model requires a channel profile with an upstream slope and an active channel width to determine potential erosion and debris-flow magnitudes.

The most susceptible materials for erosion in the Manival are the unconsolidated gravel wedges developed from bedload transport. This material has a smooth surface within the rugged channel which can be automatically mapped with a 20 cm DEM from either TLS or ALS by calculating roughness with a one meter window. This provides an automatic assessment of erodible areas in a channel at the time of the laser scan survey.

2 OUTCOMES AND PERSPECTIVES

We have developed a conceptual model which provides a better understanding on seasonal cycles of scour and fill. Some authors provide similar sediment routing schemes but at a much longer timescale (Benda, 1990). The presented model provides valuable input for assessing current and potential hazards (seasonal and extreme). The determination of where and when important storages occur allows for more effective management in these catchments.

Debris-flows were shown to have a very dynamic propagation which is difficult to predict. Despite their complexities, these debris-flow events have consistent trends of sediment transport with high yield rates. The combination of post-event surveying and high-frequency monitoring stations needs to become a standard approach to accurately describe the varying propagation of debris-flow events and their important interactions with the channel.

Standard measurements for a dimensionless scour depth and upstream slope can be used for predicting debris-flow volumes. The envelope of the logarithmic relationship still needs to be better understood. We suspect that the thickness of the erodible bed and the pore-water pressures must be important contributing factors. These parameters at varying slopes need to be further explored in both laboratory experiments and field monitoring of debris-flows. Multi-date cross-section surveying has shown to be very useful for measuring scour depths. They are cost and time efficient for measuring and data processing. Pore-water pressures are more difficult which require monitoring stations located in the erodible beds.

This study has contributed to the need of quantitative field observations in the realm of debris-flow research. Complete and thorough databases were obtained by integrating multi-date cross-section surveys, multi-date laser scans, and high-frequency monitoring stations. Quantified evidence revealing

sediment transfers, channel interactions/controls, debris-flow dynamics, and storage characterizations in two different catchments provides a strong basis in the development of conceptual and statistical models. These observations also highlighted the significant field parameters that have an influence on debris-flows and steep catchment systems.

REFERENCES

- Ancey, C., 1999. Rhéologie des lave torrentielles: final scientific report PNRN 1998-99, CEMAGREF, Grenoble, France.
- Arattano, M., Marchi, L., Cavalli, M., 2012. Analysis of debris-flow recordings in an instrumented basin: confirmations and new findings. *Natural Hazards and Earth System Science*, 12(3), 679-686.
- Arnaud-Fassetta, G., Astrade, L., Bardou, E., Corbonnois, J., Delahaye, D., Fort, M., Gautier, E., Jacob, N., Peiry, J., Piégay, H., Penven, M., 2009. Fluvial geomorphology and flood-risk management. *Géomorphologie: relief, processus, environnement*, 2, 109-128.
- Ashmore, P.E., Church, M.A., 1998. Sediment transport and river morphology: A paradigm for study. In: P.C. Klingeman, R.L. Beschta, P.D. Komar, J.D. Bradley (Eds.), *Gravel-Bed Rivers in the Environment*. Water Resource Publications, LLC, Highlands Ranch, Colorado, pp. 115-148.
- Ayotte, D., Hungr, O., 2000. Calibration of a runout prediction model for debris-flows and avalanches. In: G.F. Wieczorek, N.D. Naeser (Eds.), *2nd International Conference on Debris-Flow Hazards Mitigation: Mechanics, Prediction, and Assessment*. Balkema, Rotterdam, Taiwan, pp. 505-514.
- Badoux, A., Graf, C., Ryhner, J., Kuntner, R., McArdell, B.W., 2008. A debris-flow alarm system for the Alpine Illgraben catchment: design and performance. *Natural Hazards*, 49(3), 517-539.
- Bardou, E., Ancey, C., Bonnard, C., Vulliet, L., 2003. Classification of debris-flow deposits for hazard assessment in alpine areas. In: D. Rickenmann, C.-L. Chen (Eds.), *Debris-flow Hazards Mitigation: Mechanics, Prediction, and Assessment*. Millpress, Rotterdam, pp. 799-808.
- Benda, L., 1990. The influence of debris flows on channels and valley floors in the Oregon Coast Range, USA. *Earth Surface Processes & Landforms*, 15(5), 457-466.
- Benda, L., Dunne, T., 1987. Sediment routing by debris flows. In: R.L. Beschta, T. Blinn, G.E. Grant, G.G. Ice, F.J. Swanson (Eds.), *Erosion and Sedimentation in the Pacific Rim*. IAHS Publication, pp. 213-223.
- Benda, L., Dunne, T., 1997. Stochastic forcing of sediment supply to channel networks from landsliding and debris flow. *Water Resources Research*, 33(12), 2849-2863.
- Benda, L., Hassan, M.A., Church, M., May, C.L., 2005. Geomorphology of steepland headwaters: the transition from hillslopes to channels. *Journal of the American Water Resources Association*, 41(4), 835-851.
- Benda, L., Veldhuisen, C., Black, J., 2003. Debris flows as agents of morphological heterogeneity at low-order confluences, Olympic Mountains, Washington. *Geological Society of America Bulletin*, 115(9), 1110-1121.
- Berger, C., McArdell, B.W., Schlunegger, F., 2011a. Direct measurement of channel erosion by debris flows, Illgraben, Switzerland. *Journal of Geophysical Research*, 116(F01002).
- Berger, C., McArdell, B.W., Schlunegger, F., 2011b. Sediment transfer patterns at the Illgraben catchment, Switzerland: Implications for the time scales of debris flow activities. *Geomorphology*, 125(3), 421-432.
- Berti, M., Simoni, A., 2007. Prediction of debris flow inundation areas using empirical mobility relationships. *Geomorphology*, 90(1-2), 144-161.
- Berti, M.R., Genevois, R., LaHusen, R.G., Simoni, A., Tecca, P.R., 2000. Debris flow monitoring in the Acquabona watershed in the Dolomites (Italian Alps). *Phys. Chem. Earth, Part B*, 25(9), 707-715.
- Berti, M.R., Genevois, R., Simoni, A., Tecca, P.R., 1999. Field observations of a debris flow event in the Dolomites. *Geomorphology*, 29, 265-274.
- Besl, P.J., McKay, N.D., 1992. A method for registration of 3-D shapes. *IEEE Transactions on Pattern Analysis and Machine Intelligence*, 14(2), 239-256.
- Bigelow, P.E., Benda, L.E., Miller, D.J., Burnett, K.M., 2007. On debris flows, river networks, and the spatial structure of channel morphology. *Forest Science*, 53(2), 220-238.
- Blijenberg, H.M., 2007. Application of physical modelling of debris flow triggering to field conditions: Limitations posed by boundary conditions. *Engineering Geology*, 91(1), 25-33.

- Bollschweiler, M., Stoffel, M., Ehmisch, M., Monbaron, M., 2007. Reconstructing spatio-temporal patterns of debris-flow activity using dendrogeomorphological methods. *Geomorphology*, 87, 337-351.
- Bovis, M.J., Jakob, M., 1999. The role of debris supply conditions in predicting debris flow activity. *Earth Surface Processes and Landforms*, 24(11), 1039-1054.
- Breien, H., De Blasio, F.V., Elverhøi, A., Høeg, K., 2008. Erosion and morphology of a debris flow caused by a glacial lake outburst flood, Western Norway. *Landslides*, 5, 271-280.
- Bremer, M., Sass, O., 2012. Combining airborne and terrestrial laser scanning for quantifying erosion and deposition by a debris flow event. *Geomorphology*, 138(1), 49-60.
- Bull, J.M., Miller, H., Gravley, D.M., Costello, D., Hikuroa, D.C.H., Dix, J.K., 2010. Assessing debris flows using LIDAR differencing: 18 May 2005 Matata event, New Zealand. *Geomorphology*, 124(1-2), 75-84.
- Caine, N., 1980. The Rainfall Intensity-Duration Control of Shallow Landslides and Debris Flows. *Geografiska Annaler*, 62 A(1-2), 23-27.
- Cavalli, M., Tarolli, P., Marchi, L., Dalla Fontana, G., 2008. The effectiveness of airborne LiDAR data in the recognition of channel-bed morphology. *Catena*, 73(3), 249-260.
- Chambon, G., Richard, D., 2004. Diagnostic du fonctionnement torrentiel du bassin versant du Réal (Péone-Alpes Maritimes). 04/0482, CEMAGREF.
- Chambon, G., Richard, D., Segel, V., 2010. Diagnostic du fonctionnement torrentiel d'un bassin versant générateur de laves torrentielles et estimation de l'aléa : le cas du Réal (Alpes-Maritimes, France). *Sciences Eaux et Territoires*, 2, 140-150.
- Charollais, J., D., D., Ginet, C., A., L., Muller, J.P., Rosset, J., Ruchat, C., 1986. Carte géol, France (1/50.000), Feuille Domène (33-34). In: B.R.G.M. Orléans (Ed.).
- Chen, C.L., 1987. Comprehensive review of debris flow modeling concepts in Japan. In: J.E. Costa, G.F. Wieczorek (Eds.), *Reviews in engineering geology*, vol VII. Debris flows/ avalanches: process, recognition, and mitigation., Boulder, CO, pp. 13-29.
- Coe, J.A., Kinner, D.A., Godt, J.W., 2008. Initiation conditions for debris flows generated by runoff at Chalk Cliffs, central Colorado. *Geomorphology*, 96(3-4), 270-297.
- Conway, S.J., Decaulne, A., Balme, M.R., Murray, J.B., Towner, M.C., 2010. A new approach to estimating hazard posed by debris flows in the Westfjords of Iceland. *Geomorphology*, 114(4), 556-572.
- Costa, J.E., 1984. Physical geomorphology of debris flows. In: J.E. Costa, P.J. Fleisher (Eds.), *Developments and Applications in Geomorphology*. Springer Verlag, pp. 268-317.
- Coussot, P., Meunier, M., 1996. Recognition, classification and mechanical description of debris flows. *Earth-Science Reviews*, 40, 209-227.
- D'Agostino, V., Cesca, M., Marchi, L., 2010. Field and laboratory investigations of runout distances of debris flows in the Dolomites (Eastern Italian Alps). *Geomorphology*, 115(3-4), 294-304.
- D'Agostino, V., Marchi, L., 2001. Debris flow magnitude in the Eastern Italian Alps: Data collection and analysis. *Physics and Chemistry of the Earth, Part C: Solar, Terrestrial and Planetary Science*, 26(9), 657-663.
- Dahal, R.K., Hasegawa, S., 2008. Representative rainfall thresholds for landslides in the Nepal Himalaya. *Geomorphology*, 100, 429-443.
- DeLeon, A.A., Jeppson, R.W., 1982. Hydraulic and numerical solutions of steady-state but spatially varied debris flow. *Hydraulics and hydrology series*, UWRL/H-82/03, Utah State Univ., Logan, Utah.
- Dietrich, W.E., Dunne, T., 1978. Sediment budget for a small catchment in mountainous terrain. *Zeitschrift für Geomorphologie*, 29(SUPPL.), 191-206.
- Ding, M., Wei, F., Hu, K., 2012. Property insurance against debris-flow disasters based on risk assessment and the principal-agent theory. *Natural Hazards*, 60, 801-817.
- Djrboua, A., 2001. Prédétermination des pluies et crues extrêmes dans les Alpes franco-italiennes: prévision quantitative des pluies journalières par la méthode des analogues. PhD thesis PhD, Institute National Polytechnique de Grenoble, Grenoble, 212 pp.
- Djrboua, A., Lang, M., 2007. Comparaison de différents modes d'échantillonnage pour l'estimation du gradex des pluies. *Revue des Sciences de l'Eau*, 20(1), 111-125.

- Egashira, S., Honda, N., Itoh, T., 2001. Experimental study on the entrainment of bed material into debris flow. *Phys. Chem. of the Earth*, 26(9), 645-650.
- Everest, F.H., Beschta, R.L., Scrivener, J.C., Koski, K.V., Sedell, J.R., Cederholm, C.J., 1987. Fine sediment and salmon production: A paradox. In: E.O. Salo, T.W. Cundy (Eds.), *Streamside management, forestry and fishery interactions*. Univ. of Wash. Inst. of For. Res.
- Fannin, R.J., Wise, M.P., 2001. An empirical-statistical model for debris flow travel distance. *Can. Geotech. J.*, 38, 982-994.
- Ferguson, R.I., Ashworth, P.J., 1992. Spatial patterns of bedload transport and channel change in braided and near-braided rivers. In: P. Billi, R.D. Hey, C.R. Thorne (Eds.), *Dynamics of Gravel-Bed Rivers*. Wiley, Chichester, pp. 477-496.
- Fuller, I.C., Marden, M., 2010. Rapid channel response to variability in sediment supply: Cutting and filling of the Tarndale Fan, Waipaoa catchment, New Zealand. *Marine Geology*, 270(1-4), 45-54.
- Gartner, J.E., Cannon, S.H., Santi, P.M., Dewolfe, V.G., 2008. Empirical models to predict the volumes of debris flows generated by recently burned basins in the western U.S. *Geomorphology*, 96(3-4), 339-354.
- Gidon, M., 1991. *Géologie de la Chartreuse - Sentiers de la Chartreuse: Circuit de la Dent de Crolles*, Association "A la découverte du Patrimoine de Chartreuse". publ. 1d, 1^o éd., 20 p., 9 fig., www.Geol-alp.com.
- Godt, J.W., Coe, J.A., 2007. Alpine debris flows triggered by a 28 July 1999 thunderstorm in the Central Front Range, Colorado. *Geomorphology*, 84, 80-97.
- Gregoretti, C., Fontana, G.D., 2008. The triggering of debris flow due to channel-bed failure in some alpine headwater basins of the Dolomites: analyses of critical runoff. *Hydrological Processes*, 22, 2248-2263.
- Guthrie, R.H., Hockin, A., Colquhoun, L., Nagy, T., Evans, S.G., Ayles, C., 2010. An examination of controls on debris flow mobility: evidence from coastal British Columbia. *Geomorphology*, 114(4), 601-613.
- Guzzetti, F., Peruccacci, S., Rossi, M., Stark, C.P., 2008. The rainfall intensity-duration of shallow landslides and debris flows: an update. *Landslides*, 5, 3-17.
- Harvey, A.M., 2001. Coupling between hillslopes and channels in upland fluvial systems: implications for landscape sensitivity, illustrated from the Howgill Fells, northwest England. *Catena*, 42, 225-250.
- Haschenburger, J.K., 1999. A probability model of scour and fill depths in gravel-bed channels. *Water Resources Research*, 35(9), 2857-2859.
- Helsen, M.M., Koop, P.J.M., Van Steijn, H., 2002. Magnitude-frequency relationship for debris flows on the fan of the Chalance Torrent, Valgaudemar (French Alps). *Earth Surface Processes and Landforms*, 27, 1299-1307.
- Heritage, G.L., Milan, D.J., 2009. Terrestrial Laser Scanning of grain roughness in a gravel-bed river. *Geomorphology*, 113(1-2), 4-11.
- Hungr, O., 2000. Analysis of debris flow surges using the theory of uniformly progressive flow. *Earth Surf. Process. Landforms*, 25, 483-495.
- Hungr, O., 2005. Classification and terminology. In: M. Jakob, O. Hungr (Eds.), *Debris-flow Hazards and Related Phenomena*. Springer-Praxis, Berlin, pp. 9-23.
- Hungr, O., Evans, S.G., Bovis, M., Hutchinson, J.N., 2001. Review of classification of landslides of flow type. *Environmental and Engineering Geoscience*, VII, 221-238.
- Hungr, O., McDougall, S., Bovis, M., 2005. Entrainment of material by debris flows. In: M. Jakob, O. Hungr (Eds.), *Debris-Flow Hazards and Related Phenomena*. Springer, Berlin Heidelberg, Germany, pp. 135-158.
- Hungr, O., McDougall, S., Wise, M., Cullen, M., 2008. Magnitude-frequency relationships of debris flows and debris avalanches in relation to slope relief. *Geomorphology*, 96(3-4), 355-365.
- Hungr, O., Morgan, G.C., Kellerhals, R., 1984. Quantitative analysis of debris torrent hazards for design of remedial measures. *Canadian Geotechnical Journal*, 21, 663-677.
- Hürlimann, M., Rickenmann, D., Graf, C., 2003. Field and monitoring data of debris-flow events in the Swiss Alps. *Canadian Geotechnical Journal*, 40(1), 161-175.

- Hutchinson, J.N., 1968. Mass movement. Encyclopedia of Geomorphology. Reinhold Publishers, New York.
- Iavarone, A., Vagners, D., 2003. Sensor fusion: Generating 3D by combining airborne and tripod mounted lidar data. International Archives of Photogrammetry, Remote Sensing and Spatial Information Sciences, 34.
- Imaizumi, F., Sidle, R.C., Tsuchiya, S., Ohsaka, O., 2006. Hydrogeomorphic processes in a steep debris flow initiation zone. Geophysical Research Letters, 33(10).
- Imaizumi, F., Tsuchiya, S., Ohsaka, O., 2005. Behaviour of debris flows located in a mountainous torrent on the Ohya landslide, Japan. Can. Geotech. J., 42, 919-931.
- Itakura, Y., Inaba, H., Sawada, T., 2005. A debris-flow monitoring device and methods bibliography. Natural Hazards and Earth System Sciences, 5, 971-977.
- Iverson, R.M., 1997. The physics of debris flows. Reviews of Geophysics, 35(3), 245-296.
- Iverson, R.M., LaHusen, R., Major, J.J., Zimmermann, C.L., 1994. Debris flow against obstacles and bends: dynamics and deposits. EOS, Trans. Am. Geophys. Union, 75, 274.
- Iverson, R.M., LaHusen, R.G., Costa, J.E., 1992. Debris-flow flume at H. J. Andrews Experimental Forest, Oregon, U.S. Geological Survey Open-File Report 92-483, 2 p.
- Iverson, R.M., Reid, M.E., Logan, M., LaHusen, R.G., Godt, J.W., Griswold, J.P., 2011. Positive feedback and momentum growth during debris-flow entrainment of wet sediment. Nature Geoscience(4), 116-121.
- Jaboyedoff, M., Baillifard, F., Couture, R., Locat, J., Locat, P., 2004. Toward preliminary hazard assessment using DEM topographic analysis and simple mechanic modeling. In: W.A. Lacerda, M. Ehrlich, A.B. Fontoura, A. Sayo (Eds.), Landslides Evaluation and Stabilization. Balkema, London, pp. 191-197.
- Jaboyedoff, M., Derron, M.H., 2005. A new method to estimate the infilling of alluvial sediment of glacial valleys using a sloping local base level. Geografia Fisica e Dinamica Quaternaria, 28(1), 37-46.
- Jakob, M., Anderson, D., Fuller, T., Hungr, O., Ayotte, D., 2000. An unusually large debris flow at Hummingbird Creek, Mara Lake, British Columbia. Canadian Geotechnical Journal(37), 1109-1125.
- Jakob, M., Bovis, M., Oden, M., 2005. The significance of channel recharge rates for estimating debris-flow magnitude and frequency. Earth Surface Processes and Landforms, 30, 755-766.
- Jakob, M., Friele, P., 2010. Frequency and magnitude of debris flows on Cheekye River, British Columbia. Geomorphology, 114(3), 382-395.
- Jakob, M., Hungr, O., Thomson, B., 1997. Two debris flows with anomalously high magnitude, 1st Int. Conf. on Debris-Flow Hazards Mitigation: Mechanics, Prediction and Assessment. ASCE, San Francisco, California, pp. 382-394.
- Jakob, M., Jordan, P., 2001. Design flood estimates in mountain streams - The need for a geomorphic approach. Canadian Journal of Civil Engineering, 28(3), 425-439.
- Johnson, A.M., 1970. Physical processes in Geology. Freeman-Cooper, San Francisco, CA.
- Johnson, A.M., Rodine, J.R., 1984. Debris flow. In: D. Brunsten, D.B. Prior (Eds.), Slope stability. John Wiley & Sons, New York, N.Y., pp. 257-361.
- Jomard, H., 2003. Origine et évolution des instabilités gravitaires: approches géologique, géophysique et mécanique. Application au vallon du Réal, commune de Péone (Alpes-Maritimes), DEA de l'Université de Nice-Sophia Antipolis.
- Jomelli, V., Brunstein, D., Grancher, D., Pech, P., 2007. Is the response of hill slope debris flows to recent climate change univocal? A case study in the Massif des Ecrins (French Alps). Climatic Change, 85(1-2), 119-137.
- Jomelli, V., Pech, V.P., Chochillon, C., Brunstein, C., 2004. Geomorphic variations of debris flows and recent climatic changes in the French Alps. Climatic Change, 64, 77-102.
- Koch, T., 1998. Testing various constitutive equations for debris flow modelling. In: K.e.a. Kovar (Ed.), Hydrology, Water Resources and Ecology in Headwaters. IAHS, Publ. No. 248, Merano, Italy, pp. 249-257.
- Lavigne, F., Suwa, H., 2004. Contrasts between debris flows, hyperconcentrated flows and stream flows at a channel of Mount Semeru, East Java, Indonesia. Geomorphology, 61, 41-58.

- Liébault, F., Laronne, J.B., 2008. Evaluation of bedload yield in gravel-bed rivers using scour chains and painted tracers: the case of the Esconavette Torrent (Southern French Prealps). *Geodinamica Acta*, 21(1-2), 23-34.
- Liébault, F., Remaître, A., Peteuil, C., in press. Géomorphologie des rivières de montagne. In: A. Recking, D. Richard (Eds.), *Dynamique et Aménagement des Torrents et Rivières de Montagne*. Quae, Paris.
- Lopez Saez, J., Corona, C., Stoffel, M., Gotteland, A., Berger, F., Liébault, F., 2011. Debris-flow activity in abandoned channels of the Manival torrent reconstructed with LiDAR and tree-ring data. *Natural Hazards and Earth System Sciences*, 11, 1247-1257.
- Loye, A., 2012. Budgeting rockfall and modelling sediment delivery in torrent systems. PhD thesis, Université de Lausanne, Lausanne.
- Loye, A., Jaboyedoff, M., Pedrazzini, A., Theule, J., Liébault, F., Metzger, R., 2011. Morphostructural analysis of an alpine debris flows catchment: implication for debris supply. In: R. Genevois, D.L. Hamilton, A. Prestininzi (Eds.), *5th International Conference on Debris-Flow Hazards Mitigation: Mechanics, Prediction and Assessment*. Italian Journal of Engineering Geology and Environment, Padua, Italy, 14-17 June 2011, pp. 115-125.
- Loye, A., Pedrazzini, A., Theule, J.L., Jaboyedoff, M., Liébault, F., Metzger, R., 2012. Influence of bedrock structures on the spatial pattern of erosional landforms in small alpine catchments. *Earth Surface Processes and Landforms*.
- Major, J.J., Iverson, R.M., 1999. Debris-flow deposition: effects of pore-fluid pressure and frictions concentrated at flow margins. *Geological Society of America Bulletin*, 111(10), 1424-1434.
- Mangeny, A., 2011. Geomorphology: Landslide boost from entrainment. *Nature Geoscience*, 4(2), 77-78.
- Mangeny, A., Roche, O., Hungr, O., Mangold, N., Faccanoni, G., Lucas, A., 2010. Erosion and mobility in granular collapse over sloping beds. *Journal of Geophysical Research*, 115(F03040).
- Mao, L., Cavalli, M., Comiti, F., Marchi, L., Lenzi, M.A., Arattano, M., 2009. Sediment transfer processes in two Alpine catchments of contrasting morphological settings. *Journal of Hydrology*, 364(1-2), 88-98.
- Marchi, L., Arattano, M., Deganutti, A.M., 2002. Ten years of debris-flow monitoring in the Moscardo Torrent (Italian Alps). *Geomorphology*, 46, 1-17.
- Marchi, L., D'Agostino, V., 2004. Estimation of debris-flow magnitude in the Eastern Italian Alps. *Earth Surface Processes and Landforms*, 29, 207-220.
- Martin, Y., Church, M., 1995. Bed-material transport estimated from channel surveys: Vedder River, British Columbia. *Earth Surface Processes and Landforms*, 25, 1011-1024.
- McArdell, B.W., Bartelt, P., Kowalski, J., 2007. Field observations of basal forces and pore pressure in a debris flow. *Geophysical Research Letters*, 34, L07406.
- McCoy, S.W., Kean, J.W., Coe, J.A., Staley, D.M., Wasklewicz, T.A., Tucker, G.E., 2010. Evolution of a natural debris flow: in situ measurements of flow dynamics, video imagery, and terrestrial laser scanning. *Geology*, 38(8), 735-738.
- Miller, D.J., Benda, L.E., 2000. Effects of punctuated sediment supply on valley-floor landforms and sediment transport. *Geological Society of America Bulletin*, 112(12), 1814-1824.
- Miller, D.J., Burnett, K.M., 2008. A probabilistic model of debris-flow delivery to stream channels, demonstrated for the Coast Range of Oregon, USA. *Geomorphology*, 94(1-2), 184-205.
- National Research Council, 2004. Partnerships for reducing landslide risk-assessment of the national landslide hazards mitigation strategy. National Academies Press, Washington.
- Navratil, O., Liébault, F., Bellot, H., Travaglini, E., Theule, J., in press. High-frequency monitoring of debris-flow propagation along the Réal Torrent, Southern French Prealps. *Geomorphology*.
- Navratil, O., Liébault, F., Laigle, D., Bellot, H., Ravanat, X., Theule, J., Bacq, B., Demirdjian, J.L., Segel, V., Ficquet, M., 2012. Presentation of high-frequency flash floods and debris-flow monitoring in the French Alps. *Mémoire de la Société de Sciences Naturelles Vaudoises*.
- Nawa, R.K., Frissell, C.A., 1993. Measuring scour and fill of gravel streambeds with scour chains and sliding-bead monitors. *N. Am. J. Fish Manag.*, 13, 634-639.

- Ni, H.Y., Zheng, W.M., Tie, Y.B., Su, P.C., Tang, Y.Q., Xu, R.G., Wang, D.W., Chen, X.Y., 2012. Formation and characteristics of post-earthquake debris flows: a case study from Wenjia gully in Mianzhu, Sichuan, SW China. *Natural Hazards*, 61, 317-335.
- Nyman, P., Sheridan, G.J., Smith, H.G., Lane, P.N.J., 2011. Evidence of debris flow occurrence after wildfire in upland catchments of south-east Australia. *Geomorphology*, 125, 383-401.
- O'Connor, J.E., Costa, J.E., 1993. Geologic and Hydrologic Hazards in Glacierized Basins in North America Resulting from 19th and 20th Century Global Warming. *Natural Hazards*, 8, 121-140.
- Otto, J.-C., Schrott, L., Jaboyedoff, M., Dikau, R., 2009. Quantifying sediment storage in a high alpine valley (Turtmanntal, Switzerland). *Earth Surface Processes and Landforms*, 34(13), 1726-1742.
- Papa, M., Egashira, S., Itoh, T., 2004. Critical conditions of bed sediment entrainment due to debris flow. *Natural Hazards and Earth System Science*, 4(3), 469-474.
- Pelfini, M., Santilli, M., 2008. Frequency of debris flows and their relation with precipitation: A case study in the Central Alps, Italy. *Geomorphology*, 101(4), 721-730.
- Peteuil, C., Maraval, C., Bertrand, C., Monier, G., 2008. Torrent du Manival: Schéma d'aménagement et de gestion du bassin versant contre les crues, Unpublished technical report; Office National des Forêts, Service de Restauration des Terrains en Montagne de l'Isère, Grenoble, France.
- Phillips, C.J., Davies, T.R.H., 1991. Determining rheological parameters of debris flow material. *Geomorphology*, 4, 101-110.
- Pierson, T.C., 1986. Flow behavior of channelized debris flows, Mt. St. Helens, Washington. *Hillslope Processes*. Allen & Unwin, Boston.
- Pierson, T.C., Costa, J.E., 1987. A rheological classification of subaerial sediment-water flows. In: J.E. Costa, G.F. Wieczorek (Eds.), *Debris flows/avalanche: process, recognition, and mitigation*. The Geological Society of America, Boulder, Colo., pp. 1-12.
- Pierson, T.C., Scott, K.M., 1985. Downstream Dilution of a Lahar: Transition From Debris Flow to Hyperconcentrated Streamflow. *Water Resources Research*, 21(10), 1511-1524.
- Powell, D.M., Brazier, R., Wainwright, J., Parsons, A., Kaduk, J., 2005. Streambed scour and fill in low-order dryland channels. *Water Resour. Res.*, 41, W05019.
- Prochaska, A.B., Santi, P.M., Higgins, J.D., Cannon, S.H., 2008. A study of methods to estimate debris flow velocity. *Landslides*, DOI 10.1007/s10346-008-0137-0.
- Quélenec, R.E., Rouire, J., 1981. Etude des problemes d'erosion dans les bassins du Réal at du Tuébi (en amont de Péone -Alpes Maritimes), Etude BRGM 81 SGN 544 PAC. 87 p.
- Rabatel, A., Deline, P., Jailliet, S., Ravel, L., 2008. Rock falls in high-alpine rock walls quantified by terrestrial lidar measurements: A case study in the Mont Blanc area. *Geophysical Research Letters*, 35(10).
- Raven, E.K., Lane, S.N., Ferguson, R.I., Bracken, L.J., 2009. The spatial and temporal patterns of aggradation in a temperate, upland, gravel-bed river. *Earth Surface Processes and Landforms*, 34(9), 1181-1197.
- Reid, S.C., Lane, S.N., Berney, J.M., Holden, J., 2007. The timing and magnitude of coarse sediment transport events within an upland, temperate gravel-bed river. *Geomorphology*, 83(1-2), 152-182.
- Remaître, A., Malet, J.-P., Maquaire, O., 2005. Morphology and sedimentology of a complex debris flow in a clay-shale basin. *Earth Surface Processes and Landforms*, 30, 339-348.
- Remaître, A., W. J. Van Asch, T., Malet, J.P., Maquaire, O., 2008. Influence of check dams on debris-flow run-out intensity. *Natural Hazards and Earth System Science*, 8(6), 1403-1416.
- Rickenmann, D., 1990. Debris flows 1987 in Switzerland: Modelling and sediment transport. In: O. Sinniger, M. Monbaron (Eds.), *Hydrology in Mountainous Regions II*. IAHS Publ. No. 194, Lausanne, Switzerland.
- Rickenmann, D., 1994. An alternative equation for the mean velocity in gravel-bed rivers and mountain torrents. In: G.V. Cotroneo, R.R. Rumer (Eds.), *ASCE 1994 National Conf. on Hydraulics Engineering*. ASCE, New York, pp. 672-676.
- Rickenmann, D., 1995. Beurteilung von Murgängen. *Schweizer Ingenieur und Architekt*, 48, 1104-1108.
- Rickenmann, D., 1999. Empirical relationships for debris flows. *Natural Hazards*, 19(1), 47-77.

- Rickenmann, D., Koch, T., 1997. Comparison of debris flow modeling approaches. In: C.L. Chen (Ed.), 1st international Conference on Debris-Flow Hazards Mitigation: Mechanics, Prediction, and Assessment. ASCE, San Francisco, California, pp. 576-585.
- Rickenmann, D., Koschni, A., 2010. Sediment loads due to fluvial transport and debris flows during the 2005 flood events in Switzerland. *Hydrological Processes*, 24(8), 993-1007.
- Rickenmann, D., McArdell, B.W., 2007. Continuous measurement of sediment transport in the Erlenbach stream using piezoelectric bedload impact sensors. *Earth Surf. Process. Landforms*(32), 1362-1378.
- Rickenmann, D., Weber, D., 2000. Flow resistance of natural and experimental debris-flows in torrent channels. In: G.F. Wieczorek, N.D. Naeser (Eds.), *Debris-flow hazards mitigation: mechanics, prediction, and assessment*. Balkema, Rotterdam, Taiwan, pp. 245-254.
- Rickenmann, D., Weber, D., Stepanov, B., 2003. Erosion by debris flows in field and laboratory experiments. In: D. Rickenmann, C.L. Chen (Eds.), *Debris-Flow Hazards Mitigation: Mechanics, Prediction, and Assessment*. Millpress, Rotterdam, The Netherlands, pp. 883-894.
- Rickenmann, D., Zimmermann, M., 1993. The 1987 debris flows in Switzerland: documentation and analysis. *Geomorphology*, 8, 175-189.
- Scheidl, C., Rickenmann, D., 2010. Empirical prediction of debris-flow mobility and deposition on fans. *Earth Surface Processes and Landforms*, 35(2), 157-173.
- Scheidl, C., Rickenmann, D., Chiari, M., 2008. The use of airborne LiDAR data for the analysis of debris flow events in Switzerland. *Natural Hazards and Earth System Science*, 8(5), 1113-1127.
- Schlunegger, F., Badoux, A., McArdell, B.W., Gwerder, C., Schnydrig, D., Rieke-Zapp, D., Molnar, P., 2009. Limits of sediment transfer in an alpine debris-flow catchment, Illgraben, Switzerland. *Quaternary Science Reviews*, 28(11-12), 1097-1105.
- Schürch, P., Densmore, A.L., Rosser, N.J., Lim, M., McArdell, B.W., 2011a. Detection of surface change in complex topography using terrestrial laser scanning: application to the Illgraben debris-flow channel. *Earth Surface Processes and Landforms*, 36(14), 1847-1859.
- Schürch, P., Densmore, A.L., Rosser, N.J., McArdell, B.W., 2011b. Dynamic controls on erosion and deposition on debris-flow fans. *Geology*, 39(9), 827-830.
- Shroder, J., Marston, R.A., Stoffel, M., 2012. *Treatise on Geomorphology*, 7. Elsevier B. V, Amsterdam, The Netherlands.
- Simoni, S., Zanotti, F., Bertoldi, G., Rigon, R., 2008. Modelling the probability of occurrence of shallow landslides and channelized debris flows using GEOTop-FS. *Hydrological Processes*, 22(4), 532-545.
- Staley, D.M., Wasklewicz, T.A., Coe, J.A., Kean, J.W., McCoy, S.W., Tucker, G.E., 2011. Observations of debris flows at Chalk Cliffs, Colorado, USA: Part 2, Changes in surface morphometry from terrestrial laser scanning in the summer of 2009. In: R. Genevois, D.L. Hamilton, A. Prestininzi (Eds.), 5th Int. Conf. on Debris-Flow Hazards; Mitigation, Mechanics, Prediction and Assessment. Casa Editrice Università La Sapienza, Padova, pp. 715-724.
- Stock, J., Dietrich, W.E., 2003. Valley incision by debris flows: evidence of a topographic signature. *Water Resources Research*, 39(4).
- Stock, J.D., Dietrich, W.E., 2006. Erosion of steepland valleys by debris flows. *Geological Society of America Bulletin*, 118(9/10), 1125-1148.
- Stoffel, M., 2010. Magnitude-frequency relationships of debris flows - A case study based on field surveys and tree-ring records. *Geomorphology*, 116, 67-76.
- Stoffel, M., Beniston, M., 2006. On the incidence of debris flows from the early Little Ice Age to a future greenhouse climate: a case study from the Swiss Alps. *Geophysical Research Letters*, 33(L16404).
- Stoffel, M., Bollschweiler, M., Hassler, G., 2006. Differentiating past events on a cone influenced by debris-flow and snow avalanche activity - a dendrogeomorphological approach. *Earth Surf. Process. Landforms*, 31, 1424-1437.
- Swanson, F.J., Kratz, T.K., Caine, N., Woodmansee, R.G., 1988. Landform effects on ecosystem patterns and processes: Geomorphic features of the earth's surface regulate the distribution of organisms and processes. *BioScience*, 38(2), 92-98.

- Takahashi, T., 1981. Estimation of potential debris flows and their hazardous zones; soft countermeasures for disaster. *J. Nat. Disaster Sci.*, 3(1), 57-89.
- Tecca, P.R., Genevois, R., 2009. Field observations of the June 30, 2001 debris flow at Acquabona (Dolomites, Italy). *Landslides*, 6, 39-45.
- Theler, D., Reynard, E., Lambiel, C., Bardou, E., 2010. The contribution of geomorphological mapping to sediment transfer evaluation in small alpine catchments. *Geomorphology*.
- Toyos, G., Gunasekera, R., Zanchetta, G., Oppenheimer, C., Sulpizio, R., Favalli, M., Pareschi, M.T., 2008. GIS-assisted modelling for debris flow hazard assessment based on the events of May 1998 in the area of Sarno, Southern Italy: II. Velocity and dynamic pressure. *Earth Surface Processes and Landforms*, 33(11), 1693-1708.
- Varnes, D.J., 1978. Slope movement types and processes. *Landslides, Analysis and Control, Special Report 176*. Transportation Research Board, National Academy of Sciences, Washington DC.
- Veyrat-Charvillon, S., Memier, M., 2006. Stereophotogrammetry of archive data and topographic approaches to debris-flow torrent measurements: calculation of channel-sediment states and a partial sediment budget for Manival torrent (Isère, France). *Earth Surface Processes and Landforms*, 31, 201-219.
- Wilford, D.J., Sakals, M.E., Innes, J.L., Sidle, R.C., Bergerud, W.A., 2004. Recognition of debris flow, debris flood and flood hazard through watershed morphometrics. *Landslides*, 1, 61-66.
- Zanuttigh, B., Lamberti, A., 2007. Instability and surge development in debris flows. *Reviews of Geophysics*, 45(3).

APPENDIX: list of publications

Peer-reviewed articles:

- Navratil, O., Liébault, F., Bellot, H., Travaglini, E., **Theule, J.**, (in revision). High-frequency monitoring of debris-flow propagation along the Réal Torrent, Southern French Prealps. *Geomorphology*.
- **Theule J. I.**, Liébault F., Laigle D., Jaboyedoff M., Loye A., 2012. Sediment budget monitoring of debris-flow and bedload transport in the Manival Torrent, SE France, *Nat. Hazards Earth Syst. Sci.*, 12, 731-749.
<http://www.nat-hazards-earth-syst-sci.net/12/731/2012/nhess-12-731-2012.pdf>
- Loye A., Pedrazzini A., **Theule J. I.**, Jaboyedoff M., Liébault F., and Metzger R., 2012. Influence of bedrock structures on the spatial pattern of erosional landforms in small alpine catchments, *Earth Surface Processes and Landforms*.
- Navratil, O., Liébault, F., Laigle, D., Bellot, H., Ravanat, X., **Theule, J.**, Bacq, B., Demirdjian, J.L., Segel, V., Ficquet, M., 2012. Presentation of high-frequency flash floods and debris-flow monitoring in the French Alps. *Mémoire de la Société de Sciences Naturelles Vaudoises*.

Conference proceedings:

- Navratil, O., Liébault, F., Bellot, H., **Theule, J.**, Ravanat, X., Ousset, F., Laigle, D., Segel, V., et Ficquet, M., (2012). High Frequency Monitoring of Debris-Flows in the French Alps. 12th Congress INTERPRAEVENT 2012, Grenoble France.
- **Theule, J. I.**, Liébault, F., Loye, A., Laigle, D., and Jaboyedoff, M., 2011, Sediment Budget Monitoring of a Debris-Flow Torrent (French Prealps), *in* 5th International Conference on Debris-Flow Hazards Mitigation: Mechanics, Prediction and Assessment 2011, Padova, Italy.
- Loye A., Jaboyedoff M., Pedrazzini A., **Theule J. I.**, Liébault F., and Metzger R., 2011, Morphostructural Analysis of an Alpine Debris-Flow Catchment: Implication for Debris Supply, *in* 5th International Conference on Debris-Flow Hazards Mitigation: Mechanics, Prediction and Assessment 2011, Padova, Italy.
- **Theule, J. I.**, Liébault, F., Loye, A., Laigle, D., and Jaboyedoff, M., 2011. Sediment budget monitoring of a debris-flow torrent (French Prealps). *Journée de Rencontre sur les Dangers Naturels 2011*, Lausanne, Switzerland
- Navratil, O., Liébault, F., Bellot, H., **Theule, J. I.**, Ravanat, X., Ousset, F., Laigle, D., Segel, V., and Ficquet, M., 2011. Installation d'un suivi en continu des crues et laves torrentielles dans les Alpes française. *Journée de Rencontre sur les Dangers Naturels 2011*, Lausanne, Switzerland

Communications (conferences):

- **Theule, J. I.**, Liébault, F., Loye, A., Laigle, D., and Jaboyedoff, M., 2011, Sediment budgets and channel scouring of two alpine debris-flow torrents (SE France), *in* American Geophysical Union Fall Meeting 2011, San Francisco, California, USA. (Oral)

- Navratil O., Liébault F., Travaglini E., Bellot H., **Theule J. I.**, Ravanat X., Ousset F., Laigle D., Segel V., and Ficquet M., 2011, Development of a debris-flow monitoring system in the Réal Torrent (Southern French Alps), *in* American Geophysical Union Fall Meeting 2011, San Francisco, California, USA. (Poster)
- Loye A., **Theule J. I.**, Jaboyedoff M., Liébault F., Pedrazzini A., and Metzger R., 2011, Geological and morphostructural implication for sediment and debris supplying channels of small alpine catchments prone to debris flow, *in* EGU General Assembly 2011, Vienna, Austria. (Poster)
- Navratil O., Liébault F., Laigle D., Hervé B., Ravanat X., Ousset F., **Theule J. I.**, Demirdjian J., Segel V., and Ficquet M., 2011, High-frequency monitoring of debris-flows and flash floods in the French Alps, *in* EGU General Assembly 2011, Vienna, Austria. (Poster)
- **Theule, J. I.**, Liébault, F., Loye, A., Laigle, D., and Jaboyedoff, M., 2010, Catchment-scale sediment transport in torrents: the case of the Manival (French Prealps), *in* EGU General Assembly 2010, Vienna, Austria. (Poster)
- **Theule, J. I.**, Loye, A., Liébault, F., Laigle, D., and Jaboyedoff, M., 2009, Sediment budget of a debris flow event in the French Prealps, *in* American Geophysical Union Fall Meeting 2009, San Francisco, California, USA. (Oral)
- **Theule, J. I.**, Liébault, F., Peteuil, C., and Laigle, D., 2009, Coarse sediment transport and production in torrents: preliminary results of a starting project in the Northern French Alps, *in* EGU General Assembly 2009, Vienna, Austria. (Poster)